**Tectonics of the Ålen Area, Central Norway**

by

Charles W. Mandeville

Thesis Papers I & II submitted to the Faculty of the

Virginia Polytechnic Institute and State University

in partial fulfillment of the requirements for the degree of

Master of Science

in

Geological Sciences

APPROVED:

Lynn Glover III, Chairman

Robert J. Tracy

Richard D. Law

August, 1988

Blacksburg, Virginia

**Tectonics of the Ålen Area, Central Norway: I Tectonic Setting of the Tremadocian - Lower Ordovician Fundsjø Group, Central Norway**

by

Charles W. Mandeville

Lynn Glover III, Chairman

Geological Sciences

(Abstract)

Investigation of primary features preserved within the Tremadocian - Lower Ordovician Fundsjø Group indicate that the succession accumulated in a deep water environment. The ca. 4-5 km thick Fundsjø Group exposed in the Ålen area is dominated by thin bedded, terrigenous clastic metasediments which exhibit gradational contacts with mafic dominated bi-modal volcanics. Blastoporphyritic to blasto-ophitic diabase sills (0.5 - 3 m thick) compose ca. 20 - 30% of the metavolcanic Hersjø and Reitan Formations, and were emplaced as shallow intrusive units contemporaneous with volcanic activity. Localized preservation of relict coarse pyroclastic textured rocks and clast-within-clast fragments attest to the occasional occurrence of phreatomagmatic explosions. Very thin bedded, fine grained amphibolite which exhibits mm scale planar parallel laminae and non-erosive contacts suggests deposition by marine fallout. Primary features preserved within the terrigenous clastic Gudå, Kjurudal, and Slågrov Formations indicate deposition by turbidity currents throughout the succession.

A new stratigraphic correlation between the *Dictyonema* schist of the Nordaunevol locality, with the Kjurudal Fm. of this paper is proposed based on recent detailed mapping in the Ålen and southeast Haltdalen area. This correlation suggests that the Fundsjø Group is largely of Tremodocian - Lower Ordovician age.

The lithofacies contained within the oldest (Gudå Fm.) to youngest (Slågrov Fm.) formations in the Fundsjø Group suggest that this succession represents an accumulation of syn-rift to post-rift sediments deposited oceanward of the hinge zone of the Baltoscandian continent.

# Acknowledgements

This work was completed as part of my Master's Thesis research at Virginia Polytechnic Institute & State University, Blacksburg, Virginia. I wish to thank my advisor Dr. Lynn Glover III, for initially suggesting this project to me, for providing guidance through both the 1986 and 1987 field seasons, and for having enough confidence in my abilities to provide me with such an opportunity. Special thanks are extended to Dr. Robert J. Tracy and Dr. Richard Law for reviewing this manuscript, helpful comments, and readily providing expertise in their fields. I am grateful to the Department of Geological Sciences at Virginia Tech and Dr. Dave A. Hewitt (Chairman) for providing partial support of this project.

This work was made possible by the generous financial, logistical, and technical support of Norges Geologiske Undersøkelse (NGU), and the extended efforts of Dr. Fredrik Chr. Wolff and Dr. Brian A. Sturt, of the bedrock mapping division. Special thanks are extended to Dr. Odd Nilsen of the University of Oslo for providing expertise in Sør Trøndelag geology and logistical support during the 1986 and 1987 field seasons, but most especially for his encouragement and hospitality.

I am grateful for the support provided by Dr. David G. Gee and Dr. Michael B. Stephens of Sveriges Geologiska Undersökning (SGU), for spending time in the field with me, and pro-

viding me with opportunities to see portions of Scandinavian Caledonides outside the Ålen study area.

Special thanks are extended to ı, and ı n of A/S Killingdal Grubeselskab, for living accommodations during the 1986 and 1987 field seasons, and hospitality.

This work was partially supported by a Grant-In-Aid of research awarded in 1987 from Sigma Xi, The Scientific Research Society. Additional support was provided by a research grant from the Geological Society of America awarded in 1987. I am grateful for the support and encouragement provided by , Program Support Technician and Illustrator of the Orogenic Studies Lab. I would like to thank for her professionalism, expertise, and patience. Her help was appreciated. Special thanks are extended to for his help with computer applications, and tc

, and the many other graduate students who provided support, advice and lively discussion.

I would like to thank my parents for the support they have given me throughout this endeavor. Their encouragement helped me through the rough spots. Finally I wish to acknowledge the support of my grandmother and dedicate this work to her and to my late grandfather .

## TABLE OF CONTENTS

# List of Illustrations

# List of Tables

# Introduction

The emphasis of this investigation was to examine the lithofacies assemblage of the Fundsjø Group, Meråker Nappe, of the Ålen area in Sør Trøndelag, and to determine whether a magmatic arc, rifted arc, or rifted continental margin was the likely tectonic framework of accumulation. This investigation was undertaken in order to evaluate whether the overall characteristics of the stratigraphic section represented by the Fundsjø Group support or refute the immature, rifted island arc interpretation of Grenne and Lagerblad, (1985). Determination of the likely mode of emplacement of the volcanic lithologies in this ancient sequence is fundamental to the evaluation of the tectonic environment of accumulation. Furthermore, present tectonic models (Stephens and Gee, 1985, Roberts et. al., 1985) for the development history of the central Scandinavian Caledonides have also incorporated the immature, rifted island arc interpretation for the Fundsjø Group. The primary features preserved within the Fundsjø Group of the Meråker Nappe (Wolff and Roberts, 1980, Roberts and Wolff, 1981, Gee et. al., 1985) suggest that a sedimentological approach incorporating facies description of primary features preserved in these metamorphic rocks may resolve stratigraphic problems in this ancient sequence. The sedimentologic data derived from these rocks was used in conjunction with structural data (Mandeville, 1988) to determine relative ages of mappable units and the stratigraphy. This paper presents a redefined Fundsjø Group stratigraphy based on contact

relations observed between formations mapped in the Ålen quadrangle and southeastern portion of the Haltdalen quadrangle of Sør Trøndelag, Norway.

The Meråker Nappe (Fig. 1) (Wolff and Roberts, 1980, Roberts and Wolff, 1981) forms the eastern portion of the Trondheim Nappe Complex (Guezou, 1978). The stratigraphy within the Meråker Nappe bears gross similarities to the stratigraphy of the Støren Nappe (Wolff, 1967, 1973, 1979, Gee et. al., 1985). The Støren Nappe and Meråker Nappes are separated by a central unit referred to as the Gula Nappe Complex (Roberts and Wolff, 1981) which contains a heterogeneous sequence of banded gneisses, pelitic schists, migmatites, and minor amphibolites. A lower grade, unfossiliferous phyllite rich unit, (Fig. 1) called the Tronget unit (Krill, 1980), contains rocks similar to those within the Støren Nappe and comprises an intervening unit between the lower grade Støren Nappe and the higher grade rocks of the Gula Nappe Complex (Gee, et. al., 1985). The lower grade phyllite unit has been interpreted (Horne, 1979) as possibly representing a mélange, though Wolff (1979) correlates this unit with the Lower Hovin Group. Recent work by Nilsen (1983) in the Støren and Soknedal area indicates that the mélange is of olistostrome origin, and most likely deposited after Silurian nappe emplacement and metamorphism. The correlation of the stratigraphies of the Støren and Meråker Nappes (Wolff, 1979, Gee et. al., 1985) is briefly summarized below. A more thorough discussion of the correlation between the stratigraphy of the Støren Nappe and that of the Meråker Nappe can be found in Gee et. al., (1985). The names of the correlative stratigraphic groups are listed in parentheses with names of groups within the Støren Nappe given first, followed by the name of the correlative unit in the Meråker Nappe. The basal units of the stratigraphy in both the Støren and Meråker Nappes are composed of greenstone sequences (Støren Group and Fundsjø Group). These are succeeded by mixed volcanic and sedimentary sequences (Lower Hovin Group and Sulåmo Group) which are followed by dominantly sedimentary sequences (Upper Hovin Group and Kjøhaugan Group) composed largely of greywackes and conglomerates (Horg Group and Slågån Group including the Liafjellet Group(?) of Hardenby (1980)).

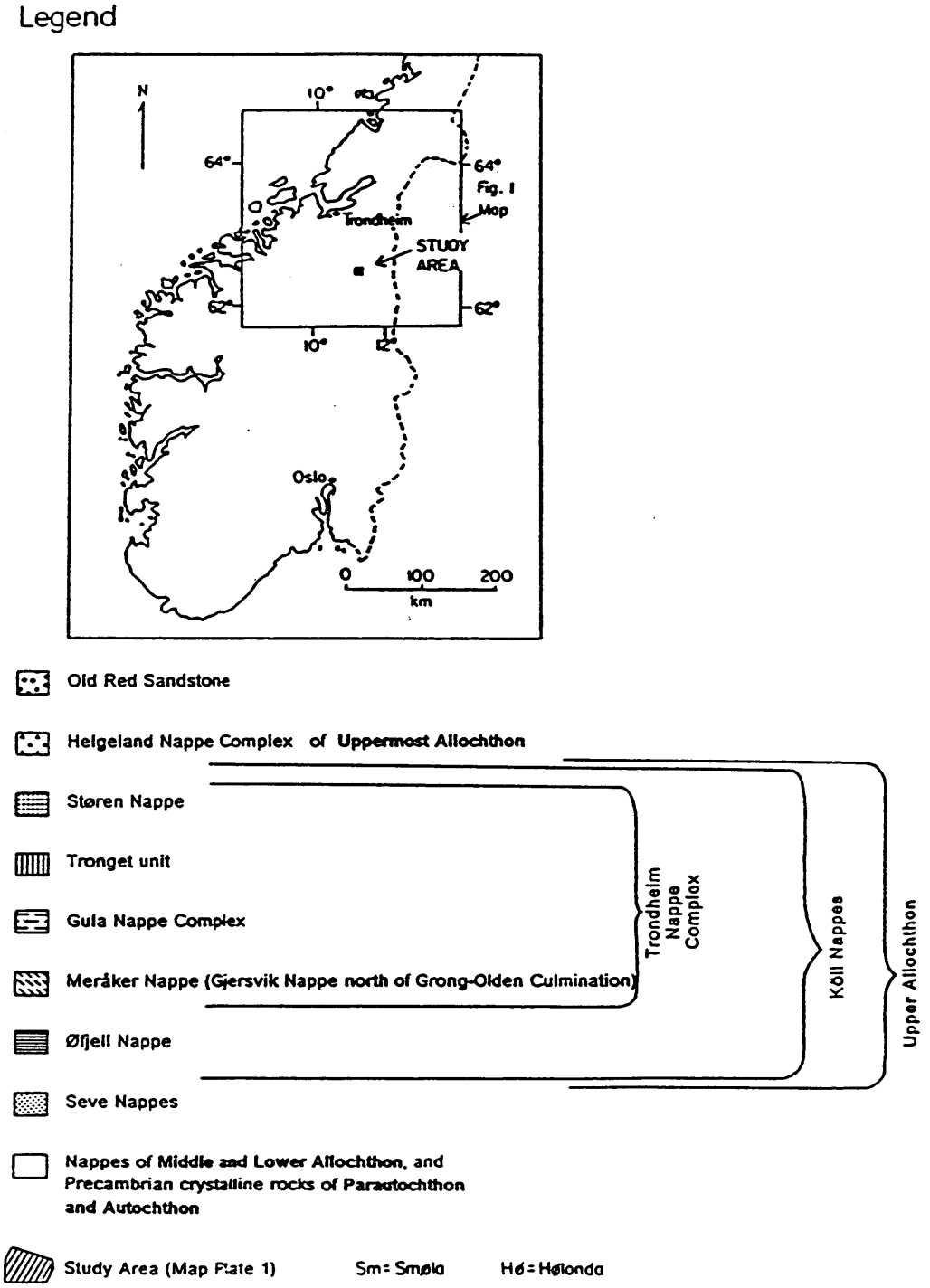


Figure 1. Tectonostratigraphic map of the Trondheim Region, Central Norway modified from Gee et. al., (1985).

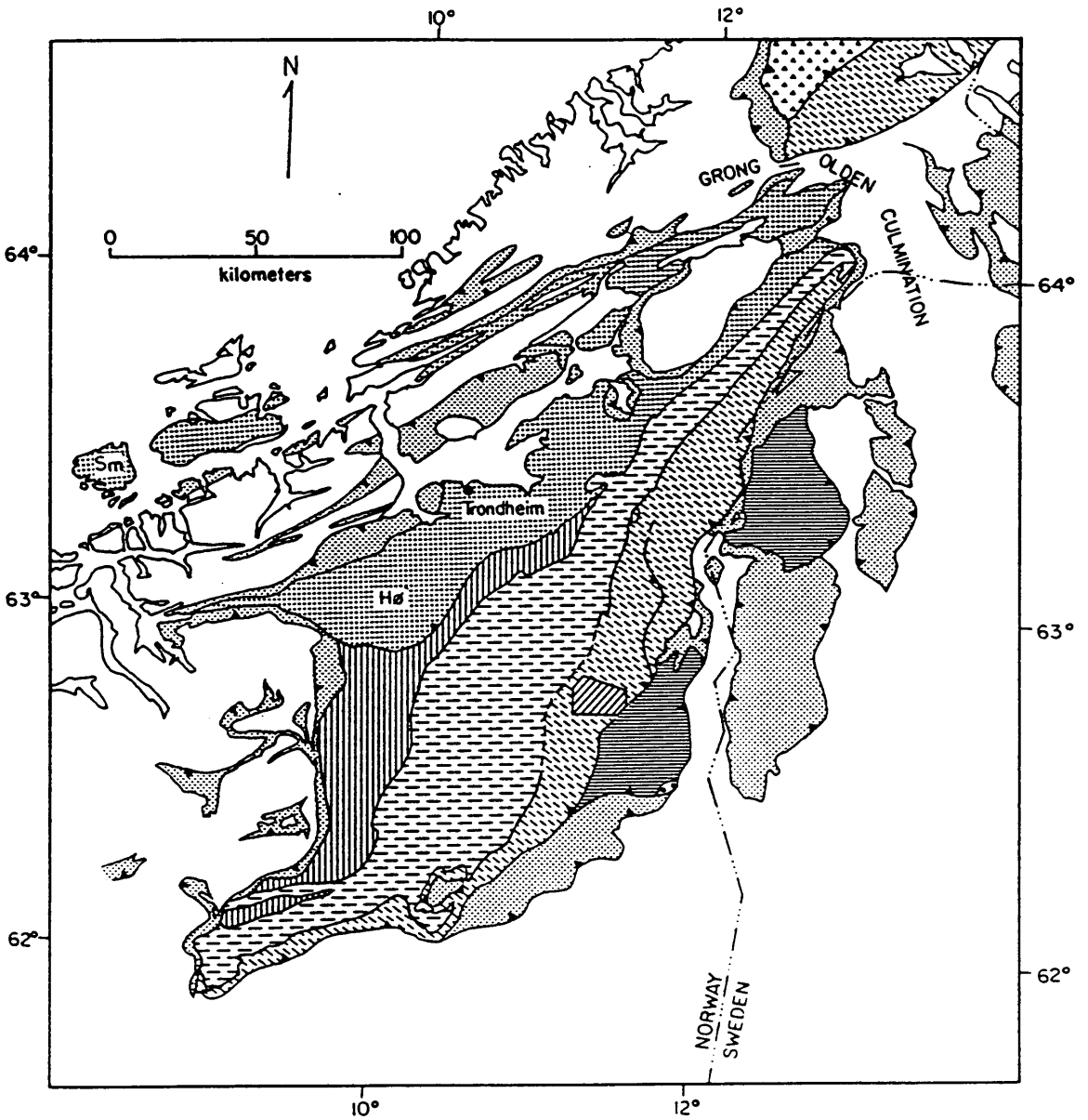
10°
12°
N
GRONG
OLDEN
CULMINATION
0
50
100
kilometers
64°
64°
Sm
Trondheim
63°
Hø
63°
62°
62°
NORWAY
SWEDEN
10°
12°

The Lower Hovin Group of the Støren Nappe contains abundant and diverse fossils (Bruton et. al., 1985) of late Arenig-early Llanvirn age including graptolites, brachiopods, trilobites, cephalopods, echinoderms, gastropods, and conodonts. Elements within the fauna show North American provincial affinity (Bruton and Bockelie, 1980). The Upper Hovin Group contains shelly faunas of Caradoc-Ashgill age (Bruton and Meråker Nappe are sparse and the rocks comprising the lower portion of the succession (e.g. Fundsjø Group) are of higher metamorphic grade (Lagerblad, 1984, Mandeville, 1988). A *Dictyonema* bearing graphitic schist (Vogt, 1889, Vogt, 1940, Størmer, 1941) which is intimately associated with the metavolcanics of the Fundsjø Group indicates a Tremadocian age for at least part of the Fundsjø Group (Gee et. al., 1985). Black phyllites of the Slågån Group contain graptolites (Getz, 1890, Wolff, 1979, Gee et. al., 1985) of Llandovery age. From the Middle Ordovician and upwards, the distinction between North American and Baltic faunas is progressively less pronounced (Bockelie, et. al., 1985). The stratigraphies of the Støren and Meråker Nappes cannot be traced continually around the intervening pelitic to semipelitic schists, and upper amphibolite grade banded gneisses of the Gula Nappe Complex (Gee et. al., 1985, Guezou, 1978).

# Stratigraphy

## General

The mappable rock-stratigraphic units which crop out in the Ålen area comprise an approximately 4-5 km thick succession of material which appears to record a prolonged period of deep water marine sedimentation and submarine volcanism. This succession has been subdivided into five mappable, named formations, each of which will be discussed below. This subdivision distinguishes formations which are dominantly of terrigenous clastic, non-volcanic origin, from those which are dominated by volcaniclastic material which record periods of active volcanism (pyroclastic rocks) or weathering of volcanic source terrains (epiclastic rocks). These rock-stratigraphic units commonly exhibit gradational boundaries. The dominantly non-volcanic terrigenous clastic formations commonly contain beds of volcanic material. Conversely, the dominantly volcaniclastic formations commonly contain material of non-volcanic origin. The physical characteristics of the material composing the non-volcanic formations, are quite similar throughout the succession from the oldest formation (Gudå Fm.) to the stratigraphically intermediate (Kjurudal Fm.) and youngest (Slågrov Fm.) formations. These formational units most likely originated from similar sedimentation processes, and it appears that these processes operated throughout the deposition of this sequence. Likewise,

the volcanic formations (Hersjø Fm. and Reitan Fm.) have similar physical characteristics in terms of bulk chemical compositions present (and proportions), and nature of the volcanism reflected by the deposits. The consistencies exhibited throughout the succession warrants a group designation for the sequence represented by the five formations (listed in order of oldest to youngest), Gudå Fm., Hersjø Fm., Kjurudal Fm., Reitan Fm., Slågrov Fm. to be discussed below. This sequence of formations contains lithologies similar to those included in the Fundsjø Group of the Færen area by Wolff (1973) and this name is therefore retained.

The Fundsjø Group rocks of the Ålen area have undergone lower amphibolite - middle amphibolite facies metamorphism (Mandeville, 1988) and consequently are extensively recrystallized. It can be assumed that the "meta" prefix precedes all lithic terms, but it has been omitted for sake of discussion where primary features are obviously preserved. Despite the extensive recrystallization, primary features are locally preserved in the formations containing psammitic and pyroclastic beds. The fortuitous preservation of such features in a couple of significant locations (discussed below, e.g., proximity to a lithologic contact and/or structural position) have been used to determine the relative ages of the formations.

The stratigraphy of the Fundsjø Group in the Ålen area is predominated by metamorphic semipelites, psammites, and calcareous schists with gradational contacts with mafic dominated, bi-modal metavolcanic units. Minor psammitic beds within the semipelitic Kjurudal Fm. of Rui (1972) and this paper, exhibit planar laminae and thin, normally-graded beds. These preserved primary features have been used to determine stratigraphic facing directions and relative ages of the formations. The localized preservation of these features along a macroscopic fold limb and also within the vicinity of a macroscopic fold hinge (locations 165 and 701 respectively, of Appendix A, and Plate 1) indicates widespread inversion of the stratigraphy. General inversion of stratigraphy at this structural and stratigraphic level has been recognized by several workers in the Caledonides of central Norway including Roberts (1967), Rui (1972), Wolff (1973), and Hardenby (1980).

The metasedimentary units (Gudå Schist, Kjurudal Fm., Slågrov Fm.) within the Fundsjø Group in the Ålen area show gradational contacts with the metavolcanic units and are never

totally devoid of intercalated volcanics. The bulk compositions of many beds within the metasedimentary units (reflected by high amounts of chlorite, biotite, and subhedral plagioclase) suggests a significant volcaniclastic component. This volcanic material could have been primary pyroclastic, reworked pyroclastic, or epiclastic in origin (Fisher and Schminke, 1984). Likewise, the Hersjø Fm. and Reitan Fm. have intercalations of metasediment within them which resemble beds found within the Gudå Fm., Kjurudal Fm., and Slågrov Fm. with respect to both mineralogy and bulk composition. These metasediment layers within the volcanics are probably representative of the background sedimentation taking place within the basin between eruptive phases. A summary of the named formations to be discussed below, is provided in Table 1.

Table 1 Summary of stratigraphy and proposed correlation

| | This paper | | Wolff (1967, 1973, 1979) | Olesen et. al., (1973) | Rui (1972) |
|---|---|---|---|---|---|
| | | Upper Ordovician Kjølhuagan Group | grey-green phyllites, phyllitic greywackes and greywackes | | Røros schists |
| Middle Ordovician Sulåmo Group | Røros Schists (Rui, 1972) | | Vektarhaug Fm., crystalline limestone, calcareous metasandstones, grey phyllites and metagreywacke, Lille Fundsjø Conglomerate (Wolff, 1973) | grey and green phyllite, greenschist, partly conglomeratic, | Dark phyllitic schists<br>Sætersjø Fm.,<br>Kjurudal Fm. |
| | | | unconformity | | |
| Tremadocian - Lower Ordovician Fundsjø Group | Slågrov Fm. | | Mica schist with layers of amphibolite (Wolff, 1979) | Micaschist and minor amphibolite (mafic tuffs) | |
| | Reitan Fm.<br>Sætersjø mbr. of Kjurudal Fm.<br>Kjurudal Fm. (includes *Dictyonema* schist) | | | | |
| | Hersjø Fm. | | Greenstone, Amphibolite, Porphyrititic Greenstone, Quartz Keratophyre, Greenstone and Quartz Keratophyre (Finely interbanded) (Wolff, 1973) | Metamorphosed mafic extrusive rocks, mafic and felsic intrusive rocks, tuffs and agglomerates, relict pillow structures | Hersjø Fm. |
| | Gudå Fm. | | Mica schist and gneiss with garnet, partly with staurolite and sillimanite, Graphite Phyllite, Biotite Amphibolite, Crystalline Limestone, Metaquartzite conglomerate to metagreywacke with biotite and garnet, also partly with staurolite and kyanite (Wolff, 1973) | garnet-quartz micaschist and staurolite, kyanite, garnet, and hornblende bearing biotite schist,<br>calcite marble, partly micaceous conglomerate, fine grained and thinly layered amphibolite | Gula schists (includes *Dictyonema* schist) |

## Gudå Formation

The Gudå Formation of this paper was named after the Gudå Conglomerate Zone of Wolff (1964) for which the type locality is near the village of Gudå (Fig. 2). Quartzite conglomerates with a matrix composed of biotite, quartz, diopside, amphibole and plagioclase ± calcite occur at this type locality. A limestone is intercalated with the conglomerates of the type locality. Greenstones are present to the east of the conglomerates of the Gudå sequence and a series of staurolite-kyanite bearing pelites occur to the west of the conglomerates (Wolff, 1964). Wolff (1964, 1967) included the lithologies of the Gudå Conglomerate Zone in the Gula Group, a dominantly metasedimentary unit that lies to the west of the Fundsjø volcanics. In his map and description of the Færen area, Wolff (1973) named a unit at the base of the Fundsjø Group, the Gudå Formation. The description of the formation includes metaquartzite conglomerate to biotite + garnet bearing metagreywacke which may also contain staurolite and kyanite. Wolff (1973) correlated the Gudå Formation with the Gudå Conglomerate of the preceding (Wolff, 1964, 1967) papers, due to the similarities of the metaquartzite conglomerates. Wolff (1973) stated that, " ... the Gudå conglomerate zone consists of metaconglomerates, metagreywackes, limestone, hornblende biotite fels and two-mica schists." Metabasalts and quartz keratophyre extrusive rocks are found to the east of the conglomerate and a series of staurolite-kyanite bearing pelitic schists are found to the west of the conglomerates at the type locality near the village of Gudå (Fig. 2).

The Gudå Formation of the Ålen area is mostly biotite quartz schist, some of which is graphitic; there are local intercalations of garbenschist, calc-silicate layers, quartz-plagioclase psammite, and mafic tuff. The term garbenschist is used here to describe calcareous schists whose mineralogy is composed of plagioclase, hornblende, quartz, and chlorite, ± calcite, ± garnet. The hornblende crystals can be up to 2 cm long and randomly or weakly alligned within the foliation. The Gudå Formation is the oldest formation within the Fundsjø Group (as herein defined) of the Ålen area.

Legend


Gabbro-metagabbro

Calcareous phyllite, garnet mica schist garbenschist and gneiss

Grey-green metagraywacke, banded metatuff

Quartz keratophyre

Grey sandstone (S&aetersjø Fm. of Rui, 1972)

Grey-green metatuff

Grey and black phyllite (Kjurudal Fm. of Rui, 1972)

Migmatite

Fundsjø greenstones

Metaquartzite conglomerate

Crystalline limestone

Gudå Fm. (Åsli Fm. of Nilsen, 1978)

thrust fault 

F = Færen
LFC = Lille Fundsjø Conglomerate
G = Gudå (village)
M = Meråker
Fo = Fongen
Hy = Hyllingen
N = Nordaunevol
Å = Ålen
R = Reitan Station
S = Sætersjøen

Figure 2. Regional map of Meråker Nappe modified from Wolff (1973,1979) and Nilsen and Wolff (1988).

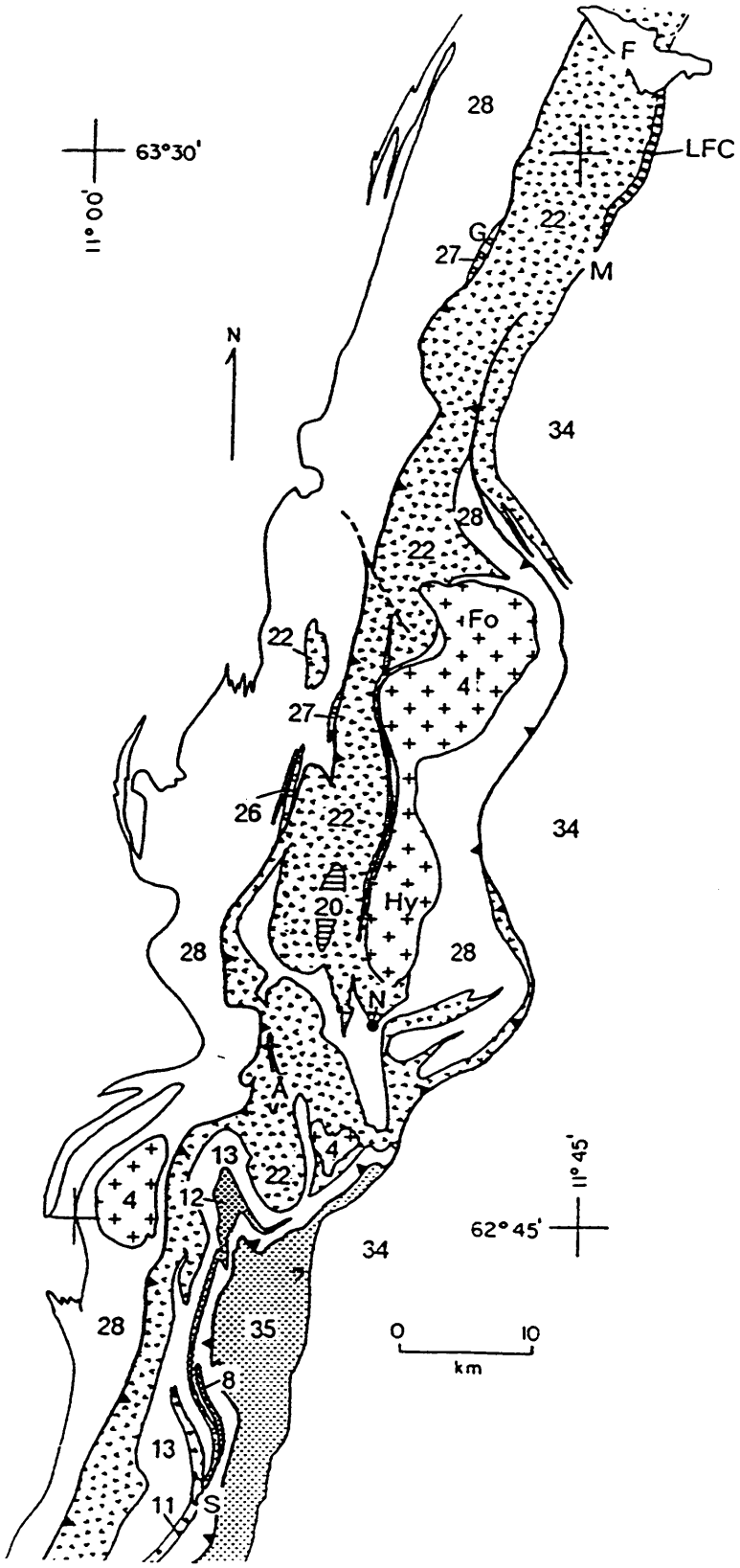
63°30'
11°00'
N
F
LFC
G
M
27
28
22
34
Fo
4
Hy
20
26
N
S
13
12
35
8
11
62°45'
11°45'
0
10
km

*Semipelites and minor psammites.* Semipelitic schists are the dominant lithofacies of the Gudå Fm. Thin beds of grey-brown biotite + quartz + muscovite ± garnet schist, biotite + muscovite + quartz phyllite-schist and biotite + quartz + muscovite + garnet ± staurolite ± kyanite schist compose most of the formation. Quartz + plagioclase + biotite ± muscovite ± garnet psammite, beds, which commonly grade upwards into fine grained semipelitic schist. These psammite rich beds are found as thin interbeds within the finer grained semipelitic schists. Primary sedimentary features are locally preserved within the semipelitic and psammitic beds. These consist of thin parallel laminae (mm-cm scale), graded beds, and rare ripple cross-stratification. The lower (stratigraphic bottom) contacts of the coarse grained laminae with the underlying fine grained laminae are sharp. Individual beds range from 1 cm - 10 cm in thickness. Normally graded beds are massive at the base and fine upwards into thin mm scale laminae.

*Graphitic schists and phyllites.* Thin 1-3 cm beds of dark grey biotite + quartz + muscovite + graphite ± kyanite ± staurolite schists are intercalated with the semipelitic and psammitic beds and are devoid of primary structures. In one outcrop, thin beds of biotite + quartz + muscovite + graphite phyllite are interbedded with semipelites and calcareous sediments.

*Calcareous metasediments.* In the Ålen area, the Gudå Fm. commonly contains intercalations of plagioclase + quartz + hornblende ± chlorite garbenschist, plagioclase + hornblende + quartz calc silicate layers, and minor light to dark grey marble layers. All of these lithotypes occur as minor 1-10 cm thick beds within the semipelite and psammite dominated sequences. Thin bedding is the only primary structure preserved in these lithofacies. The garbenschists and thin marble beds become more abundant towards the contact with the Hersjø Fm.

*Fine grained amphibolite.* Fine grained dark green amphibolite occurs as thin 2-10 cm beds within the semipelite and garbenschist dominated sequences. They are more abundant near the contact with the Hersjø Fm.

At one locality along the contact of the Gudå Schist with the Hersjø Fm. volcanics, (location 505 of Appendix A) a narrow zone of strongly rodded quartz is present within the biotite +

garnet schists. Some of these quartz rods may represent quartz clasts typical of the type Gudå conglomerate. Directly in contact with this quartz-rod bearing schist is a narrow zone of calc silicate schist, minor amphibolite, and impure marble. These lithologies are at a similar stratigraphic level to the Gudå Conglomerate Zone of Wolff (1964, 1967) at its type locality.

### *Interpretation*

The 1 cm-10 cm graded beds with massive bases which grade upwards into thin 1 mm-2 mm laminae are interpreted as A and B horizons of the Bouma (1962) sequence. Rare ripple cross-stratification in the upper parts of the graded beds are interpreted as representing the A, B, and C horizons of the Bouma (1962) sequence. The protolith for the semipelitic - psammitic beds was most likely a lithic arenite - lithic wacke (classification of Tucker, 1982). Organic rich marine shale or siltstone is a likely protolith for the graphitic schist layers within the Gudå. A turbidity current (Kuenen and Migliorini, 1950, Bouma, 1962, Walker, 1967, 1984) mode of deposition is likely for the semipelitic - psammitic beds. Layers composed almost exclusively of plagioclase, hornblende ± quartz ± calcite which commonly exhibit an internal layering parallel to bedding, (due to variation in modal hornblende and plagioclase) are present as intercalations between psammitic beds. A resedimented carbonate origin is proposed for these beds. The carbonate material may have been periplatform/perireefal detritus diluted by mixture with terriginous clastic/volcaniclastic material. The more calcareous layers within the Gudå Formation are likely to have originated from the redeposition of periplatform/perireefal detritus due to the lack of true pelagic carbonate in the Lower Paleozoic (McIlreath and James, 1984) and on their facies association with turbidite deposits.

The presence of fine grained amphibolite (mafic tuff) interbedded with impure marble (location 505 of Appendix A) indicates the transition to more prolonged volcanicity (represented by the Hersjø Fm.). Furthermore, detailed mapping in the eastern portion of the Haltdalen quadrangle indicates that bi-modal volcanism and coarse pyroclastic deposition occurred

(Lynn Glover III, pers. comm.) below the stratigraphic level of the mafic tuffs mentioned above. This indicates that volcaniclastic material within the Gudå Fm. is partially of primary pyroclastic origin and not solely due to weathering of Fundsjø Group volcanics as implied by Lagerblad (1984). The mineralogy and bulk composition of the Gudå Formation as well as position within the stratigraphic sequence, indicate that this unit is probably correlative with the biotite + garnet ± staurolite ± kyanite metagreywacke of Wolff's (1973) Gudå Formation which includes the Gudå Conglomerate Zone (Wolff, 1964, 1967). The Gudå Fm. is also correlative with the Åsli Formation of Nilsen (1978), the staurolite + kyanite + garnet + hornblende bearing biotite schist of Olesen et. al., (1973), and the Drøia Schist Group of Flatebö (1968).

Lagerblad (1984) described two profiles from east to west from the Fundsjø Group to the Gula Group of Wolff (1967). One of the profiles is from the Inndalen valley. The other lies 2 km north of lake Færen (Fig. 2). Both of the profiles described by Lagerblad (1984) indicate a gradation from the greenstones in the east to pelites and semipelites in the west. The gradation is by interleaving. When these are compared to a profile from east to west of the type section of Wolff (1964) it is apparent that the biotite + garnet ± staurolite ± kyanite schists are common to all three profiles. In all three profiles, pelites are found in the western portion. Minor differences are due to the presence or absence of staurolite or kyanite, intrusives, and intercalated volcanics.

## Hersjø Formation

The Hersjø Formation is an interbedded sequence of dark green, fine grained amphibolite, 1-2 m thick porphyritic diabase, minor layers of light grey fine grained quartz plagioclase semischist to gneiss, and localized occurrences of metamorphosed grey-green coarse pyroclastic rocks. The sequence is mafic dominated and bi-modal.

The contact with the stratigraphically overlying, structurally underlying Kjurudal Fm. is gradational by interleaving. The lower contact of the Hersjø Fm. with the structurally overlying, stratigraphically underlying, Gudå Fm. is most likely a bedding plane fault (tectonic slide of Hutton, (1981). This is indicated by the disharmonic geometry of this contact relative to the upper contact of the Hersjø Fm. with the Kjurudal Fm. (Plate 1). This fault contact probably becomes a a primary contact in the southwest portion of the study area as the evidence of a space problem diminishes and the geometry of the contact between the Hersjø Fm. and Gudå Fm. becomes more conformable. The presence of lithofacies typical of the Gudå to Fundsjø transition (e.g. conglomeratic beds, minor marble beds, and fine grained amphibolite beds) at location 505 along this fault contact suggests that little, if any, section was excised from the sequence as a result of faulting. The contact between the Hersjø Fm. and Gudå Fm. has not been encountered within a single outcrop but can be located to within 50-100 m in several localities. No distinct metamorphic or structural break exists across this bedding plane fault (Mandeville, 1988 , map Plate 1) which would suggest that it is of major tectonic significance.

The Hersjø Formation takes its name from the Hersjø Formation of Rui (1972), and is correlated by the author with an unnamed unit included in the Fundsjø Group of Wolff (1979) which consists of greenstone, and greenschists with layers of quartz keratophyre. The Hersjø Fm is also correlated by this author with the "finely interbanded" greenstone and quartz keratophyre, quartz keratophyre, porphyritic greenstone, and greenstone-amphibolite units of the Fundsjø Group of the Færen area (Wolff, 1973).

*Metamorphosed pyroclastics* In the Ålen area the Hersjø Fm. contains several types of metamorphosed pyroclastic rocks. These consist predominantly of interbedded fine grained dark green amphibolite mafic tuff, light grey quartz keratophyre tuff, plagioclase quartz crystal tuff, and crystal-lapilli tuff. Minor occurences of tuff breccia, and coarse pyroclastic breccia are present in some of the bedded sequences. The coarse grained pyroclastic breccias contain subangular to subrounded pyroclasts up to 15 cm long which are similar in mineralogy and texture to the blastoporphyritic diabase sills. The relatively coarse grained matrix of the pyroclastic breccias contains euhedral plagioclase phenocrysts and lithic fragments. It is

relatively poor in fine grained material which also suggests hydraulic separation of the finer materials from the coarser fractions. This separation process may be accentuated in the deposits derived from submarine eruptions (Fisher and Schminke, 1984) and becomes more effective with increased water depth (Fiske, 1963). Classification of the pyroclastic rocks is according to Fisher (1966) and Fisher and Schminke, (1984). Despite the amphibolite grade metamorphism, primary features are well preserved in several localities (locations 26, 31, 48, and 600 of Appendix A). At these localities, primary pyroclastic textures preserved allow for the direct interpretation of the sequence as pyroclastic in origin. It should be noted that the "meta" prefix has been omitted here, even though all the lithologies have been metamorphosed. The light grey and dark green banding in the tuffaceous sequences is interpreted to be primary planar bedding. This banding is due to alternating modal variation in plagioclase and hornblende content on a mm-cm scale. It is conformable to contacts between layers of marked grain size difference and/or relict phenocryst or lithic fragment content (e.g. contact between crystal lapilli tuff and tuff breccia, for example). This layering is also parallel to the contacts of minor terrigenous metasediment intercalations within the pyroclastic sequences.

*Sills.* Concordant blastoporphyritic diabase sills on the order of 1-2 m thick which display both upper and lower fine grained margins are common in the Hersjø Formation and comprise a siginificant volume of the Formation (approximately 20-30%). These sills are rarely observed, but present, in the epiclastic units, and quite abundant within this volcanic formation. Thin 10 - 50 cm thick blasto-ophitic diabase sills are also observed within the Hersjø Fm. but are less abundant than the blastoporphyritic variety.

*Intercalated terrigenous clastics.* Thin (5-15 cm) beds of quartz + plagioclase + biotite ± garnet ± hornblende semischist, and biotite + quartz ± garnet ± hornblende schist are commonly observed in outcrops dominated by the pyroclastic lithologies. The biotite quartz rich semipelitic layers are similar in composition to the formations stratigraphically below and above the volcanics of the Hersjø Fm.

*Impure marble and calcareous metasediments.* A single outcrop of light grey impure marble with minor amounts of quartz, albite, tremolite, chlorite and biotite occurs along highway 30 in the village of Ålen (location 80 of Appendix A) and is designated, Fhm, on Plate 1. It is common to find beds of plagioclase + quartz + hornblende ± chlorite ± garnet garbenschist, up to 1 m thick intercalated with the pyroclastics. These are present throughout the Hersjø Fm.

## *Interpretation*

The very fine grained, thin beds of amphibolite which commonly have mm-cm scale planar laminations of lighter colored, more plagioclase rich laminations within them are probably representative of mafic marine fall out. Evidence for this lies in the facies association of these deposits with coarser grained material of clearly pyroclastic origin in the better preserved sequences. The light grey layers of plagioclase quartz rich semischists to gneiss probably reflect thicker accumulations of felsic tuff which have probably undergone potassium loss and are thus interpreted as quartz keratophyre tuffs. The metasedimentary material rich in plagioclase and hornblende within the Hersjø reflects possible reworking of tuffaceous material and its admixture with perireefal/periplatform detritus either by bioturbation or deposition by turbulent flows. The lack of true pelagic carbonates in the early Paleozoic (McIlreath and James, 1984) also suggests that the calcareous layers are probably a result of redeposited carbonate mixed in various amounts with non-biogenic material. The biotite quartz rich semipelitic to quartzo-felspathic layers similar in composition to beds within the Gudå and Kjurudal formations are probably representative of background turbidite-hemipelagic deposition. A marl protolith is interpreted for the impure marble, Fhm, which crops out along highway 30 in Ålen. Contacts of this impure marble are poorly exposed and an olistostromal origin cannot be ruled out. Facies associations with clearly marine lithologies indicates that the volcanicity took place in a submarine environment (Fisher and Schminke, 1984).

The presence of large porphyritic diabase pyroclasts within the coarse pyroclastic breccias suggests that the sills are contemporaneous with the volcanicity and were probably emplaced as shallow intrusives into wet pyroclastic deposits. The surrounding pyroclastic tephra is interpreted to be the result of submarine phreatomagmatic explosions (Fisher and Schminke, 1984). At one locality near the center of Ålen, (location 600 of Appendix A) coarse pyroclastic breccia is exposed, which contains clast-within-clast, fragments. These pyroclasts suggest proximity to an eruptive center where repeated phreatomagmatic explosions lead to the redeposition of previously deposited pyroclastic fragments. Emplacement of shallow diabase sills into deep water sediments has been reported from the late Quaternary in the Guaymas Basin of the Gulf of California by Kelts et. al., (1982), and Einsele et. al., (1980). Saunders et. al., (1982) also suggest that this may be an important process of ocean crust formation in the early stages of ocean and marginal basin development when sedimentation rates are relatively high (such as in the Guaymas Basin of the Gulf of California; 1000 m/Ma). It is common to observe mm scale bedding preserved in the metatuffs directly adjacent to the contacts with the diabase sills and at one locality (location 31 of Appendix A) a large sill apparently has a pillowed termination within the tuff. Zones of peperite intrusion into the tuff host were not observed. However, relatively undisturbed laminations in sediments apparently unconsolidated at the time of sill emplacement have been reported by Kokelaar (1982). Notably lacking from the contacts at location 31 and in the better preserved pyroclastic sequences in the study area are horizons of hyaloclastite breccia or flow foot rubble (Busby-Spera, 1987). These deposits are commonly formed at the foot of an advancing basalt flow and are subsequently burried as the flow advances farther (Busby-Spera, 1987). This also suggests that most of the diabase was emplaced as sills. It is possible that some of the more massive textured diabase could also be submarine lava flows, because in some outcrops it is not possible to distinguish whether there are both upper and lower fine grained margins present due to poor exposure. Guezou (1978) reports the occurrence of pillowed porphyritic greenstones from the Dombås-Lesja area at this stratigraphic level. Pillow lavas are present within the Fundsjø Group

greenstones in the vicinity of the Fongen-Hyllingen layered basic intrusive complex (Olesen et. al., 1973, Nilsen, 1978).

## Kjurudal Formation

This unit was named the Kjurudal Formation by Rui (1972). The formation is composed predominantly of thin bedded (2-10 cm) semipelitic biotite quartz schists, biotite + quartz + chlorite schists and phyllites, minor graphitic schists, and quartz-plagioclase rich psammites. Minor layers of thin bedded (2-4 cm) calc silicate schists to impure marble are also interbedded with the semipelitic to psammitic beds. This unit was previously described by Rui (1972) as being predominantly dark phyllite. In the Ålen area however, there is a great deal of variation in this unit with respect to bulk compositon and mineralogy.

The lower contact of the Kjurudal Fm. with the Hersjø Fm. is gradational by interleaving. The schists of the Kjurudal Fm. commonly become richer in chlorite and/or hornblende adjacent to the contact with the Hersjø Fm. The complete transition from the Kjurudal Fm. to Hersjø Fm. was not observed within a single outcrop but was located to within 50 m in several locations. The amount of garbenschist in both formations also tends to increase near the contact. The upper contact of the Kjurudal Fm. with the Reitan Fm. is also gradational by interleaving and there is also an increase in the chlorite content of the schists of the Kjurudal Fm. and an increase in the proportion of garbenschists or thin amphibolite beds near the contact.

*Semipelites and psammites.* These lithofacies are closely associated in the Kjurudal Fm. and are the dominant lithotypes. Primary sedimentary features preserved in this unit are thin parallel laminae (mm-cm scale) and graded beds. These are best preserved in the psammitic schists (such as at location 701 of Appendix A). Contacts between coarse grained laminae and underlying fine grained laminae are sharp. The coarse grained laminae are massive at the base and grade upwards into fine grained, mm scale, parallel laminae.

*Biotite + quartz + chlorite schists and phyllites.* Thin bedded, dark grey-green biotite-chlorite-rich schists and phyllites are subordinate to the semipelitic schists but are commonly interbedded with the latter throughout most of the Kjurudal Fm. This lithofacies also commonly contains thin beige (mm scale) laminae that are rich in carbonate. This biotite-chlorite-rich lithofacies is commonly associated with garbenschists, and thin beds of fine grained amphibolite.

*Graphitic phyllites and schists.* Thin (2-10 cm) beds of dark grey biotite + quartz + muscovite + graphite phyllite and schist are interbedded with the semipelites and are more common near the contact with the Hersjø Formation. These graphitic beds are devoid of primary structures and are strongly cleaved.

*Calcareous schists.* Dark blue-grey calcareous schists, with abundant biotite, quartz and chlorite, are present as thin beds within the semipelitic to psammitic beds. Some of these calcareous layers of 1-3 cm thickness are rich enough in carbonate to be considered impure marble.

## *Sætersjø Member of Kjurudal Formation*

This stratigraphic unit takes its name from the Sætersjø Formation of Rui (1972). Though it does not occur in the Ålen area, it would occupy a position in the stratigraphy within the Kjurudal Fm. and stratigraphically below the Reitan Formation. This unit which is given member status in this paper was named from the type localities to the south of Sætersjøen (Fig. 2). This unit has been described by Rui (1972) as consisting of "alternating polymict conglomerates, grey feldspathic metasandstones, and semipelitic schists."

Reconnaissance work carried out during the summer of 1987 in the Sætersjøen area revealed that the polymict conglomerates interbedded with the semipelitic schist, have clast populations which are dominated by felsic volcanic fragments with minor clasts of dark grey phyllite/schist, and light grey tonalite and trondjheimite clasts. Clast size is generally in the

pebble to cobble range although 2 meter (long dimension) sized clasts of dark schist have been observed. Other less abundant clasts are briefly described and listed in Appendix B .

The contacts of the Sætersjø member of the Kjurudal Fm. are gradational by interleaving with the surrounding biotite + quartz ± chlorite ± graphite schists and phyllites of the Kjurudal Fm. Dark grey schists and phyllites are present as intercalations throughout the Sætersjø member.

Primary features preserved within the Sætersjø member consist of normally graded and inversely graded beds within the conglomeratic horizons, and large rip-up clasts of dark semipelitic schist. Flame structure has also been observed at one locality at the contact of a coarse conglomeratic bed with an underlying dark semipelitic schist.

Petrographic examination of polished slabs and several thin sections indicates that the felsic volcanic fragments are porphyritic quartz keratophyre clasts with euhedral plagioclase and quartz phenocrysts preserved in a finer grained pilotaxitic groundmass of plagioclase and quartz (Fig. 3). Rare diabase clasts exhibit blasto-ophitic textures and now consist of intergrown plagioclase and hornblende. The tonalite and trondjheimite clasts exhibit coarse blasto-hypidiomorphic granular textures. Isolated and slightly elongate clots of biotite and chlorite are also present. The matrix of these beds, is composed of euhedral-subhedral plagioclase, polycrystalline quartz, relict quartz phenocrysts, crudely alligned biotite and chlorite, and accessory zoisite.

## *Interpretation*

The thin graded beds and planar laminae preserved within the psammitic layers of the Kjurudal Fm. are interpreted as Bouma (1962) A and B horizons and deposition by turbidity currents is likely (Kuenen and Migliorini, 1950, Bouma, 1962, Walker, 1967, 1984). The increase in chlorite and hornblende content of the schists and psammites suggests an increase in volcaniclastic component to the primary protoliths. This material may have been epiclastic

Figure 3. Photomicrograph of felsic volcanic rock fragment from Sætersjø Member of the Kjurudal Fm. (cross polarized light).

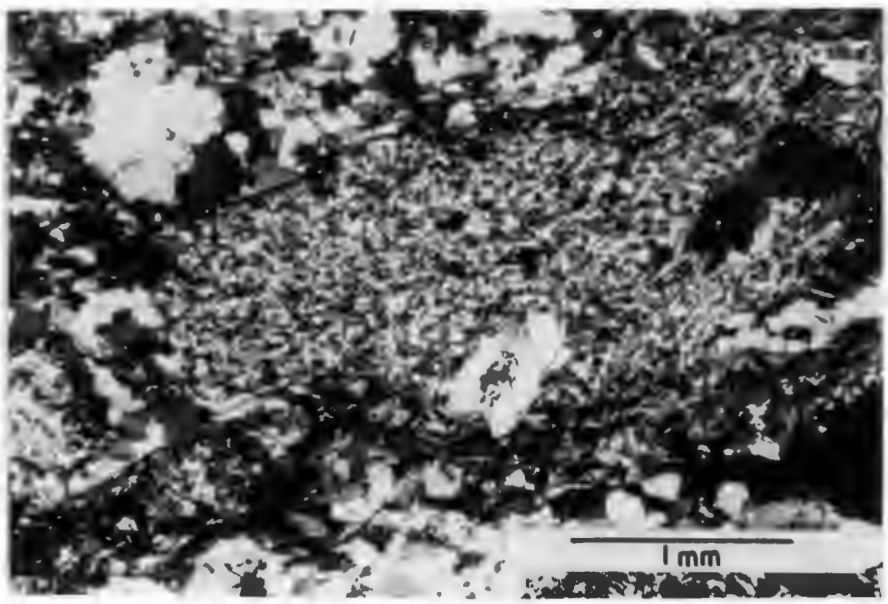
1 mm

or pyroclastic in origin. The presence of thin fine grained amphibolite layers in the Kjurudal Fm. which are interpreted as mafic tuffs suggest that some of this volcaniclastic material may have been of pyroclastic origin. Thin bedded marine mudstones-siltstones with varying amounts of organic and minor graphitic schists. The calcareous beds are likely to have been a deep water marl due to their facies association with turbidites.

The elongated clots of biotite and chlorite contained within the conglomeratic layers of the Sætersjø member contain isolated plagioclase phenocrysts and patches of zoisite. These clots may represent relict mafic tuff clasts subjected to tectonic flattening.

The compositons of the dominant felsic volcanic clasts, their subangular shapes, (much of which is due to tectonic flattening) and the composition of the matrix, suggests that these "polymict conglomerates" are volcaniclastic conglomerates which are most likely of epiclastic origin (Fisher and Schminke, 1984). The dominance of felsic volcanic clasts and the amount of euhedral plagioclase in the matrix in some of the conglomerate horizons may also indicate a reworking of pyroclastic material. There is a general lack of clasts which have a pre-existing structural fabric oriented independently of the prominent fabric in the rocks. The clasts which show the most deformation are the felsic volcanic clasts and dark schist fragments and the fabric present is essentially parallel in all the clasts. This suggests that the Sætersjø member is an intraformational conglomerate within the Kjurudal Formation. A moderate amount of sorting and normally graded basal units within some coarse pyroclastic beds suggests some hydraulic separation of coarse and fine fragments. Deposition was likely to have been from low concentration sediment gravity flows where the flow was probably turbulent. Rip-up clasts of dark phyllite and schist within the coarse beds suggest that the flow was probably turbulent (and erosive) and not laminar. Conversely, those conglomeratic beds which display inversely graded basal zones were probably deposited from high concentration sediment gravity flows (Sigurdsson et. al., 1980, Fisher, 1984). Deposition by sediment gravity flows originating from the slumping of unstable slopes (Fisher, 1984) composed predominantly of felsic volcaniclastic debris is likely. The presence of conglomeratic beds with normally graded basal zones and those with inversely graded basal zones suggests that flow transformation (Fisher, 1983) may

have occurred. Very large (up to several meters) fragments of the dark semipelitic schist beds are present as rip-up clasts within the coarse volcaniclastic beds. Alternatively, some of these very large schist fragments may represent accidental fragments originating from phreatomagmatic explosions. These may have subsequently been entrained with the volcaniclastic debris in subaqueous sediment gravity flows. The flame structure mentioned above is indicative of fluid escape from the underlying unit as a result of possible loading due to the overriding sediment gravity flow.

The protolith of the dark phyllitic schists was most likely a fine grained lithic-wacke, or lithic-arenite, possibly interbedded with minor amounts of mudstone. A turbidite origin is likely for the fine grained dark phyllitic schist. The Sætersjø member of the Kjurudal Fm. is interpreted as an interbedded sequence of turbidites, and sediment gravity flows of both high and low concentration which apparently remobilized debris of dominantly felsic volcanic origin.

## *Implications of new mapping and proposed correlation*

Present mapping (Plate 1) indicates that the Kjurudal Formation is stratigraphically continuous into what has previously been mapped as Gudå Formation (Fig. 4, from Nilsen and Wolff, 1988). Almost continous exposure along the Gaula river (Plate 1) indicates that what was previously shown as a lithologic contact between the Hersjø Fm. volcanics and the Gudå Formation is actually a zone (locations 630 and 634 of Appendix A) spanning approximately 50 m where the schist is extensively intruded by porphyritic and fine grained sills. To the west of this zone however, one encounters continuous exposures of metapsammite and semipelite which can be mapped continuously into the Kjurudal Fm. of Rui (1972) which also corresponds to unit 13 (Dark Phyllitic Schists) of the NGU 1 : 250,000 scale Røros and Sveg quadrangle of Nilsen and Wolff (1988), (Fig. 4). The new mapping presented in this paper (Fig. 5 and Plate 1), has important implications for the age of the lower part of the Fundsjø Group based on the

*Dictyonema* occurrence at Nordaunevol (Vogt, 1889, Vogt, 1940, Størmer, 1941). This new mapping suggests that the *Dictyonema* bearing graphitic schist is part of the Kjurudal Fm. of this paper. Gee et. al., (1985) indicate that the Fundsjø Group is "in part of Tremadoc age?" based on the correlation of the *Dictyonema* schist with Gudå Formation of this paper, the Gudå Formation (Wolff, 1973), and Gudå Conglomerate Zone (Wolff, 1964, 1967). The mapping in Figure 5 and Plate 1 indicates that the Hersjø Fm. and Kjurudal Fm. are of Tremodocian age. Moreover, it suggests that the Fundsjø Group as defined herein, is largely of Tremadocian - Lower Ordovician age. This makes the correlation (Table 1) of the Kjurudal Fm. of Rui (1972) with the Sulåmo Group of Wolff et. al., (1967) unlikely.

The correlation proposed in this paper, (Table 1) is that the Røros Schists of Rui (1972) are correlative with the Sulåmo Group of Wolff (1967, 1973, 1979). Both units contain partly graphitic phyllites and schists, grey to grey-green phyllites and schists, calcareous metasandstones and siltstones (Rui, 1972, Wolff, 1973, Hardenby, 1980). This is in agreement with the work of Olesen et. al., (1973) in the Tydal area which lies to the northeast of Ålen.

The upper and lower contacts of the Kjurudal Fm. of this paper are gradational with the Reitan Volcanics and Hersjø Fm. respectively, and are conformable. No evidence for an unconformable contact is recognized between the Kjurudal Fm. and the stratigraphically underlying Hersjø Fm. (Fundsjø greenstone correlative) in the Ålen area. This is unlike the contact relationship described between the Fundsjø Group and Sulåmo Group in the Meråker and Færen areas (Wolff, 1973). Hardenby (1983) in his description of the structural geology of the Kjølhaugan area, also reports a distinct structural break reflected by the change in the orientation of fold axes observed within the Fundsjø relative to the orientation of fold axes observed within the Sulåmo and younger groups. The structural break is at the level of the unconformity represented by the Lille Fundsjø conglomerate. No structural break of this sort was encountered in the study area (Mandeville, 1988) and as mentioned above, evidence for an unconformity at the level of the Hersjø Fm.- Kjurudal Fm. contact was not observed. This suggests that the Kjurudal Fm. is not a correlative of the Sulåmo Group if one accepts the validity of the unconformity (Chaloupsky and Fediuk, 1967, Wolff, 1973).

## Legend

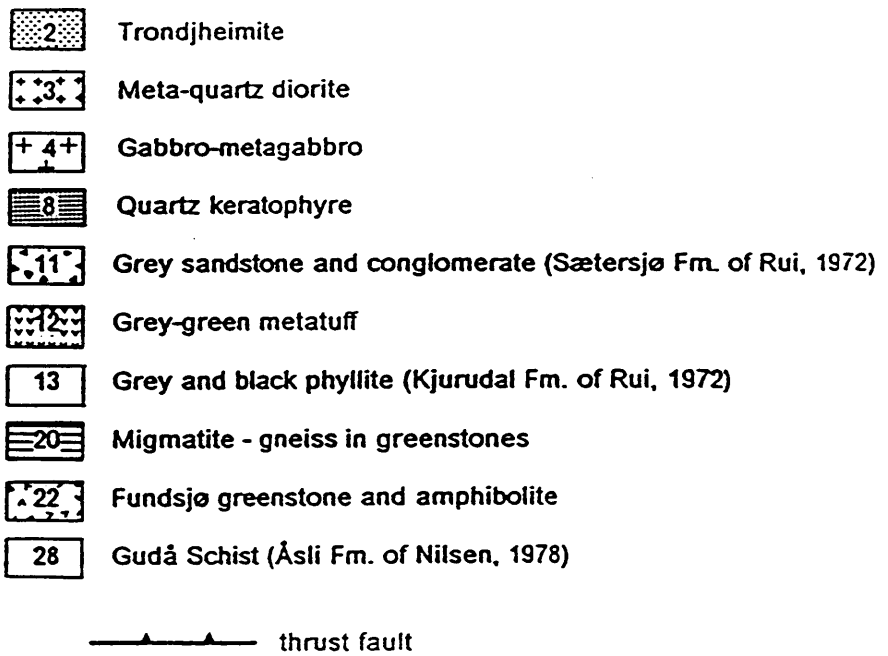


Ga = Gaulåsen
Gr = Graftås
Hy = Hyllingen
N = Nordaunevol
Å = Ålen
R = Reitan Station
S = Sætersjøen

Figure 4. Regional map over Ålen Area compiled from Wolff (1973, 1979) and Nilsen and Wolff (1988).

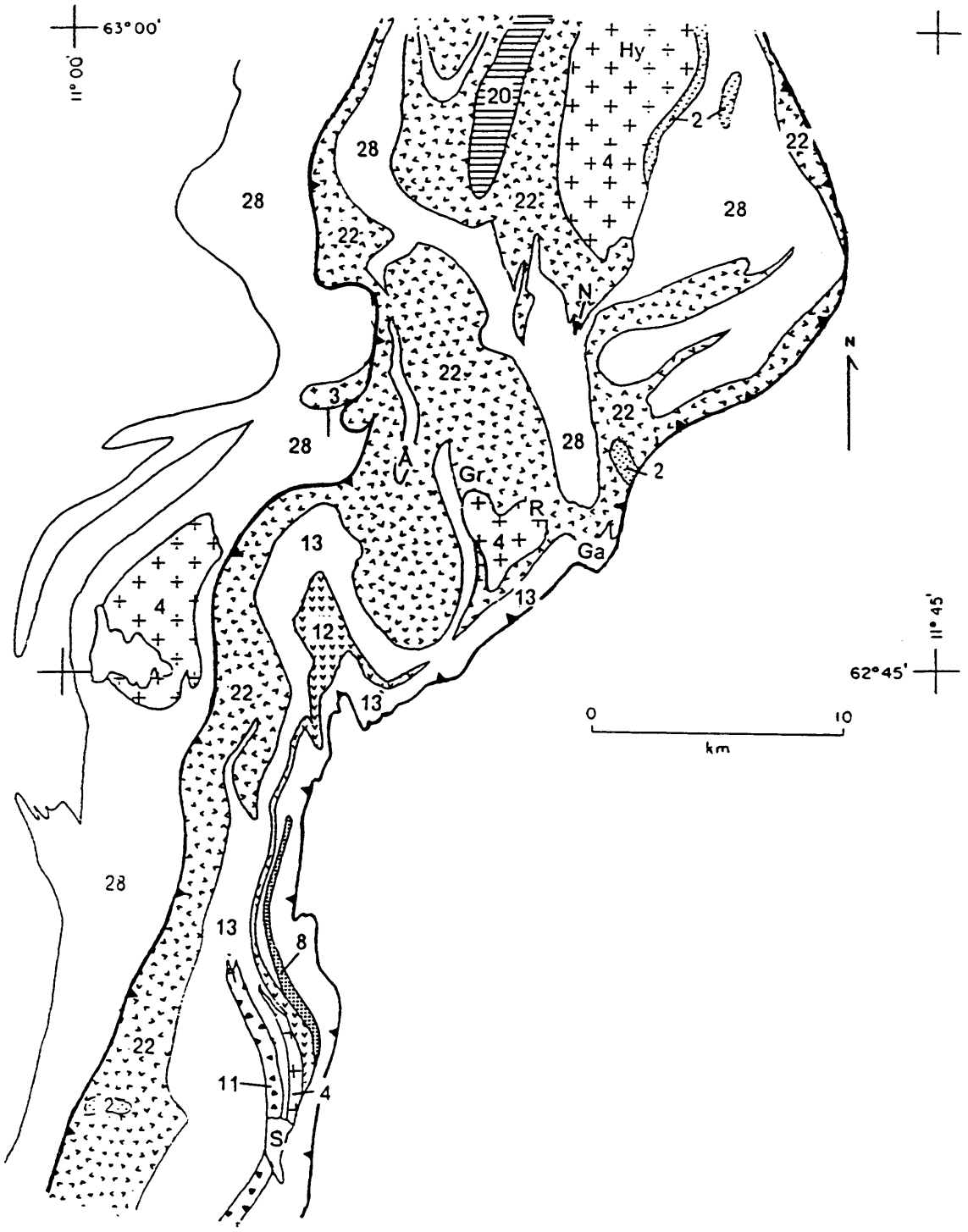
63°00'
11°00'
11°45'
62°45'
Hy
20
2
4
22
28
N
3
A
Gr
R
Ga
13
12
8
11
S
0
10
km

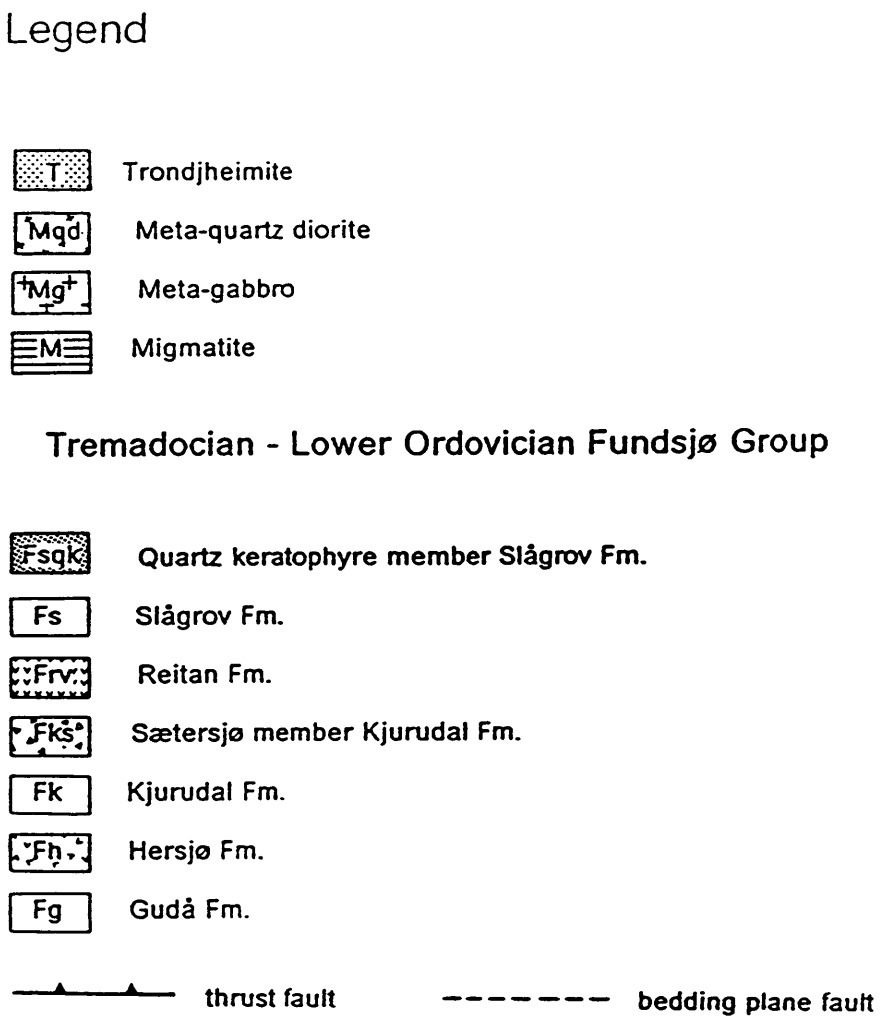


Figure 5. Regional map over Ålen Area showing modifications (this study) of 1 : 250.000 Røros and Sveg quadrangle of Nilsen and Wolff (1988).

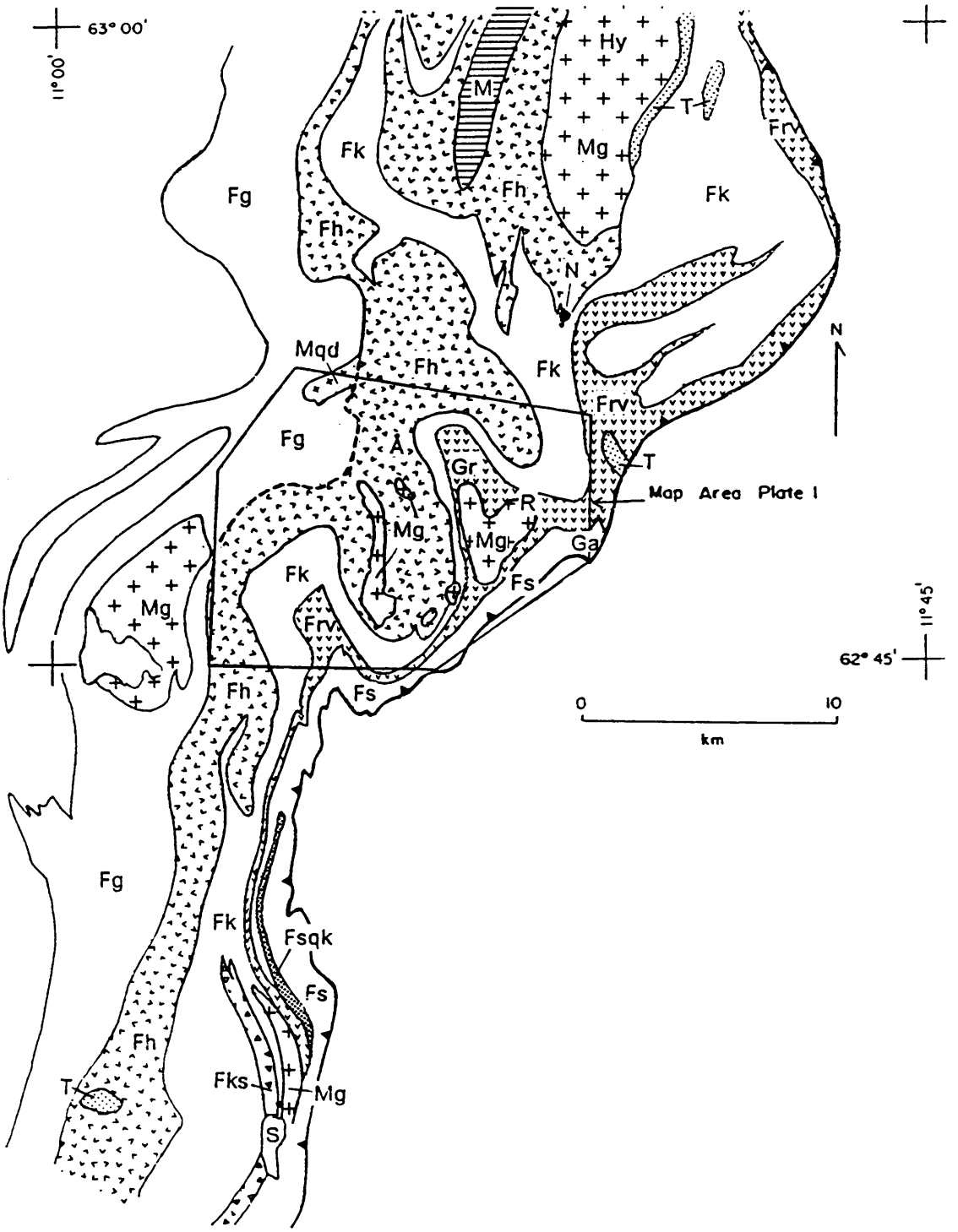
63° 00'
11° 00'
Hy
M
T
Fr
Fk
Mg
Fg
Fh
Fk
N
Mqd
Fh
Fk
Frv
Fg
A
Gr
T
R
Map Area Plate I
Mg
Mgr
Ga
Fk
Fs
Mg
Frv
Fh
Fs
0
10
km
11° 45'
62° 45'
Fg
Fk
Fsqk
Fs
Fh
T
Fks
Mg
S

## Reitan Formation

This unit is named for good exposures along the road to Tydal, approximately 2 km to the east of Reitan Station. This unit is very similar to the Hersjø Fm. in that it is predominantly interbedded fine grained dark green amphibolite, fine grained grey-green plagioclase quartz semischist to gneiss, with visible plagioclase phenocrysts, medium to fine grained diabase, and grey-green metamorphosed pyroclastic rocks. composition to those found within the lithologies of the Hersjø Fm. The relative proportion of mafic to felsic rocks is similar to that of the Hersjø Fm. and the formation is mafic dominated and bi-modal. Localized preservation of primary pyroclastic textures (e.g. location 675 of Appendix A) indicates that portions of this formation are clearly composed of metamorphosed pyroclastic rocks. Relict euhedral clinopyroxene phenocrysts have been observed in only one of the pyroclastic rocks (a tuff breccia). Most primary igneous pyroxene has been replaced by blue-green hornblende.

The contact relationships of the Reitan Fm. with the stratigraphically underlying Kjurudal Fm. and stratigraphically overlying Slågrov Fm. are gradational by interleaving. The Reitan Fm.-Slågrov Fm. contact is poorly exposed and has been mapped according to where the bedrock is dominantly composed of volcaniclastic material.

A minor occurrence of impure marble and calc silicate schist designated Frm, on the map (Plate 1), and in gradational contact with the bedded pyroclastics is exposed along the railroad tracks just north of Graftås. Intercalations of biotite + quartz + plagioclase $\pm$ garnet $\pm$ chlorite schist, and plagioclase + hornblende + quartz $\pm$ chlorite $\pm$ calcite garbenschist are common within the Reitan Fm.

This unit is similar to the Hersjø Fm. in that it is intruded by concordant sills which comprise a significant volume of the formation. The sills within the Reitan Volcanics however tend to be thinner (less than 0.5 m) and finer grained than the porphyritic diabase sills of the Hersjø Fm. Porphyritic diabase sills are found only occasionally within the Reitan Formation.

### *Interpretation*

The abundance (20-30%) of concordant metadiabase sills, some of which exhibit blastoporphyritic textures similar to those found as large pyroclasts within the tuff breccias implies contemporaneity of sill emplacement and volcanic eruptions of phreatomamatic origin. Lack of flow foot rubble/hyaloclastite breccias (Busby-Spera, 1987) in the Reitan Fm. also suggests that the concordant metadiabase represents shallow sills emplaced into wet tuffaceous sediments, similar to those reported by Kelts et. al., (1982) Saunders et. al., (1982) and Einsele et. al., (1980). The Reitan Formation contains several varieties of metamorphosed pyroclastic rocks. These include fine grained dark green mafic tuff, grey-green plagioclase quartz crystal tuff, olive colored mafic lapilli tuff, and grey-green tuff breccia. The tuff breccias contain fragments (up to 10 cm long) of blastoporphyritic diabase and less abundant quartz keratophyre tuff in a matrix of hornblende, chlorite, quartz and plagioclase. Mafic lapilli in the tuff breccias and mafic lapilli tuffs consist of clots of dark blue-green hornblende and chlorite. The best preserved bedded pyroclastic deposits occur on the north flank of Gaulåsen (location 675 of Appendix A) where concordant sills intruded fine grained mafic tuff, crystal tuff, crystal lapilli tuff, and tuff breccia. The bi-modal compositions of the relict porphyroclasts suggests that many are probably accidental fragments.

The semipelitic beds are similar to those found within the Kjurudal Fm. and Slågrov Fm and are likely to be the result of turbidite influx between eruptive phases. Mixture of pyroclastic material with pelagic carbonate or periplatform/perireefal debris is the interpreted origin of the calcareous metasediments.

## Slågrov Formation

This unit takes its name from exposures along the railroad tracks just west of Highway 30 near Slågrovsvollan in the southern portion of the Ålen 1 : 50,000 scale quadrangle (location

298 of Appendix A). The formation is composed of thin bedded dark grey to dark grey-brown schists and phyllites with minor layers of grey-green chlorite + quartz + plagioclase schists, quartz plagioclase rich psammites, and fine grained amphibolite.

The contact relationship with the stratigraphically underlying Reitan Fm. is not well exposed, but appears to be gradational by interleaving. Indication of a gradational contact is in the form of thin (2-4 cm) beds of fine grained amphibolite and/or chlorite + quartz + plagioclase schist which are more abundant in exposures nearer the contact with the Reitan Fm. (e.g. location 724 of Appendix A).

The Slågrov Formation is dominantly interbedded dark grey muscovite + biotite + quartz ± graphite phyllite, biotite + muscovite + quartz ± graphite schist, and muscovite + quartz + biotite schist. Common intercalations of plagioclase + quartz + biotite semischist and quartz + plagioclase + biotite ± garnet psammite are also present and comprise most of the beds exposed near the summit of Gaulåsen. These beds are extensively recystallized and do not exhibit preservation of primary grading, although compositional changes occur on a mm scale and have the appearance of thin planar laminae.

## *Interpretation*

The psammitic beds are interpreted as metatuffaceous sandstones due to their relatively high content of chlorite and plagioclase. The thin beds of chlorite + quartz + plagioclase schist may represent an increase in the amount of epiclastic material in the sediments. The thin beds of fine grained amphibolite are interpreted as mafic tuff horizons. The thin bedding within this unit and plane parallel laminae suggest depositon by turbidity currents.

The Slågrov formation is correlative with an unnamed unit described by Rui (1972), as mainly dark phyllitic schists.

## Age of the Fundsjø Group

Constraints on the ages of the lithologies exposed in the Ålen area are derived from outside the field area shown in Plate 1. The Nordaunevol fossil locality found by J.H.L. Vogt (1889) and described by T. Vogt (1940) and Størmer (1941), lies approximately 15 km to the north of the Ålen area (Fig. 2). The presence of *Dictyonema* bearing graphitic schists that are intimately associated with pillow lavas of the Fundsjø Group (Gee et. al. 1985) indicates that the metasediments are Tremodocian in age. The graphitic schist at this locality, has been correlated (Gee et. al., 1985, Nilsen and Wolff, 1988) with the Gudå Conglomerate Zone (Wolff, 1964), part of the Åsli Formation of Nilsen (1978), and is also included in the Holta Group of Guezou et. al., (1980) (Fig. 4). However, recent detailed mapping carried out during 1986 and 1987, (Fig. 5, and Plate 1) indicates that the graphitic schist at the Nordaunevol locality is probably correlative with the Kjurudal Formation (Rui, 1972) as redefined in this paper. This correlation would place the lower part of the Fundsjø Group within the Tremadocian.

In the Meråker and Færen areas to the north (Fig. 2), a polymict conglomerate called the Lille Fundsjø Conglomerate (Chaloupsky and Fediuk, 1967, Wolff, 1973) separates the Fundsjø Group volcanics from the stratigraphically overlying Sulåmo Group. This polymict conglomerate which forms the base of the Sulåmo Group, contains pebbles derived from the stratigraphically underlying Fundsjø Group and marks an unconformity between the two groups. This unconformity indicates a previous deformation, uplift, and metamorphism of the Fundsjø Group (Wolff 1967, Furnes et. al., 1980, Hardenby, 1980). No evidence for this unconformity has been recognized in the Ålen area, nor has a distinct break in metamorphic grade been found. If the interpretation of an unconformity separating the Fundsjø and Sulåmo groups is valid, then the lack of evidence for this unconformity in the Ålen area may be due to the absence of true Sulåmo age rocks in the stratigraphic section. The lack of evidence for this unconformity in the Ålen area suggests that the various formations which crop out in the

Ålen area most probably belong within the Fundsjø Group. This correlation differs from that proposed by Rui (1972), (Table 1).

The Trondheim and Ostersund 1 : 250,000 quadrangle map of Wolff (1979) shows an unnamed unit included within the Fundsjø Group composed of mica schist with layers of amphibolite (See Fig. 2) located in a NNE striking belt on the east side of the Fongen-Hyllingen layered basic intrusive complex (Wilson et. al., 1981, Wilson, 1985). The three youngest formations within the Fundsjø Group of this paper (Kjurudal Fm., Reitan Fm., and Slågrov Fm.) are correlative with this unit and are the result of its further subdivision in the Ålen area. This is in agreement with previous work done to the east of the Fongen-Hyllingen complex by Olesen et. al., (1973). They indicate a mica schist and minor amphibolite (mafic tuffs) unit on their map (their fig. 1, pp. 260-261.)

# *Intrusive Rocks*

## Meta-Gabbro

This unit consists of grey-green, medium to coarse grained, blasto-ophitic - blastogranular textured rock composed of plagioclase and hornblende. The unit commonly forms small hills and mounds in the study area. This lithology is readily distinguished from the volcanic lithologies due to its medium-coarse grained, equigranular texture. Strongly foliated and/or lineated varieties also occur along the margins of the larger bodies and as smaller isolated bodies. The mineralogy of this unit consists almost entirely of plagioclase partially altered to zoisite and sericite, and dark blue-green hornblende. Accessory phases include garnet and sulphides. Dikes of similar composition and equigranular texture are also present within the Gudå Formation, and Hersjø Formation. Several small bodies and one larger body occur

within Kjurudal and Reitan formations. Some of the bodies may be coeval with the mafic volcanism within the Fundsjø Group and thus may represent magma chambers. The complete replacement of original igneous pyroxene or hornblende by dark blue-green metamorphic hornblende indicates that the gabbro bodies were metamorphosed to amphibolite grade along with the surrounding country rocks (Mandeville, 1988).

## Meta-Quartz diorite

This lithology is commonly associated with the meta-gabbro and is composed of fine-coarse grained, grey to light grey, blastogranular textured to strongly foliated and/or lineated plagioclase + hornblende + quartz rock. Exposures east of the Reitan Station contain numerous elongated mafic xenoliths of possibly cogenetic gabbro. The mineralogy of the Meta-Quartz diorite consists of plagioclase, quartz, biotite, dark blue-green hornblende, and chlorite with accessory phases consisting of zoisite, sphene, epidote, and calcite. Bodies of Meta-Quartz diorite are present within the Gudå Formation and the nature of the contact is clearly intrusive. The Gudå Formation of this paper is extensively intruded by gabbro, diorite, and trondjhemite. There are perhaps a few generations of these intrusive rocks. At one locality along highway 30 to the west of Ålen, diorite, quartz diorite and trondjheimite - tonalite are mutually intrusive into the Gudå Fm. The more felsic varieties are predominant and appear to post date the more mafic dioritic varieties based on cross cutting relations. Meta-Quartz diorite is found along the periphery of the large meta-gabbro body in the vicinity of Reitan Station and is probably a late-stage differentiate of the gabbro.

## Trondjhemite

This lithology is readily distinguishable from the other intrusives by its extremely low modal amounts of mafic minerals and light color. Several textural varieties of this unit are present in the Ålen area. Fine-coarse grained, massive equigranular varieties are most common. Strongly foliated and/or lineated varieties are present mostly as dikes within the metasedimentary units, and also associated with the Meta-Gabbro. The mineralogy of these light colored intrusive rocks consists of plagioclase, quartz, and biotite, occasionally with accessory garnet. Structural overprinting relationships indicate that there are perhaps more than one generation of Trondjhemite in the Ålen area.

# Discussion

The Fundsjø Group as descibed above, consists of an approximately 4-5 km thick succession of metamorphosed thin bedded semipelites, quartz rich psammites, and calcareous schists, which exhibit gradational contacts with bi-modal, mafic dominated metavolcanics. The semipelites and psammites dominate the terrigenous clastic sediments, and the primary features preserved within them indicate deposition by turbidity currents. Notably lacking, or present in minor amounts (e.g. Sætersjø member of Kjurudal Fm.) in the terrigenous clastic portions of the Fundsjø Group, are coarse grained debris flows. High concentration sediment gravity flows are common in the proximal portion of submarine fans (Walker, 1984). There is also a general lack of channeling in the terrigenous clastic sequences which also suggests deposition mainly in the non-channeled lower (distal) fan portion of the submarine fan environment (Walker, 1984).

Volcanic activity was most likely submarine as indicated by facies association with clearly marine facies such as turbidites, and deep water marls. Features indicative of shallow marine volcanism, and/or eruption well above the pressure compensation level (Fisher, 1984) such as amygdule rich flow tops in basalt flows, and highly vessiculated material are absent from the best preserved sections. However, the presence of finely bedded (mm scale) mafic tuffs which most likely represent marine fallout and associated bedded pyroclastic deposits does

indicate that at least some of the volcanic activity was explosive. These explosions were most likely phreatomagmatic.

Grenne and Lagerblad (1985) have presented major, trace, and REE chemical data from amphibolites of the Fundsjø Group collected in the Meråker-Verdal area. They also recognize the bi-modal nature of the volcanics. They distinguish "type I" amphibolites (low in Fe and Ti) from "type II & III" amphibolites which have MORB affinities. The interpretation put forth by Grenne and Lagerblad (1985), based on the chemical data is that the "type I" amphibolites represent basalts generated in an immature island arc setting. They interpret the "type II & III" amphibolites as MORB type basalt generated during subsequent rifting of the immature arc. The stratigraphic relationship between the various types of amphibolites is not specified, so it is not possible to place these two possibly different metabasalt types in any chronologic framework. This makes it difficult to evaluate their interpretation. There is a great deal of scatter in the data as evidenced by the various trace element discrimination plots used. These authors also report that the amphibolites of the Fundsjø Group show a wide range in $SiO_2$ (ranging from basalt - andesite). Whether this range in silica content reflects primary variation in magma compositions or $SiO_2$ mobilization during metamorphism is inconclusive. Unfortunately, major elements except for Ti and possibly P (Gottfried et. al., 1978, Garcia, 1978) can suffer significant modification during alteration and low grade metamorphism. This problem may be worse at higher metamorphic grades.

Grenne and Lagerblad (1985) stated that the island arc interpretation was supported by intercalated pyroclastic, volcaniclastic, and sedimentary material which partly consists of shallow water deposits. They do not specify the criteria used to distinguish some of the sediment as shallow water deposits.

The turbidite facies preserved in the terrigenous clastic formations of the Fundsjø Group indicate that deep water sedimentation was dominant throughout the sequence. This is also reflected by the terrigenous clastic material intercalated with the volcanic formations.

Criteria proposed by Garcia (1978) for the recognition of ancient volcanic arc complexes include: 1) predominant pyroclastic texture of volcanic rocks, and 2) thick sequences of

volcaniclastic rocks. Both of these criteria have a high probability of being preserved in ancient sequences. These two criteria were used by Grenne and Lagerblad (1985) in support of the immature island arc interpretation. Garcia (1978) reports that in the Marianas where volcanism is tholeiitic, 90% of the volcanic rock is of fragmental textural types. Fragmental pyroclastic rocks are commonly preserved in the Fundsjø Group in the Ålen area, but they do not comprise 90% of the volcanic rocks. Coarse pyroclastic rocks (e.g. tuff breccias, pyroclastic breccias) are present in minor amounts. A significant portion of the Hersjø Fm is composed of porphyritic sills or fine grained sills which this author recognizes as contemporaneous with the pyroclastic sequences. Olesen et. al., (1973) also recognized a close association of the porphyritic diabase with pillow lavas of the Fundsjø Group in the Tydal area and interpreted these as shallow level intrusives. These could represent the subvolcanic complex (Cas, 1983) of an arc, but in the Ålen area there is no increase in the proportion of coarse pyroclastic rocks preserved within the Reitan Fm. stratigraphically higher in the section. Fine grained diabase and minor porphyritic diabase sills compose a substantial portion of this formation. Coarse pyroclastic rocks are present in this formation but are not dominant. The addition of approximately 1.5-2 km of overlying material (represented by the Kjurudal Fm. and lower portion of the Reitan Fm.) apparently did not cause a change in the style of volcanism (pyroclastic dominated) as might be expected near a shoaling arc volcano (Carey and Sigurdsson, 1984, Busby-Spera, 1988).

The abundance of quartz rich terrigenous clastic material within the Fundsjø Group indicates proximity to a continental source (Cas and Wright, 1987). This is also supported by the calcareous beds present throughout the sequence and interpreted as deep water marls/resedimented carbonate. No metamorphosed equivalents of pelagic sediments such as cherts, or Fe rich abyssal clays, are present in the Fundsjø Group in the Ålen area. This indicates the dominance of continent derived terrigenous clastic sedimentation in the sequence (Karig and Moore, 1975, Leitch, 1984, Klein, 1985).

The most characteristic feature of volcanogenic sedimentation in an island arc setting (including immature arcs) is the development of a thick volcaniclastic apron (Karig and Moore,

1975, Carey and Sigurdsson, 1984, Busby-Spera, 1988). Coarse tuff breccia and pyroclastic breccia facies are more common in the proximal portion of the apron whereas the more distal portions are composed mostly of finer grained volcaniclastic rocks (Carey and Sigurdsson, 1984, Bogen, 1985, Busby-Spera, 1988). As noted previously there is no increase in the relative proportion of coarse pyroclastic material from the Hersjø Formation to the stratigraphically higher Reitan Formation. This appears to be inconsistent with the build up of a submergent arc volcano, or the progradation of a volcaniclastic apron as a result of renewed volcanic activity.

The development history exhibited by present day marginal basins of the Southwest Pacific (e.g. Havre Trough, Taupo Rotorua Depression) indicates that rifting in the marginal basins of the Southwest Pacific commenced within thick crust (Leitch, 1984) in either continental or island arc settings, and not on thin oceanic crust. A seismic refraction profile across the Colville ridge (remnant arc) and Kermadec arc presented by Karig (1970), indicates that the crust of the Colville ridge is approximately 15 km thick. If 8 out of the 15 km of material represents typical oceanic crust then approximately 7 km of material could be attributed to the formation of the arc block (Cas and Wright, 1987). This arc block would consist of a variably deformed sequence of volcanic/volcaniclastic rocks, pelagic sediments, and associated mafic intrusive complex. The approximate thickness of the entire Fundsjø Group from the Gudå Fm. to the Slågrov Fm. in the Ålen area is 4-5 km. Terrigenous clastic material apparently composes 50-60% of the sequence. This seems inconsistent with the volcanic/volcaniclastic-subvolcanic intrusive complex dominated crust of a rifted remnant arc setting.

The bi-modal volcanism represented by the Hersjø and Reitan formations is indicative of initial ocean basin rifting whereas back-arc basins open adjacent to or within volcanic chains (Cas and Wright, 1987) dominated by basic-intermediate rocks of arc tholeiite or calc-alkaline affinities. The basement underlying the Fundsjø Group at the time of its accumulation was most likely a transitional attenuated continental crust. The felsic volcanics present within the Fundsjø Group may be the result of fusion of the lower crust due to heat supplied from rising

basaltic magmas. Alternatively, the primary composition of the felsic volcanics may have been of alkalic affinity and the result of differentiation from parental magmas of alkalic affinity.

The mafic dominated bi-modal volcanism within the Fundsjø Group can be contrasted with the felsic dominated bi-modal volcanism of the Taupo Rotorua Depression in New Zealand. Volcanism in the Taupo Rotorua Depression is dominated by rhyolitic eruptions associated with the development of an ensialic marginal basin (Cole, 1984, Lewis and Pantin, 1984). Crustal thickness flanking the Taupo Rotorua Depression is estimated to be 30-35 km (Thomson and Evison, 1962) from seismic refraction data.

Seismic data from modern passive margins on the Galicia-Portugal, and Northern Biscay margins (Chenet et. al., 1982) and the passive margin off eastern Canada (Keen and deVoogd, 1988) have shown the deep structure of the rifted margins. In both of these studies, thin continental crust approximately 12 km thick is present near the continental-oceanic crust boundary. The attenuation of the continental crust is the result of extension presumed to have taken place during the rifting process (Falvey, 1974, MacKenzie, 1978, Royden and Keen, 1980, Chenet et. al., 1982). The ratio of the crustal thickness of a point on the margin relative to the thickness of the crust of the adjacent continent was defined (Chenet et. al., 1982) as the thinning ratio, $\beta$. The value of $\beta$ for the Galicia-Portugal margin which includes the post-rift sediments as part of this crust was 3. A theoretical model developed by Cochran (1983) to take into account the effect of lateral heat loss from the rifted area during an extended rift phase indicates that the syn-rift portion of subsidence is increased relative to the post-rift subsidence. The model of Cochran (1983) also shows that for a rifting event of 50 m.y. duration and $\beta$ value of 2, up to 4 km of subsidence is possible. This model also indicates that the portion of the stratigraphic column composed of syn-rift deposits is increased relative to that of post-rift deposits.

The approximately 3 km thick sequence composed of the Gudå Fm. through the Reitan Fm. most likely represents a syn-rift sequence which accumulated during an extended rift phase. It is also possible that the Slågrov Fm. accumulated during the rift phase but the rift to drift transition is placed above the Reitan Fm. as a conservative estimate of the syn-rift sequence.

The absence of rift basin deposits of subaerial-shallow marine facies within the Fundsjø Group is probably due to the initiation of sedimentation seaward of the hinge zone (Wehr and Glover, 1985). The rift phase could have begun during the Late Cambrian due to the minimum age constraint placed on the volcanics of the Hersjø Fm. by the *Dictyonema* schist occurrence at Nordaunevol. Perhaps the major transgression recorded in the platform and foreland sequence (Bruton et. al., 1985) of the Baltoscandian margin during the Tremodoc, reflects a syn-rift to post-rift phase of tectonic subsidence (Cochran, 1983) associated with a prolonged rift phase and thermal relaxation of the rift area. This may be supported by the presence of bi-modal volcanics within the Gudå Fm. The rift phase could have continued into the early Middle Ordovician.

## Tectonic Implications

The primary features preserved within the Fundsjø Group and the overall characteristics of the succession are consistent with a rifted continental margin setting. The proposed correlation of the *Dictyonema* schist at the Nordaunevol locality with the Kjurudal Fm. of this paper also suggests that the lowermost unit of the Fundsjø Group (Gudå Fm.) may be of late Cambrian age. The presence of bi-modal, mafic dominated volcanics in this formation and in the stratigraphically overlying Hersjø and Reitan formations is interpreted to be representative of a prolongued rifting event. This rifting event most likely began at approximately 665 ± 10 Ma. as indicated by the Ar/Ar and K/Ar study by Claesson and Roddick (1983) on the diabase dikes of the Särv Nappe. As mentioned in the discussion above, the effect of a prolongued rifting event is to increase the thickness of the syn-rift deposits relative to the post-rift deposits (Cochran, 1983). The ca. 4-5 km thick succession represented by the Fundsjø Group as defined herein, was more likely to have accumulated during a prolongued rifting event on thinned continental crust as illustrated in Figure 6. This interpretation differs markedly from the immature, rifted island arc interpretation (Grenne and Lagerblad, 1985) for the Fundsjø

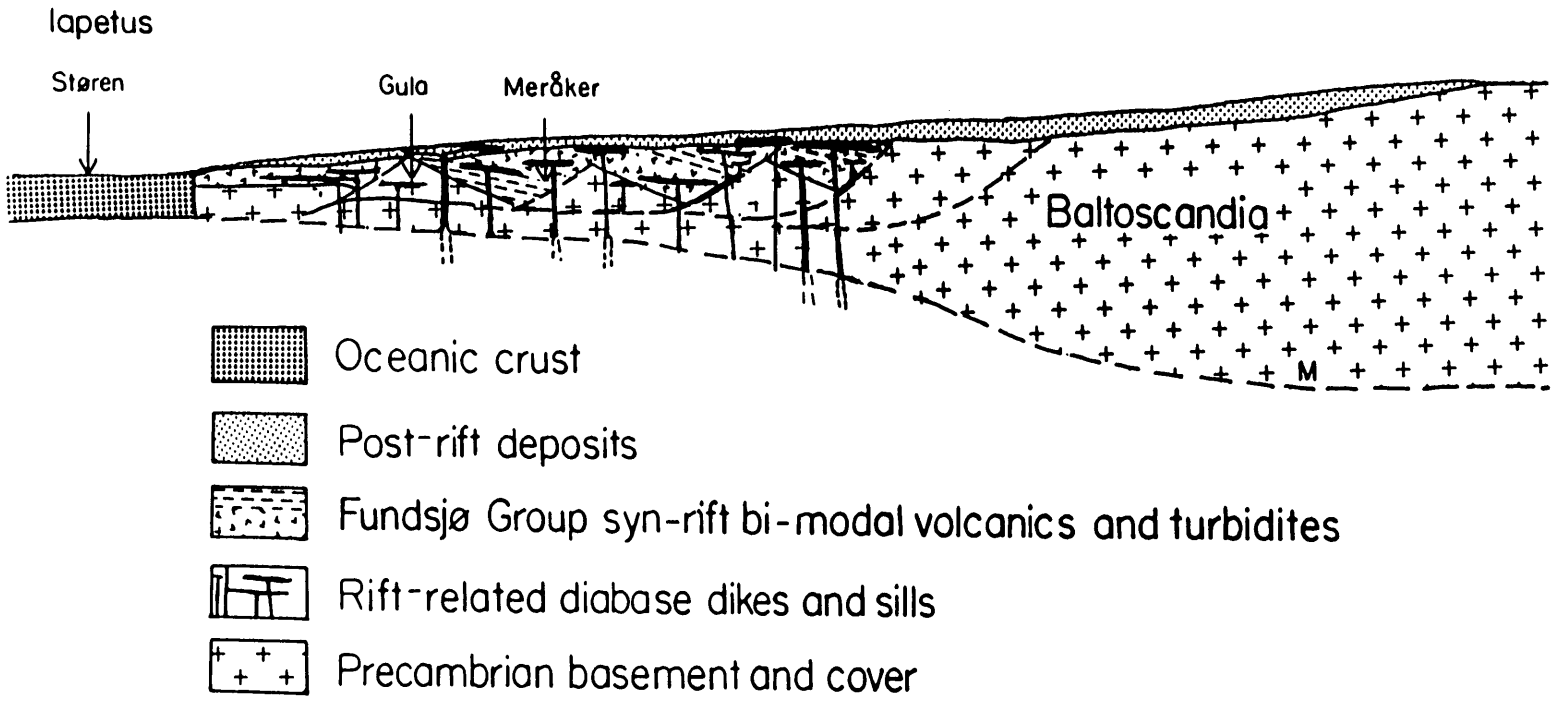


Figure 6. Illustration of the rifted margin tectonic setting interpreted for the Fundsjø Group of the Meråker Nappe.

Group which has been incorporated in current tectonic models (Stephens and Gee, 1985, Roberts et. al., 1985) for the development of the central Scandinavian Caledonides.

No lower Ordovician fossils of North American affinity have been found within the Fundsjø Group at present. Therefore, there does not appear to be any compelling reason to place the tectonic unit now represented by the Meråker Nappe proximal to the Laurentian margin as indicated by Stephens and Gee, (1985,) (the Gjersvik-Meråker "main magmatic arc"). Furthermore, the presence of Llandovery black shales (Getz, 1890) in the Slågan Group (Wolff, 1979) which pass up into a coarsening upwards greywacke succession is similar to the sequence of similar age present in the Baltoscandian margin (Stephens and Gee, 1985).

The tectonic model proposed by Roberts et. al., (1985) recognizes the Fundsjø Group as an immature ensimatic volcanic arc, partly of Tremadocian age developed during the initial stages of Iapetus ocean closure. In contrast to the Roberts et. al., (1985) model, the model proposed here is that the Fundsjø Group represents continued Iapetus ocean opening. This rifting phase most likely came to a close by mid-Arenig time due to mature arc/marginal basin collision with the outermost portion of the Baltoscandian margin.

# Conclusions

1) The mapping shown in Fig. 5 and Plate 1 indicates that the Fundsjø Group defined herein, is of Tremodocian-Lower Ordovician age and is inverted. This mapping also indicates that the *Dictyonema* schist occurrence at Nordaunevol is probably correlative with the Kjurudal Fm. of this paper. This point requires additional mapping.

2) The Gudå Fm. of this paper has a gradational upper contact with the Hersjø Fm., despite localized complication due to a bedding plane fault (tectonic slide of Hutton, 1981). The lithofacies present in the Gudå Fm as defined herein do not contrast markedly with those contained within the overlying formations of the Fundsjø Group to justify a separate group status. The Gudå Fm., therefore, is included as the basal formation of the Fundsjø Group as redefined in this paper.

3) The lithofacies and primary features preserved within the Fundsjø Group indicate that the sequence accumulated in a rift that led to the opening of an ocean basin. This is represented by a 4-5 km thick sequence dominated by deep water terrigenous clastics which exhibit gradational contacts with mafic dominated, bi-modal volcanics.

4) The Gudå, Hersjø, Kjurudal, and Reitan formations represent an approximately 3 km thick accumulation of syn-rift deposits. Initial sedimentation took place seaward of the hinge zone and was dominated by turbidite deposits. Volcanism was submarine as indicated by facies association with marine lithofacies, and lack of shallow marine-subaerial features. Explosions were of phreatomagmatic origin. Much of the metavolcanic sequence is composed of concordant sills contemporaneous with the bedded pyroclastic deposits, and emplaced at shallow levels into wet pyroclastics and less commonly, terrigenous clastic sediments.

**Tectonics of the Ålen Area, Central Norway: II Metamorphism and Deformation within the Fundsjø Group of the Meråker Nappe, Ålen Area, Central Norway**

by

Charles W. Mandeville

Lynn Glover III, Chairman

Geological Sciences

(Abstract)

Detailed mapping within the Fundsjø Group of the Meråker Nappe, Ålen area central Norway indicates downward facing structures and general inversion of the stratigraphic section. Evidence derived from overprinting relationships and structural facing indicates that the stratigraphy was overturned prior to the second phase of folding. This second fold phase resulted in the formation of macroscopic (map scale) reclined folds. Parallelism of $F_2$ axes and mineral stretching lineation indicates probable rotation of fold axes into the ESE transport direction.

The $D_1$ - $D_2$ deformations probably represents a continuum as evidenced by continued growth of lower-middle amphibolite facies mineral assemblages throughout the deformation. A relatively static period represented by post-tectonic porphyroblast growth and thermal annealing of strain features separates $D_1$ - $D_2$ from a late stage deformation, $D_3$, represented by microfaults, kink folds, cataclasite, and pseudotachylite.

Metamorphic mineral assemblages in the Fundsjø Group indicate that the metamorphism was of lower-middle amphibolite, medium pressure facies throughout the study area. Post-tectonic garnet-biotite pairs yield 530° - 590° C temperatures. A pressure estimate derived from the QGAP geobarometer of 8.0 kb was obtained and indicates an overburden of 26 - 28 km. Tectonic thickening as a result of Caledonian orogenesis could account for up to 15 km of this overburden.

# Introduction

The development history of a substantial portion of the central- southern Scandinavian Caledonides is recorded by the structures and metamorphic mineral assemblages contained within the nappes of the Trondheim Nappe Complex (Guezou, 1978, Gee et. al., 1985). This study was concentrated within the Fundsjø Group (Wolff, 1973, 1979, Mandeville, 1988) of the Meråker Nappe (Wolff and Roberts, 1980, Roberts and Wolff, 1981, Gee et. al., 1985) Sør Trøndelag Norway (Fig. 1). The emphasis of this study was the examination of deformational features and metamorphic mineral assemblages contained within a ca. 4-5 km thick succession dominated by metamorphosed semipelites - psammites in gradational contact with bi-modal, mafic dominated volcanics (Mandeville, 1988). The Fundsjø Group consists (from oldest to youngest) of the Gudå Fm., Hersjø Fm., Kjurudal Fm., Reitan Fm., and Slågrov Fm.

The Meråker Nappe (Wolff and Roberts, 1980, Roberts and Wolff, 1981) forms the eastern portion (Fig. 1) of the Trondheim Nappe Complex (Guezou, 1978, Gee et. al., 1985). The Upper Allochthon (Gee et. al., 1985) of the central-southern portion of the Scandinavian Caledonides consists largely of the various nappes of the Trondheim Nappe Complex. Gross similarities in the stratigaphies of the Støren Nappe, which occurs to the west of the Gula Nappe Complex (Roberts and Wolff, 1981) (Fig. 1) and the Meråker Nappe in the east, has led to various interpretations of the regional structure. These interpretations range from that of a large mush-

room shaped antiform (Roberts and Wolff, 1981) to a large recumbent fold (Rui, 1972), to a series of imbricate thrusts (Gee and Zachrisson, 1974, Guezou, 1977, Gee, 1978). The interpretation of the regional structure represented by the Trondheim Nappe Complex is still controversial (Gee et.al., 1985). A review of the various interpretations is provided by Wolff (1967) and Gee et. al., (1985). Moreover, recent studies (Grenne and Lagerblad, 1985, Lagerblad, 1984, Nilsen, 1983, Horne, 1979, Hardenby, 1983, Krill, 1980) indicate that there is some asymmetry to the Trondheim Nappe Complex. This asymmetry is reflected by the difference in the metamorphic grade (Hardenby et. al., 1981) between the Støren Group greenstones (Grenne and Lagerblad, 1985) forming the lower portion of Støren Nappe in the west, and the Fundsjø Group which comprises the lower portion of the Meråker Nappe in the east (Fig. 1). Differences in the nature of the greenstone sequences as represented by the Støren Group and Fundsjø Group also exist. The greenstones of the Støren Group are mafic dominated and are of MORB chemical affinity, whereas, the amphibolites of the Fundsjø Group exhibit greater chemical variation, and the sequence is mafic dominated and bi-modal (Grenne and Lagerblad, 1985).

The stratigraphy of the Meråker Nappe (Wolff, 1973, 1979, Hardenby, 1980) is composed (from oldest to youngest) of the Fundsjø Group, the Sulåmo Group (a mixed volcanic and sedimentary sequence), the Kjøhaugan Group (a dominantly sedimentary sequence), and the Slågan and Liafjellet Groups (composed largely of metagreywackes and conglomerates).

A detailed structural and metamorphic study was conducted in the Fundsjø Group in order to resolve two fundamental questions concerning the stratigraphy: 1) Is the stratigraphy inverted, and if so, during which deformation phase did the overturning occur? 2) Does a structural break exist between the Hersjø Fm. and stratigraphically overlying Kjurudal Fm. similar to that reported to occur (Hardenby, 1983) at the boundary between the Fundsjø and Sulåmo Groups? This structural break occurs at the stratigraphic level of the Lille Fundsjø Conglomerate (Chaloupsky and Fediuk, 1967, Wolff, 1973) which contains pebbles derived from the Fundsjø Group and marks an unconformity between the Fundsjø Group and the Sulåmo Group. Evaluation of the metamorphic grade within the Meråker Nappe in the Ålen area, was neces-

sary to confirm whether a decrease in metamorphic grade is present in the eastern portion of the study area. A decrease in metamorphic grade was reported by Lagerblad (1981, 1984) from the Fundsjø Group to the Sulåmo Group in the northern portion of the Meråker Nappe in the Inndalen Valley north of lake Færen (Fig. 2).

Ultimately, the determination of metamorphic grade and deformation history can be used to group nappes which share similar development histories (Gula Nappe, and Meråker Nappe, as in Hardenby et. al., 1981, Lagerblad, 1981, 1984). Complete characterization of metamorphism and deformation within the Fundsjø Group is an integral step towards the generation of structural models which account for the development of the Trondheim Nappe Complex. Furthermore, models of the tectonic evolution of the Trondheim Nappe Complex must be constrained by the metamorphism and deformation exhibited by the various nappes.

# Metamorphism

Regional metamorphism in the Ålen area is of the Barrovian (Barrow, 1912, Read, 1952) or "medium-pressure" (Miyashiro, 1973) type. This is indicated by the relatively ubiquitous appearance of zoned almandine garnet, the presence of staurolite and kyanite in the semipelitic- quartzo-feldspathic lithologies and absence of andalusite and cordierite. Notably lacking within both metabasaltic and semipelitic lithologies, are high pressure mineral phases such as jadeite, glaucophane, and lawsonite (Miyashiro, 1973, Turner, 1981). The thermal peak associated with regional metamorphism is likely to have roughly coincided with the 426 $\pm^{8}/_{2}$ Ma zircon U-Pb age (Wilson, et. al., 1983) of late stage quartz bearing ferrosyenites within the Fongen-Hyllingen layered basic complex (Wilson, 1985). The intrusion of more mafic gabbroic magmas took place prior to 426 Ma. and was the likely heat source for the development of the contact aureole. The contact aureole was overprinted by regional metamorphism on the western side of the layered intrusion (Olesen et. al., 1973). Xenoliths of foliated and folded country rock are present within the layered intrusive (Wilson and Pederson, 1981) which suggests the regional metamorphism commenced prior to emplacement of the mafic intrusive (Olesen et. al., 1973). The Rb-Sr whole rock age of 405 ±9 Ma (Wilson and Pederson, 1981) has been reinterpreted by Wilson (1985) as representing a cooling age after amphibolite facies regional metamorphism. Olesen et. al., (1973) report polymorphic reaction of contact aureole

andalusite → kyanite from the western side of the Fongen-Hyllingen layered intrusive complex, which suggests that regional metamorphism overprints the contact metamorphism.

Two phases of prograde regional metamorphism, $M_1$ and $M_2$, have been distinguished within the Fundsjø Group of the Ålen area. A third metamorphism $M_3$, is a retrograde event that appears to be associated with late deformation. The $M_1$ and $M_2$ events are of lower to middle amphibolite, medium pressure facies. Quite possibly, the $M_1$ and $M_2$ events represent a continuum such that there is really only one protracted, prograde metamorphic event. Until geochronologic evidence is obtained from this area which confirms a significant time period between $M_1$ and $M_2$ it is best to refer to $M_1$ - $M_2$ collectively as $M_{1-2}$ due to the lack of evidence for significant changes in pressure and temperature conditions. However, the age of the Fundsjø Group (Tremadocian - Lower Ordovician) implied by new mapping in the Ålen area (Mandeville, 1988) certainly allows for the possibility of a pre-Middle Ordovician metamorphism and deformation of the Fundsjø Group as reported by Lagerblad (1981, 1984) and Hardenby et. al., (1981). The $M_{1-2}$ event appears to have spanned both the $D_1$ and $D_2$ deformations. A summary of metamorphic and structural features present in the Fundsjø Group in the Ålen area is provided in Table 2.

## $M_1$ Mineral Assemblages

Within the semipelitic to psammitic schists of the Gudå Formation, garnet, staurolite, and kyanite porphyroblasts are commonly observed. The mineral assemblage, quartz, muscovite, biotite, garnet, staurolite, kyanite ± chlorite ± ilmenite ± graphite within the semipelitic schists of the Gudå Formation is characteristic of middle amphibolite facies regional metamorphism (Miyashiro, 1973, Turner, 1981).

The $M_1$ assemblage in the semipelitic to psammitic rocks within the Kjurudal and Slågrov formations is quartz, biotite, chlorite, garnet, ± muscovite ± epidote/zoisite ± graphite ± ilmenite. However, staurolite and kyanite porphyroblasts are absent from the semipelitic and

Table 2 Summary of structural features and metamorphism

| Deformation event | Surfaces S | Folds F | Lineations L | Metamorphism M |
|---|---|---|---|---|
| $D_1$ | $S_1$; penetrative schistosity parallel to $S_0$ (bedding) and axial planar to mesoscopic isoclinal folds, extensive development of layer parallel quartz veins | $F_1$; rare mesoscopic isoclinal folds, WNW trending axes | $L_1$; weak hornblende lineation in $S_1$, rare $S_0/S_1$ intersection lineation | $M_1$; lower amphibolite -middle amphibolite |
| $D_2$ | $S_2$; spaced cleavage, axial planar crenulation cleavage which transposes $S_1$, rarely a continuous cleavage | $F_2$; predominant mesoscopic open-tight folds, WNW-WSW trending, moderately plunging axes, mean orientation of axial surfaces 351°/38°W | $L_2$; intersection lineation of $S_1$ continuous and $S_2$ spaced cleavage, crenulation lineation on $S_1$, mineral lineation defined by hornblende and/or elongated plagioclase and quartz grains, all above parallel to $F_2$ fold axes | $M_2$; lower amphibolite -middle amphibolite |
| Post $D_2$ - Pre $D_3$ static event | | | | $M_2$; thermal peak, static garnet, biotite, kyanite and staurolite porphyroblast growth, thermal annealing and strain recovery; lower amphibolite -middle amphibolite |
| $D_3$ | $S_3$; rare spaced cleavage, microfaults, generally NS striking, commonly associated with pseudotachylite | $F_3$; NS trending, shallow plunging, minor kink folds | $L_3$; crenulation lineation on $S_1/S_2$ surfaces | $M_3$; localized retrograde greenschist facies metamorphism, replacement of garnet by chlorite |

psammitic schists of the Kjurudal and Slågrov formations. This may be due to low aluminum content, as these minerals are absent from even the most muscovite rich samples. This might also be due to a decrease in $M_1$ metamorphic grade from west (Gudå Fm.) to east (Kjurudal Fm. and Slågrov Fm.).

The assemblage within the impure marble and calc-silicate schists occurring in the Hersjø Fm. (Fhm), and Reitan Fm. (Frm), is calcite, quartz, zoisite (less commonly epidote), tremolite, plagioclase, biotite, ± chlorite ± pyrite ± ilmenite ± sphene. The assemblage calcite, quartz, tremolite, zoisite (or epidote) ± grossularite is also found in the calcareous nodules of the Gudå Formation and was probably developed during the $M_1$ metamorphism. The stability of the hydrous phase, zoisite, well into the middle amphibolite facies (as indicated by the surrounding semipelitic schists of the Gudå Fm.) may be due to high $pH_2O$ as a result of dehydration reactions taking place in the surrounding schists. If the $H_2O$ rich fluid had moved into the calcareous nodule it could have had a buffering effect on a "type 3" dehydration reaction (Kerrick, 1974) such as:

$$4 \text{ Zoisite} + 7 \text{ Quartz} \rightarrow \text{Grossular} + 5 \text{ Anorthite} + 4H_2O$$

thereby stabilizing the hydrous phase zoisite, to higher temperature.

The $M_1$ assembleges within the metamorphosed mafic tuffs of the Hersjø Fm. and Reitan Fm. are similar and consist predominantly of plagioclase (oligoclase), blue-green hornblende, and chlorite, ± ilmenite ± epidote/zoisite. Electron microprobe traverses of several amphiboles within a few fine grained amphibolites of the Hersjø formation reveal magnesio-hornblende cores grading out to ferro pargasitic - ferro edenitic hornblende rims (classification Leake (1978)). The plagioclase in equilibrium with these amphibole cores is likely to have been in the oligoclase range although plagioclase inclusions are relatively rare. These amphiboles are blue-green to dark blue-green in plane light and may show slight indication of zoning. Amphiboles within the various meta-gabbro and meta-quartz diorite bodies throughout the field area are similar in color to those described above. It is likely that these are the result of $M_1$ metamorphism of the gabbro and quartz diorite intrusives. No relict igneous pyroxene or hornblende phenocrysts have been identified in any of the intrusive

rocks. Quite commonly, the meta-gabbro and meta-quartz diorite intrusives exhibit blasto-hypidiomorphic granular to blasto-ophitic textures, where not strongly tectonized. Relict igneous plagioclase phenocrysts are commonly replaced by zoisite, quartz and oligoclase. These features indicate that some of the gabbro and quartz diorite occurring in the Ålen area was probably metamorphosed during $M_1$ and that some meta-gabbro and meta-quartz diorite may represent magma chambers coeval with Hersjø Fm. or Reitan Fm. shallow intrusive and/or extrusive activity. Most certainly, all of the gabbro and quartz diorite bodies were metamorphosed by the end of $M_{1-2}$ and the close of $D_2$

## $M_2$ Assemblages

The $M_2$ assemblage in the semipelitic to quartzo-feldspathic schists of the Gudå Fm. is quartz, muscovite, biotite, garnet, staurolite, kyanite ± chlorite ± ilmenite ± graphite. These phases are present in the $M_1$ assemblages and indicate continued growth of middle amphibolite facies assemblages in $M_2$. The $M_2$ assemblages are distinguished from the $M_1$ assemblages on textural criteria. Porphyroblasts of amphibolite facies indicator minerals which postdate the $D_2$ deformation can be distinguished from those which are likely to have grown during $D_1$. The assemblages in two samples from the Gudå Fm. used for thermobarometry, CM87-495 and LG86-11D, (See Fig. 7 and Appendix A for map locations) are plotted in their respective AKFM diagrams projected from quartz, muscovite, plagioclase, ilmenite, and $H_2O$ excess (Figures 8a & 8b) (Thompson, 1957). The assemblages present within the semipelitic to quartzo-feldspathic schists of the Kjurudal and Slågrov formations are: 1) quartz, biotite, muscovite, chlorite, almandine garnet, oligoclase ($An_{20}$- $An_{27}$) ± epidote ± zoisite ± graphite ± ilmenite (2) quartz, biotite, chlorite, muscovite, zoisite ± oligoclase ± almandine garnet (3) quartz, biotite, chlorite, almandine garnet, oligiclase ± epidote ± zoisite ± ilmenite. The assemblage in sample CM87-793 from the Kjurudal Fm, which was used for thermometry, (See Fig. 7 and Appendix A for map location) is plotted in

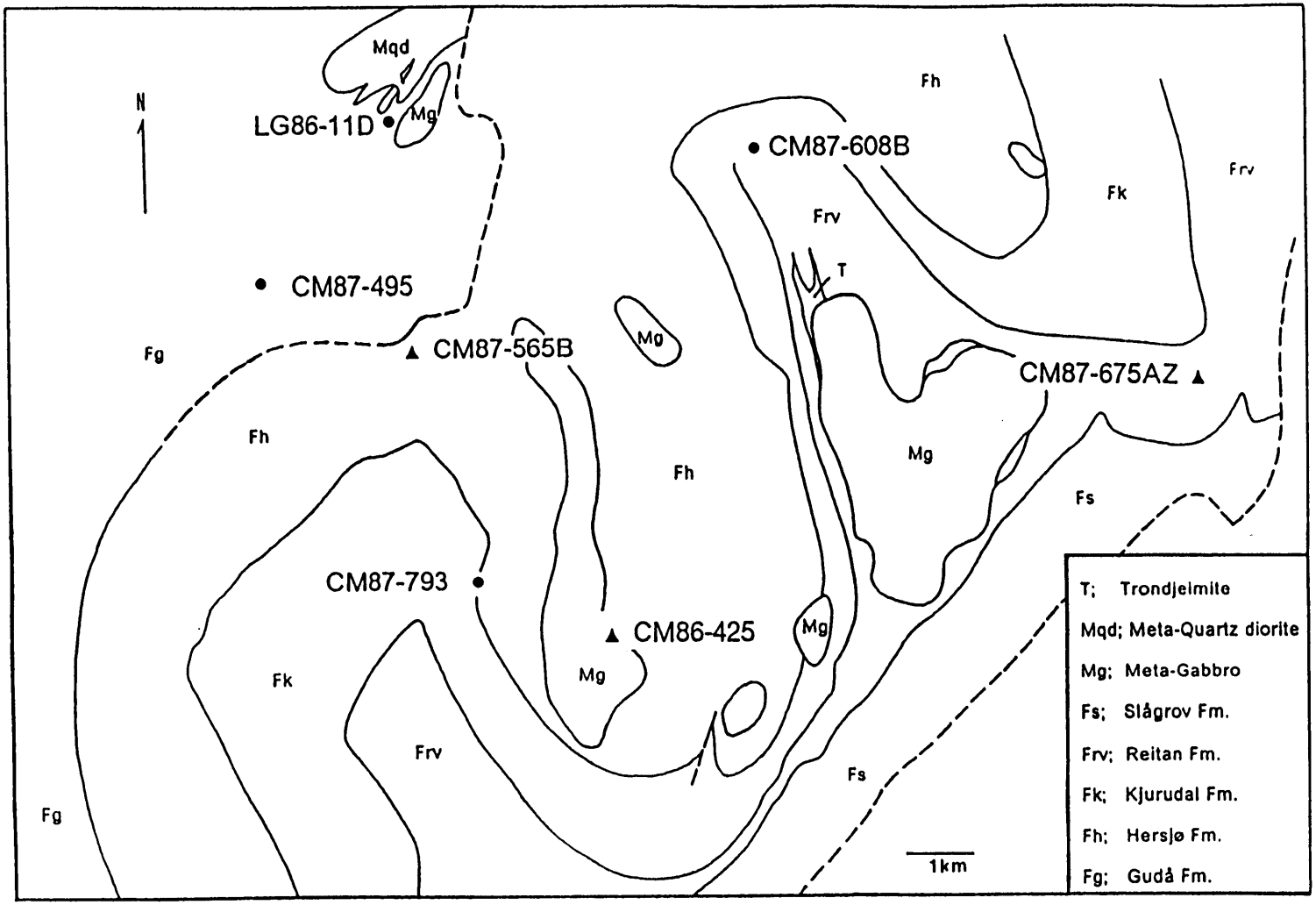


Figure 7. Simplified sample location map for samples used in metamorphic study. Solid triangles indicate mafic rocks, solid circles indicate semipelitic - psammitic schists.

Figure 8. AKFM projections of mineral assemblages in semipelitic - psammitic schists used for thermobarometry. Representative garnet rim compositions and average matrix biotite compositions are plotted. (a) mineral assemblage in CM87-495, (b) mineral assemblage in LG86-11D, (c) mineral assemblage in CM87-793.

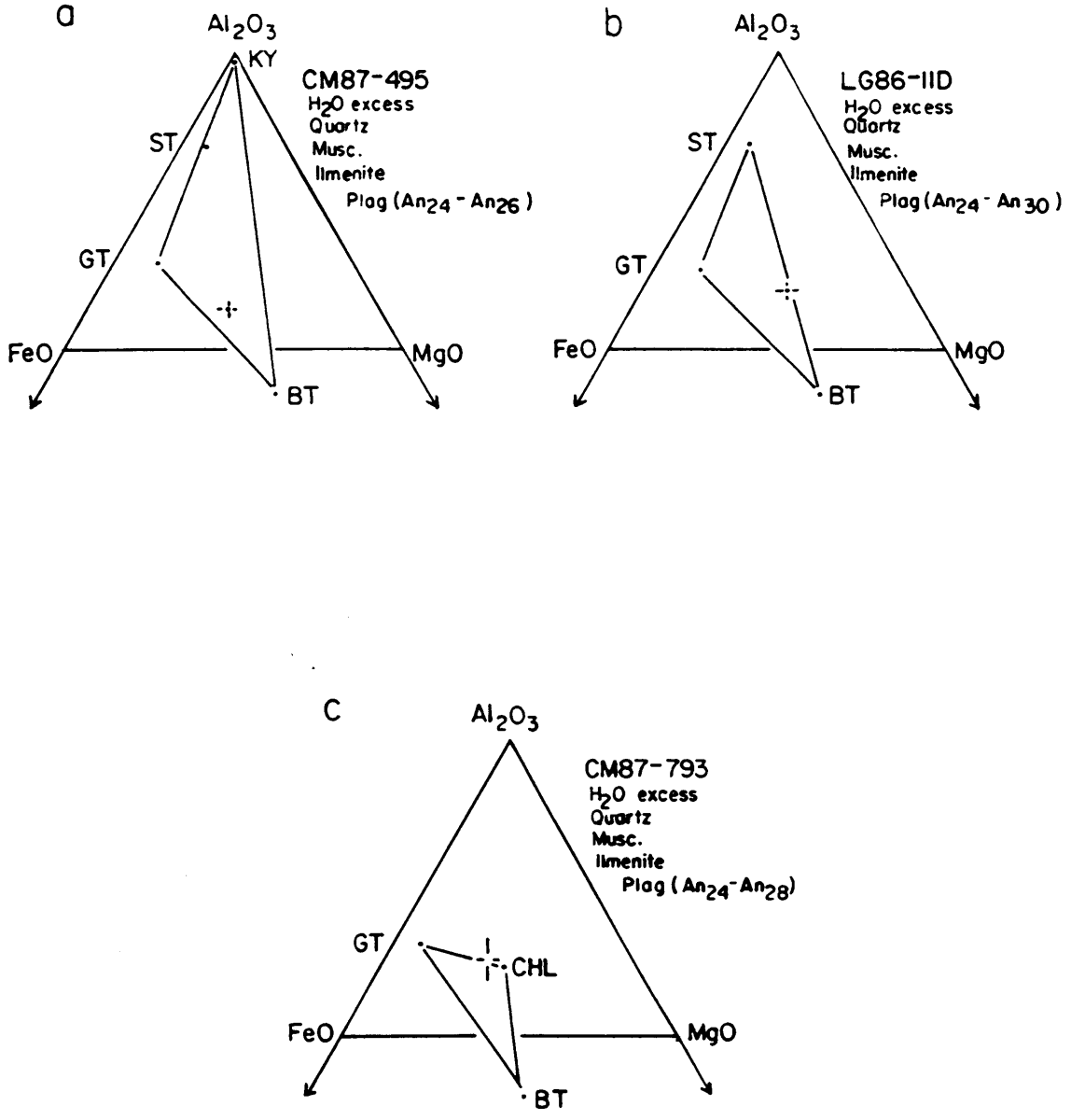


-┼- = Calculated bulk composition of sample

an AFM (Thompson, 1957) diagram projected from quartz, muscovite, plagioclase, ilmenite, and $H_2O$ excess (Fig. 8c). Sample CM87-608B (See Fig. 7 and Appendix A for map location) from the Kjurudal Fm. which was used for thermometry contains no modal muscovite. The assemblage in + chlorite+ garnet + epidote + zoisite + ilmenite. These assemblages within the Kjurudal and Slågrov formations also lack $M_2$ staurolite and kyanite possibly for the same reasons postulated to explain the absence of these phases from the $M_1$ assemblages in these formations. A preliminary investigation utilizing the garnet-biotite geothermometer (Thompson, 1976, Ferry and Spear, 1978) was undertaken in order to determine whether metamorphic temperature estimates would indicate an $M_2$ gradient across the field area (temperatures higher in the west to lower in the east) possibly accounting for the absence of staurolite and kyanite in the eastern portion of the field area. Acquisition of quantitative temperature data from a few samples in various parts of the field area was undertaken in order to resolve this problem. Assesment of metamorphic grade in mafic schists (Laird and Albee, 1981) of the study area was accomplished by obtaining mineral composition data from these types of rocks. Mineral compositon data from a few samples of fine grained mafic schists from the western to eastern portion of the field area were obtained so as to monitor whether somewhat more continuous modal and mineral compositional changes have taken place in the mafic rocks from the east side of the field area to the west.

The investigation was restricted to the $M_2$ mineral assemblages within the semipelitic-quartzo-feldspathic schists and mafic schists for two reasons. First, it is unlikely that the matrix biotite in the semipelitic to psammitic rocks retained its $M_1$ composition. Temperature estimates for these rocks are determined from the temperature-dependent Fe-Mg partitioning between garnet and biotite as empirically calibrated by Thompson (1976) and experimentally calibrated by Ferry and Spear (1978). Garnet rim compositions were used for thermometry because these are most likely to be in to be in equilibrium with matrix biotite (Tracy et. al., 1976). The $M_2$ post-kinematic garnets analyzed by electron microprobe and used in subsequent thermobarometric calculations exhibit compositional zoning profiles consistent with prograde growth (Fig. 9). Second, it is no longer possible to determine the composition of the

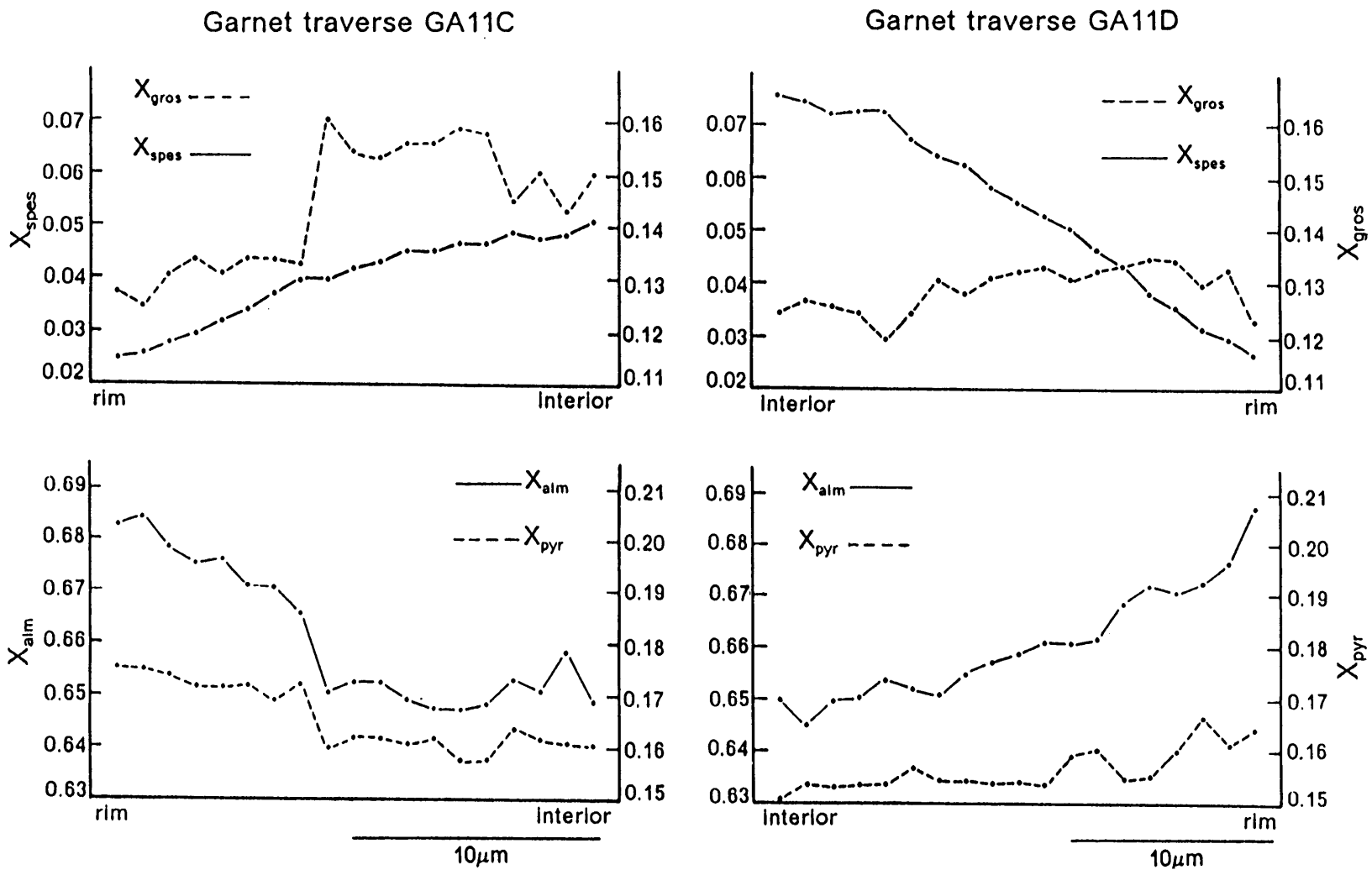


Figure 9. Electron microprobe traverses GA11C and GA11D of garnet from sample LG86-11D. Compositional profiles are consistent with prograde garnet growth.

matrix plagioclase that was likely to be in equilibrium with calcic amphibole of $M_1$ in the mafic schists because of the lack of plagioclase inclusions in the relatively small (.15 mm long) amphiboles. The matrix plagioclase compositions that have been determined by electron microprobe analysis most likely represent the $M_2$ metamorphic peak. These plagioclase grains are homogenous in composition as indicated by microprobe traverses.

Microprobe traverses across amphiboles from three fine grained amphibolites indicate a slight increase in Al, Na, and Fe towards the rims with relatively Mg- and Si-rich cores. Two of these traverses, one from sample CM87-565B and one from sample CM86-425 (See Fig. 7 and Appendix A for map locations) are shown in Figures 10a and 10b respectively. The error bars represent the $2\sigma$ level for each of the elements, and are shown as vertical bars along a few of the data points in each traverse to avoid clutter. These error bars were derived from 50 analyses of a Kakanui hornblende reference standard conducted during the same microprobe session. The chemical zonation exhibited by the amphiboles from CM87-565B and CM86-425 is of larger magnitude than the error bars associated with the microprobe analyses. This chemical zonation therefore appears to be a real feature which cannot be attributed to microprobe error. Similar changes in amphibole composition have been observed within experimentally synthesized amphiboles (Spear, 1981) with increasing temperature under constant fluid pressure and on a given oxygen fugacity buffer. Laird (1980) and Laird and Albee (1981) have observed such changes in composition in natural amphiboles as a result of increased metamorphic grade (as monitored by assemblages in intercalated pelitic schists). The composition changes in amphiboles which take place with increase in metamorphic grade can be represented by substitution into the basic tremolite formula, $\square Ca_2Mg_5Si_8O_{22}(OH)_2$ (Spear, 1981). The $\square$ in the formula, denotes a vacancy in the A site in the amphibole structure (Robinson et. al., 1982). A few of the substitutions which take place in amphiboles within mafic schists (Laird and Albee, 1981, Spear, 1981) are:

1. Edenite, $Na + Al(IV) \rightarrow \square + Si$
2. Tschermakite, $Al(IV) + Al(VI) \rightarrow Mg + Si$
3. Glaucophane, $2Na(M4) + 2Al(VI) \rightarrow 2Ca(M4) + 2Mg(VI) + Si$

Figure 10. Electron microprobe traverses of amphiboles from samples CM87-565 and CM86-425.

Figure 10a. Electron microprobe traverse of amphibole from CM87-565.

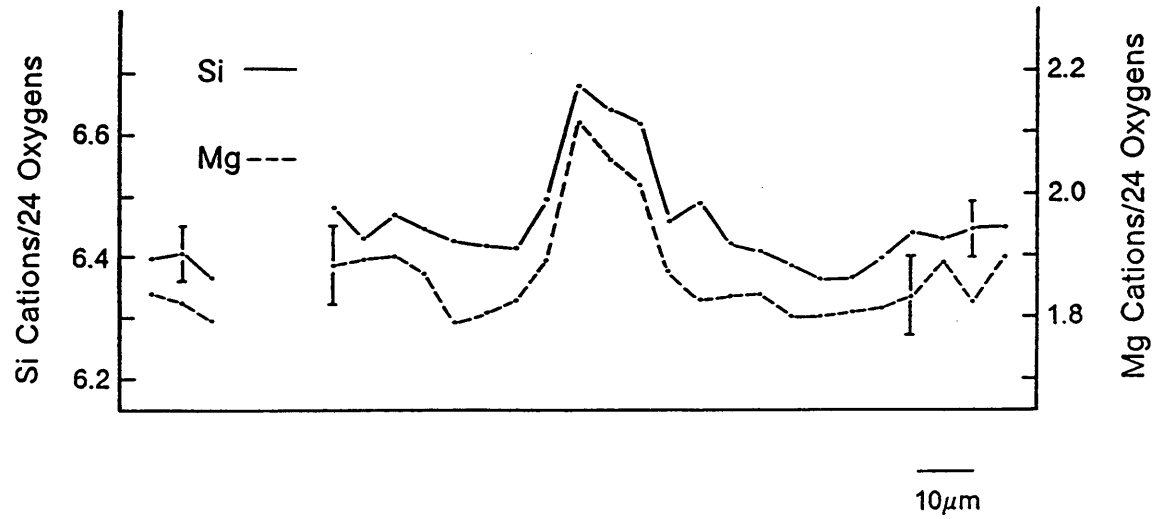
Si Cations/24 Oxygens
Si
Mg
6.6
6.4
6.2
2.2
2.0
1.8
Mg Cations/24 Oxygens
10μm

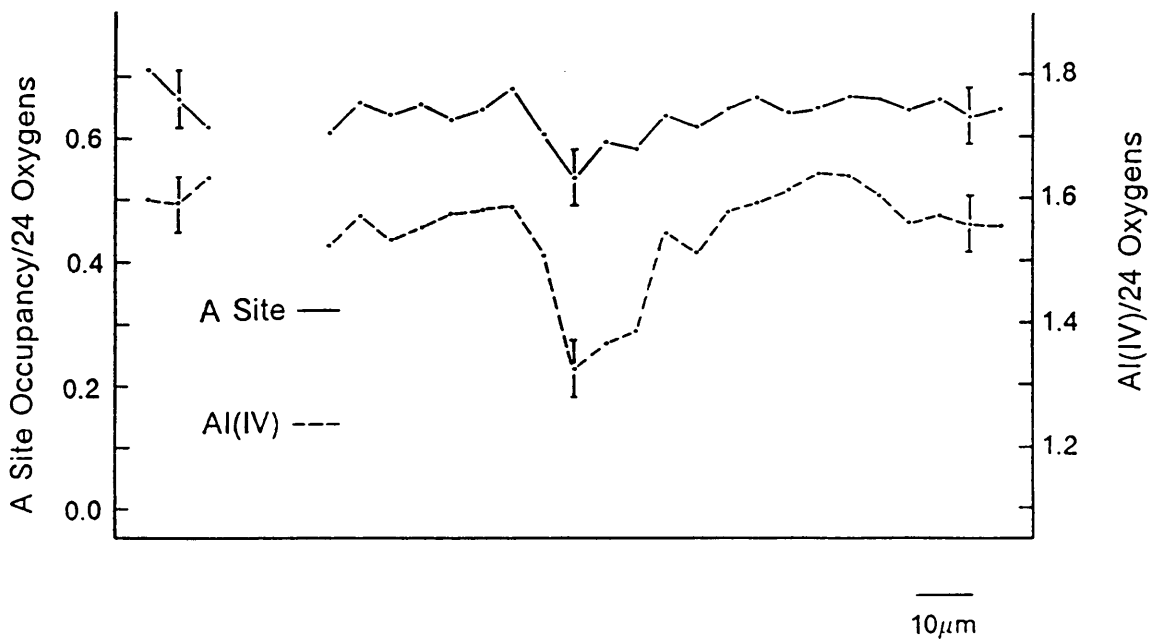
A Site Occupancy/24 Oxygens
A Site
Al(IV)
0.6
0.4
0.2
0.0
1.8
1.6
1.4
1.2
Al(IV)/24 Oxygens
10μm

Figure 10. cont.

Figure 10b. Electron microprobe traverse of amphibole from CM86-425.

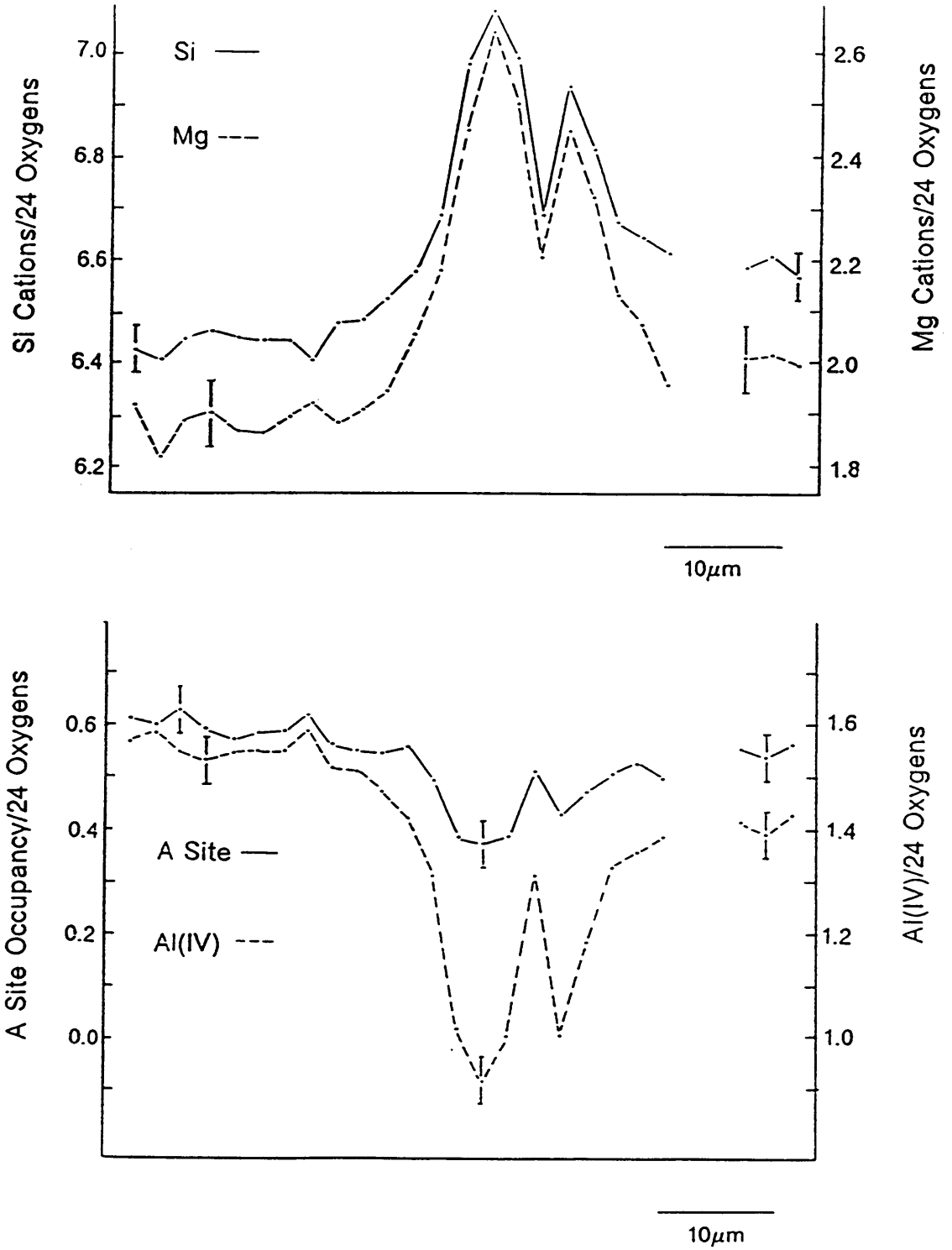
Si Cations/24 Oxygens
7.0
6.8
6.6
6.4
6.2
Si
Mg
2.6
2.4
2.2
2.0
1.8
Mg Cations/24 Oxygens
10μm
A Site Occupancy/24 Oxygens
0.6
0.4
0.2
0.0
A Site
Al(IV)
1.6
1.4
1.2
1.0
Al(IV)/24 Oxygens
10μm

4. Ferritschermakite, $Al(IV) + Fe^{3+}(VI) \rightarrow Mg + Si$

5. Ti tschermakite, $2Al(IV) + Ti(VI) \rightarrow 2Si(IV) + Mg(VI)$

Laird and Albee (1981) presented amphibole composition data from world wide occurrences of mafic schist from low pressure, medium pressure, and high pressure facies series. Their data indicated that glaucophane substitution dominates in high pressure facies series metamorphism, whereas the edenite and tschermakite substitutions dominate during low pressure facies series metamorphism. The data presented by Laird and Albee (1981) also indicates that amphiboles from medium pressure facies series have compositions which are intermediate between those of the high pressure and low pressure facies series. The zoning displayed in the microprobe traverses of amphiboles from samples CM87-565B and CM86-425 (Fig. 10a and 10b, analyses in Tables 3a and 3b of Appendix C) suggest that both the edenite and tschermakite substitutions have operated during the growth of these amphiboles. This may indicate a temperature increase during the growth of these amphiboles. It should also be noted that the cores of these amphiboles were not distinguishable optically. They are not rimmed by inclusions suggesting two relatively separate growth periods. They are also generally free of inclusions. Although some amphibole growth took place in $M_1$, these amphiboles suggest post tectonic $M_2$ growth under static conditions. They are thus interpreted as post kinematic analogues of the post kinematic $M_2$ zoned garnet porphyroblasts in the semipelitic and quartzo-feldspathic schists. Noteworthy also, is the fact that the smaller amphiboles ($< 60\mu m$) within a single sample (CM87-565B, CM87-675AZ, or CM86-425) have homogenous compositions which are similar to the rim compositions of the larger amphiboles within the same sample (analyses of smaller amphiboles from samples CM87-565B, CM86-425 and CM87-675AZ are provided in Tables 3a , 3b, and 3c respectively of Appendix C). This is also taken as evidence of continued $M_2$ middle amphibolite facies mineral growth. Modal data (Table 4) for these samples suggests that the amphiboles are likely to have formed at the expense of chlorite and epidote (or zoisite), as these minerals are present in minor amounts

TABLE 4 Modal analyses (400 pts.) of mafic rocks

| Sample | CM87-675AZ | CM87-565B | CM86-425 |
|---|---|---|---|
| Quartz | 6.0 | 5.5 | 0.25 |
| Plag.(Olig.) | 28.0 | 36.0 | 34.0 |
| Hornblende | 48.0 | 52.0 | 56.0 |
| Epidote | 10.0 | --- | 2.5 |
| Ilmenite | 3.0 | 6.25 | 6.0 |
| Chlorite | 2.0 | tr. | tr. |
| Zoisite | 3.0 | --- | 0.75 |
| Biotite | --- | --- | 0.5 |
| Hematite | tr. | 0.25 | --- |

| Sample | Rock Type | Loc. Ref. No. | Map Sheet |
|---|---|---|---|
| CM87-675AZ | fine grained amphib. sill | 32VPQ254668 | Alen |
| CM87-565B | fine grained mafic tuff | 32VPQ138675 | Alen |
| CM86-425 | fine grained mafic tuff | 32VPQ166633 | Alen |

Loc. Ref. No. = Location reference number given in UTM grid coordinates

in CM87-675AZ and CM86-425. In CM87-565B there is just a trace amount of chlorite (not analyzed by electron microprobe), and no epidote or zoisite. Sphene is absent from the mafic schists from the eastern (CM87-675AZ), central (CM86-425), and western (CM87-565B) portions of the study area (Fig. 7). The Ti phase in these samples and throughout the study area is ilmenite and less commonly, rutile. Both of these Ti oxide minerals tend to replace sphene in amphibolite facies parageneses of the medium pressure facies series (Robinson et. al., 1982). The assemblages in the mafic schists, (CM87-565B, CM86-425, and CM87-675AZ) are shown in Figures 11a, 11b, 11c, respectively projected into the CaO, FMO (FeO + MgO + MnO), $Al_2O_3$, $Na_2O$ tetrahedron (Laird, 1980) from quartz and ilmenite as excess phases with $\mu H_2O$ externally controlled. Representative hornblende rim compositions and the most An-rich plagioclase composition in each of the samples have been plotted in order to show the prograde assemblage. There is reason to suspect that sample CM86-425 may have been subject to localized retrograde metamorphism as the plagioclase composition in this rock generally is on the order of $An_3$ - $An_5$. However, there are patches within the plagioclase grains where the composition is approximately $An_{18}$ . Electron microprobe analyses of the plagioclase and chlorite (with the exception of CM87-565B) from samples CM87-565B, CM86-425, and CM87-675AZ are listed in Tables 5a, 5b, 5c, (respectively) of Appendix C.

## Geothermometry and Geobarometry

The possible existence of a metamorphic gradient suggested by the presence of staurolite and kyanite porphyroblasts in the western portion of the field area and their absence from $M_2$ assemblages in the east was addressed by obtaining temperature estimates based on the Fe-Mg exchange reaction between garnet and biotite as calibrated by Ferry and Spear (1978) and Thompson (1976b). Samples CM87-495, CM87-793, CM87-608B, and LG86-11D were selected for their strategic location (Fig. 7), the presence of prograde, post tectonic garnet porphyroblasts and semipelitic to quartzo-feldspathic bulk compositions. It would have been

Figure 11. Projection of mineral assemblages in mafic rocks into $Al_2O_3$, $Na_2O$, CaO, FMO tetrahedron. Olig = oligoclase, Ep = epidote, Hbl = hornblende, Chl = chlorite, (a) Mineral assemblage in CM87-565B, (b) Mineral assemblage in CM86-425, (c) Mineral assemblage in CM87-675AZ.

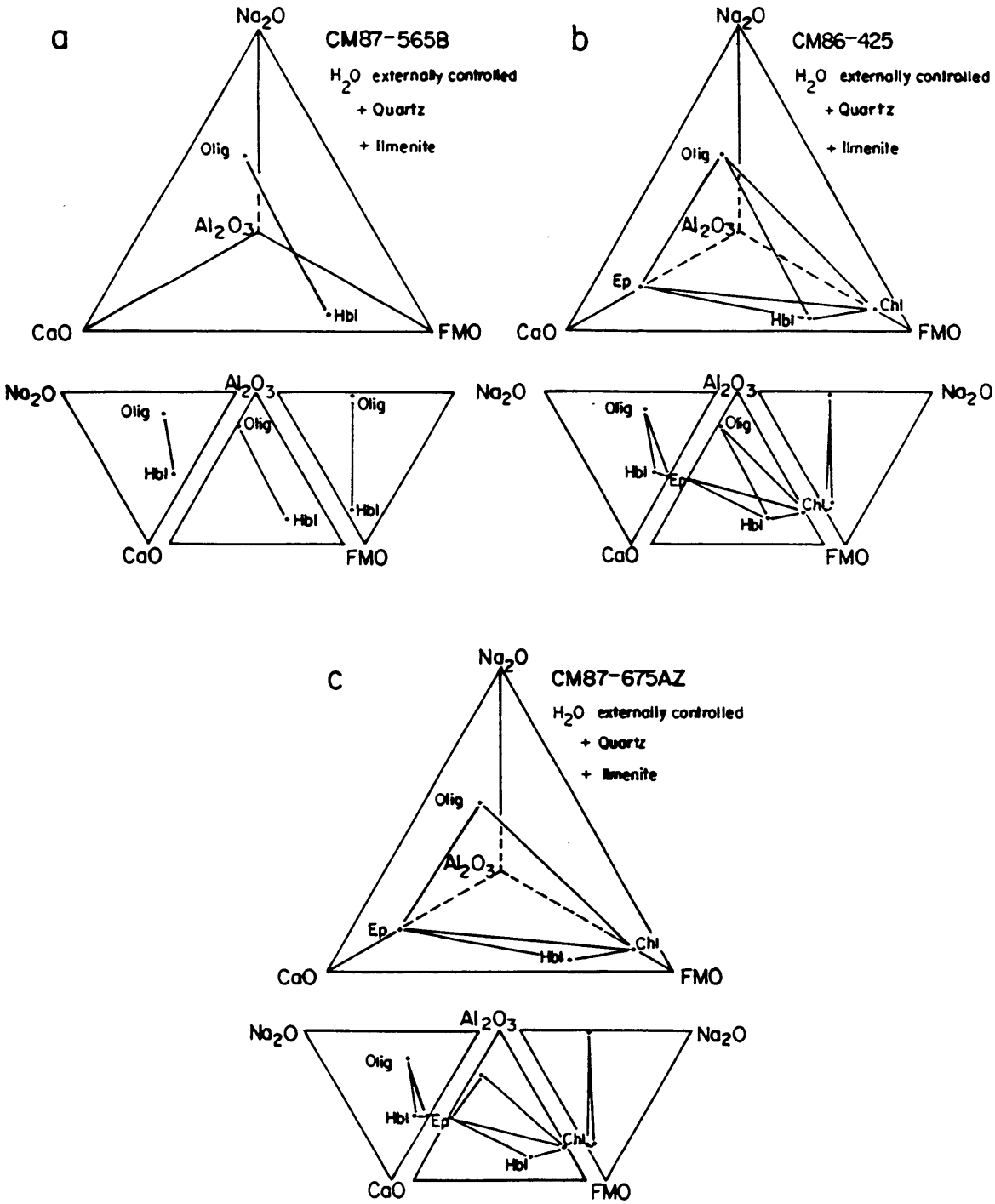


FMO = (FeO + MgO + MnO)

preferable to select samples with identical bulk composition, but the gradually changing nature of the metasediments across the study area made this impossible. The bulk FeO/(FeO + MgO) ratio of the rock does have some control on the lowest temperature at which garnet may first appear in a rock (neglecting the affects of additional components, e.g. Ca and Mn), as well as the composition of the matrix biotite in equilibrium with it. If one views the garnet-biotite exchange reaction as a closed loop in T - $X_{FeO}$ space (Thompson, 1976a), then once garnet is formed, its composition and that of the coexisting biotite should become more Mg-rich with increasing temperature (or decreasing $\mu H_2O$). This is shown schematically for two rocks of different bulk FeO/(FeO + MgO) ratio in Figure 12. If both rocks were raised to equal temperature during metamorphism, and garnet continued to grow by continuous prograde reaction in each of the rocks, then the garnet-biotite pairs in each of the rocks should theoretically be of identical composition and should yield equal partition coefficient (Kd) values regardless of initial bulk FeO/(FeO + MgO) ratio. Garnet initially formed at $T_1$ in rock A, with higher FeO/(FeO + MgO), will change composition along path *a* to the new equilibrium composition at $T_3$. The composition of the biotite in equilibrium with this garnet will also change composition along path *a'*. Similarly, garnet formed at a slightly higher temperature in rock B, with lower bulk FeO/(FeO + MgO) at temperature $T_2$, will change compositon to the equilibrium composition at $T_3$, along path *b*. The biotite in equilibrium with this garnet changes composition along path *b'*. It is assumed that differing Kd values for the garnet-biotite exchange reaction in separate samples corresponds to differences in peak temperatures (or decrease in $\mu H_2O$) encountered by each sample provided the garnet and biotite have not been subject to retrograde reaction.

A bulk chemical composition (Table 6) for each of the samples used for geothermometry has been calculated according to the method of Tracy et. al., (1983). This was accomplished by converting modal analysis data (based on 1000 points) to moles per 100 $cm^3$ of rock by dividing the modal percent of the phases by the appropriate molar volumes obtained from Robie et. al., (1978), and Helgeson et. al., (1978). Microprobe analyses of minerals with variable compositions were used to determine molar volumes and densities assuming ideal mixing.

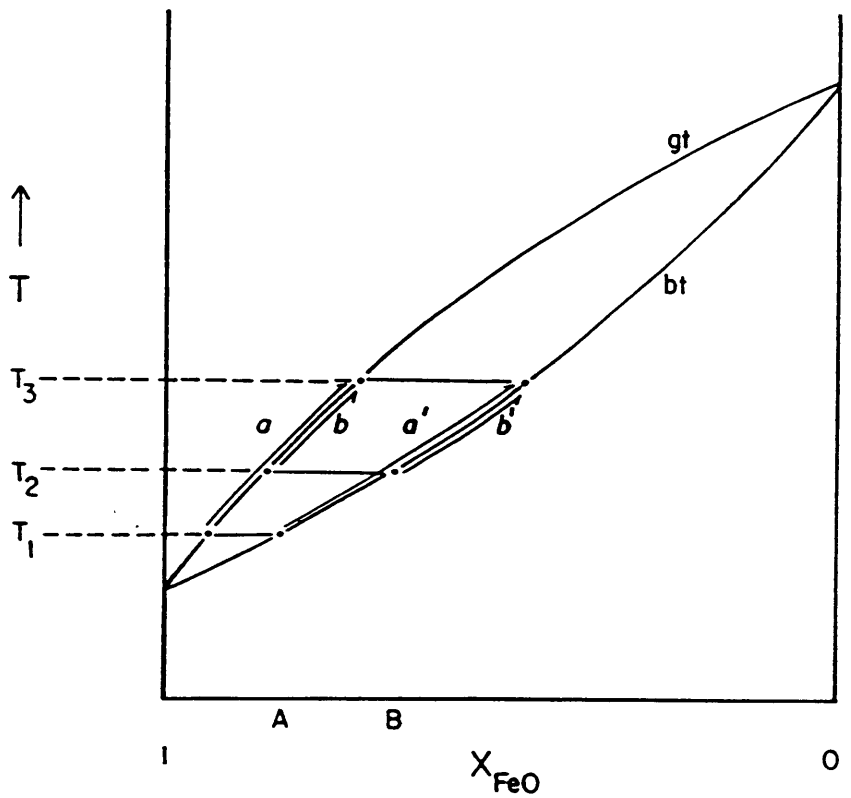


Figure 12. Schematic illustration of garnet - biotite pairs in T - $X_{FeO}$ space for rocks with different FeO/(FeO + MgO) ratios.

TABLE 6 Modal analyses and calculated bulk compositions of semipelitic/psammitic schists

| Sample | CM87-495 | LG86-11D | CM87-793 | CM87-608B |
|---|---|---|---|---|
| Modes | | | | |
| Quartz | 13.0 | 27.4 | 41.9 | 41.5 |
| Plagioclase | 7.8 | 15.0 | 21.2 | 21.9 |
| Biotite | 50.4 | 44.6 | 27.2 | 15.0 |
| Muscovite | 15.3 | 7.5 | 2.1 | --- |
| Chlorite | 6.7 | 1.4 | 1.75 | 10.8 |
| Garnet | 2.9 | 1.6 | 0.3 | 3.8 |
| Kyanite | 0.8 | --- | --- | --- |
| Staurolite | 1.9 | 2.0 | --- | --- |
| Epidote | --- | --- | --- | 5.3 |
| Zoisite | --- | --- | 2.2 | 0.7 |
| Ilmenite | 1.2 | 0.4 | 1.0 | 1.0 |
| Apatite | tr. | --- | --- | --- |
| Tourmaline | tr. | tr. | --- | --- |
| Moles/100cm$^3$ | | | | |
| Quartz | 0.57 | 2.95 | 1.84 | 1.83 |
| Plagioclase | 0.08 | 0.20 | 0.21 | 0.22 |
| Biotite | 0.33 | 0.29 | 0.18 | 0.10 |
| Muscovite | 0.11 | 0.06 | 0.02 | --- |
| Chlorite | 0.03 | 0.01 | 0.02 | 0.05 |
| Garnet | .025 | .014 | .002 | .032 |
| Kyanite | .018 | --- | --- | --- |
| Staurolite | .008 | .010 | --- | --- |
| Epidote | --- | --- | --- | .005 |
| Zoisite | --- | --- | .016 | .005 |
| Ilmenite | .038 | .009 | .032 | .032 |
| Apatite | --- | --- | --- | --- |
| Tourmaline | --- | --- | --- | --- |
| Calculated Compositions (Weight percent oxides) | | | | |
| $SiO_2$ | 65.8 | 81.6 | 87.5 | 84.6 |
| $TiO_2$ | 3.0 | 1.0 | 1.4 | 1.3 |
| $Al_2O_3$ | 13.0 | 7.4 | 4.6 | 4.8 |
| FeO | 8.0 | 3.6 | 2.8 | 4.9 |
| MgO | 4.0 | 2.4 | 1.1 | 0.9 |
| MnO | 0.1 | 0.1 | tr. | 0.1 |
| CaO | 0.5 | 0.6 | 0.7 | 1.6 |
| $Na_2O$ | 0.8 | 1.0 | 0.8 | 0.7 |
| $K_2O$ | 2.9 | 1.4 | 0.7 | 0.4 |
| $H_2O$ | 1.9 | 0.9 | 0.4 | 0.7 |
| FeO/FeO + MgO | .53 | .46 | .59 | .76 |

Densities for the endmember phases were obtained from Deer, Howie, and Zussman (1963). The density of the phase multiplied by the number of moles/100 $cm^3$ multiplied by the weight percent of the oxide (X) in the mineral yields the contribution of that phase to the total amount of oxide (X) in the rock. These oxide contributions from each of the phases are then summed and normalized to yield a calculated bulk chemistry. Replicate point counts of the same thin section indicate that the error associated with the modal analysis is approximately 0.5 - 1.0 percent. For a phase of relatively high density, such as ilmenite (4.78, Deer et. al., 1963), this error can result in a significant change in bulk FeO/FeO + MgO ratio. Error bars associated with a 0.5 percent error in the modal amount of ilmenite are shown for each of the samples, CM87-495, LG86-11D, CM87-793, in their respective AKFM (Thompson, 1957) diagrams (Figures 8a, 8b, 8c) projected from quartz, muscovite, plagioclase, ilmenite, and $H_2O$ excess. Sample CM87-608B is not shown because it contains no modal muscovite. The calculated bulk composition of CM87-495 is within the semipelitic range (Miyashiro, 1973), whereas the calculated bulk compositions of CM87-793, CM87-608B, and LG86-11D are in the quartzo-feldspathic range. This is also indicated by the modal data of Table 6.

Garnet rim compositions from samples CM87-608B and CM87-793, contain a higher mole fraction of grossular ($X_{gros}$ = 0.15 - 0.19, see Table 7 of Appendix C) than garnet rim compositions from samples CM87-495 and LG86-11D ($X_{gros}$ = 0.12 - 0.13, see Table 7 of Appendix C). Ferry (1980) noted in his study that garnet rim compositions with $X_{gros}$ greater than 0.1 yielded low temperatures when using the garnet-biotite geothermometer when compared to temperature estimates based on other geothermometers. The garnet rim compositions used for geothermometry in this study area (see Tables 7a, 7b, 7c, 7d of the Appendix C) meet the criteria of combined $X_{gros}$ + $X_{spes}$ not in excess of 0.3 as recommended by Ferry (1980). Representative matrix biotite compositions from the samples used for thermobarometry are provided in Tables 8a, 8b, 8c, and 8d of Appendix C. However, in all samples, the mole fraction of grossular in the garnet rim compositions exceeds 0.1. For this reason, the garnet activity model of Hodges and Crowley (1985) has been used in the geothermometry calculations. This

activity model accounts for the non-ideal mixing behavior of the grossular-pyrope binary and appears as follows:

$$a_{alm} = [X_{alm} \cdot \exp(((1.5T(K) - 3300) \cdot (X_{pyr}X_{gr}))/RT(K))]^3 \quad (1)$$

$$a_{pyr} = [X_{pyr} \cdot \exp(((3300 - 1.5T(K)) \cdot (X_{gr}^2 + X_{alm}X_{gr} + X_{gr}X_{sp}))/RT(K))]^3 \quad (2)$$

If one writes the Fe-Mg exchange reaction between garnet and biotite in the following fashion:

almandine + phlogopite → pyrope + annite

then the equilbrium constant written in terms of mole fractions (Kd) for this reaction reduces to:

$$Kd = [(X_{pyr}^{Gar}/X_{alm}^{Gar})/(X_{phl}^{Bi}/X_{ann}^{Bi})] \quad (3)$$

If one writes the equilibrium constant in terms of activities, the expression will have the following appearance:

$$K^* = [(a_{pyr}^{Gar}/a_{alm}^{Gar})/(a_{phl}^{Bi}/a_{ann}^{Bi})] \quad (4)$$

If ideal mixing in biotite is assumed, then,

$$a_{phl}^{Bi} = X_{phl}^{Bi} \quad (5)$$

The resulting $K^*$ value is substituted back into the original equilibrium constant equation of Ferry and Spear (1978):

$$0 = 12454 - 4.662T(K) + 0.057P(bars) + RT(K) \ln K^* \quad (6)$$

Temperature estimates can be derived by obtaining a pressure estimate, garnet rim compositions and matrix biotite compositions. Exchange reactions such as this between garnet

and biotite tend to have small $\Delta V$ (Thompson, 1976b, Essene, 1982) and relatively large $\Delta S$ values making them largely independent of pressure and suitable for geothermometry. A minimum pressure estimate of 4.0 kb was chosen for the study area based on the presence of kyanite as the aluminosilicate phase in sample CM87-495, and lack of andalusite in the study area suggesting pressures above the aluminosilicate triple point of Holdaway (1971).

The equilibrium constant equation of Thompson (1976b), based on an empirically derived calibration of natural garnet data for the reaction;

$$\text{pyrope} + \text{annite} \rightarrow \text{almandine} + \text{phlogopite}$$

is as follows:

$$0 = lnKd + \Delta Vs(P/RT(K) + 1.560 - 2{,}740/T(K) \quad (7)$$

where,

$$Kd = [(X^{Gar}_{alm})(X^{Bi}_{phl})/(X^{Gar}_{pyr})(X^{Bi}_{ann})] \quad (8)$$

The original equation of Thompson (1976b) has been modified by replacing the mole fraction almandine and mole fraction pyrope terms with the activities of almandine and pyrope derived from the Hodges and Crowley (1985) activity model for garnet. Ideal mixing in biotite is assumed.

Temperature estimates (Table 9a) for sample CM87-495 were determined by using the modified (garnet activity model of Hodges and Crowley (1985)) Ferry and Spear (1978) calibration of the garnet-biotite exchange reaction and a minimum pressure estimate of 4.0 kb. These temperature estimates were then used to obtain a more accurate pressure determination based on the quartz-garnet-aluminosilicate-plagioclase (QGAP) geobarometer of Newton and Haselton (1981), with revisions by Koziol and Newton (1988). The data is shown in Table 9b and indicates pressures in the 8.0 kb $\pm$500 bar range. A second iteration with an 8.0 kb pressure estimate derived from the QGAP geobarometer and the modified versions of

TABLE 9a Temperature estimates for CM87-495 (4 kb pressure estimate)

| Garnet rim analysis no. | $F/FM_{bio}$* | Modified (Thompson, 1976b) ln Kd | Modified (Thompson, 1976b) T (C) | Modified (Ferry and Spear, 1978) ln k | Modified (Ferry and Spear, 1978) T (C) |
|---|---|---|---|---|---|
| 24 | .394 | 1.838 | 560 | -1.838 | 538 |
| 44 | .394 | 1.759 | 580 | -1.759 | 564 |
| 64 | .394 | 1.786 | 573 | -1.786 | 555 |
| 84 | .394 | 1.742 | 584 | -1.742 | 569 |
| 104 | .394 | 1.786 | 573 | -1.786 | 555 |
| 124 | .394 | 1.808 | 568 | -1.808 | 548 |
| 223 | .394 | 1.761 | 580 | -1.761 | 563 |

* $F/FM_{bio}$ = average mole fraction of annite in biotite (34 analyses)
Std. dev. = 0.005

TABLE 9b Pressure estimates for CM87-495 derived from QGAP geobarometer of Newton and Haselton (1981) with revisions from Koziol and Newton (1988)

| Garnet rim analysis no. | F&S's T* | $X_{an}$ (rim) | $a_{gr}$ | $a_{an}$ | DVrxn | P(kb) |
|---|---|---|---|---|---|---|
| 24 | 538 | .264 | .139 | .483 | -63.09 | 7.7 |
| 44 | 564 | .264 | .143 | .461 | -63.01 | 8.5 |
| 64 | 555 | .264 | .137 | .468 | -63.16 | 8.1 |
| 84 | 569 | .264 | .144 | .457 | -62.96 | 8.6 |
| 104 | 555 | .264 | .146 | .468 | -62.89 | 8.3 |
| 124 | 548 | .264 | .155 | .474 | -62.71 | 8.4 |
| 223 | 563 | .264 | .145 | .462 | -62.95 | 8.5 |

* F&S's T = temperature estimates derived from activity model modified Ferry and Spear (1978) calibration.

the Ferry and Spear (1978) and Thompson (1976b) calibrations of the garnet-biotite exchange reaction yielded the temperature values listed for this sample in Table 9c.

The pressure estimates for sample CM87-495 derived from the QGAP geobarometer of Newton and Haselton (1981) make use of the revised expression for P° (kb) from Koziol and Newton (1988), where,

$$P°(kb) = -1093 + 22.80T(°C) \quad (9)$$

for the end member reaction with kyanite as the aluminosilicate phase. The activities of grossular and anorthite were calculated according to the original equations of Newton and Haselton (1981). Partial molal volumes along the almandine-grossular binary join and pyrope-grossular join were calculated according to the equations listed in Newton and Haselton (1981). The molar volume of the multicomponent garnet was determined by a weighted average of the pyrope-grossular and almandine-grossular molal volumes. The pressure estimates from garnet rim compositions and a plagioclase rim composition from CM87-495, are listed in Table 9b. Chemical analyses of the garnet and plagioclase are listed in Tables 7a and 10a respectively, of Appendix C.

The temperature estimates derived from the activity model modification of the Ferry and Spear (1978) calibration are probably more reasonable for samples CM87-495 (Table 9c) and LG86-11D (Table 11), than those derived from the modified version of the Thompson (1976b) calibration. This is based on the middle amphibolite facies assemblage present in the two samples and absence of migmatite zones in these rocks. At approximately 8 kb, and temperatures in excess of 600°C, the water saturated granite melting (Turner, 1981) curve would be encountered yet the Gudå Fm. does not exhibit migmatite zones in the study are. Temperature estimates for samples CM87-793 (Table 12) and CM87-608B (Table 13) derived from the modified Ferry and Spear (1978) calibration are reasonable, whereas the temperatures from the modified Thompson (1976b) calibration may be somewhat high for the given assemblage in these samples. Laird and Albee (1981) report that samples from the garnet oligoclase zone in Vermont were probably metamorphosed at 525° ± 50°C, whereas samples

TABLE 9c Temperature estimates for CM87-495 (8.0 kb pressure estimate from QGAP geobarometer)

| Garnet rim analysis no. | $F/FM_{bio}$* | Modified (Thompson, 1976b) ln kd | T (C) | Modified (Ferry and Spear, 1978) ln k | T(C) |
|---|---|---|---|---|---|
| 24 | .394 | 1.842 | 587 | -1.842 | 551 |
| 44 | .394 | 1.763 | 607 | -1.763 | 577 |
| 64 | .394 | 1.790 | 600 | -1.790 | 568 |
| 84 | .394 | 1.747 | 611 | -1.747 | 583 |
| 104 | .394 | 1.791 | 600 | -1.791 | 568 |
| 124 | .394 | 1.813 | 594 | -1.813 | 561 |
| 223 | .394 | 1.765 | 607 | -1.765 | 576 |

* $F/FM_{bio}$ = average mole fraction of annite in biotite (34 analyses)
Std. dev. = 0.005

TABLE 11 Temperature estimates for LG86-11D (8.0 kb pressure estimate)

| Garnet rim analysis no. | $F/FM_{bio}$* | Modified (Thompson, 1976b) ln kd | T (C) | Modified (Ferry and Spear, 1978) ln k | T (C) |
|---|---|---|---|---|---|
| 385 | .383 | 1.704 | 623 | -1.704 | 597 |
| 389 | .383 | 1.724 | 618 | -1.724 | 590 |
| 399 | .383 | 1.731 | 616 | -1.731 | 588 |
| 400 | .383 | 1.737 | 614 | -1.737 | 586 |
| 434 | .383 | 1.707 | 622 | -1.707 | 596 |
| 436 | .383 | 1.748 | 611 | -1.748 | 582 |

* $F/FM_{bio}$ = average mole fraction of annite in biotite (16 analyses)
Std. dev. = 0.004

TABLE 12 Temperature estimates for CM87-793 (8 0 kb pressure estimate)

| Garnet rim analysis no. | $F/FM_{bio}$* | Modified (Thompson, 1976b) ln kd | T (C) | Modified (Ferry and Spear, 1978) ln K | T (C) |
|---|---|---|---|---|---|
| 544 | .467 | 1.907 | 571 | -1.907 | 532 |
| 546 | .467 | 1.879 | 577 | -1.879 | 540 |
| 559 | .467 | 1.895 | 573 | -1.895 | 535 |
| 560 | .467 | 1.787 | 601 | -1.787 | 569 |
| 638 | .467 | 1.883 | 576 | -1.883 | 539 |

* $F/FM_{bio}$ = average mole fraction of annite in biotite (8 analyses)
Std. dev. = 0.005

TABLE 13 Temperature estimates for CM87-608B (8.0 kb pressure estimate)

| Garnet rim analysis no. | $F/FM_{bio}$* | Modified (Thompson, 1976b) ln kd | T (C) | Modified (Ferry and Spear, 1978) ln k | T (C) |
|---|---|---|---|---|---|
| 159 | .491 | 1.886 | 576 | -1.886 | 538 |
| 160 | .491 | 1.783 | 602 | -1.783 | 570 |
| 184 | .491 | 1.807 | 596 | -1.807 | 563 |
| 253 | .491 | 1.828 | 590 | -1.828 | 556 |
| 254 | .491 | 1.829 | 590 | -1.829 | 556 |
| 255 | .491 | 1.821 | 592 | -1.821 | 558 |

* $F/FM_{bio}$ = average mole fraction annite in biotite (27 analyses)
Std. dev. = 0.008

from the staurolite plus kyanite zone in Vermont probably were metamorphosed at 550° ± 50°C. These temperatures reported by Laird and Albee (1981) were consistent with temperature estimates derived from other independent geothermometers.

Regardless of the calibration chosen, temperature estimates for CM87-495 and LG86-11D are slightly higher than the estimates obtained for samples CM87-793 and CM87-608B. The general consensus in the literature (Hodges and Crowley, 1985, Laird and Albee, 1981, Ferry and Spear, 1978) is that the error associated with the garnet-biotite geothermometer is ± 50°. Certainly the difference in estimated temperatures between samples CM87-495, LG86-11D, CM87-608B, and CM87-793 are well within the margin of error estimated for this geothermometer. This suggests that the absence of staurolite and kyanite in the eastern portion of the study area is due to bulk composition (low aluminum) and not to differences in intensive parameters (e.g. temperature or $\mu H_2O$). Most importantly, the majority of the temperature estimates derived from each of the samples indicate that middle amphibolite facies P - T conditions persisted after deformation. This is consistent with the evidence for prevalent thermal annealing and post-tectonic porphyroblast growth to be discussed in the structural geology section below.

Of particular significance is that the pressure estimate of 8 kb ± 500 bars, implies that the study area was buried to a depth of 26-28 km assuming $\simeq$0.28 kb/km$^1$ (Best, 1982). Up to 15 km of this overburden could be accounted for by tectonic thickening culminating in the Scandian (Gee et. al., 1985, Roberts and Sturt, 1980) phase of Caledonian orogenesis. If one assumes an average $M_2$ temperature of 565°C for the study area, then the 8 kb pressure estimate implies a geothermal gradient of approximately 21°C/km$^1$. This is assuming that the maximum pressure and temperature were recorded in the rock simultaneously. It is likely that the temperature was recorded in the rock along one thermal gradient developed during the relaxation of initially depressed isotherms. The pressure may have been recorded independently along another thermal gradient. This data however, is in the range of the average geothermal gradient (20°C/km$^1$) for medium pressure series (Miyashiro, 1973) metamorphism.

The mineral compositions contained within the mafic schists indicates that amphibolite facies metamorphism was attained throughout the study area. The anorthite content of plagioclase in sample CM87-675 from the eastern portion of the study area (See Fig. 7 for sample locations) is in the $An_{19}$ - $An_{23}$ range. In sample CM87-565B from the western portion of the study area, the anorthite content of the plagioclase is $An_{16}$ - $An_{21}$. The anorthite content of plagioclase in CM86-425 from the central portion of the study area, is generally $An_3$ - $An_5$. However, a few analyses from the core of a plagioclase grain in this sample reach $An_{17}$ . This suggests that CM86-425 may have undergone localized retograde metamorphism. Plagioclase compositions from samples CM87-565B (west) and CM87-675(east) seem to support the implications of the garnet-biotite geothermometry. The aluminum content of the calcic amphiboles in samples CM87-565B, CM86-425, and CM87-675, are also similar, ranging from 12 - 14 weight percent $Al_2O_3$ in both eastern and western sections. Microprobe analyses of amphiboles from samples CM87-565B, CM86-425, and CM87-675AZ are listed in tables 3a, 3b, 3c, of Appendix C. The similarity of plagioclase and amphibole compositions from the eastern and western portions of the field area suggests that similar- grade amphibolite facies metamorphism was prevalent throughout the Fundsjø Group as redefined (Mandeville, 1988) in the Ålen area.

## $M_3$ Assemblage

A retrograde metamorphic event $M_3$, affected the rocks of the Fundsjø Group only on a very localized scale. The major evidence for this greenschist facies retrograde metamorphism is in the Kjurudal Fm. where garnets have been replaced partially to completely by chlorite. A few samples of amphibolite from the Hersjø Fm contain coarse (0.5-2.0 mm) dark blue-green hornblendes which show ragged edges rimmed by chlorite. Sample CM86-425 from the Hersjø Fm. contains plagioclase grains which appear to have been subject to local retrograde metamorphism and now consist largely of albitic plagioclase. One sample from the Reitan

Fm. in the southern portion of the study area (Sample CM86-285, location given in Appendix A) contains very light blue-green actinolitic amphibole. This sample of greenschist was also deformed by cataclasis and this retrograde metamorphism is probably associated with fluids migrating through this zone.

The general lack of widespread retrograde metamorphism may be due to relatively rapid uplift and/or slow reaction kinetics of (Turner, 1981) the retrograde reactions. The positive slope of most prograde dehydration reactions in P - T space also would suggest that reaction curves are crossed at higher temperature in the compression path, whereas the same reaction curves may be crossed at lower temperature in the decompression path (Turner, 1981). This could enhance the kinetics of the prograde reactions and reduce those of the retrograde reactions.

# Structural Geology

Three deformation episodes have been distinguished in the Alen area. They have been distinguished by classical criteria such as overprinting relationships, varying geometrical orientation, structural styles, and with respect to the separation of $D_2$ from $D_3$, an intervening period of post-kinematic porphyroblast growth and thermal annealing. This annealing is indicated by strain-free quartz, feldspar, and micas. The first two episodes possibly represent a single progressive tectonic event for reasons which will be discussed below and in the discussion of metamorphism. The $D_1$ phase is characterized by a penetrative schistosity which is almost always parallel to $S_0$ (primary bedding). This fabric is interpreted as a tectonic fabric and is axial planar to $F_1$ mesoscopic isoclinal folds which, despite their rarity, have been observed. The $D_2$ phase is characterized by open to tight folds which fold the pre-existing $S_1$ fabric and early isoclinal folds. A spaced axial planar cleavage is associated with these $F_2$ folds and transects the $S_1$ fabric. A period of thermal annealing and static mineral growth most probably associated with the metamorphic peak separates the $D_2$ and $D_3$ phases of deformation. The $D_3$ phase of deformation is characterized by structures typically associated with more brittle deformation under conditions of low confining pressure and/or high strain rates. These features include, kink folds, microfaults, and the generation of cataclasite and pseudotachylite. Moreover, strain features associated with the $D_3$ deformation are still pre-

served within the mineral phases, and have not been obliterated by post deformational strain recovery.

It should be pointed out that the criteria used to distinguish the various deformations in this area yield only a local, relative sequence of events, and not an absolute dating, nor even a relative dating from place to place (Williams, 1985) as absolute relationships are likely to vary in time and space across an orogen. For example, a $D_1$ feature at one locality does not imply that it is the same absolute age as a similar $D_1$ feature at another locality. The generation of imbricate thrusts and duplexes, for example (Dahlstrom, 1970, Boyer and Elliot, 1982, Butler, 1982), illustrates that not all thrusts were formed simultaneously. Grouping of deformation features into generations (denoted by numerical subscripts) is based on overprinting relationships observed in individual outcrops. In a single outcrop, a $D_2$ structure will be younger than a $D_1$ structure, but without absolute age data, it cannot be implied that all $D_2$ structures are younger than all $D_1$ structures in a given area (Hobbs et. al., 1976, Williams, 1985). Structural features associated with each generation are summarized in Table 2 and listed in the map legend of Plate 1

## $D_1$

The $D_1$ phase is characterized by a widespread penetrative schistosity almost always parallel to original bedding ($S_0$). The penetrative $S_1$ fabric is due to preferred shape orientation of amphiboles in the amphibolites (mafic tuffs and fine grained mafic sills of the Hersjø and Reitan Formations) and alignment of biotite, chlorite, muscovite, and less commonly, staurolite and kyanite in the semipelitic to psammitic schists.

In rare instances where early isoclinal $F_1$ fold hinges can be observed, (Fig. 13) this penetrative fabric transects $S_0$. The penetrative schistosity is axial planar to the $F_1$ isoclinal folds. It is defined by the parallel to subparallel arrangement of chlorite, biotite, muscovite, or zoisite, and in the fine grained amphibolites by the subparallel allignment of hornblende.

Figure 13. Photograph of $F_1$ isoclinal fold and $S_1$ parallel quartz veins folded by tight $F_2$ fold. View looking towards west.

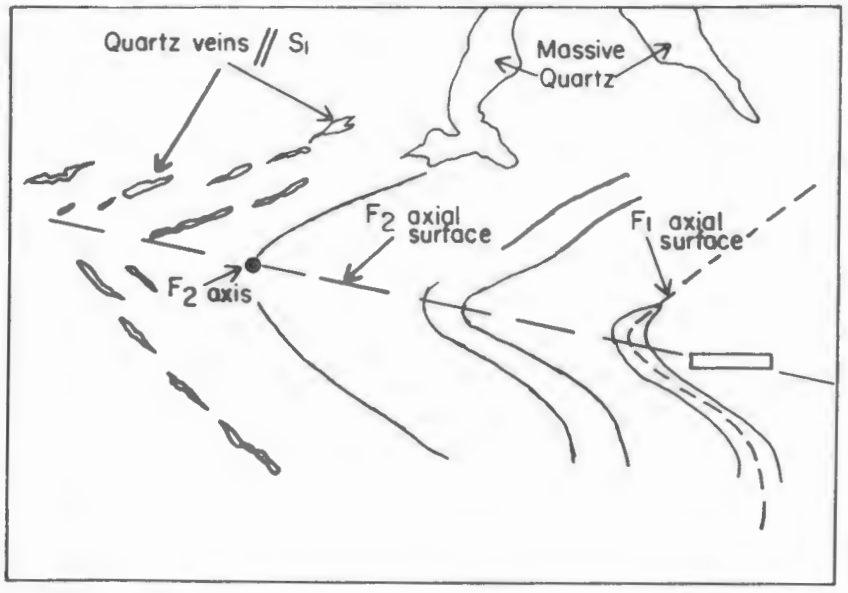
Quartz veins // S1
Massive Quartz
F2 axial surface
F1 axial surface
F2 axis

There may have been some parallel allignment of platy/elongate minerals in the sedimentary/volcanic protoliths, but the extent of recrystallization and the strongly penetrative nature of the fabric suggest that it is of tectonic origin. In one sample, a rarely observed intersection lineation between $S_0$ and $S_1$ is deformed about an $F_2$ fold axis.

Quartz veins, generally 0.5 - 2.0 cm thick, and laterally extensive for several meters, are parallel to the early $S_1$ cleavage, and are ubiquitous within the various formations of the Ålen area (Fig. 13). They are probably the result of localized pressure solution and precipitation of quartz which probably took place during $D_1$. Isoclinally folded quartz veins have been observed and these were deformed during $D_2$ along with the bedding parallel cleavage ($S_1$). These quartz veins serve as useful relative strain indicators, and often enable one to distinguish $D_1$ structures from $D_2$ structures at outcrop level (Cosgrove, 1980, Platt and Lister, 1985a).

The mesoscopic $F_1$ isoclinal folds observed at outcrop level are relatively small scale features (amplitudes of several - 10's of cms). Orientation data of $F_1$ folds is lacking due to their relative rarity, and also to lack of good three dimensional exposure where they have been observed. One measured $F_1$ axis oriented 290°/40° plunge, is subparallel to the mean of the $F_2$ axes. It cannot be unequivocally determmined whether this $F_1$ fold axis was initiated roughly orthogonal to the $F_2$ axial direction and then rotated into near coincidence with $F_2$, or whether it was initially generated subparallel to the mean $F_2$ axial direction. The type 3 fold patterns (Ramsay, 1967) commonly observed where one can see overprinting of $F_1$ folds by more open $F_2$ folds (Fig. 13) suggests that the subsequent $F_2$ axes may have been coincident with the earlier $F_1$ axes. Type 3 interference patterns are commonly developed where recumbent folds are refolded by younger folds with steeply inclined axial surfaces (Ramsay, 1967).

No large map scale $F_1$ isoclines have been identified to date. However, medium to large scale folds are suggested by inversion of the stratigraphy. The definition of a fold nappe given in Dennis et. al., (1981) states that, "a fold nappe is an allochthonous tectonic unit which exhibits large scale stratigraphic inversion and may have initiated from large recumbent folds.

The underlying limbs of these folds may be sheared out into thrust faults." The inverted stratigraphy of the Ålen area therefore may represent the inverted limb of a recumbent fold similar to those described by Platt and Lister, (1985b) from the Vanoise Massif in the French Alps, and by Ramsay (1981), and Ramsay et. al., (1983), from the Helvetic nappes of Switzerland. Recognition of inverted stratigraphy at the tectono-stratigraphic level of the Meråker Nappe has been reported by several workers (Roberts, 1967, Rui, 1972, Wolff, 1973, Hardenby, 1980, 1983). Generation of such widespread stratigraphic inversion for distances up to 100 km along strike would require several regionally extensive recumbent folds. A possible mechanism of generating such large scale recumbent folds is by simple shear deformation acting within a nappe as illustrated by Ramsay et. al., (1983) for the formation of the Morcles nappe. Many of the individual folds in the central and western Helvetic region can be traced for distances in excess of 50 km (Ramsay, 1981).

The larger features in the Ålen area which are likely to be of $D_1$ generation are the fault surfaces. They are deformed by the $F_2$ phase folds. The fault surface separating the Gudå Fm. from the Hersjø Fm. on the west side of the map (Plate 1) is likely to be a tectonic slide as defined by Hutton (1981). Tectonic slides often occur along lithological boundaries (Hutton, 1981) and lie within zones of intensified regional cleavage-deformation. They form under metamorphic conditions between lower greenschist facies and upper amphibolite facies. It is inferred from strain studies that tectonic slides initiate under conditions of elevated temperature and pressure because of differing response of contrasting rock types to syn-metamorphic strains (Hutton, 1981). There does not seem to be any truncation or dramatic change in orientation of $S_1$ cleavage at the boundary between the Gudå Fm. and Hersjø Fm. Tectonic slides are rarely associated with cataclasis, local bedding or foliation discordance. The $S_2$ spaced cleavage (oriented sub-orthogonal to the $S_1$ cleavage) does not change orientation significantly across the fault in locations (locations 551, and 557 of Appendix A) where the fault can be located to within 50 m. This suggests that the fault is a $D_1$ feature. It is apparent from the map pattern (Plate 1) that a zone of decoupling is present, as the Gudå Fm. is not folded harmonically with the Hersjø Fm. and Kjurudal Fm. in the western portion of the

map. The relationship shown on the map (Plate 1) suggests that the Hersjø Fm. volcanics were thrust over the Gudå Fm.. This is the relationship indicated on the NGU 1 : 250,000 scale Røros and Sveg quadrangle map of Nilsen and Wolff (1988) and is in agreement with the interpretation of Heim (1972). No evidence to prove or disprove this interpretation has been found. The fault is indicated where an apparent space problem is suggested by the disharmonic nature of the Gudå Fm.-Hersjø Fm. contact relative to that between the Hersjø Fm. and Kjurudal Fm. This tectonic slide probably dies out to the south where the lithologic contacts appear to be more harmonic.

The "thrust" fault indicated in the eastern portion of the map has been recognized by Rui (1972), Færden (1949), Olesen et. al., (1973), Kisch (1962, his Heina zone), and Nilsen and Wolff (1988). Mylonite zones are reported (Rui, 1972) to be associated with this fault farther to the north. The outcrop evidence for this fault in the Ålen area is poor. The fault zone does not form outcrops in the vicinity of Gaulåsen (Plate 1), but was encountered in a drill hole approximately 1500 m west of the surface entrance to the Killingdal Mine (Ø. Pettersen, and H. Moan, pers. comm.). There is again suggestion of a tectonic slide in this area however, based on the disharmonic nature of the lithologic contacts to the south of the meta-gabbro body at Reitan Station. It is likely that another zone of decoupling occurs here. This fault is recognized as a thrust by other workers (Færden, 1949, Kisch, 1962, Olesen et. al., 1973) where it does crop out at the surface and is probably a $D_1$ generation feature.

## $D_2$

The mesoscopic folds in the Ålen area are predominantly of $D_2$ generation. These folds are open - tight in profile (Fleuty, 1964) and clearly refold the $F_1$ isoclinal folds, the associated $S_1$ fabric, and $S_1$ parallel quartz veins (Fig. 13). They commonly have a well developed axial planar cleavage (Fig. 14a) and are parasitic to the large macroscopic folds indicated in the map area (Plate 1). The axial traces of the macroscopic $F_2$ folds (Fig. 15) were located by the

Figure 14. Photographs of $F_2$ fold features.

Figure 14a. Photomicrograph of $S_2$ axial planar cleavage. Sample from location 793 of Appendix A. Note strain free quartz (cross polarized light).

Figure 14b. Photograph of mesoscopic $F_2$ S fold at location 793. View looking towards west.

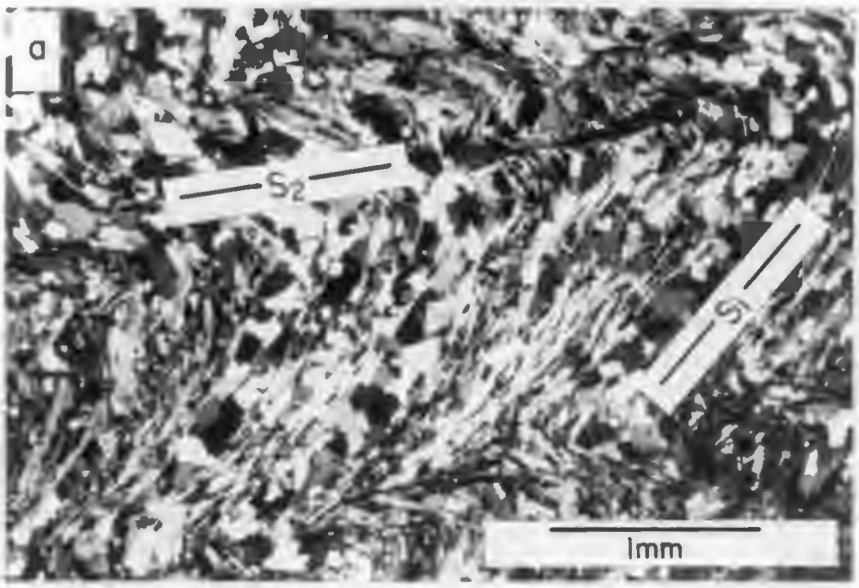
a
S2
S1
1mm

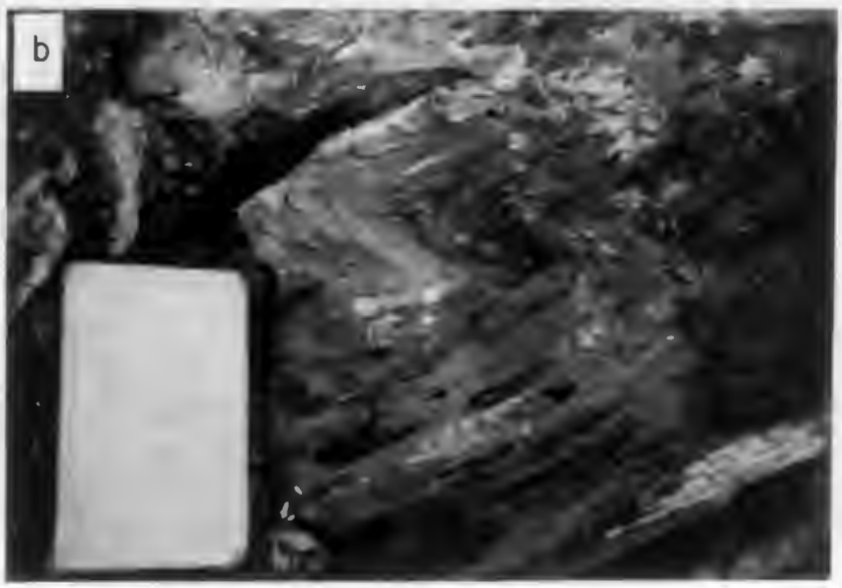
b

Figure 14. cont.

Figure 14c. Photograph of mesoscopic $F_2$ Z fold at location 116 of Appendix A. View looking towards northwest.

Figure 14d. $F_2$ zonal crenulation cleavage developed in fine grained amphibolite from location 116 (cross polarized light).


c

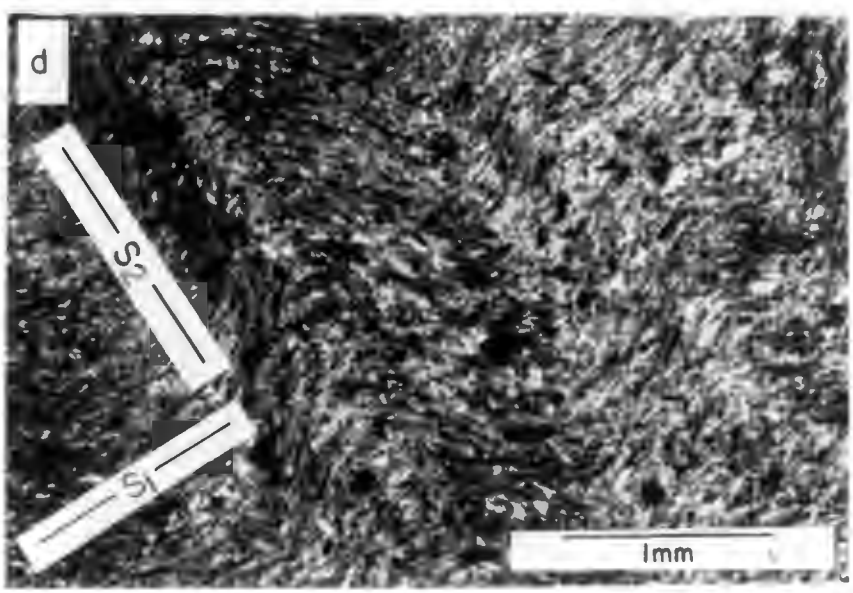
d
S2
S1
1mm

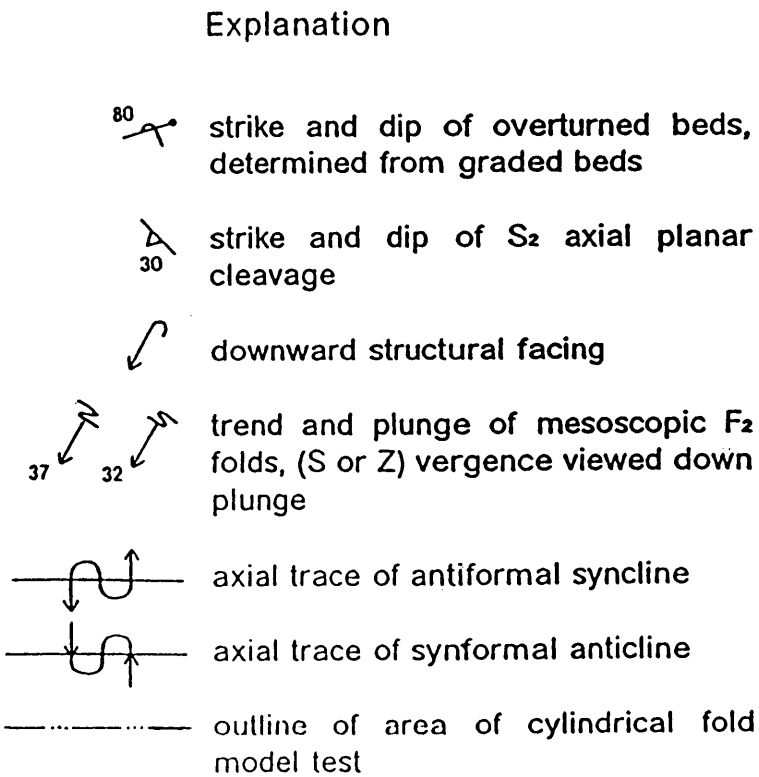


Figure 15. Generalized map showing important structural/stratigraphic features. R = Reitan Station.

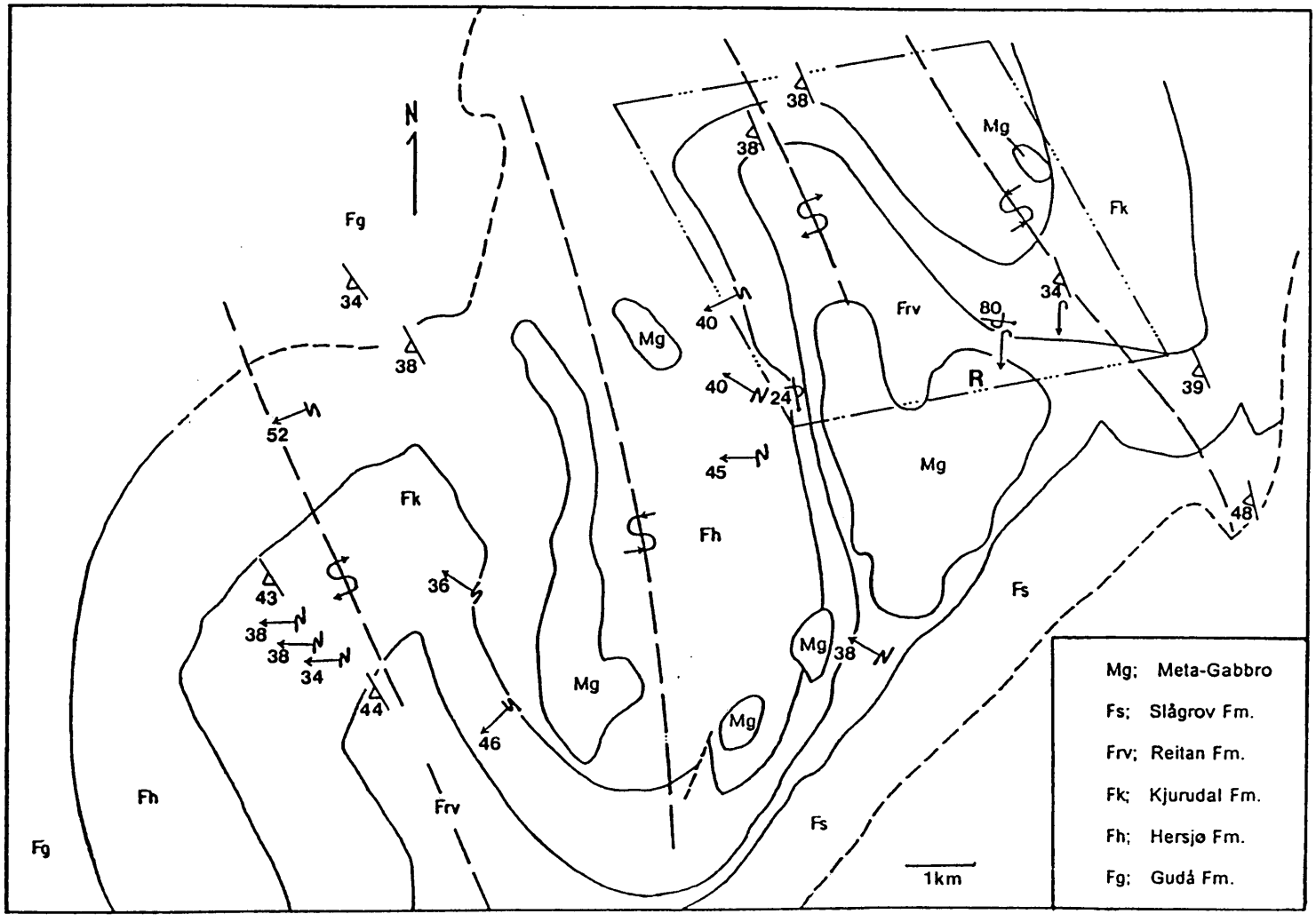
N
Fg
34
38
52
Fk
43
38
38
34
44
36
46
Mg
Mg
Mg
Fh
Frv
Fh
Fg
38
38
Mg
Fk
40
Frv
80
34
40
24
R
39
45
Mg
48
Fs
Mg
38
Fs
1km
Mg; Meta-Gabbro
Fs; Slågrov Fm.
Frv; Reitan Fm.
Fk; Kjurudal Fm.
Fh; Hersjø Fm.
Fg; Gudå Fm.

change in vergence (S or Z, looking down plunge, or north vs. south vergence in the usage of Bell (1981)) of the mesoscopic $F_2$ folds and where the $S_2$ cleavage is nearly orthogonal to the $S_1$ bedding parallel schistosity. Representative examples from two of the localities shown in Figure 15 (793 and 116 of Appendix A) are pictured in Fig. 14b and Fig. 14c respectively. The $F_2$ folds are reclined to moderately inclined, and moderately plunging according to the definitions of fold attitudes of Fleuty (1964). Many of the $F_2$ folds in the Ålen area are reclined. Their hinge lines are parallel to the dip direction of the axial plane (or axial surface when non-planar) (Ramsay, 1967). The point maxima (168 data) of poles to $S_2$ (Fig. 16a) indicates that the mean orientation (strike and dip) of $S_2$ is approximately 351°/38°W. The mean orientation of the $F_2$ axes, 273°/37°, is nearly parallel to the dip direction of $S_2$, indicating the general reclined attitudes of the folds (Fig. 16b)

The axial planar cleavage $S_2$ associated with the $F_2$ folds can range from a very finely spaced (0.25-0.5mm) crenulation of $S_1$ to a more widely spaced (2-4mm) crenulation or asymmetric microfolding (Hanmer, 1979) of the $S_1$ fabric within the mica rich metasediments. In the fine grained amphibolites, spaced crenulation cleavage is zonal, (Powell, 1979) sporadically developed, and consists of slightly differentiated (amphibole rich) microfold limbs (Fig. 14d).

The Pi diagram (Ramsay, 1967) shown in Fig. 16c shows a strong $\pi$ great circle distribution of $S_1$ (541 data) about a $\pi$ axis plunging approximately 275°/40°. The point maxima of the $F_2$ axes (115 data) falls approximately in this orientation (275°/38°). This indicates that the $S_1$ fabric is sub-cylindrically folded about the $F_2$ axes throughout the field area (Ramsay and Huber, 1987) as 90 percent of the data falls within $\pm$ 10° of the $\pi$ great circle. An additional test of the sub-cylindrical fold hypothesis was carried out by plotting the $S_1$ data (91 data) from the limbs and hinge area of the macroscopic fold cored by the meta-gabbro body at Reitan Station (Area in dashed outline in Figure 15) and all the mesoscopic $F_2$ folds (13 data) which occur in this area. A strong $\pi$ great circle distibution of the data ($\pi$ great circle at approximately 356° 49°W) about a $\pi$ axis oriented 265° 41° results (Fig. 17a). This $\pi$ axis is nearly parallel to the $F_2$ fold axes maxima indicated in Figure 15b. Approximately 90 percent of the $S_1$ data falls within $\pm$ 10 degrees of the indicated $\pi$ circle (Fig. 17a), and this indicates sub-

Figure 16. Stereographic projections of: (a) Poles to $S_2$ cleavage, (b) $F_2$ fold axes, (c) Poles to $S_1$ penetrative schistosity.

POLES TO $S_2$

168 DATA

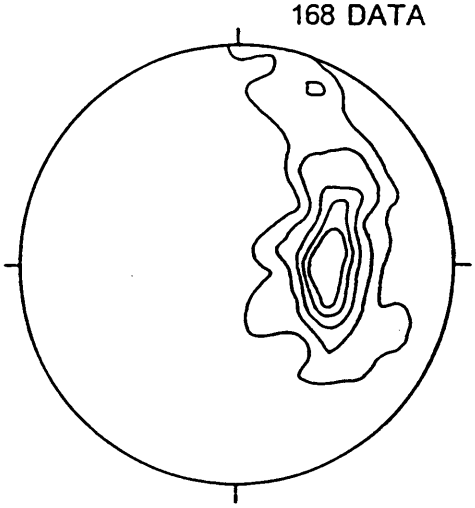

CONTOURED AT 1 3 6 9 12%

$F_2$ AXES

115 DATA

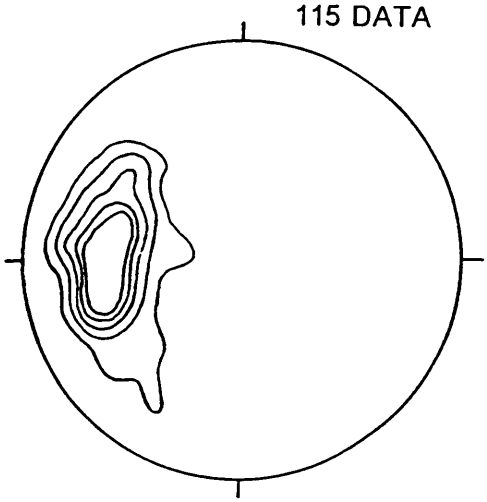

CONTOURED AT 1 3 6 9 12%

POLES TO $S_1$

541 DATA

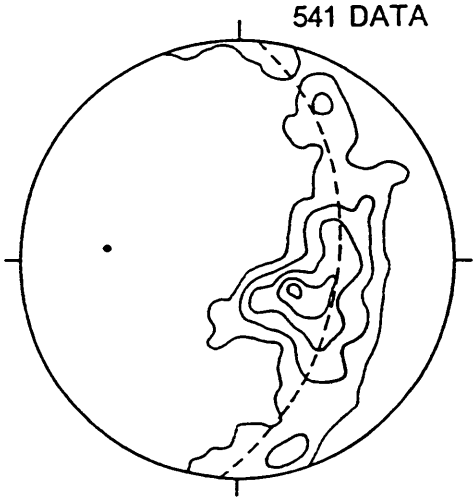

CONTOURED AT 1 3 6 9 12%

Figure 17. Stereographic projections of: (a) Poles to $S_1$ schistosity from area in dashed outline in Figure 15, (b) $L_2$ ($S_1/S_2$) lineations, (c) Mineral elongation lineations, (d) Boudin long axes, closed circles indicate orthogonal relation to nearby $F_2$ mesoscopic fold axes, open circles indicate subparallel relationship to fold axes.

POLES TO $S_1$

91 DATA

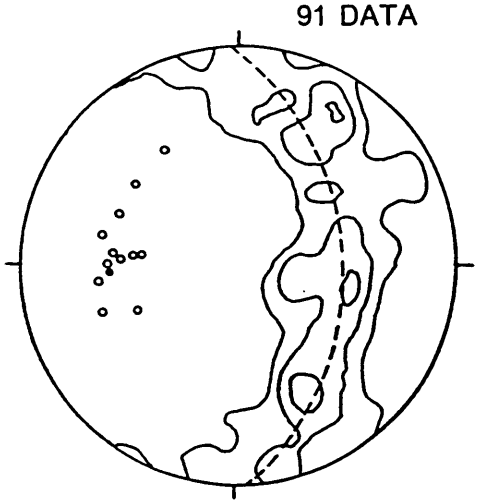

CONTOURED AT 1 3 5%

$L_2$ ($S_1/S_2$) LINEATIONS

92 DATA

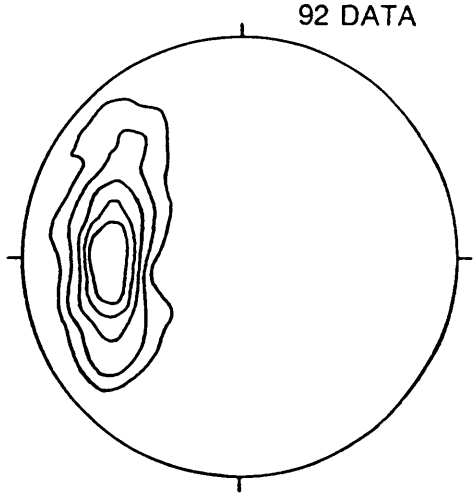

CONTOURED AT 1 3 6 9 12%

MINERAL LINEATIONS ($L_2$)

75 DATA

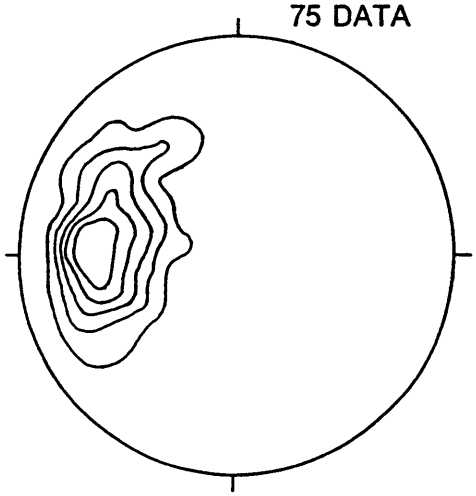

CONTOURED AT 1 3 6 9 12%

BOUDIN LONG AXES

22 DATA

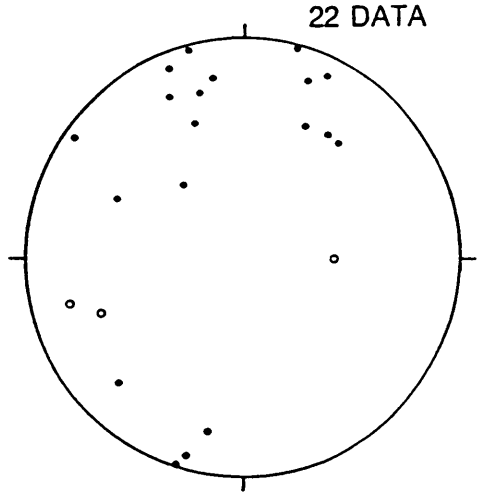

cylindrical folding in this portion of the field area. The structural data has not been further subdivided into domains because the orientation of the $F_2$ folds appears to be relatively constant throughout the study area. This constancy in the orientation of the $F_2$ fold axes differs from that reported by Hardenby (1983) from the Kjølhaugan area in the northern portion of the Meråker Nappe. In the Kjølhaugan area, a structural break is indicated by the change in orientation of the $F_2$ axes. $F_2$ fold axes in the Gula and Fundsjø Groups are EW trending and steeply plunging, whereas $F_2$ axes in the unconformably overlying, structurally underlying Sulåmo Group (Wolff, 1973, Hardenby, 1983) are NNE-SSW trending and shallow plunging. The lack of a corresponding break in the orientation of the $F_2$ axes in the Ålen area at the level of the Hersjø Fm. - Kjurudal Fm. contact supports the inclusion of the Kjurudal Fm., Reitan Fm., and Slågrov Fm. in the Fundsjø Group (See Table 1, Mandeville, 1988).

A stereo net plot (Fig. 17b) of the intersection lineation produced by $S_1/S_2$, ($L_2$), indicates a point maxima at approximately 270°/40° (the data from the entire Ålen area is shown) parallel to the $F_2$ fold axes maxima. This is expected since even where cleavage is refracted, the intersection lineation remains parallel to the fold axes (Ramsay, 1967, Ramsay and Huber, 1987).

A pervasive mineral lineation (stretching lineation) defined by hornblende, and/or elongated plagioclase and quartz grains is present in most of the formations in the Ålen area. It is usually best developed in the volcanic and intrusive lithologies by the parallel allignment of hornblende and plagioclase. It is represented by zones of strongly rodded quartz in the metasedimentary lithologies (e.g. in the Gudå Fm.). This lineation parallels the $F_2$ fold axes as shown in Fig. 17c, and exhibits a point maxima oriented approximately 272°/36°. Although there is some hornblende lineation in $S_1$, the nearly coincident orientation with the $F_2$ fold axes suggests that this lineation may be a late $D_2$ generation feature.

The generalized map of Fig 18 illustrates the orientation of $F_2$ fold axes or $L_2$ intersection lineations within the $S_2$ axial planar cleavage. Structural data from localities 629, 634, 702, and 704 (locations given in Appendix A) indicate that the $L_2$ intersection lineations ($S_1/S_2$) which parallel the $F_2$ fold axes, pitch towards the direction (northwest) in which the macroscopic fold

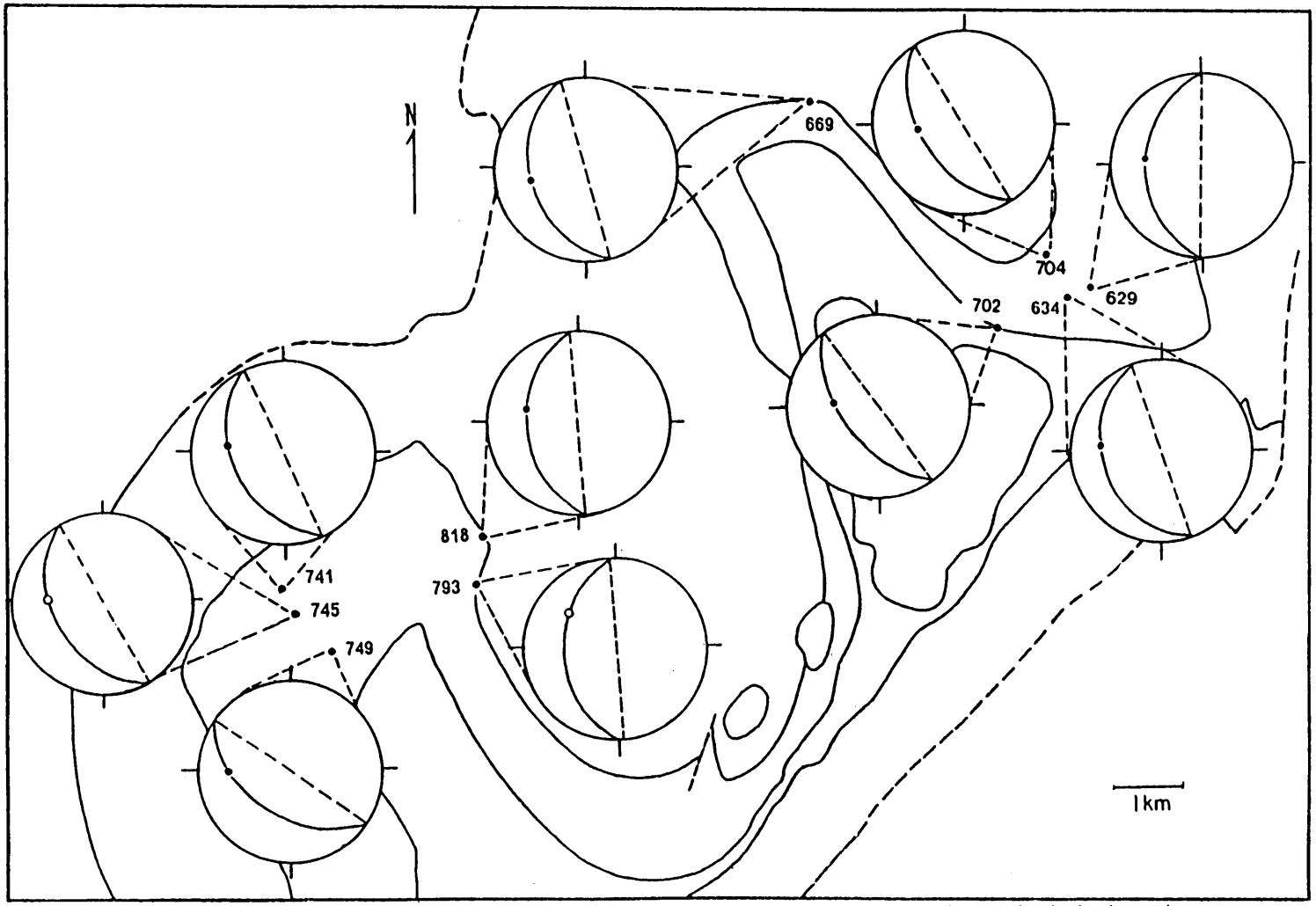


Figure 18. Generalized map illustrating $S_1/S_2$ intersection lineations (closed circles) and mesoscopic $F_2$ fold axes (open circles) plotted within $S_2$ axial planar cleavage.

opens. This indicates that the macroscopic fold is synformal. Preserved graded bedding at locations 701 and 636 along the Gaula River (locations given in Appendix A) indicate a downward structural facing (Shackleton, 1956, Boradaille, 1976) when the direction of younging is projected along the $S_2$ cleavage. The downward structural facing indicates that the macroscopic fold in the northeast portion of the map is a synformal anticline (Fleuty, 1964). There is currently no evidence in the form of a change in structural facing (to upwards) at the Hersjø Fm.- Kjurudal Fm. contact which would indicate crossing of an earlier $F_1$ axial trace within the Kjurudal Fm. It is this relationship which indicates the relative ages of the formations in the Ålen area and demonstrates the general stratigraphic inversion. Moreover, this indicates that the stratigraphy was inverted prior to the $F_2$ folding. The downward structural facing suggests that the stratigraphic inversion is likely to have resulted from the formation of an early recumbent fold.

Orientations of $S_1/S_2$ intersection lineations and $F_2$ fold axes lying within the $S_2$ axial planar cleavage, from localities 741, 745, 749, 793, and 818, (of Appendix A and Fig. 18) pitch towards the direction (north) in which a large macroscopic $F_2$ fold closes. The downward structural facing directions of localities 701 and 636, and the younging direction at location 165 indicates that this structure is an antiformal syncline (Ramsay, 1967). The intervening macroscopic fold closure to the east which closes to the south, and is cored by the Hersjø Fm. and meta-gabbro bodies is probably a synformal anticline. The macroscopic fold closure which lies to the east of this synformal anticline, (area enclosed within dashed outline in Fig. 15) closes to the north, and is cored by the Reitan Fm. and meta-gabbro body at Reitan Station, is an antiformal syncline. This structure is analogous to the macroscopic fold closure near localities 741, 745, 749, 793, and 818, in the southwest portion of the map (Fig. 18).

Many of the mesoscopic $F_2$ folds in the study area are boudined. These are well demonstrated in the Gudå Fm. but are also quite common in all of the Fundsjø Group formations. In the Gudå Fm., competent calcareous beds (mineralogy consisting largely of plagioclase, hornblende, and quartz) surrounded by less competent semipelitic schist beds, are commonmly observed. These interbeded sequences have been folded about $F_2$ axes while in

a shortening field (with respect to the finite strain ellipsoid). These $F_2$ folds most probably entered an elongation field (with respect to the infinitesimal strain ellipsoid) and were subsequently boudined. Although boudinage can take place under conditions of pure shear as well as under conditions of simple shear, this suggests, along with syntectonic rotated garnet porphyroblasts, that the principal axes of the finite strain ellipse have not remained in coincidence with the principal axes of the infinitesimal strain ellipse during the deformation $D_2$. This suggests that the $D_2$ deformation was most probably non-coaxial.

The long axes of boudins were measured throughout the study area and they show a weak distribution roughly orthogonal to the mineral (stretching) lineation (Fig. 17d) and the E-ESE transport direction. When measurements of the orientation of boudin long axes are compared to the orientation of the nearest $F_2$ axis or the $L_2$ intersection lineation within the same outcrop, the common observation is that the boudin long axis is suborthogonal. In a few instances, the long axis of the boudin is subparallel to the fold axis. One would expect that if the boudinage was due to a progressive rotational deformation (Ramsay 1967, Hobbs et. al., 1976) and subsequent extension of a previously formed fold, that the boudin long axis developed would be subparallel to the fold axis (provided that the shear direction remains constant). The cases where boudin long axes are suborthogonal to the nearest fold axis or intersection lineation, might suggest that boudinage took place after the fold axis reorientation (Escher and Watterson, 1974, Roberts and Sturt, 1980) towards the elongation direction. It cannot be assumed that all $F_2$ axes developed simultaneously (Williams 1985), nor can it be assumed that all folds entered the extension field simultaneously. Whether or not a fold axis enters the extension field, and when during the course of the deformation it enters that field, is a function of original orientation (Ramsay, 1967, Hobbs et. al., 1976). The variation exhibited in the relationships between boudin long axes and $F_2$ axes can be explained with regards to these factors. More importantly, the data illustrated in Fig. 17d are consistent with boudinage developed during the latter part of $D_2$ in response to elongation in the direction of transport. At one roadcut along Highway 30 (location 61 of Appendix A), a trondjheimite dike which

clearly truncates $S_1$ and quartz veins parallel to $S_1$, is folded by a mesoscopic $F_2$ fold and is boudined along one limb.

The meta-gabbro bodies which commonly core the $F_2$ folds (Plate 1) are pre-syn $D_2$. Evidence for this is derived from the following field observations: 1) they are affected by the elongation lineation $L_2$, 2) they can be strongly foliated locally (particularly along their margins), 3) they are quite commonly boudined especially where the gabbro is present as dikes within the bedded volcanic lithologies. The S surface developed in these intrusive rocks has been designated $S_i$ on the map of Plate 1 because in many areas $S_1$ and $S_2$ are nearly parallel. The subscript 'i' designates foliation developed in intrusive igneous lithologies. Without primary bedding features in the intrusive rocks (e.g. rhythmic layering) it is not possible to discriminate whether these surfaces are $S_1$ or $S_2$ Even if rhythmic layering were present, it most likely would not have been parallel to the compositional layering in the surrounding host lithologies. Tectonic surfaces of both generations however, are probably present. There does not appear to be any significant change in mineral assemblage from $D_1$ to $D_2$ as indicated by the phases defining the $D_1$ fabrics to those defining $D_2$ fabrics. The semipelitic to quartzo-feldspathic schists of the Gudå Fm. contain syn- to post-tectonic porphyroblasts of garnet, staurolite, and kyanite, indicating that the culmination of the $D_1$- $D_2$ progressive deformation was followed by the continued growth of middle amphibolite facies mineral assemblages. Evidence for syn-$D_1$ growth of garnet is exhibited by the quartzo-feldspathic schists of the Kjurudal Fm. which show garnet porphyroblasts with S internal inclusion patterns truncated by the S external foliation of the matrix (Fig. 19a). This late porphyroblast growth was also accompanied by coarsening of matrix biotite, muscovite, and chlorite, and thermal annealing of strain features in quartz and feldspar. Moreover, mineral phases such as garnet which are syntectonic (Fig. 19b) with respect to $D_2$ as evidenced by internal inclusion trails (Spry, 1969, Jamieson and Vernon, 1987, Ramsay and Huber, 1987), also occur as post-tectonic porphyroblasts which truncate $S_2$ foliation (Ferry, 1980) and are relatively free of inclusions. Minerals which have grown syn-tectonically with respect to $D_1$ and post-tectonically with respect to $D_2$ include: garnet, kyanite, staurolite, amphibole, biotite, chlorite, and muscovite.

Figure 19. Photomicrographs of garnet and biotite porphyroblasts and associated microstructurefeatures.

Figure 19a. Photomicrograph of syn-$D_1$ garnet from Kjurudal Fm. S internal inclusion pattern truncated by $S_2$ of the matrix (cross polarized light).

Figure 19b. Photomicrograph of syn-$D_2$ garnet from Kjurudal Fm. S internal inclusion pattern roughly parallels $S_2$ fabric of the matrix near porphyroblast margins (cross polarized light).

Figure 19c. Photomicrograph of helicitic biotite porphyroblasts overgrowing weak $S_2$ zonal crenulation cleavage of matrix (plane light).

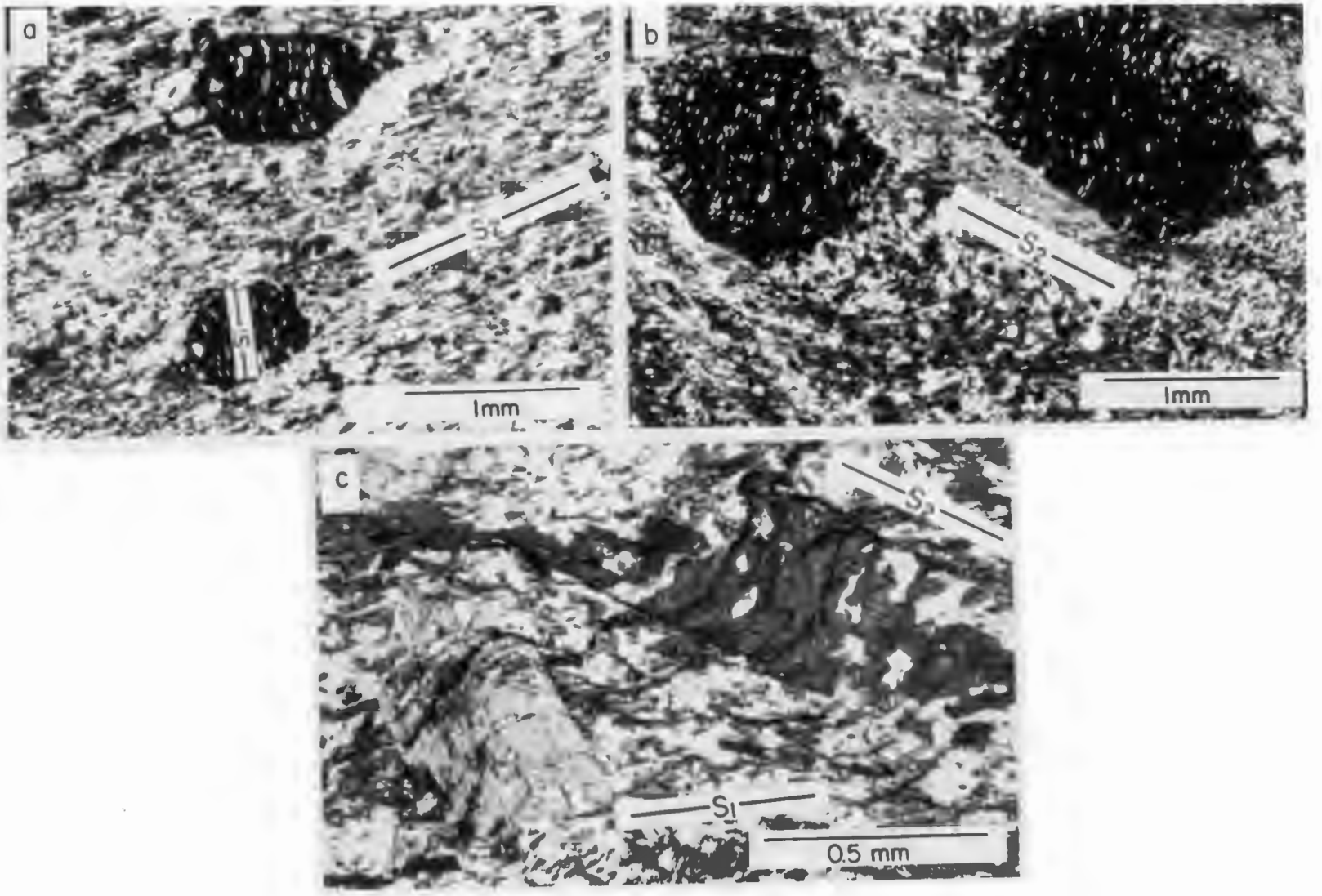
a
S1
1mm
b
S2
1mm
c
S2
S1
0.5 mm

In a few samples, biotite porphyroblasts exhibit helicitic (Spry, 1969) overgrowth of crenulated $S_1$ (Fig. 19c), suggesting that porphyroblast growth was taking place while the $S_2$ crenulation cleavage was being formed in the rock. It is also possible that biotite porphyroblast growth in this sample continued after $D_2$ because the crenulation developed in the matrix does not tighten relative to that preserved in the porphyroblast (Jamieson and Vernon, 1987). In samples where the $S_2$ spaced cleavage is nearly penetrative, interstitial quartz and oligoclase are relatively strain free, polygonized, and exhibit uniform extinction. Quartz and feldspar have undergone extensive recrystallization as a result of post $D_2$ annealing and strain features (e.g. deformation bands, subgrains) in these phases are rare probably due to thermally activated recovery (Nicholas and Poirier, 1976, Bell and Etheridge, 1976). This period of thermal annealing is most likely the result of a metamorphic peak after $D_2$ which is evidenced by post-tectonic porphyroblast growth, and grain size coarsening of the $M_{1-2}$ mineral assemblages. Therefore, the $D_1$-$D_2$ deformation is interpreted as a continuum, separated from $D_3$ by a static period of strain recovery perhaps associated with the peak of regional metamorphism.

The meta-gabbro bodies may have nucleated the macroscopic $F_2$ folds. The lack of such large $F_2$ folds along strike to the south of the Ålen area (Fig. 5) may be due to the lack of such large meta-gabbro bodies there. This suggests an association between the intrusives and the macroscopic $F_2$ folds.

The relative constancy in the orientation of the $F_2$ folds allowed for the construction of a three dimensional diagram to show the approximate orientations of the enveloping surfaces of the map scale $F_2$ folds. This diagram (Fig. 20) accompanies the map of Plate 1 and is substituted in place of a standard geologic cross section because it is more informative. It was constructed by creating an "up-plunge" fold profile according to the method of Wilson (1967) as outlined in Ragan (1968), which takes topographic relief into account, and assumes cylindrical folding. An average $F_2$ fold axis orientation of 275° 35° plunge was assumed over the entire map area because variations from this orientation do not appear to be large nor systematic from one portion of the study area to the next. For illustrative purposes, this as-

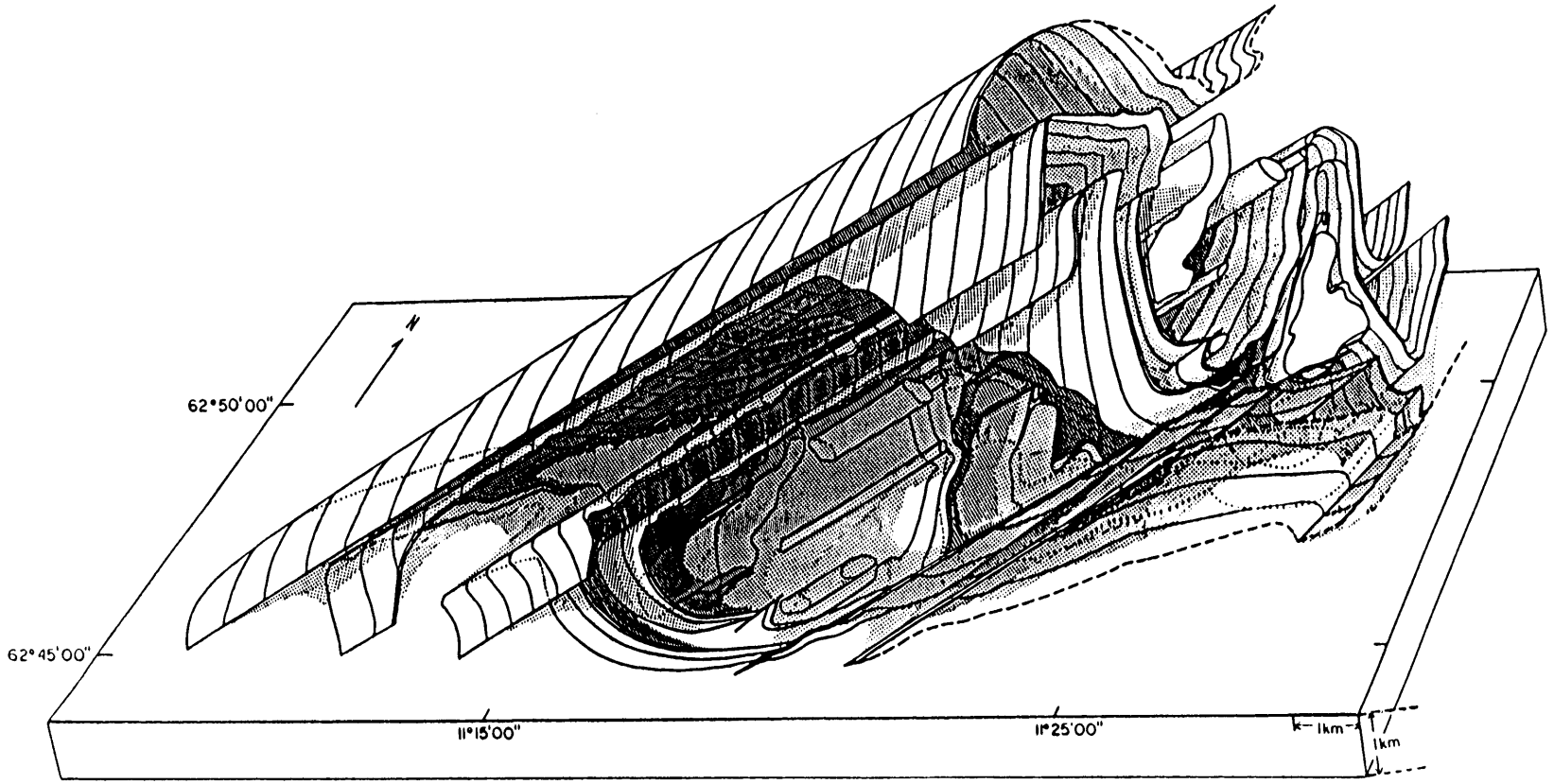


Figure 20. Three dimensional diagram of macroscopic $F_2$ fold enveloping surfaces. Gabbro intrusives are shown as solid cylinders.

sumption of constant fold orientation is justified in that it probably introduces less error into the construction than trying to integrate several smaller fold profiles (each constructed using different $F_2$ axis orientations). Both the map of Plate 1 and the up-plunge fold profile were then transferred to 3 point perspective grids (plan 15° - 75°, altitude 30°). The final stage in the construction of the diagram was to connect the surfaces in the perspective view of the fold profile to their actual down plunge locations on the perspective view of the geologic map. Cutaway surfaces were then prepared to show as many of the enveloping surfaces as possible. Although unrealistic in detail, the shapes of intrusive rock bodies were projected as solid cylinders without shape change because no data are available to constrain their shapes in the up-plunge profile and they also serve as "landmarks" for a viewer's eye.

The possibility that the $F_2$ fold axes may have been rotated into coincidence with the maximum elongation direction also raises the question as to whether a significant amount of the deformation was by simple shear. To address this problem thin sections were prepared from hand samples which have the appearance of mylonites developed within the fine grained amphibolites. These were prepared such that the thin section is oriented parallel to the elongation lineation, (X), and perpendicular to the foliation as illustrated in Simpson (1986). In several samples there is evidence of grain size reduction by crystal-plastic processes, type 3 quartz ribbons (Boullier and Bouchez, 1978) and preferred length orientation of amphiboles. However, kinematic indicators in the samples prepared up to present are not consistent on the scale of a thin section and it is therefore not possible to verify unequivocally that there has been west over east movement. A significant part of the problem in the Ålen area is the general fine grain size of the lithologies, and the post tectonic thermal annealing which appears to have caused extensive recrystallization. Both of these factors contribute to the difficulty in identifying true mylonites in the field and to the determination of movement sense within those samples presumed to be mylonites. It is also possible that much of the ductile deformation was not partitioned into discrete zones during the deformation but was more homogenously distributed.

## $D_3$

Features associated with the $D_3$ phase of deformation generally are oriented NS. These features are relatively smaller scale than that of $D_1$ - $D_2$, and are suggestive of deformation under somewhat more brittle conditions. This phase of deformation is likely to have been achieved by "elastico-frictional" processes (Sibson, 1977).

The $F_3$ folds in the study area are kink folds which have a NS trend and shallow plunge (Fig. 21a). The experimental work of Anderson (1974) indicates that the requirements for the generation of kink folds are that the rock must possess a strong planar isotropy, and that compression acts along the plane of the anisotropy. In this case the anisotropy is due to the penetrative $S_1 \pm S_2$ schistosity. The generally NS orientation of the $F_3$ axes suggests a compression in an EW direction in the direction of transport. As mentioned previously, the simple shear model (Escher and Watterson, 1974) for the reorientation of fold axes towards the stretching lineation suggests that later formed folds are likely to remain at a high angle to this direction. The NS orientation of the $F_3$ axes may reflect their formation relatively late in the deformation history. These small-scale structures were most likely generated during the Scandian (or Scandinavian) phase of orogenesis (Roberts and Sturt, 1980, Gee et. al., 1985).

The relatively small-scale nature of the $D_3$ structures is suggested by the lack of redistribution of poles to $S_2$ axial planar cleavage about the NS $F_3$ axes (Fig. 21a). Nor is there any strong indication of redistribution of the $F_2$ axes (Fig. 16b) by the $F_3$ axes.

The $L_3$ lineation which is a crenulation lineation developed on $S_1$ or $S_2$ planes is also generally NS trending and shallow plunging (Fig. 21b). In a few localities this lineation is observed to fold a preexisting $L_2$ crenulation in the same rock. A rare $S_3$ spaced cleavage and the orientation of axial planes of $F_3$ folds have a NS trend and upright orientation.

In several localities within the study area, the kink folds are associated with late brittle microfaullts which commonly have zones of cataclasite and pseudotachylite veins (Philpotts, 1964, Sibson, 1975, 1977, Sibson, et. al., 1981) developed along them. The variety of kink bands

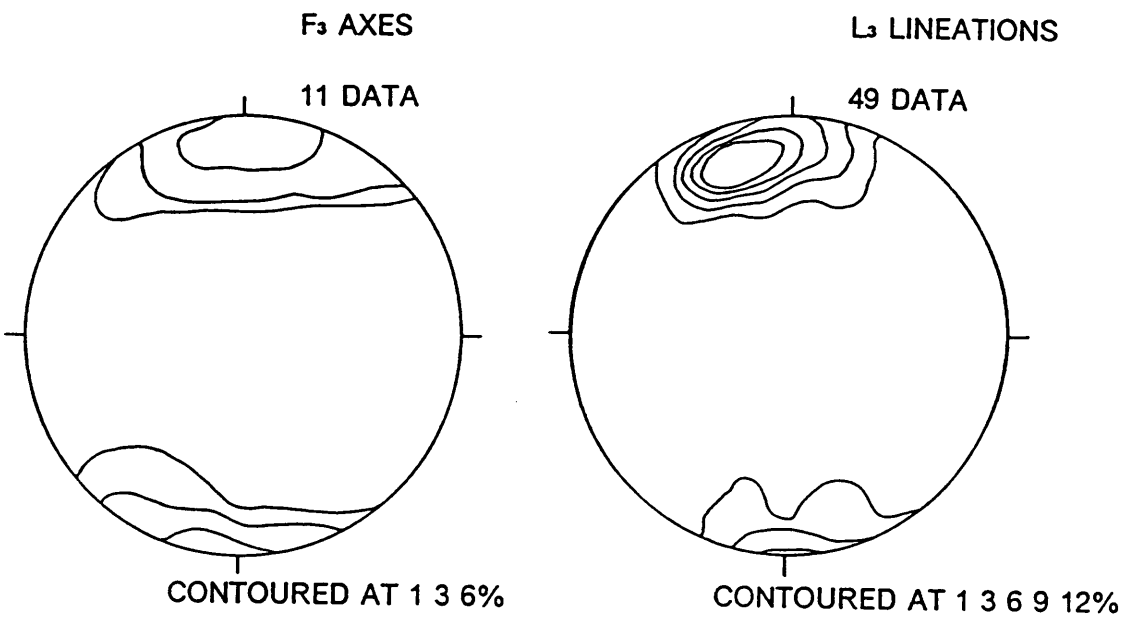


Figure 21. Stereographic projection of: (a) $F_3$ fold axes, (b) $L_3$ lineations.

developed are the contractional type as illustrated in Ramsay and Huber (1987) and Fig. 22a. These commonly progress into brittle microfaults which have been grouped with the $D_3$ structures. Similar microfaults were generated in the experimental work of Anderson (1974). These small-scale structures are likely to represent features generated during the later stages of nappe translation.

Strain features associated with $D_3$ are present in the rocks affected by this deformation. On the thin section scale these features include: deformation bands in quartz, kinked biotite porphyroblasts, small scale asymmetric kink folds which progress to through-going microfaults, intergranular fractures associated with protocataclasite-cataclasite (Sibson, 1977). Commonly the cataclasite is in zones parallel to the preexisting foliation. Injection veins (Sibson, 1975) of pseudotachylite intrusive into the protocataclasite-cataclasite are present (Fig. 22b). This material is interpreted to be of frictional melt origin as reported by (Philpotts, 1964, Sibson, 1975, 1977, Allen, 1979, Maddock, 1983). Though it is somewhat devitrified, the pseudotachylite is largely isotropic and shows indication of a chilled margin relatively free of country rock fragments. It is assumed here that devitrification would be much more extensive had this material been generated prior to the metamorphic peak. Microstructural features of $D_3$ generation indicate deformation dominantly by cataclasis (Rutter, 1986) or elastico-frictional processes (Sibson, 1977).

## Structure of Intrusive Rock Units

Most of the intrusive rocks in the Ålen area have been affected by the $D_2$ deformation. In most cases the igneous lithologies are strongly lineated and foliated. In the meta-quartz diorite bodies, elongated country rock xenoliths are quite common and are alligned with the stretching lineation in the surrounding metasediments. The meta-gabbro bodies are commonly tectonized particularly along their boundaries, and exhibit a marked mineral lineation and foliation similar in orientation to those found in the surrounding

Figure 22. Photographs of $D_3$ generation structural features.

Figure 22a. Photograph of $F_3$ kink folds in the Kjurudal Fm. View looking towards south. Note small microfault below cm bar scale.

Figure 22b. Photomicrograph of pseudotachylite injection vein, and cataclasite developed within fine grained amphibolite of the Hersjø Fm. (cross polarized light). Sample from location 26 of Appendix A.

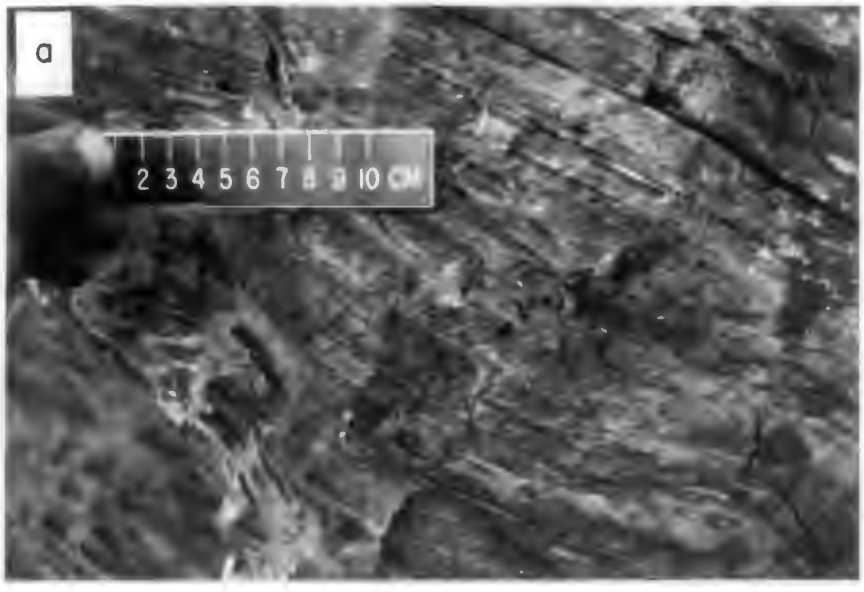
a
2 3 4 5 6 7 8 9 10 CM

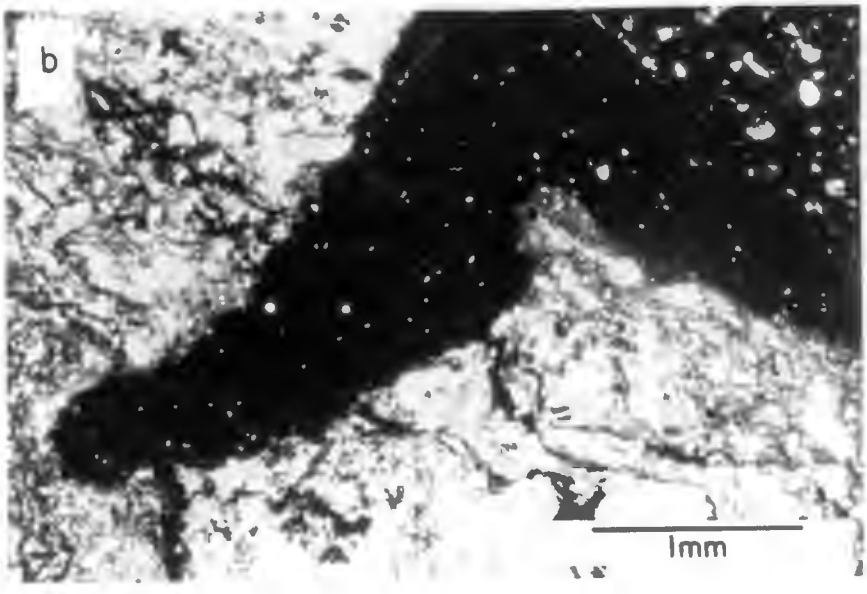
b
1mm

metavolcanics/metasediments. In the southern part of the map (Plate 1), the contacts of a smaller meta-gabbro body are discordant to the lithologic boundary between the Hersjø Fm. and Kjurudal Fm., indicating post depositional emplacement. Numerous meta-gabbro dikes have also been observed within the bedded metavolcanics of the Hersjø Fm., but in most cases, these are either conformable, or subsequent boudinage has made the contact relationships less clear.

The map pattern of the larger meta-gabbro body at Reitan Station also indicates local discordance to the lithologic boundaries and bedding parallel schistosity of the surrounding Reitan and Kjurudal Formations. However, no mesoscopic $F_1$ isoclinal folds (which have $S_1$ as axial planar cleavage) clearly cross-cut by meta-gabbro were observed. It is possible that at least some of the gabbro in the Ålen area may have been emplaced prior to $D_1$ and may represent localized magma chambers associated with the concordant blastporphyritic sills (Mandeville, 1988) and fine grained sills found within the metavolcanic sequences. The close field association of the meta-quartz diorite with the meta-gabbro bodies also suggests that some of the quartz diorite emplacement may have taken place prior to $D_1$ The most convincing evidence of intrusive activity prior to $D_1$ is the presence of isoclinally folded Trondjheimite veins and dikes within the Hersjø Formation. These field relationships along with the age constraint placed on the Fundsjø Group by the *Dictyonema* occurrence at Nordaunevol, (Vogt, 1889, Vogt, 1940, Stømer, 1941) suggest that gabbro, quartz diorite, and trondjheimite intrusion may have taken place during the Early Ordovician (possibly Tremadocian).

At one road cut along highway 30 (location 61 of Appendix A) approximately 4 km. south of Ålen, a trondjheimite dike which clearly cross-cuts the bedding parallel schistosity ($S_1$) as well as $S_1$ parallel quartz veins, is itself folded about an $F_2$ fold axis, suggesting pre-syn $D_2$ emplacement. A few relatively massive textured, relatively undeformed trondjheimite dikes are also present within the Kjurudal Formation. These occurrences indicate that there is more than one generation of Trondjheimite and that intrusive activity probably ranges into the Silurian.

## Discussion

The parallelism of mesoscopic fold axes and a pronounced mineral lineation (elongation lineation) has been recognized in the Caledonides of the Scottish Highlands (Wilson, 1953, McClay and Coward 1981), the Grenville front (Dalziel et. al. 1969) the Central Appalachians (Cloos 1946, Bryant and Reed 1969), the Scandinavian Caledonides (Kvale 1953, Hossack 1968, Roberts and Sturt, 1980) and in Alpine Corsica (Mattauer, et. al., 1981). Parallelism of the $F_2$ fold axes with the mineral elongation lineation in this study area is indicated in Figures 16b and 17c. It is generally assumed that fold axes initiate normal to the compression direction (Cloos, 1946). This would imply from the orientation of the $F_2$ fold axes in this study area, that compression was due to a NNE - SSW trending stress couple and that the movement direction was either to the NNE or SSW. Yet the recognized transport direction for the nappes in this central portion of the Norwegian Caledonides is E - ESE (Hardenby 1983, Hossack and Cooper 1986, Roberts and Sturt 1980). It is possible that this parallelism is the result of deformation involving simple shear and progressive rotation of the fold axes within their axial planes, into near coincidence with the direction of maximum elongation, X (where $X \geq Y \geq Z$) as suggested by Bryant and Reed (1969) and Escher and Watterson (1974). If the fold axes initiate exactly parallel to the intermediate elongation direction (Y), and the simple shear deformation is homogenous, then the fold axis is not reoriented towards X with further increments of shear strain. However, if the fold axis originated slightly oblique to Y, and the simple shear strain is slightly inhomogenous, the fold axis can be reoriented towards X with increased strain as shown by (Escher and Watterson 1974).

Sanderson (1973) showed that a Gaussian distribution of fold axes about a mean corresponding in orientation with Y, may be reoriented towards X with low strain (X/Y) if the standard deviation of the original data is large. Conversely, high strain is required to reorient the original axes towards X if the standard deviation of the original data is small.

Notably lacking in the Ålen area are $F_2$ folds which are orthogonal to the mineral elongation direction. Generally the $F_2$ axes and mineral elongation X are subparallel - parallel. This suggests that rotation of fold axes may have taken place, and possibly to an advanced stage.

A significant aspect of the model presented by Escher and Watterson (1974), is that folds formed later in the deformation are more likely to remain at high angles to the stretching direction than earlier folds. The subparallel orientation of the $F_1$ and $F_2$ folds might be explained by such a process. The NS trending $F_3$ folds which are relatively shallow plunging and orthogonal to the elongation lineation probably retain their original orientations.

A pertinent question raised by the observed parallelism of $F_1$, $F_2$ axes, the intersection lineation, $L_2$ ($S_1/S_2$), and the mineral (elongation) lineation, is whether the macroscopic folds are sheath (or tergiversate) folds as described by Dearman (1969), Bell (1978), and Cobbold and Quinquis (1980). The characteristic feature of sheath folds is the change in direction of the fold axis within the axial plane up to 90° (Dearman 1969). If the macroscopic $F_2$ fold surfaces shown in the 3 dimensional diagram (Fig. 20) accompanying the map of Plate 1 are of this type, then it is possible that the folds close to the east in the direction of transport. None of the larger mesoscopic $F_2$ axes observed turned back on themselves within a single exposure. However, at one roadcut along Highway 30 to the west of Ålen, what appear to be small scale isoclinal sheath folds defined by calcareous beds within a semipelitic matrix were observed above highway level. These were grouped with the $F_1$ folds based on their isoclinal geometry. The data accumulated up to present does not prove or disprove the existence of macroscopic $F_2$ sheath folds. However, the mesoscopic analogues of these appear to be rare in the Ålen area. The sub-cylindrical geometry exhibited by the $S_1$ data would suggest very large simple shear strain if these structures do close in an easterly direction.

An alternative hypothesis and one that is currently favored due to the lack of abundant mesoscopic sheath folds, would be that the folds do not close in an easterly direction but perhaps decrease in amplitude to the east. The folds may have originally been generated by differential movement along some portions of the bounding thrusts and may have had more

of a NE or E vergence. The original vergence direction of these macroscopic folds has probably been significantly modified due to tectonic transport.

## Tectonic Implications

There is accumulating evidence (Klingspor and Gee, 1981, Hardenby et. al., 1981, Hardenby, 1983, Lagerblad, 1981, 1984, Andreasson and Gorbatschev, 1980) which suggests that the Gula Nappe and lower portion of the Meråker Nappe (represented by the Fundsjø Group) have undergone similar pre-Middle Ordovician deformation and metamorphism. The Fundsjø Group and Gula Group (Wolff, 1967, 1973,) contain middle amphibolite grade mineral assemblages (Olesen et. al., 1973, Guezou, 1978, Lagerblad, 1984) which postdate the second phase of deformation. In the Fundsjø Group of the Ålen area, it has been possible to distinguish the $S_1$ foliation from the $S_2$ foliation more readily than in areas further north or south within the Meråker Nappe. The textural evidence presented in this paper indicates that amphibolite facies metamorphism accompanied $D_1$ and that these P -T conditions persisted beyond the close of $D_2$. This differs slightly from the relationship described by Lagerblad (1984) which states that high grade metamorphism began during $D_2$.

The $D_1$ deformation exhibited in the Ålen area most probably began during pre-Middle Arenig time. In the lower grade Støren Nappe to the west there is evidence of a pre-Middle Arenig deformation (Furnes et. al., 1980, Roberts et. al., 1985) related to ophiolite obduction. If the unconformity represented by the Lille Fundsjø Conglomerate (Chaloupsky and Fediuk, 1967, Wolff, 1973, Hardenby, 1983) separating the Sulåmo Group from the stratigraphically underlying Fundsjø Group is contemporaneous with the ophiolite obduction in the west, then it is likely that amphibolite facies metamorphism and $D_1$ of this paper are of this age or older. This early deformation and amphibolite facies metamorphism may represent a late stage of the Finnmarkian (Sturt et. al., 1978, Roberts and Sturt, 1980). U/Pb data (zircon) and Rb/Sr whole-rock studies (Klingspor and Gee, 1981) of trondjheimites cross-cutting isoclinal folds

within the Gula Nappe have yielded Lower-Middle Ordovician ages. The pressure, temperature and mineral chemistry data reported in this paper indicate that the Fundsjø Group attained middle amphibolite P - T conditions during a relatively static period following $D_2$. Lagerblad (1984), and Andréasson and Gorbatschev (1980) report that the Gula Group and Fundsjø Group reached middle- upper amphibolite grade during a relatively static period prior to, or at an early stage of the Mid-Late Silurian (Roberts and Sturt, 1980, Gee et.al., 1985) Scandian phase of orogenesis. The 8.0 kb ± 500 b. pressure estimate obtained from the Fundsjø Group in this study suggests that the Fundsjø Group of the Meråker Nappe and the Gula Nappe share a common early Ordovician development history distinct from that of the lower grade Støren Nappe which contains fragmented ophiolites (Furnes et. al., 1980), and late Arenig-early Llanvirn fossils of North American provincial affinity (Bruton and Bockelie, 1980). In light of these findings, the sequence of metamorphosed lithologies present in the Fundsjø Group (Mandeville, 1988) and the Gula Nappe may be of distal Baltic continental margin affinity. These characteristics appear to be more consistent with the Seve Nappes or Lower Köli Nappes which commonly show a gradational contact with the Seve nappes (Stephens and Gee, 1985). Furthermore, the lack of fossils of North American provincial affinity, within the Lower Ordovician of both the Gula and Meråker Nappes, allows for their derivation from the Baltoscandian margin during the Finnmarkian phase of orogenesis.

This work impacts current plate tectonic models (Stephens and Gee, 1985, Roberts et. al., 1985) developed for the Upper Allochthon of the central Scandinavian Caledonides because it suggests that the Fundsjø Group of the Meråker Nappe and the Gula Nappe share an early Ordovician development history distinct from that of the lower grade, ophiolite bearing Støren Nappe and are unrelated to an island arc environment. Both Stephens and Gee (1985) and Roberts et. al., (1985) incorporate an immature island arc represented by the Fundsjø Group into their tectonic models. The island arc tectonic setting interpreted (Grenne and Lagerblad, 1985) for the Fundsjø Group was based primarily on geochemical data. A more recent study of the Fundsjø Group (Mandeville, 1988) adopted a facies analysis approach and characterized the likely mode of emplacement of the volcanics and overall nature of the succession. This

more recent study indicated that a rifted Baltoscandian margin setting is more consistent with the general characteristics of the succession. Therefore, this author does not favor the correlation of the Meråker Nappe with the "Gjersvik Terrane" of Stephens and Gee (1985) which suggests that it is part of a "main magmatic arc" but proposes that the Fundsjø Group of the Meråker Nappe is more likely a rift related succession which accumulated in the distal portion of the Baltoscandian margin.

The simplified tectonic model (Fig. 23) proposed in this paper for the Upper Allochthon of the central Scandinavian Caledonides incorporates the predecessors of the Meråker and Gula Nappes into the rifted Baltoscandian margin in the Tremadocian (Fig. 23a). The Støren Nappe and mature island arc/marginal basin couplet (Roberts et. al., 1985) represented on the island of Smøla and in the Hølonda area (Fig. 1) is placed on the Laurentian side of Iapetus due to the presence of late Arenig-early Llanvirn fossils of North American provincial affinity (Bruton and Bockelie, 1980). This mature arc may have initially developed as early as the Tremadocian on the Laurentian side oflapetus. A segment of oceanic crust perhaps related to marginal basin development separates the island arc from the Laurentian margin (Figure 23a). It is also possible that the island arc initially developed on the Laurentian margin and it may not have had an associated ensimatic marginal basin lying to the west of it.

The pre-mid Arenig deformation exhibited by the Støren Nappe (Holtedahl, 1920, Furnes et. al., 1980, Gee et. al., 1985) is shown (Fig. 23b) as possibly related to a change in subduction polarity which may also have involved some ophiolite obduction.

The Middle Ordovician deformation exhibited by the Gula Nappe (Klingspor and Gee, 1981) and Meråker Nappe (Hardenby et. al., 1981, Hardenby, 1983, Lagerblad, 1981, 1984, and this paper) and pre-Scandian? amphibolite facies metamorphism of the Gula and Meråker nappes is attributed (fig. 23c) to mature arc/marginal basin collsion with the outermost portion of the Baltoscandian margin. It is inferred that the Gula and Meråker nappes are of higher metamorphic grade and higher strain due to their position below the overriding arc/marginal basin complex. This model implies that the Støren, Gula and Meråker nappes were assem-

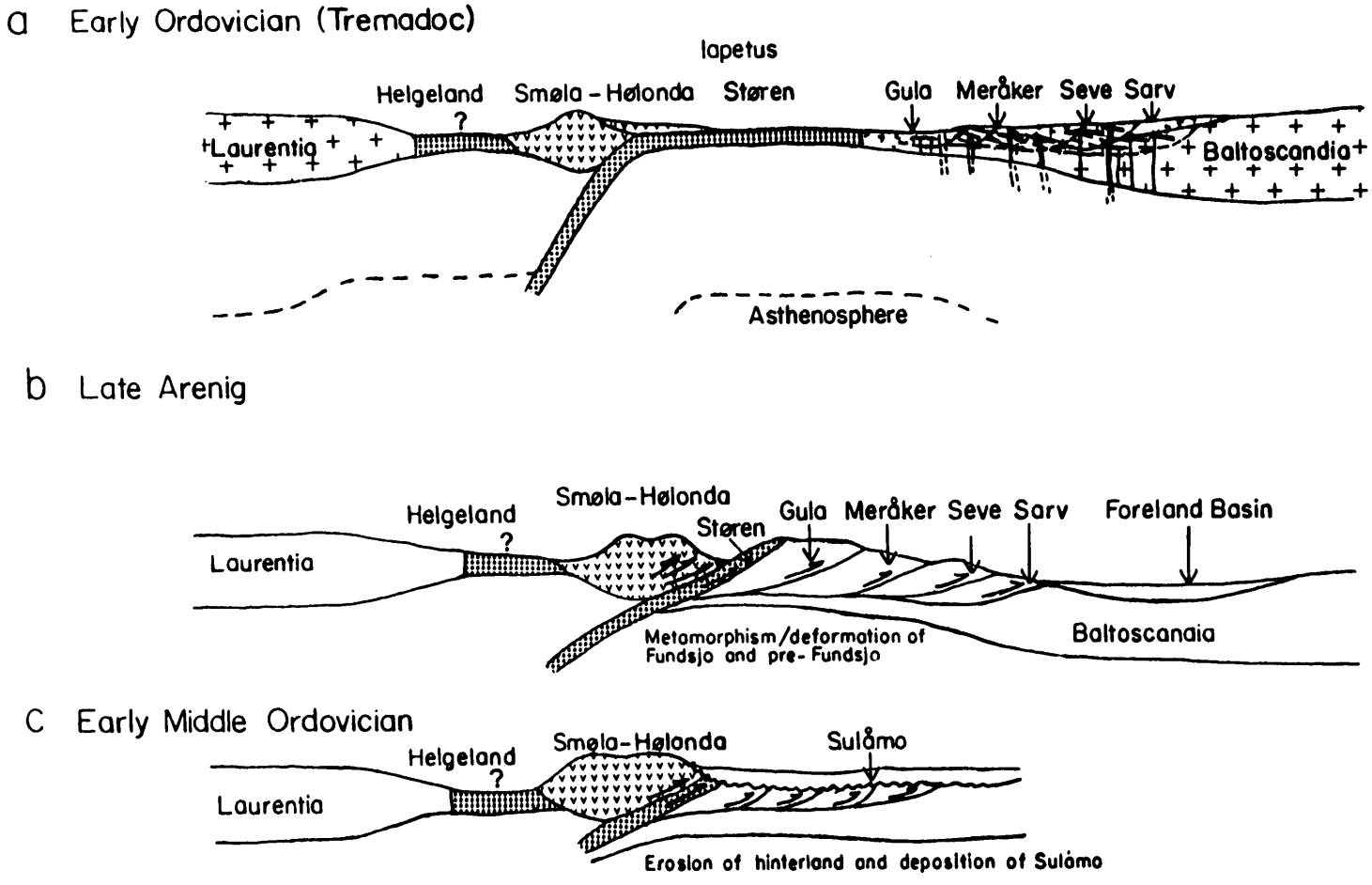


Figure 23. Simplified tectonic model for the Upper Allochthon of the Trondheim Region, central Scandinavian Caledonides.

bled prior to final emplacement onto the Baltoscandian margin during the Scandian phase of orogenesis.

# Conclusions

1) The stratigraphy of the Fundsjø Group in the Ålen area was inverted prior to the $D_2$ phase of folding, as indicated by downward structural facing in the Kjurudal Fm. The overturned sequence probably originated as the highly strained lower limb of a $D_1$ recumbent fold.

2) The map scale folds of the Ålen area are $D_2$ features and are generally reclined in orientation, but can be locally moderately inclined, and moderately plunging.

3) Parallelism of fold axes and stretching lineation implies passive rotation of fold axes into the ESE transport direction and deformation by approximate simple shear. The orientation of boudin long axes are consistent with this interpretation.

4) The $D_1$ and $D_2$ deformations represent a continuum as indicated by dominantly ductile deformation and by accompanying amphibolite facies mineral assemblages. This continuum may represent a late stage of the Finnmarkian phase of orogenesis. The $D_3$ deformation was

achieved largely by cataclasis or elastico-frictional processes and probably took place during the later stages of the Scandian phase of orogenesis.

5) Regional metamorphism was of the medium pressure facies series and lower - middle amphibolite grade during the $D_1$ - $D_2$ continuum. These P - T conditions maintained after the close of this event as evidenced by post-tectonic mineral growth. Post-tectonic garnet-biotite pairs yield temperatures which range from 530° C - 590° C. Pressure estimates derived from the QGAP geobarometer range from 7.5 - 8.5 kb and indicate an overburden of 26 - 28 km thickness. Tectonic thickening which likely culminated in the Scandian phase of orogenesis may account for up to 15 km of this overburden.

6) The differences in temperature estimates derived from the eastern to the western portions of the study area lie within the margin of error associated with the garnet-biotite geothermometer, and suggest that the absence of staurolite and kyanite in the east is due to low aluminum bulk compositions. This is supported by similar amphibole and plagioclase chemistry within amphibolites from the eastern and western portions of the study area.

7) The Fundsjø Group of the Meråker Nappe, and the Gula Nappe most likely represent the outermost portion of the rifted Baltoscandian margin. This outermost portion of the Baltoscandian margin was deformed and metamorphosed to amphibolite grade during a pre-mid Arenig collision with a mature arc/marginal basin complex. This early Ordovician deformation resulted in the initial assembly of the Trondheim Nappe Complex. Subsequent deformation during the Scandian phase of orogenesis resulted in further transport of the Trondheim Nappe Complex onto more proximal portions of the Baltoscandian margin.

# Bibliography

Allen, A.R., 1979. Mechanism of frictional fusion in fault zones, Journal of Structural Geology, v. 1, pp. 231-249.

Anderson, T.B., 1974. The relationship between kink bands and shear fractures in experimental deformation of slate: Journal of the Geological Society of London, v. 130, pp. 231-243.

Andréasson, P.G., and Gorbatschev, R., 1980. Metamorphism in extensive nappe terrains: a study of the Central Scandinavian Caledonides, Geologiska Föreningens i Stockholm Förhandlingar, v. 102, pt. 4, pp. 335-357.

Asklund, B., 1938. Hauptzüge der Tektonik and Stratigraphie der mittleren Kaldoniden in Schweden, Sveriges Geologiska Undersökning, C417, 99 pp.

Bell, A.M., 1981. Vergence: an evaluation, Journal of Structural Geology, v. 3, no. 3, pp. 197-202.

Bell, T.H., 1978. Progressive deformation and reorientation of fold axes in a ductile mylonite zone: the Woodroffe thrust: Tectonophysics, v. 44, pp. 285-321.

Bell, T.H., and Etheridge, M.A., 1976. The deformation and recrystallization of quartz in a mylonite zone, Tectonophysics, v. 32, pp. 235-267.

Bence, A.E., and Albee, A.L., 1968. Empirical correction factors for the electron microanalysis of silicates and oxides, Journal of Geology, v. 76, pp. 382-403.

Best, M.G., 1982. Igneous and Metamorphic Petrology. W.H. Freeman and Company, San Francisco, 630pp.

Bogen, N.L., 1985. Stratigraphic and sedimentologic evidence of a submarine island-arc volcano in the lower Mesozoic Penon Blanco and Jasper Point Formations, Mariposa County, California, Geological Society of America Bulletin, v. 96, no. 10, pp. 1322-1331.

Boradaille, G.J., 1976. "Structural facing" (Shackelton's Rule) and the paleozoic rocks of the Malaguide Complex near Vélez Rubio, SE Spain, Proccedings of the Koninklijke Nederlandse Akademie van Wetenschapen, Amsterdam, series B, v. 79, no. 5, pp. 330-336.

Boullier, A.M., and Bouchez, J.L. 1978. Le quartz en rubans dans les mylonites: Bulletin de le Societe Geologique de France, v. 7, pp. 253-262.

Bouma, A.H., 1962. Sedimentology of some Flysch Deposits: A graphic approach to facies interpretation: Elsevier, Amsterdam, pp. 168.

Boyer, S.E., and Elliot, D., 1982. Thrust systems, American Association of Petroleum Geologists Bulletin, v. 66, pp. 1192-1230.

Bruton, D.L., and Bockelie, J.F., 1980. Geology and paleontology of the Hölonda area, western Norway-a fragment of North America? in Wones, D.R., (ed.), The Caledonides in the U.S.A., Dept. of Geological Sciences, Virginia Polytechnic Institute & State University Memoir 2, pp. 41-47.

Bruton, D.L., and Bockelie, J.F., 1982. The Løkken-H&osl,landa- Støren areas, in Bruton, D.L., and Williams, S.H. (eds.), Field excursion guide IV, Int. symp. Ordovician system. Paleont. Contr. Univ. of Oslo v. 279, pp. 77-86.

Bruton, D.L., Lindström, M., and Owen, A.W., 1985. The Ordovician of Scandinavia, in Gee, D.G., and Sturt, B.A. (eds.), The Caledonide Orogen-Scandinavia and related Areas. John Wiley & Sons Ltd., New York, pp. 273-282.

Bryant, B., and Reed, J.C., 1969. Significance of lineation and minor folds near major thrust faults in the southern Appalachians and the British and Norwegian Caledonides: Geological Magazine, v. 106, no. 5, pp. 412-429.

Busby-Spera, C.J., 1986. Depositional features of rhyolitic and andesitevolcaniclastic rocks of the Mineral King submarine caldera complex, Sierra Nevada, California: Journal of Volcanology and Geothermal Research, v. 7, pp. 67-86.

Busby-Spera, C.J., 1987. Lithofacies of deep marine basalts emplaced on a Jurassic backarc apron, Baja California (Mexico), Journal of Geology, v. 95, pp. 671-686.

Busby-Spera, 1988. Evolution of a Middle Jurassic back arc basin, Cedros Island, Baja California: Evidence from a marine volcaniclastic apron, Geological Society of America Bulletin, v. 100, no. 2, pp. 218-233.

Butler, R.W.H., 1982. The terminology of structures in thrust belts, Journal of Structural Geology, v. 4, pp. 239-245.

Carey, S.N., and Sigurdsson, H., 1984. A model of volcanogenic sedimentation in marginal basins, in Kokelaar, B.P., and Howells, M.F. (eds.), Marginal Basin Geology, Geological Society of London Special publication no. 16, pp. 37-58.

Cas, R.A.F., 1983. A review of the paleogeographic and tectonic development of the Paleozoic Lachlan fold belt of Southeastern Australia, Geological Society of Australia Special Publication no. 10. pp. 1-104.

Cas, R.A.F., and Wright, J.V., 1987. Volcanic Successions: Modern and Ancient. Allen and Unwin, London, 528 pp.

Chaloupsky, J., and Fediuk, F., 1967. Geology of the western and north-eastern part of the Meråker area: Norges Geologiske Undersøkelse, v. 245, pp. 9-21.

Chenet, P., Montadert, L., Gairaud, H., and Roberts, D., 1982. Extension ratio measurement on the Galicia, Portugal, and Northern Biscay continental margins: Implications for evolutionary models of passive continental margins, in Watkins, J.S., and Drake, C.L.(eds.), Studies in Continental Margin Geology, American Association of Petroleum Geologists Memoir 34, pp. 703-715.

Claesson, S., and Roddick, J.C., 1983. 40Ar/39Ar data on the age and metamorphism of the Ottfjället dolerites, Särv Nappe, Swedish Caledonides, Lithos, v. 16, pp. 61-73.

Cobbold, P.R., and Quinquis, H., 1980. Development of sheath folds in shear regions: Journal of Structural Geology, v. 2, pp. 119-126.

Cole, J.W., 1984. Taupo-Rotorua Depression: an ensialic marginal basin of North Island, New Zealand, in Kokelaar, B.P., and Howells, M.F. (eds.), Marginal Basin Geology, Geological Society of London Special Publication no. 16, pp. 109-120.

Cosgrove, J.W., 1980. The tectonic implication of some small scale structures in the Mona Complex of Holy Isle, North Wales: Journal of Stuctural Geology, v. 1, pp. 383-396.

Dahlstrom, C.D.A., Structural geology in the eastern margin of the Canadian Rocky Mountains, Bulletin of Canadian Petroleum Geology, v. 18, no. 3, pp. 332-406.

Dalziel, I.W., Brown, J.M. and Warren, T.E., 1969. The structural and metamorphic history of the rocks adjacent to the Grenville front near Sudbury Ontario, and Mount Wright Quebec: Geological Association of Canada Special Paper no. 5, pp. 207-224.

Deer, W.A., Howie, R.A., and Zussman, J., 1963, Rock-Forming Minerals (5 v), London, Longmans, Green and Co.

Dearman, W.R., 1969. Tergiversate folds from South-West England: Proceeds of the Usher Society, v. 2, pp. 112-115.

Dennis, J.G., Price, R.A., Sales, J.K., Hatcher, R., Bally, A.W., Perry, W.J., Laubscher, H.P., Williams, R.E., Elliot, D., Norris, D.K., Hutton, D.W., and T. Emmet, 1981. What is a Thrust? What is a Nappe? Discussion compiled by K.R. McClay, in McClay, K.R., and Price, N.J. (eds.), Thrust and Nappe Tectonics, Geological Society Special Publication No. 9, pp. 7-9.

Escher, A. and Watterson, J., 1974. Stretching fabrics, folds and crustal shortening: Tectonophysics, v. 22, pp. 223-231.

Einsele, G., Gieskes, J.M., Curray, J., Moore, D.M., Aguayo, E., et. al., 1980. Intrusion of basaltic sills into highly porous sediments, and resulting hydrothermal activity: Nature, v. 283, pp. 441-445.

Færden, J., 1949. Petrografisk og tektonisk beskrivelse fra Kjøli-Øvre Tydal. Unpublished cand. real. thesis at the University of Oslo, 59 pp.

Falvey, D.A., 1974. The development of continental margins in plate tectonic theory, Journal of the Australian Petroleum Exploration Association, v. 14, pp. 95-106.

Ferry, J.M., 1980. A comparative study of geothermometers and geobarometers in pelitic schists from south-central Maine: American Mineralogist, v. 65, pp. 720-732.

Ferry J.M., and Spear, F.S., 1978. Experimental calibration of the partitioning of Fe and Mg between biotite and garnet: Contributions to Mineralogy and Petrology, v. 66, pp. 113-117.

Fisher, R.V., 1966. Rocks composed of volcanic fragments and their classification: Earth-Science Reviews. v. 1, pp. 287-298.

Fisher, R,V., 1979. Models for pyroclastic surges and pyroclastic flows: Journal of Volcanology and Geothermal Research, v.6, pp. 305-318.

Fisher, R.V., 1984. Submarine volcaniclastic rocks, in Kokelaar, B.P., and Howells, M.F., (eds.), Marginal Basin Geology, Geological Society of London Special Publication no. 16. pp. 5-27.

Fisher, R.V., 1983. Flow transformations in sediment gravity flows, Geology, v. 11, pp. 273-274.

Fisher, R.V., and Schminke, H.U., 1984. Pyroclastic Rocks. Springer- Verlag, New York, 472 p.

Fiske, R.S., 1963. Subaqueous pyroclastic flows in the Ohanepecosh Formation, Washington: Geological Society of America Bulletin, v. 74, pp. 391-406.

Flatebö, R., 1968. En geologisk undersøkelse i området Ålen - Haltdalen, Sö- Tröndelag. Unpubl. Thesis, University of Oslo, 1968, 139 pp.

Furnes, H., Roberts, D., Sturt, B.A., Thon, A., & Gale, G.H., 1980. Ophiolite fragments in the Scandinavian Caledonides: Proceedings of the International Ophiolite Symposium 1979, Cyprus Geological Survey Department, pp. 582-600.

Garcia, M.O., 1978. Crtiteria for the identification of ancient volcanic arcs, Earth Science Reviews, v. 14, pp. 147-165.

Gee, D.G., Guezou, J.C., Roberts, D., and Wolff, F. C., 1985. The central-southern part of the Scandinavian Caledonides: in Gee, D.G., and Sturt, B.A. (eds.), The Caledonide Orogen-Scandinavia and Related Areas. John Wiley & Sons Ltd., New York, pp. 109-133.

Getz, A., 1890. Graptoliførende skiferzoner i de trondhjemske, Nyt Mag. for Naturv., Christiana (Oslo), v. 3, pp. 41-42.

Gottfried, D., Annell, C.S.,and Schwarz, L.J., 1978. Geochemistry of subsurface basalt from the deep corehole (Clubhouse Crossroads Corehole 1) near Charleston, South Carolina-Magma type and tectonic implications, United States Geological Survey Paper P 1028, Studies related to the Charleston, South Carolina, Earthquake of 1886- A Preliminary Report, Edited by D.W. Rankin, pp. 91-113.

Hanmer, S.K., 1979. The role of discrete heterogeneites and linear fabrics in the formation of crenulations: Journal of Structural Geology, v. 1, pp. 81-89.

Hanna, S.S., and N. Fry, 1979. A comparison of methods of strain determination from south-west Dyfed (Pembrokeshire) and adjacent areas: Journal of Structural Geology, v. 1, no. 2, pp. 155-162.

Hardenby, C., 1983. Structural geology of the Kjølhaugan area, easternmost Trøndelag, central Scandinavian Caledonides: Geologiska Föreningens i Stockholm Förhandlingar, v. 104, pp. 345-365.

Hardenby, C., 1980. Geology of the Kjøhaugan area, eastern Trøndelag, central Scandinavian Caledonides: Geologiska Föreningens i Stockholm Förhandlingar, v. 102, pp. 475-492.

Hardenby, C., Lagerblad, B., and Andreasson, P.G., 1981. Structural development of the northern Trondheim Nappe Complex, central Scandinavian Caledonides, (Abstract), Terra Cognita, v. 1, no. 1, p. 50.

Helgeson, H.C., Delaney, J.M., Nesbitt, H.W., and Bird, D.K., 1978. Summary and critique of the thermodynamic properties of rock-forming minerals, American Journal of Science, v. 278-A, 229 pp.

Hobbs, B.E., Means, W.D., and Williams, P.F., 1976. An Outline of Structural Geology. John Wiley & Sons, Inc., New York, 571 pp.

Hodges, K.V., and Crowley, P.D., 1985. Error estimation and empirical geothermobarometry for pelitic systems: American Mineralogist, v. 70, pp. 702-709.

Holdaway, M.J., 1971. Stability of andalusite and the aluminum silicate phase diagram: American Journal of Science, v. 271, pp. 97-131.

Horne, G.S., 1979. Mélange in the Trondheim Nappe suggests a new tectonic model for the central Norwegian Caledonides, Nature, London, v. 281, pp. 267-270.

Hossack, J.R., 1968. Pebble deformation and thrusting in the Bygdin area (southern Norway): Tectonophysics, v. 5, 315-339.

Hossack, J.R., and Cooper, M.A., 1986. Collision tectonics in the Scandinavian Caledonides: in Coward, M.P., and Ries, A.C., (eds.), Collision Tectonics, Geological Society Special Publication no. 19, pp. 287-304.

Hutton, D.H.W., 1981. Tectonic slides in the Caledonides, in McClay, K.R., and Price, N.J. (eds.), Thrust and Nappe Tectonics, Geological Society of London Special Publication No. 9, pp. 261-265.

Jamieson, R.A., and Vernon, R.H., 1987. Timing of porphyroblast growth in the Fleur de Lys Supergroup, Newfoundland: Journal of Metamorphic Geology, v. 5, pp. 271-288.

Karig, D.E,1970. Ridges and basinsof the Tonga-Kermadec Island arc system, Journal of Geophysical Research, v. 75, pp. 239-255.

Karig, D.E., and Moore, G.F., 1975. Tectonically controlled sedimentation in marginal basins, Earth and Planetary Science Letters, v. 26, pp. 233-238.

Keen, C.E., and de Voogd, J.B., 1988. The continent-ocean boundary at the rifted margin off eastern Canada: new results from deep seismic reflection studies, Tectonics, v. 7, no. 1, pp. 107-124.

Kelts, K., Curray, J.R., and Moore, D.G., 1982. Introduction and Explanatory Notes: Initial Reports of the Deep Sea Drilling Project Leg 64, V. 64, Washington, U.S. Government Printing Office, pp. 5-26.

Kerrick, D.M., 1974. Review of metamorphic mixed-volatile ($H_2O$- $CO_2$) equilibria: American Mineralogist, v. 59, pp. 729-762.

Kisch, H.J., 1962. Petrographical and Geological Investigations in the Southwestern Tydal Region, Sör-Tröndelag, Norway. Acad. Proefschrift, Amsterdam, 136 pp.

Klein, G. d V., 1985. The control of depositional depth, tectonic uplift, and volcanism on sedimentation processes in the back-arc basins of the western Pacific Ocean, Journal of Geology, v. 93, pp. 1-25.

Klingspor, I., and Gee, D.G., 1981. Isotopic age determination studies of the Trøndelag trondjheimites, (Abstract) Terra Cognita, v. 1, pp. 55

Kokelaar, B.P., 1982. Fluidization of wet sediments during the emplacement and cooling of various igneous bodies, Journal of the Geological Society of London, v. 139,pp. 21-33.

Koziol, A.M., and Newton, R.C., 1988. Redetermination of the anorthite breakdown reaction and improvement of the plagioclase-garnet- $Al_2SiO_5$-quartz geobarometer. American Mineralogist, v. 73, pp. 216-223.

Krill, A.G., 1980. Tectonics of the Oppdal area, central Norway, Geologiska Föreningens i Stockholm Föhandlingar, v. 102, pp. 523- 530.

Kuenin, PH.H., and Migliorini, C.I., 1950. Turbidity currents as a cause of graded bedding: Journal of Geology, v. 58, pp. 91-127.

Kvale, A., 1953. Linear structures and their relationship to movement in the Caledonides of Scandinavia and Scotland: Quarterly Journal of the Geological Society of London, v. 109, pp. 51-74.

Lagerblad, B., 1984. Tectono-metamorphic relationships of the Gula Fundsjø Group contact zone in the Inndalen-Færen area, Trøndelag, central Norwegian Caledonides: Geologiska Föreningens i Stockholm Förhandlingar, v. 105, pt. 2, pp. 131-153.

Lagerblad, B., 1981. Metamorphism and metamorphic regime in the Gula Group and adjacent units in the Trondheim Nappe Complex, central Norway, Terra Cognita, v. 1, no. 1, p. 57.

Laird, J., 1980. Phase equilibria in mafic schist from Vermont: Journal of Petrology, v. 21, part 1, pp. 1-37.

Laird, J., and Albee, A.L., 1981. Pressure temperature, and time indicators in mafic schist: their application to reconstructing the polymetamorphic history of Vermont: American Journal of Science, v. 281, pp. 127-175.

Leake, B.E., 1978. Nomenclature of amphiboles: American Mineralogist, v. 63, pp. 1023-1053.

Leitch, E.C., 1984. Marginal basins of the SW Pacific and the preservation and recognition of their ancient analogues: a review, in Kokelaar, B.P., and Howells, M.F.(eds.), Marginal Basin Geology, Geological Society of London Special Publication no. 16, pp. 97-108.

Lewis, K.B., and Pantin, H.M., 1984. Intersection of a marginal basin with a continent: structure and sediments of the Bay of Plenty, New Zealand, in Kokelaar, B.P., and Howells, M.F. (eds.), Marginal Basin Geology, Geological Society of London Special Publication no.16, pp. 121-135.

MacKenzie, D.P.,1978. Some remarks on the developmentof sedimentary basins, Earth and Planetary Science Letters, v. 40, pp. 25-32.

Maddock, R.H., 1983. Melt origin of fault-generated pseudotachylytes demonstrated by textures, Geology, v. 11, pp. 105-108.

Mandeville, 1988. Tectonics of the Ålen Area, Central Norway, M. S. thesis, Virginia Polytechnic Institute & State University.

Mattauer, M., Faure, M., and Malavielle, J., 1981. Transverse lineation and large-scale structures related to Alpine obduction in Corsica: Journal of Structural Geology, v. 3, no. 4, pp. 401-409.

McClay, K.R., and Coward, M.P., 1981. The Moine Thrust Zone: an overview: in McClay, K.R., and Price, N.J. (eds.), Thrust and Nappe Tectonics, Geological Society Special Publication no. 9, pp. 241-260.

McIlreath, I.A., and James, N.P., 1984. Carbonate Slopes: in Walker, R.L., (ed.), Facies Models, Second Edition. Geoscience Canada Reprint Series 1, Geological Association of Canada, pp. 245-257.

Miyashiro, A., 1973. Metamorphism and Metamorphic Belts. Unwin Brothers Ltd., The Gresham Press, Old Woking, Surrey, Great Britain, 492pp.

Newton, R.C., and Haselton, H.T., 1981. Thermodynamics of the garnet-plagioclase-$Al_2SiO_5$-quartz geobarometer: in Newton, R.C., Navrotsky, A., and Wood, B.J., (eds.), Advances in physical geochemistry, v. 1, pp. 131-147, Springer-Verlag, New York.

Nilsen, O., 1983. The nature and tectonic setting of mélange deposits in Soknedal, near Støren, Central Norwegian Caledonides, Norges Geologiske Undersøkelse, v. 378, pp. 65-81.

Nilsen, O., 1978. Caledonian sulphide deposits and minor iron-formations from the southern Trondheim region, Norway: Norges Geologiske Undersøkelse, v. 340, pp. 35-85.

Nilsen, O., and Wolff, F.C., 1988. Preliminary bedrock map of Norway & Sveg - 1 : 250,000, NorgesGeologiske Undersøkelse.

Olesen, N. Ø., Hansen, E.S., Kristensen, L.H., & Thrystedt, T., 1973. A preliminary account on the geology of the Selbu-Tydal area, the Trondheim region, central Norwegian Caledonides: Leidse Geologische Mededelingen, v. 49, pp. 259-276.

Philpotts, A.R., 1964. Origin of psuedotachylites: American Journal of Science, v. 262, pp. 1008-1035.

Platt, J.P. and Lister, G.S., 1985a. Structure and metamorphism in the Vanoise massif, French Alps: Journal of Structural Geology, v. 7, no. 1, pp. 19-35.

Platt, J.P. and Lister, G.S., 1985b. Structural evolution of a nappe complex, southern Vanoise massif, French Penninic Alps: Journal of Structural Geology, v. 7, no. 2, pp. 145-160.

Powell, C. McA., 1979. A morphological classification of rock cleavage: Tectonophysics, v. 58, pp. 21-34.

Ragan, D.M., 1968. Structural Geology, An Introduction to Geometrical Techniques 2nd ed. John Wiley &Sons, New York, 208 pp.

Ramsay, J.G., 1967. Folding and Fracturing of Rocks. McGraw-Hill Book Company, New York, 568 pp.

Ramsay, J.G., 1981. Tectonics of the Helvetic Nappes: in K.R. McClay, and N.J. Price (eds.), Thrust and Nappe Tectonics. Geological Society of London Special Publication no. 9, pp. 293-309.

Ramsay, J.G., Casey, M., and R. Kligfield, 1983. Role of shear in the development of the Helvetic fold-thrust belt of Switzerland: Geology, v. 11, pp. 439-442.

Ramsay, J.G., and Huber, M.I., 1987. The Techniques of Modern Structural Geology Volume 2: Folds and Fractures. Academic Press, London, 700 pp.

Robie, R.A., Hemingway, B.S., and Fisher, J.R., 1978. Thermodynamic properties of minerals and related substances at 298.15K and 1 bar ($10^5$ pascals) pressure and at higher temperatures, United States Geological Survey Bulletin 1452, 456 pp.

Roberts, D., 1967. Structural observations from the Kopperå-Riksgrense area and discussion of the tectonics of Stjørdalenand the N. E. Trondheim region: Norges Geologiske Undersøkelse, v. 245, pp. 64-122.

Roberts, D., and Sturt, B.A., 1980. Caledonian deformation in Norway: Journal of the Geological Society of London, v. 137, pp. 241-250.

Roberts, D., and Wolff, F. Chr., 1981. Tectonostratigraphic development of the Trondheim region Caledonides, Central Norway, Journal of Structural Geology, v. 3, pp. 487-494.

Roberts, D., Sturt, B.A., and Furnes, H., 1985. Volcanite assemblages and environments in the Scandinavian Caledonides and the sequential development history of the mountain belt, in Gee, D.G., and Sturt, B.A. (eds.), The Caledonide Orogen-Scandinavia and Related Areas, John Wiley & Sons Ltd., New York, pp. 919-930.

Robinson, P., Spear, F.S., Schumacher, J.C., Laird, J., Klein, C., Evans, B.W., and Doolan, B.L., 1982. Phase relations of metamorphic amphiboles: Natural occurrence and theory: in Veblen, D.R., and Ribbe, P.H., (eds.), Reviews in Mineralogy v. 9B, Amphiboles: Petrology and Experimental Phase Relations. Mineralogical Society of America, BookCrafters, Inc., Chelsea, Michigan. pp. 1-227.

Rucklidge, J.C., 1971. Specifications of FORTRAN program SUPERRECAL, Department of Geology, University of Toronto, Toronto, Ont.

Rui, I.J., 1972. Geology of the Røros district, south-eastern Trondheim region with a special study of the Kjøliskarvene-Holtsjøen area: Norsk Geologisk Tidsskrift, v. 52, pp. 1-21.

Sanderson, D.J., 1973. The development of fold axes oblique to the regional trend: Tectonophysics, v. 16, pp. 55-70.

Saunders, A.D., Fornari, D.J., and Morrison, M.A., 1982. The composition and emplacement of basaltic magmas produced during the development of continental-margin basins: the Gulf of California, Mexico, Journal of the Geological Society of London, v. 139, pp. 335-346.

Shackleton, R.M., 1956. Downward-facing structures of the Highland Border, Quarterly Journal of the Geological Society of London, v. 113, pp. 361-392.

Sibson, R.H., 1975. Generation of pseudotachylyteby ancient seismic faulting: Geophysical Journal of the Royal Astronomical Society, v. 43, pp. 775-794.

Sibson, R.H., 1977. Fault rocks and fault mechanisms: Journal of the Geological Society of London, v. 133, pp. 190-213.

Sibson, R.H., White, S.H. and Atkinson, B.K., 1981. Structure and distribution of fault rocks in the Alpine Fault Zone, New Zealand: in McClay, K.R. and Price, N.J. (eds.), Thrust and Nappe Tectonics, Geological Society Special Publication no. 9, pp. 197-210.

Sigurdsson, H., Sparks, R.S.J., Carey, S.N., & Huang, T.C., 1980. Volcanogenic sedimentation in the Lesser Antilles Arc, Journal of Geology, v. 88, pp. 523-540.

Simpson, C., 1986. Determination of movement sense in mylonites: Journal of Geological Education, v. 34, pp. 246-261.

Spear, F.S., 1978. An experimental study of hornblende stability and compositional variability in amphibolite: American Journal of Science, v. 281, pp. 697-734.

Spry, A., 1969. Metamorphic Textures, Pergamon Press, Oxford.

Stephens, M.B., and Gee, D.G., 1985. A tectonic model for the evolution of the eugeoclinal terranes in the central Scandinavian Caledonides, in Gee, D.G., and Sturt, B.A. (eds.), The Caledonide Orogen- Scandinavia and Related Areas, John Wiley & Sons Ltd., New York, pp. 953- 978.

Stømer, L., 1941. *Dictyonema* shale outside the Oslo region: Norsk Geologisk Tidsskrift, v. 20, pp. 161-169.

Thompson, A.B., 1976a. Mineral reactions in pelitic rocks: I. Prediction of P-T-X(Fe-Mg) phase relations: American Journal of Science, v. 276, pp. 401-424.

Sturt, B.A., Pringle, I.R., and Ramsay, D.M., 1978. The Finnmarkian phase of the Caledonian orogeny, Journal of the Geological Society of London, v. 135, pp. 597-610.

Thompson, A.B., 1976b. Mineral reactions in pelitic rocks: II. Calculation of some P-T-X(Fe-Mg) phase relations: American Journal of Science, v. 276, pp. 425-454.

Thompson, J.B., 1957. The graphical analysis of mineral assemblages in pelitic schists: American Mineralogist, v. 42, pp. 842-858.

Thomson, A.A., and Evison, F.F., 1962. Thickness of the Earth'scrust in New Zealand, New Zealand Journal of Geology and Geophysics, v. 1, pp. 29-45.

Tracy, R.J., Robinson, P., and Thompson, A.B., 1976. Garnet composition and zoning in the determination of temperature and pressure of metamorphism, central Massachusetts: American Mineralogist, v. 61, pp. 762-775.

Tracy, R.J., Rye, D.M., Hewitt, D.A., and Schiffries, C.M., 1983. Petrologic and stable-isotopic studies of fluid-rock interactions, south- central Connecticut: I. The role of infiltration in producing reaction assemblages in impure marbles: American Journal of Science, v., 238-A, pp. 589-616.

Tucker, M.E., 1982. The Field Description of Sedimentary Rocks. John Wiley & Sons, New York, 112 p.

Turner, F.J., 1981. Metamorphic Petrology: Mineralogical, Field, and Tectonic Aspects, 2nd ed. Hemisphere Publishing Corp., Washington, 524 pp.

Vogt, J.H.L., 1889. Om fund af *Dictyonema* og Stinkkalk i Alunskifer: Foredrag 16. nov. 1888. Vidensk.-Selsk. Forh. Kristiania. Oversigt over Møder, p. 12.

Vogt, T., 1940. Geological notes on the *Dictyonema* locality and the upper Gauldal Distrikt in the Trondheim area: Norsk Geologisk Tidsskrift, v. 20, pp. 171-192.

Walker, R.L., 1967. Turbidite sedimentary structures and their relationship to proximal and distal depositional environments: Journal of Sedimentary Petrology, v. 37, pp. 25-43.

Walker,R.L., 1984. Turbidites and AssociatedCoarse Clastic Deposits: in Walker, R.L., (ed.), Facies Models, Second Edition. Geoscience Canada Reprint Series 1, Geological Association of Canada, pp. 171-188.

Wehr, F., and Glover, L., III 1985. Stratigraphy and tectonics of the Virginia-North Carolina Blue Ridge: Evolution of a lateProterozoic-early Paleozoic hinge zone. Geological Society of America Bulletin, v. 96, pp. 285-295.

Williams, P.F., 1985. Multiply deformed terrains - problems of correlation: Journal of Structural Geology, v. 7, no. 3/4, pp. 269-280.

Wilson, G., 1967. The geometry of cylindrical and conical folds: Proceedings of the Geologists' Association, v. 78, pp. 179-210.

Wilson, G., 1953. Mullion and rodding structures in the Moine Series of Scotland: Proceedings of the Geologists' Association, v. 64, pp. 118- 151.

Wilson, J.R., 1985. The synorogenic Fongen-Hyllingen layered basic complex, Trondheim region, Norway: in Gee, D.G. and Sturt, B.A., (eds.), The Caledonide Orogen-Scandinavia and Related Areas. John Wiley & Sons, Ltd., New York, pp. 717-724.

Wilson, J.R., Esbensen, K.H., and Thy, P., 1981. Igneous petrology of the synorogenic Fongen-Hyllingen layered basic complex, South-Central Scandinavian Caledonides: Journal of Petrology, v. 22, pp. 584-627.

Wolff, F. Chr., 1964. Stratigraphical position of the Gudå conglomerate zone: Norges Geologiske Undersøkelse, v. 227, pp. 85-91.

Wolff, F. Chr., 1967. Geology of the Meråker area as a key to the eastern part of the Trondheim region: Norges Geologiske Undersøkelse, v. 245, pp. 123-142.

Wolff, F. Chr., 1973. Meråker og Færen. Beskrivelse til de berggrunnsgeologiske kart (AMS-M711) 1721 I och 1722 II - 1 : 50,000. Norges Geologiske Undersøkelse, v. 295, pp. 1-42.

Wolff, F. Chr., 1979. Beskrivelse til de berggrunnsgeologiske kart Trondheim og Østersund 1 : 250,000 (med fargetrykte kart): Norges Geologiske Undersøkelse, v. 353, pp. 1-76.

Wolff, F.Chr., and Roberts, D., 1980. Geology of the Trondheim region, Norges Geologiske Undersøkelse, v. 356, pp. 117-128.

# Appendix

# Appendix A

## Field Locations

The field station numbers referred to in the text are preceded by the CM87 or CM86 prefix so that these numbers are not confused with the UTM grid system numbers on the topographic base. All field station numbers are followed by the UTM grid zone 32 location reference number (in parentheses) for precise location of the field station.

CM87-701 (32VPQ224678) NE portion of Plate 1. Outcrop on north side of Tydal private road, 100 m SW of power line intersection with Tydal private road. Thin planar laminae and graded beds preserved in Kjurudal Fm. indicate overturned stratigraphy and downward structural facing.

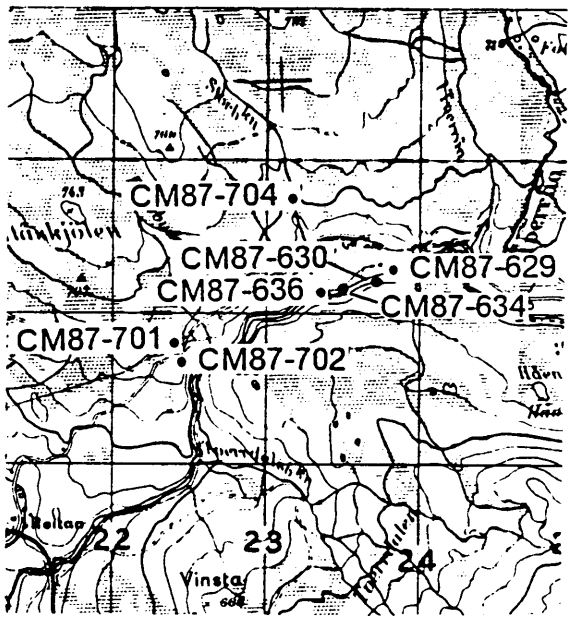


CM87-636 (32VPQ233681) Outcrop on north side of Gaula river, 100 m east of where Storbekken creek flows into Gaula. Thin planar laminae and graded beds in Kjurudal Fm. indicate overturned stratigraphy and downward structural facing.

CM87-702 (32VPQ224677) Outcrop on north side of Tydal private road 1500 m N 47° E of

Reitan Station. Gradational contact of Kjurudal and Reitan Fm. indicated by numerous 2-10 cm thick fine grained amphibolite (mafic tuff) beds and $S_1/S_2$ intersection lineation in schists is well developed.

CM87-704 (32VPQ232687) Outcrop on west side of Storbekken creek 300 m north of Tydal road. $S_1/S_2$ intersection lineation well developed in Kjurudal FM. schists.

CM87-629 (32VPQ237683) Outcrop on north side of Gaula river 700 m west of bridge over Tverråa stream. $S_1/S_2$ intersection lineation well developed in Kjurudal Fm. Small mesoscopic $F_2$ folds in outcrop.

CM87-630 (32VPQ237683) Outcrop on north side of Gaula river 750 m west of bridge over Tverråa stream. Kjurudal Fm. schists intruded by fine grained amphibolite sill.

CM87-634 (32VPQ234682) Outcrop on north side of Gaula river 1000 m west of bridge over Tverråa stream. Kjurudal Fm. schists intruded by fine - medium grained (1-1.5 m thick) amphibolite sill.

CM86-48 (32VPQ189669) Central portion of Plate 1. Outcrop on west side of Hwy. 30, 1 km south of Killindal road intersection. Thin mm scale bedding preserved in mafic tuff, and $F_2$ folded fine grained amphibolite sill present in this outcrop of Hersjø Fm.

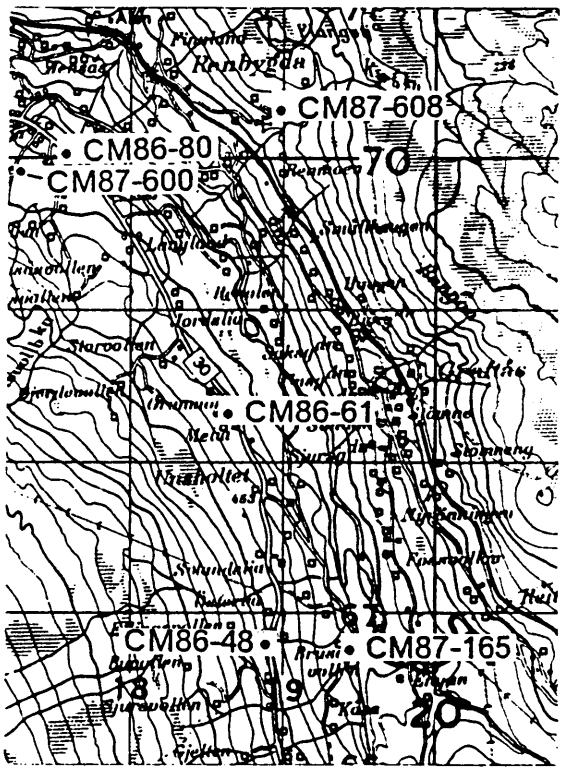


CM86-61 (32VPQ187683) Outcrop on west side of Hwy. 30, 600 m north of intersection of Killingdal road. Trondjheimite crosscutting $S_0$ and $S_1$ within Kjurudal Fm. is folded and boudined ($D_2$). Refolded $F_1$ isoclinal fold pictured in Fig. 13 is from this locality.

CM86-80 (32VPQ177699) Outcrop on southwest side of Hwy. 30, 500 m S 50° E of Graftås road intersection. Impure marble in Hersjø Fm. designated Fhm on Plate 1, is found at this locality.

CM86-165 (32VPQ194668) Outcrop on west side of small dirt road, 500 m N 72° W of bridge over Gaula river. Graded beds within psammitic schists of the Kjurudal Fm. indicate overturned beds.

CM87-600 (32VPQ172699) Outcrop on both sides of small service road to Egga residence

400 m south of Hwy. 30 intersection. Coarse pyroclastic breccia of Hersjø Fm. with clast-within-clast fragments is found at this locality.

CM87-608 (32VPQ189703) Outcrop on east side of private road, 120 m N 52° E of radio tower. Sample of biotite + quartz + chlorite + garnet + oligiclase schist from Kjurudal Fm. used for thermobarometry was collected from this locality. $S_2$ is penetrative at this locality.

CM87-675 (32VPQ254668) Eastern edge of Plate 1. Outcrop 900 mS 5° W of bridge over Gaula river on new dirt road not on current topographic base. Primary pyroclastic textures are well preserved in the Reitan Fm. at this location. Rock types include fine grained mafic tuff, crystal lapilli tuff, tuff breccia, and fine grained amphibolite sills. The sills and pyroclastic textured rocks are folded by $F_2$ folds.

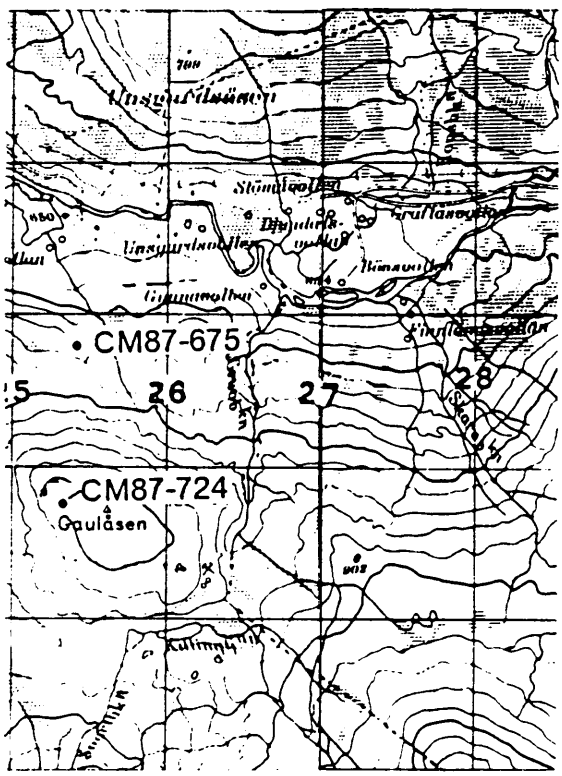


CM87-724 (32VPQ253657) Outcrop 300 m west of peak of Gaulåsen. Thin beds of fine grained amphibolite and chlorite + quartz + plagioclase schist are present within the Slågrov Fm. near contact with Reitan Fm.

CM87-505 (32VPQ123677) NW portion of Plate 1. Outcrop on east side of Hessdalen road S 80° E of bridge over Hesja river. Lithologies typical of Gudå Fm. - Hersjø Fm. contact including (from N to S) quartz-rod bearing schist, fine grained amphibolite (mafic tuff) and calc silicate schist to impure marble,

CM87-495 (32VPQ118685) Outcrop on east side of Hessdalen road 1 km south of intersection with road leading to Asnås residence. Sample of biotite + quartz + garnet + biotite + staurolite + kyanite schist from the Gudå Fm. used for thermobarometry was collected from this locality.

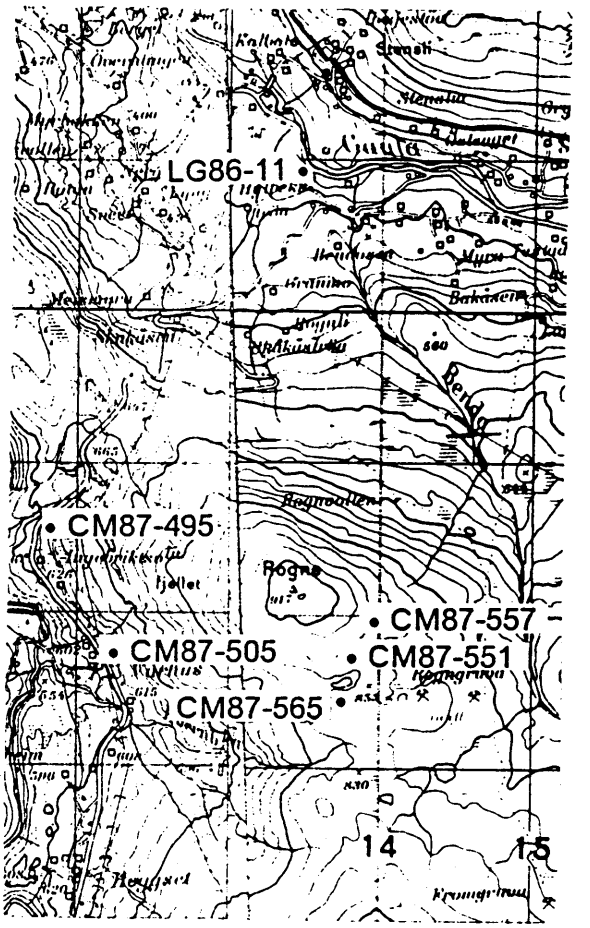


LG86-11 (32VPQ135709) Outcrop (200 m long) on south side of Hwy. 30, 800 m west of Hessdalen road intersection. Sample of biotite + quartz + garnet + staurolite schist from the Gudå Fm. used for thermobarometry was collected from this locality.

CM87-565 (32VPQ138675) Outcrop 150 m south of small pond on south side of Rogne peak. Mafic schist (mafic tuff) used for metamorphic study was collected from this locality. Small $F_1$ isoclinal folds present in the mafic schists.

CM87-551 (32VPQ138678) Outcrop 580 m S 48° E of Rogne peak. Locality in Gudå Fm. where overturned bedding plane fault is located to within 50 m and $S_2$ maintains constant orientation across fault.

CM87-557 (32VPQ139679) Outcrop 560 m S 60°E of Rogne peak. Locality in Gudå Fm. where overturned bedding plane fault is located to within 50 m and $S_2$ maintains constant orientation across fault.

CM87-741 (32VPQ119641) SW portion Plate 1. Outcrop in Rognsåa stream 700 m S 64° E of Hessdalen church. $S_1/S_2$ intersection lineation well developed in schists of Kjurudal Fm.

CM87-745 (32VPQ121638) Outcrop in Rognsåa stream 1050 m S 54° E of Hessdalen church. $F_2$ axes and $S_2$ cleavage well developed in Kjurudal Fm. schists at this locality.

CM87-749 (32VPQ127632) Outcrop in Rognsåa stream 900 m N 47° W of NW outlet of Rognsåsjøen. $S_1/S_2$ intersection lineation well developed in Kjurudal Fm. schists.

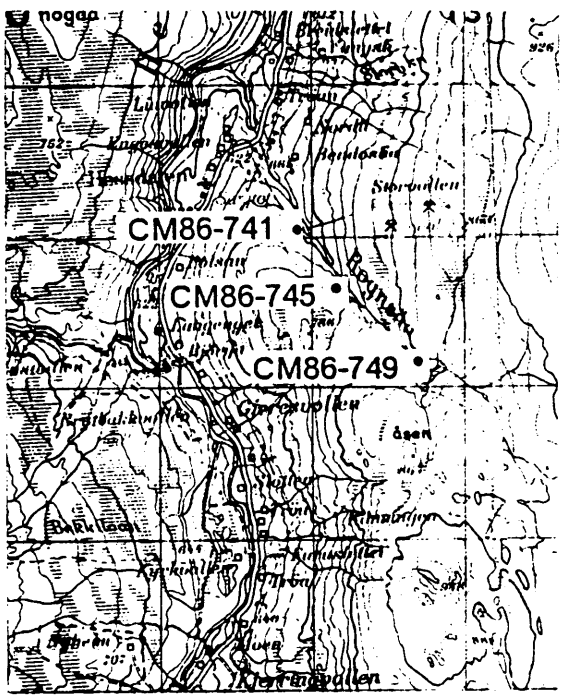

CM86-26 (32VPQ194646) South central portion of Plate 1. Outcrop on west side of Hwy. 30, 1 km north of Granlundvollen. Primary pyroclastic textures preserved in Hersjø Fm. Rock types include lapilli tuff, and tuff breccia. At north end of outcrop purple pseudotachylite veins are present in fine grained amphibolite.

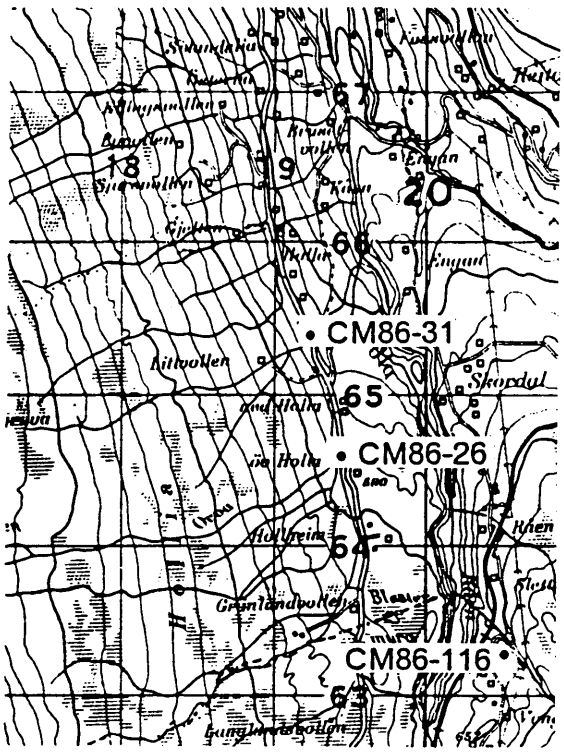


CM86-31 (32VPQ192654) Outcrop on west side of Hwy. 30, 250 m north of intersection of road to Litvollen. Thin mm scale bedding in mafic tuffs of Hersjø Fm. are preserved along with beds of crystal lapilli tuff. Bedded lithologies are in sharp contact with porphyritic diabase sills. At south end of outcrop porphyritic diabase sill becomes finer grained and pillowed.

CM86-116 (32VPQ205632) Outcrop 100 m south of hairpin turn in road, 30 m above stream valley. Fine grained amphibolite (mafic tuff) and felsic crystal tuff beds of Reitan Fm. are folded ($F_2$ Z) along with amphibolite sill pictured in Fig. 14c.

CM86-285 (32VPQ185602) Southern edge (center) of Plate 1. Outcrop along creek 900 m S 55° W of Grubba residence. Actinolitic amphiboles in cataclastically deformed mafic schist of Reitan Fm. are present at this locality.

CM86-298 (32VPQ191603) Outcrop on east side of Railroad tracks 200 m south of small trestle. Thin bedded schists and phyllites of the Slågrov Fm. are exposed at this locality near Slågrovsvollan.

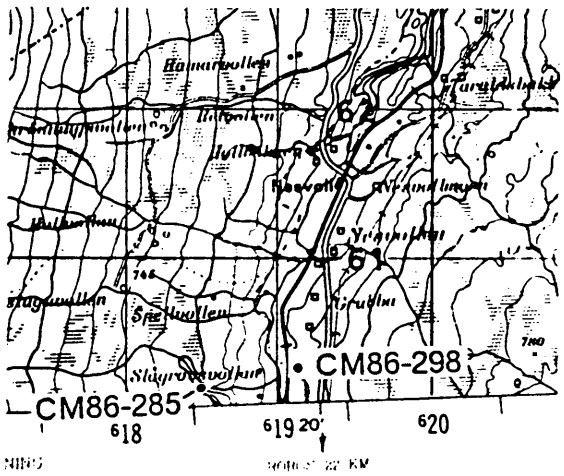

CM86-425 (323VPQ166633) South central portion of Plate 1. Outcrop along stream 600 m N 42° W of 934 m peak. Sample of mafic schist (mafic tuff) from Hersjø Fm. used in metamorphic study was collected from this locality.

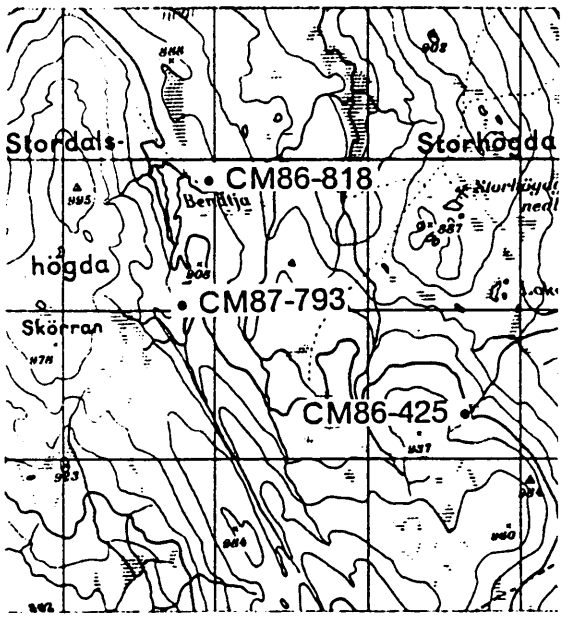


CM87-793 (32VPQ148641) Outcrop 350 m south of Bendtja lake. Sample of biotite + quartz + garnet + muscovite + oligoclase schist of Kjurudal Fm. and used for thermobarometry was collected from this locality. $F_2$ S fold pictured in Fig. 14b can be found at this locality. $S_2$ spaced cleavage is well developed at this locality.

CM87-818 (32VPQ149648) Outcrop along stream 250 m SW of small cottage on east side of Bendtja lake. $S_1/S_2$intersection lineationwell developed in Kjurudal Fm. Contact with Hersjø Fm. is gradational.

## Appendix B

The clast population of the Sætersjø Member of the Kjurudal Fm. is domonated by felsic volcanic rock fragments. Other less abundant clasts include angular, blasto-ophitic textured diabase clasts, graphitic schist/phyllite fragments and blocky rounded tonalite and

trondjheimite clasts. Elongate clots of chlorite and biotite which are tectonically flattened and contain small patches of epidote and relict plagioclase and quartz phenocrysts are interpreted as relict mafic tuff fragments.

# Appendix C

## Mineral Chemistry

Mineral chemistries were analyzed with an automated, nine spectrometer ARL-EMX electron microprobe. Natural silicate samples with well established wet chemical analyses data were used for standardization. Data reduction to weight percent oxides was according to the method of Bence and Albee (1968). Oxide weight percents were recalculated into mineral formula using the SUPERRECAL computer program (Rucklidge, 1971).

1SUPER RECAL TABLE 3A AMPHIBOLE ANALYSES (OH CALCULATED)

| | 1 | 2 | 3 | 4 | 5 | 6 | 7 | 8 |
|---|---|---|---|---|---|---|---|---|
| SIO2 | 42.08 | 42.76 | 42.60 | 42.93 | 42.98 | 43.39 | 43.26 | 43.28 |
| A2O3 | 13.24 | 13.77 | 14.66 | 13.12 | 13.43 | 13.30 | 13.48 | 14.09 |
| TIO2 | 0.52 | 0.52 | 0.51 | 0.51 | 0.53 | 0.53 | 0.54 | 0.54 |
| FEO | 19.93 | 19.62 | 19.15 | 19.21 | 19.57 | 19.33 | 19.62 | 19.48 |
| MNO | 0.36 | 0.36 | 0.38 | 0.42 | 0.40 | 0.40 | 0.43 | 0.37 |
| MGO | 8.12 | 8.17 | 8.05 | 8.37 | 8.49 | 8.55 | 8.42 | 8.10 |
| CAO | 10.74 | 10.95 | 10.82 | 10.85 | 10.93 | 10.93 | 10.84 | 10.94 |
| NA2O | 2.14 | 2.11 | 2.01 | 1.89 | 2.01 | 2.07 | 2.09 | 2.11 |
| K2O | 0.42 | 0.39 | 0.40 | 0.38 | 0.41 | 0.39 | 0.41 | 0.44 |
| BAO | 0.00 | 0.00 | 0.00 | 0.00 | 0.00 | 0.00 | 0.00 | 0.00 |
| CL | 0.00 | 0.00 | 0.00 | 0.00 | 0.00 | 0.00 | 0.00 | 0.00 |
| F | 0.00 | 0.00 | 0.00 | 0.00 | 0.00 | 0.00 | 0.00 | 0.00 |
| H2O | 1.97 | 2.00 | 2.01 | 1.99 | 2.00 | 2.01 | 2.01 | 2.02 |
| SUM | 99.52 | 100.65 | 100.59 | 99.67 | 100.75 | 100.90 | 101.10 | 101.37 |
| -O= F+CL | 0.00 | 0.00 | 0.00 | 0.00 | 0.00 | 0.00 | 0.00 | 0.00 |
| SUM | 99.52 | 100.65 | 100.59 | 99.67 | 100.75 | 100.90 | 101.10 | 101.37 |

| | | | | | | | | | | | | | | | | |
|---|---|---|---|---|---|---|---|---|---|---|---|---|---|---|---|---|
| SI | 6.398 | * | 6.404 | * | 6.362 | * | 6.478 | * | 6.428 | * | 6.467 | * | 6.445 | * | 6.422 | * |
| AL | 1.602 | 8.000 | 1.596 | 8.000 | 1.638 | 8.000 | 1.522 | 8.000 | 1.572 | 8.000 | 1.533 | 8.000 | 1.555 | 8.000 | 1.578 | 8.000 |
| AL | 0.770 | * | 0.834 | * | 0.941 | * | 0.811 | * | 0.795 | * | 0.803 | * | 0.811 | * | 0.885 | * |
| TI | 0.059 | * | 0.059 | * | 0.057 | * | 0.058 | * | 0.060 | * | 0.059 | * | 0.060 | * | 0.060 | * |
| FE | 2.534 | * | 2.457 | * | 2.392 | * | 2.424 | * | 2.448 | * | 2.410 | * | 2.444 | * | 2.417 | * |
| MN | 0.046 | * | 0.046 | * | 0.048 | * | 0.054 | * | 0.051 | * | 0.050 | * | 0.054 | * | 0.047 | * |
| MG | 1.840 | 5.250 | 1.824 | 5.220 | 1.792 | 5.230 | 1.883 | 5.229 | 1.893 | 5.246 | 1.900 | 5.222 | 1.870 | 5.240 | 1.791 | 5.201 |
| CA | 1.750 | * | 1.757 | * | 1.731 | * | 1.754 | * | 1.751 | * | 1.745 | * | 1.730 | * | 1.739 | * |
| NA | 0.631 | * | 0.613 | * | 0.582 | * | 0.553 | * | 0.583 | * | 0.598 | * | 0.604 | * | 0.607 | * |
| K | 0.081 | * | 0.075 | * | 0.076 | * | 0.073 | * | 0.078 | * | 0.074 | * | 0.078 | * | 0.083 | * |
| BA | 0.000 | 2.462 | 0.000 | 2.444 | 0.000 | 2.389 | 0.000 | 2.380 | 0.000 | 2.412 | 0.000 | 2.418 | 0.000 | 2.412 | 0.000 | 2.429 |
| CL | 0.000 | * | 0.000 | * | 0.000 | * | 0.000 | * | 0.000 | * | 0.000 | * | 0.000 | * | 0.000 | * |
| F | 0.000 | * | 0.000 | * | 0.000 | * | 0.000 | * | 0.000 | * | 0.000 | * | 0.000 | * | 0.000 | * |
| H | 2.000 | 2.000 | 2.000 | 2.000 | 2.000 | 2.000 | 2.000 | 2.000 | 2.000 | 2.000 | 2.000 | 2.000 | 2.000 | 2.000 | 2.000 | 2.000 |
| O | 24.000 | * | 24.000 | * | 24.000 | * | 24.000 | * | 24.000 | * | 24.000 | * | 24.000 | * | 24.000 | * |

1 31 AM565
2 32 AM565
3 33 AM565
4 37 AM565
5 38 AM565
6 39 AM565
7 40 AM565
8 41 AM565

1SUPER RECAL TABLE 3A AMPHIBOLE ANALYSES (OH CALCULATED)

| | 9 | 10 | 11 | 12 | 13 | 14 | 15 | 16 |
|---|---|---|---|---|---|---|---|---|
| SIO2 | 43.05 | 42.93 | 43.48 | 45.35 | 44.64 | 44.62 | 43.41 | 43.27 |
| A2O3 | 13.94 | 13.81 | 13.29 | 11.91 | 11.88 | 12.11 | 13.55 | 13.12 |
| TIO2 | 0.54 | 0.53 | 0.50 | 0.43 | 0.45 | 0.49 | 0.52 | 0.54 |
| FEO | 19.56 | 19.57 | 19.33 | 18.70 | 18.92 | 19.21 | 19.33 | 19.56 |
| MNO | 0.39 | 0.38 | 0.38 | 0.40 | 0.40 | 0.42 | 0.41 | 0.38 |
| MGO | 8.12 | 8.21 | 8.51 | 9.63 | 9.28 | 9.12 | 8.46 | 8.18 |
| CAO | 10.88 | 10.80 | 10.79 | 10.84 | 10.96 | 10.87 | 10.99 | 11.01 |
| NA2O | 2.13 | 2.25 | 1.97 | 1.83 | 1.96 | 1.93 | 2.05 | 1.96 |
| K2O | 0.41 | 0.43 | 0.39 | 0.30 | 0.33 | 0.34 | 0.42 | 0.41 |
| BAO | 0.00 | 0.00 | 0.00 | 0.00 | 0.00 | 0.00 | 0.00 | 0.00 |
| CL | 0.00 | 0.00 | 0.00 | 0.00 | 0.00 | 0.00 | 0.00 | 0.00 |
| F | 0.00 | 0.00 | 0.00 | 0.00 | 0.00 | 0.00 | 0.00 | 0.00 |
| H2O | 2.01 | 2.01 | 2.01 | 2.04 | 2.02 | 2.02 | 2.02 | 2.00 |
| SUM | 101.03 | 100.92 | 100.65 | 101.43 | 100.84 | 101.13 | 101.15 | 100.43 |
| -O= F+CL | 0.00 | 0.00 | 0.00 | 0.00 | 0.00 | 0.00 | 0.00 | 0.00 |
| SUM | 101.03 | 100.92 | 100.65 | 101.43 | 100.84 | 101.13 | 101.15 | 100.43 |

| | | | | | | | | | | | | | | | | |
|---|---|---|---|---|---|---|---|---|---|---|---|---|---|---|---|---|
| SI | 6.416 | * | 6.410 | * | 6.489 | * | 6.673 | * | 6.632 | * | 6.615 | * | 6.453 | * | 6.489 | * |
| AL | 1.584 | 8.000 | 1.590 | 8.000 | 1.511 | 8.000 | 1.327 | 8.000 | 1.368 | 8.000 | 1.385 | 8.000 | 1.547 | 8.000 | 1.511 | 8.000 |
| AL | 0.864 | * | 0.840 | * | 0.827 | * | 0.738 | * | 0.712 | * | 0.731 | * | 0.827 | * | 0.807 | * |
| TI | 0.061 | * | 0.060 | * | 0.056 | * | 0.048 | * | 0.050 | * | 0.055 | * | 0.058 | * | 0.061 | * |
| FE | 2.438 | * | 2.444 | * | 2.413 | * | 2.301 | * | 2.351 | * | 2.382 | * | 2.403 | * | 2.453 | * |
| MN | 0.049 | * | 0.048 | * | 0.048 | * | 0.050 | * | 0.050 | * | 0.053 | * | 0.052 | * | 0.048 | * |
| MG | 1.804 | 5.215 | 1.827 | 5.219 | 1.893 | 5.237 | 2.112 | 5.248 | 2.055 | 5.218 | 2.015 | 5.235 | 1.875 | 5.215 | 1.828 | 5.197 |
| CA | 1.737 | * | 1.728 | * | 1.725 | * | 1.709 | * | 1.745 | * | 1.727 | * | 1.750 | * | 1.769 | * |
| NA | 0.615 | * | 0.651 | * | 0.570 | * | 0.522 | * | 0.565 | * | 0.555 | * | 0.591 | * | 0.570 | * |
| K | 0.078 | * | 0.082 | * | 0.074 | * | 0.056 | * | 0.063 | * | 0.064 | * | 0.080 | * | 0.078 | * |
| BA | 0.000 | 2.431 | 0.000 | 2.461 | 0.000 | 2.370 | 0.000 | 2.287 | 0.000 | 2.372 | 0.000 | 2.346 | 0.000 | 2.421 | 0.000 | 2.417 |
| CL | 0.000 | * | 0.000 | * | 0.000 | * | 0.000 | * | 0.000 | * | 0.000 | * | 0.000 | * | 0.000 | * |
| F | 0.000 | * | 0.000 | * | 0.000 | * | 0.000 | * | 0.000 | * | 0.000 | * | 0.000 | * | 0.000 | * |
| H | 2.000 | 2.000 | 2.000 | 2.000 | 2.000 | 2.000 | 2.000 | 2.000 | 2.000 | 2.000 | 2.000 | 2.000 | 2.000 | 2.000 | 2.000 | 2.000 |
| O | 24.000 | * | 24.000 | * | 24.000 | * | 24.000 | * | 24.000 | * | 24.000 | * | 24.000 | * | 24.000 | * |

9 42 AM565
10 43 AM565
11 44 AM565
12 45 AM565
13 46 AM565
14 47 AM565
15 48 AM565
16 49 AM565

1SUPER RECAL TABLE 3A AMPHIBOLE ANALYSES (OH CALCULATED)

| | 17 | 18 | 19 | 20 | 21 | 22 | 23 | 24 |
|---|---|---|---|---|---|---|---|---|
| SIO2 | 42.98 | 42.87 | 42.89 | 42.56 | 42.53 | 42.99 | 43.29 | 43.26 |
| A2O3 | 13.80 | 13.85 | 14.27 | 14.45 | 14.32 | 14.19 | 13.92 | 13.74 |
| TIO2 | 0.53 | 0.52 | 0.52 | 0.51 | 0.50 | 0.47 | 0.45 | 0.49 |
| FEO | 19.43 | 19.50 | 19.67 | 19.36 | 19.40 | 19.58 | 19.29 | 19.44 |
| MNO | 0.35 | 0.40 | 0.42 | 0.41 | 0.39 | 0.39 | 0.39 | 0.40 |
| MGO | 8.23 | 8.25 | 8.12 | 8.09 | 8.11 | 8.18 | 8.27 | 8.54 |
| CAO | 10.95 | 10.82 | 10.81 | 10.85 | 10.85 | 10.84 | 10.83 | 10.83 |
| NA2O | 2.10 | 2.15 | 2.05 | 2.05 | 2.13 | 2.13 | 2.19 | 2.15 |
| K2O | 0.39 | 0.42 | 0.40 | 0.41 | 0.41 | 0.40 | 0.39 | 0.39 |
| BAO | 0.00 | 0.00 | 0.00 | 0.00 | 0.00 | 0.00 | 0.00 | 0.00 |
| CL | 0.00 | 0.00 | 0.00 | 0.00 | 0.00 | 0.00 | 0.00 | 0.00 |
| F | 0.00 | 0.00 | 0.00 | 0.00 | 0.00 | 0.00 | 0.00 | 0.00 |
| H2O | 2.01 | 2.00 | 2.01 | 2.00 | 2.00 | 2.01 | 2.01 | 2.02 |
| SUM | 100.77 | 100.78 | 101.16 | 100.69 | 100.64 | 101.18 | 101.03 | 101.26 |
| -O= F+CL | 0.00 | 0.00 | 0.00 | 0.00 | 0.00 | 0.00 | 0.00 | 0.00 |
| SUM | 100.77 | 100.78 | 101.16 | 100.69 | 100.64 | 101.18 | 101.03 | 101.26 |

| | | | | | | | | | | | | | | | | |
|---|---|---|---|---|---|---|---|---|---|---|---|---|---|---|---|---|
| SI | 6.420 | * | 6.407 | * | 6.384 | * | 6.360 | * | 6.363 | * | 6.395 | * | 6.439 | * | 6.427 | * |
| AL | 1.580 | 8.000 | 1.593 | 8.000 | 1.616 | 8.000 | 1.640 | 8.000 | 1.637 | 8.000 | 1.605 | 8.000 | 1.561 | 8.000 | 1.573 | 8.000 |
| AL | 0.849 | * | 0.846 | * | 0.887 | * | 0.905 | * | 0.888 | * | 0.883 | * | 0.879 | * | 0.832 | * |
| TI | 0.060 | * | 0.058 | * | 0.058 | * | 0.057 | * | 0.056 | * | 0.053 | * | 0.050 | * | 0.055 | * |
| FE | 2.427 | * | 2.437 | * | 2.448 | * | 2.420 | * | 2.427 | * | 2.436 | * | 2.399 | * | 2.415 | * |
| MN | 0.044 | * | 0.051 | * | 0.053 | * | 0.052 | * | 0.049 | * | 0.049 | * | 0.049 | * | 0.050 | * |
| MG | 1.832 | 5.212 | 1.838 | 5.230 | 1.801 | 5.248 | 1.802 | 5.236 | 1.809 | 5.230 | 1.814 | 5.234 | 1.833 | 5.211 | 1.891 | 5.244 |
| CA | 1.752 | * | 1.733 | * | 1.724 | * | 1.737 | * | 1.739 | * | 1.728 | * | 1.726 | * | 1.724 | * |
| NA | 0.608 | * | 0.623 | * | 0.592 | * | 0.594 | * | 0.618 | * | 0.614 | * | 0.632 | * | 0.619 | * |
| K | 0.074 | * | 0.080 | * | 0.076 | * | 0.078 | * | 0.078 | * | 0.076 | * | 0.074 | * | 0.074 | * |
| BA | 0.000 | 2.435 | 0.000 | 2.436 | 0.000 | 2.391 | 0.000 | 2.409 | 0.000 | 2.435 | 0.000 | 2.418 | 0.000 | 2.431 | 0.000 | 2.417 |
| CL | 0.000 | * | 0.000 | * | 0.000 | * | 0.000 | * | 0.000 | * | 0.000 | * | 0.000 | * | 0.000 | * |
| F | 0.000 | * | 0.000 | * | 0.000 | * | 0.000 | * | 0.000 | * | 0.000 | * | 0.000 | * | 0.000 | * |
| H | 2.000 | 2.000 | 2.000 | 2.000 | 2.000 | 2.000 | 2.000 | 2.000 | 2.000 | 2.000 | 2.000 | 2.000 | 2.000 | 2.000 | 2.000 | 2.000 |
| O | 24.000 | * | 24.000 | * | 24.000 | * | 24.000 | * | 24.000 | * | 24.000 | * | 24.000 | * | 24.000 | * |

17 50 AM565
18 51 AM565
19 52 AM565
20 53 AM565
21 54 AM565
22 55 AM565
23 56 AM565
24 57 AM565

1SUPER RECAL TABLE 3A AMPHIBOLE ANALYSES (OH CALCULATED)

| | 25 | 26 | 27 | 28 | 29 | 30 | 31 | 32 |
|---|---|---|---|---|---|---|---|---|
| SIO2 | 43.41 | 43.39 | 43.01 | 43.57 | 43.15 | 43.32 | 42.98 | 42.78 |
| A2O3 | 13.84 | 13.52 | 12.58 | 13.17 | 12.89 | 13.39 | 13.42 | 13.76 |
| TIO2 | 0.53 | 0.51 | 0.36 | 0.39 | 0.40 | 0.41 | 0.43 | 0.46 |
| FEO | 19.45 | 19.64 | 19.32 | 19.28 | 19.34 | 19.46 | 19.43 | 19.63 |
| MNO | 0.39 | 0.40 | 0.35 | 0.34 | 0.35 | 0.35 | 0.35 | 0.42 |
| MGO | 8.24 | 8.57 | 8.37 | 8.31 | 8.33 | 8.07 | 7.99 | 7.74 |
| CAO | 10.91 | 10.85 | 11.17 | 11.13 | 11.08 | 10.93 | 10.87 | 10.98 |
| NA2O | 2.13 | 2.04 | 1.81 | 1.81 | 1.84 | 1.83 | 1.98 | 2.05 |
| K2O | 0.41 | 0.40 | 0.38 | 0.39 | 0.39 | 0.38 | 0.38 | 0.38 |
| BAO | 0.00 | 0.00 | 0.00 | 0.00 | 0.00 | 0.00 | 0.00 | 0.00 |
| CL | 0.00 | 0.00 | 0.00 | 0.00 | 0.00 | 0.00 | 0.00 | 0.00 |
| F | 0.00 | 0.00 | 0.00 | 0.00 | 0.00 | 0.00 | 0.00 | 0.00 |
| H2O | 2.02 | 2.02 | 1.98 | 2.00 | 1.99 | 2.00 | 1.99 | 1.99 |
| SUM | 101.33 | 101.34 | 99.33 | 100.39 | 99.76 | 100.14 | 99.82 | 100.19 |
| -O= F+CL | 0.00 | 0.00 | 0.00 | 0.00 | 0.00 | 0.00 | 0.00 | 0.00 |
| SUM | 101.33 | 101.34 | 99.33 | 100.39 | 99.76 | 100.14 | 99.82 | 100.19 |

| | | | | | | | | | | | | | | | | |
|---|---|---|---|---|---|---|---|---|---|---|---|---|---|---|---|---|
| SI | 6.442 | * | 6.445 | * | 6.521 | * | 6.518 | * | 6.509 | * | 6.501 | * | 6.478 | * | 6.436 | * |
| AL | 1.558 | 8.000 | 1.555 | 8.000 | 1.479 | 8.000 | 1.482 | 8.000 | 1.491 | 8.000 | 1.499 | 8.000 | 1.522 | 8.000 | 1.564 | 8.000 |
| AL | 0.863 | * | 0.811 | * | 0.769 | * | 0.840 | * | 0.800 | * | 0.869 | * | 0.862 | * | 0.875 | * |
| TI | 0.059 | * | 0.057 | * | 0.041 | * | 0.044 | * | 0.045 | * | 0.046 | * | 0.049 | * | 0.052 | * |
| FE | 2.414 | * | 2.440 | * | 2.450 | * | 2.412 | * | 2.440 | * | 2.442 | * | 2.449 | * | 2.470 | * |
| MN | 0.049 | * | 0.050 | * | 0.045 | * | 0.043 | * | 0.045 | * | 0.044 | * | 0.045 | * | 0.054 | * |
| MG | 1.823 | 5.207 | 1.897 | 5.255 | 1.891 | 5.196 | 1.853 | 5.192 | 1.873 | 5.202 | 1.805 | 5.207 | 1.795 | 5.199 | 1.736 | 5.186 |
| CA | 1.735 | * | 1.727 | * | 1.814 | * | 1.784 | * | 1.791 | * | 1.757 | * | 1.755 | * | 1.770 | * |
| NA | 0.613 | * | 0.587 | * | 0.532 | * | 0.525 | * | 0.538 | * | 0.532 | * | 0.579 | * | 0.598 | * |
| K | 0.078 | * | 0.076 | * | 0.073 | * | 0.074 | * | 0.075 | * | 0.073 | * | 0.073 | * | 0.073 | * |
| BA | 0.000 | 2.425 | 0.000 | 2.390 | 0.000 | 2.420 | 0.000 | 2.383 | 0.000 | 2.404 | 0.000 | 2.363 | 0.000 | 2.407 | 0.000 | 2.441 |
| CL | 0.000 | * | 0.000 | * | 0.000 | * | 0.000 | * | 0.000 | * | 0.000 | * | 0.000 | * | 0.000 | * |
| F | 0.000 | * | 0.000 | * | 0.000 | * | 0.000 | * | 0.000 | * | 0.000 | * | 0.000 | * | 0.000 | * |
| H | 2.000 | 2.000 | 2.000 | 2.000 | 2.000 | 2.000 | 2.000 | 2.000 | 2.000 | 2.000 | 2.000 | 2.000 | 2.000 | 2.000 | 2.000 | 2.000 |
| O | 24.000 | * | 24.000 | * | 24.000 | * | 24.000 | * | 24.000 | * | 24.000 | * | 24.000 | * | 24.000 | * |

25 58 AM565
26 59 AM565
27 329 AM565
28 330 AM565
29 331 AM565
30 332 AM565
31 333 AM565
32 334 AM565

1SUPER RECAL TABLE 3A AMPHIBOLE ANALYSES (OH CALCULATED)

| | 33 | 34 | 35 | 36 | 37 | 38 | 39 | 40 |
|---|---|---|---|---|---|---|---|---|
| SIO2 | 42.48 | 42.07 | 42.30 | 42.51 | 42.24 | 42.48 | 42.98 | 43.13 |
| A2O3 | 13.98 | 14.26 | 14.27 | 14.25 | 14.13 | 13.75 | 13.58 | 13.61 |
| TIO2 | 0.49 | 0.50 | 0.53 | 0.53 | 0.54 | 0.55 | 0.54 | 0.52 |
| FEO | 19.79 | 19.76 | 19.96 | 19.94 | 19.74 | 19.69 | 19.53 | 19.38 |
| MNO | 0.36 | 0.38 | 0.36 | 0.37 | 0.39 | 0.40 | 0.39 | 0.37 |
| MGO | 7.88 | 7.68 | 7.64 | 7.76 | 7.90 | 7.94 | 8.14 | 8.14 |
| CAO | 10.92 | 10.96 | 10.90 | 10.97 | 10.91 | 10.91 | 10.95 | 11.14 |
| NA2O | 2.12 | 2.15 | 2.15 | 2.03 | 2.06 | 2.03 | 1.94 | 1.98 |
| K2O | 0.40 | 0.41 | 0.42 | 0.44 | 0.44 | 0.43 | 0.42 | 0.42 |
| BAO | 0.00 | 0.00 | 0.00 | 0.00 | 0.00 | 0.00 | 0.00 | 0.00 |
| CL | 0.00 | 0.00 | 0.00 | 0.00 | 0.00 | 0.00 | 0.00 | 0.00 |
| F | 0.00 | 0.00 | 0.00 | 0.00 | 0.00 | 0.00 | 0.00 | 0.00 |
| H2O | 1.99 | 1.99 | 1.99 | 2.00 | 1.99 | 1.99 | 2.00 | 2.00 |
| SUM | 100.41 | 100.16 | 100.52 | 100.80 | 100.34 | 100.17 | 100.47 | 100.69 |
| -O= F+CL | 0.00 | 0.00 | 0.00 | 0.00 | 0.00 | 0.00 | 0.00 | 0.00 |
| SUM | 100.41 | 100.16 | 100.52 | 100.80 | 100.34 | 100.17 | 100.47 | 100.69 |

| | | | | | | | | | | | | | | | | |
|---|---|---|---|---|---|---|---|---|---|---|---|---|---|---|---|---|
| SI | 6.385 | * | 6.345 | * | 6.357 | * | 6.367 | * | 6.356 | * | 6.400 | * | 6.442 | * | 6.446 | * |
| AL | 1.615 | 8.000 | 1.655 | 8.000 | 1.643 | 8.000 | 1.633 | 8.000 | 1.644 | 8.000 | 1.600 | 8.000 | 1.558 | 8.000 | 1.554 | 8.000 |
| AL | 0.861 | * | 0.880 | * | 0.884 | * | 0.882 | * | 0.861 | * | 0.841 | * | 0.840 | * | 0.843 | * |
| TI | 0.055 | * | 0.057 | * | 0.060 | * | 0.060 | * | 0.061 | * | 0.062 | * | 0.061 | * | 0.058 | * |
| FE | 2.487 | * | 2.492 | * | 2.509 | * | 2.497 | * | 2.484 | * | 2.481 | * | 2.448 | * | 2.422 | * |
| MN | 0.046 | * | 0.049 | * | 0.046 | * | 0.047 | * | 0.050 | * | 0.051 | * | 0.050 | * | 0.047 | * |
| MG | 1.765 | 5.215 | 1.727 | 5.204 | 1.711 | 5.210 | 1.732 | 5.218 | 1.772 | 5.228 | 1.783 | 5.218 | 1.818 | 5.217 | 1.813 | 5.185 |
| CA | 1.758 | * | 1.771 | * | 1.755 | * | 1.760 | * | 1.759 | * | 1.761 | * | 1.758 | * | 1.784 | * |
| NA | 0.618 | * | 0.629 | * | 0.626 | * | 0.589 | * | 0.601 | * | 0.593 | * | 0.564 | * | 0.574 | * |
| K | 0.077 | * | 0.079 | * | 0.081 | * | 0.084 | * | 0.084 | * | 0.083 | * | 0.080 | * | 0.080 | * |
| BA | 0.000 | 2.453 | 0.000 | 2.479 | 0.000 | 2.462 | 0.000 | 2.434 | 0.000 | 2.444 | 0.000 | 2.437 | 0.000 | 2.402 | 0.000 | 2.438 |
| CL | 0.000 | * | 0.000 | * | 0.000 | * | 0.000 | * | 0.000 | * | 0.000 | * | 0.000 | * | 0.000 | * |
| F | 0.000 | * | 0.000 | * | 0.000 | * | 0.000 | * | 0.000 | * | 0.000 | * | 0.000 | * | 0.000 | * |
| H | 2.000 | 2.000 | 2.000 | 2.000 | 2.000 | 2.000 | 2.000 | 2.000 | 2.000 | 2.000 | 2.000 | 2.000 | 2.000 | 2.000 | 2.000 | 2.000 |
| O | 24.000 | * | 24.000 | * | 24.000 | * | 24.000 | * | 24.000 | * | 24.000 | * | 24.000 | * | 24.000 | * |

33 335 AM565
34 336 AM565
35 337 AM565
36 338 AM565
37 339 AM565
38 340 AM565
39 341 AM565
40 342 AM565

1SUPER RECAL TABLE 3A AMPHIBOLE ANALYSES (OH CALCULATED)

| | 41 |
|---|---|
| SIO2 | 43.92 |
| A2O3 | 13.69 |
| TIO2 | 0.50 |
| FEO | 19.32 |
| MNO | 0.38 |
| MGO | 8.07 |
| CAO | 10.99 |
| NA2O | 1.91 |
| K2O | 0.40 |
| BAO | 0.00 |
| CL | 0.00 |
| F | 0.00 |
| H2O | 2.02 |
| SUM | 101.20 |
| -O= F+CL | 0.00 |
| SUM | 101.20 |

| | | | |
|---|---|---|---|
| SI | 6.509 | * | |
| AL | 1.491 | 8.000 | |
| AL | 0.900 | * | |
| TI | 0.056 | * | |
| FE | 2.395 | * | |
| MN | 0.048 | * | |
| MG | 1.783 | 5.181 | |
| CA | 1.745 | * | |
| NA | 0.549 | * | |
| K | 0.076 | * | |
| BA | 0.000 | 2.370 | |
| CL | 0.000 | * | |
| F | 0.000 | * | |
| H | 2.000 | 2.000 | |
| O | 24.000 | * | |

41 343 AM565

1SUPER RECAL TABLE 3B AMPHIBOLE ANALYSES (OH CALCULATED)

| | 1 | 2 | 3 | 4 | 5 | 6 | 7 | 8 |
|---|---|---|---|---|---|---|---|---|
| SIO2 | 42.65 | 42.73 | 43.14 | 43.24 | 43.38 | 43.20 | 43.26 | 42.82 |
| A2O3 | 13.92 | 14.36 | 14.05 | 13.93 | 14.29 | 14.09 | 14.05 | 14.08 |
| TIO2 | 0.40 | 0.39 | 0.40 | 0.39 | 0.40 | 0.40 | 0.41 | 0.42 |
| FEO | 18.46 | 18.71 | 18.34 | 18.29 | 18.40 | 18.51 | 18.41 | 18.42 |
| MNO | 0.31 | 0.29 | 0.30 | 0.28 | 0.29 | 0.28 | 0.28 | 0.28 |
| MGO | 8.55 | 8.13 | 8.48 | 8.55 | 8.44 | 8.40 | 8.55 | 8.62 |
| CAO | 10.69 | 10.93 | 10.80 | 10.84 | 10.89 | 11.04 | 11.10 | 11.11 |
| NA2O | 1.89 | 1.92 | 2.02 | 1.92 | 1.89 | 1.88 | 1.88 | 1.91 |
| K2O | 0.56 | 0.50 | 0.57 | 0.58 | 0.55 | 0.51 | 0.48 | 0.46 |
| BAO | 0.00 | 0.00 | 0.00 | 0.00 | 0.00 | 0.00 | 0.00 | 0.00 |
| CL | 0.00 | 0.00 | 0.00 | 0.00 | 0.00 | 0.00 | 0.00 | 0.00 |
| F | 0.00 | 0.00 | 0.00 | 0.00 | 0.00 | 0.00 | 0.00 | 0.00 |
| H2O | 1.99 | 2.00 | 2.00 | 2.00 | 2.01 | 2.01 | 2.01 | 2.00 |
| SUM | 99.42 | 99.96 | 100.10 | 100.02 | 100.54 | 100.32 | 100.43 | 100.12 |
| -O= F+CL | 0.00 | 0.00 | 0.00 | 0.00 | 0.00 | 0.00 | 0.00 | 0.00 |
| SUM | 99.42 | 99.96 | 100.10 | 100.02 | 100.54 | 100.32 | 100.43 | 100.12 |

| | | | | | | | | | | | | | | | | |
|---|---|---|---|---|---|---|---|---|---|---|---|---|---|---|---|---|
| SI | 6.428 | * | 6.409 | * | 6.449 | * | 6.466 | * | 6.450 | * | 6.447 | * | 6.445 | * | 6.407 | * |
| AL | 1.572 | 8.000 | 1.591 | 8.000 | 1.551 | 8.000 | 1.534 | 8.000 | 1.550 | 8.000 | 1.553 | 8.000 | 1.555 | 8.000 | 1.593 | 8.000 |
| AL | 0.900 | * | 0.947 | * | 0.924 | * | 0.920 | * | 0.953 | * | 0.924 | * | 0.912 | * | 0.890 | * |
| TI | 0.045 | * | 0.044 | * | 0.045 | * | 0.044 | * | 0.045 | * | 0.045 | * | 0.046 | * | 0.047 | * |
| FE | 2.327 | * | 2.347 | * | 2.293 | * | 2.287 | * | 2.288 | * | 2.310 | * | 2.294 | * | 2.305 | * |
| MN | 0.040 | * | 0.037 | * | 0.038 | * | 0.035 | * | 0.037 | * | 0.035 | * | 0.035 | * | 0.035 | * |
| MG | 1.921 | 5.233 | 1.818 | 5.193 | 1.890 | 5.190 | 1.906 | 5.192 | 1.870 | 5.193 | 1.868 | 5.183 | 1.899 | 5.185 | 1.923 | 5.201 |
| CA | 1.726 | * | 1.757 | * | 1.730 | * | 1.737 | * | 1.735 | * | 1.765 | * | 1.772 | * | 1.781 | * |
| NA | 0.552 | * | 0.558 | * | 0.585 | * | 0.557 | * | 0.545 | * | 0.544 | * | 0.543 | * | 0.554 | * |
| K | 0.108 | * | 0.096 | * | 0.109 | * | 0.111 | * | 0.104 | * | 0.097 | * | 0.091 | * | 0.088 | * |
| BA | 0.000 | 2.386 | 0.000 | 2.411 | 0.000 | 2.424 | 0.000 | 2.404 | 0.000 | 2.384 | 0.000 | 2.406 | 0.000 | 2.406 | 0.000 | 2.423 |
| CL | 0.000 | * | 0.000 | * | 0.000 | * | 0.000 | * | 0.000 | * | 0.000 | * | 0.000 | * | 0.000 | * |
| F | 0.000 | * | 0.000 | * | 0.000 | * | 0.000 | * | 0.000 | * | 0.000 | * | 0.000 | * | 0.000 | * |
| H | 2.000 | 2.000 | 2.000 | 2.000 | 2.000 | 2.000 | 2.000 | 2.000 | 2.000 | 2.000 | 2.000 | 2.000 | 2.000 | 2.000 | 2.000 | 2.000 |
| O | 24.000 | * | 24.000 | * | 24.000 | * | 24.000 | * | 24.000 | * | 24.000 | * | 24.000 | * | 24.000 | * |

1 565 AM425
2 566 AM425
3 567 AM425
4 568 AM425
5 569 AM425
6 570 AM425
7 571 AM425
8 572 AM425

1SUPER RECAL TABLE 3B AMPHIBOLE ANALYSES (OH CALCULATED)

| | 9 | 10 | 11 | 12 | 13 | 14 | 15 | 16 |
|---|---|---|---|---|---|---|---|---|
| SIO2 | 43.45 | 43.68 | 43.89 | 44.28 | 45.30 | 48.05 | 48.39 | 47.58 |
| A2O3 | 13.87 | 13.97 | 13.47 | 12.90 | 11.99 | 9.69 | 8.36 | 9.28 |
| TIO2 | 0.41 | 0.39 | 0.37 | 0.36 | 0.33 | 0.28 | 0.25 | 0.27 |
| FEO | 18.40 | 18.15 | 18.43 | 18.10 | 17.87 | 17.72 | 17.25 | 17.41 |
| MNO | 0.24 | 0.24 | 0.29 | 0.30 | 0.30 | 0.34 | 0.37 | 0.34 |
| MGO | 8.48 | 8.64 | 8.79 | 9.27 | 9.91 | 11.32 | 12.12 | 11.45 |
| CAO | 11.08 | 11.12 | 10.95 | 10.82 | 10.91 | 10.39 | 10.22 | 10.39 |
| NA2O | 1.85 | 1.88 | 1.85 | 1.95 | 1.69 | 1.45 | 1.33 | 1.38 |
| K2O | 0.45 | 0.39 | 0.35 | 0.30 | 0.26 | 0.22 | 0.19 | 0.20 |
| BAO | 0.00 | 0.00 | 0.00 | 0.00 | 0.00 | 0.00 | 0.00 | 0.00 |
| CL | 0.00 | 0.00 | 0.00 | 0.00 | 0.00 | 0.00 | 0.00 | 0.00 |
| F | 0.00 | 0.00 | 0.00 | 0.00 | 0.00 | 0.00 | 0.00 | 0.00 |
| H2O | 2.01 | 2.02 | 2.01 | 2.02 | 2.03 | 2.06 | 2.05 | 2.04 |
| SUM | 100.24 | 100.48 | 100.40 | 100.30 | 100.59 | 101.52 | 100.53 | 100.34 |
| -O= F+CL | 0.00 | 0.00 | 0.00 | 0.00 | 0.00 | 0.00 | 0.00 | 0.00 |
| SUM | 100.24 | 100.48 | 100.40 | 100.30 | 100.59 | 101.52 | 100.53 | 100.34 |

| | | | | | | | | | | | | | | | | |
|---|---|---|---|---|---|---|---|---|---|---|---|---|---|---|---|---|
| SI | 6.480 | * | 6.486 | * | 6.527 | * | 6.579 | * | 6.689 | * | 6.981 | * | 7.084 | * | 6.993 | * |
| AL | 1.520 | 8.000 | 1.514 | 8.000 | 1.473 | 8.000 | 1.421 | 8.000 | 1.311 | 8.000 | 1.019 | 8.000 | 0.916 | 8.000 | 1.007 | 8.000 |
| AL | 0.917 | * | 0.930 | * | 0.887 | * | 0.838 | * | 0.775 | * | 0.640 | * | 0.527 | * | 0.600 | * |
| TI | 0.046 | * | 0.044 | * | 0.041 | * | 0.040 | * | 0.037 | * | 0.031 | * | 0.028 | * | 0.030 | * |
| FE | 2.295 | * | 2.254 | * | 2.292 | * | 2.249 | * | 2.207 | * | 2.153 | * | 2.112 | * | 2.140 | * |
| MN | 0.030 | * | 0.030 | * | 0.037 | * | 0.038 | * | 0.038 | * | 0.042 | * | 0.046 | * | 0.042 | * |
| MG | 1.885 | 5.173 | 1.912 | 5.170 | 1.948 | 5.206 | 2.053 | 5.218 | 2.181 | 5.237 | 2.451 | 5.316 | 2.645 | 5.357 | 2.508 | 5.321 |
| CA | 1.770 | * | 1.769 | * | 1.745 | * | 1.723 | * | 1.726 | * | 1.617 | * | 1.603 | * | 1.636 | * |
| NA | 0.535 | * | 0.541 | * | 0.533 | * | 0.562 | * | 0.484 | * | 0.408 | * | 0.378 | * | 0.393 | * |
| K | 0.086 | * | 0.074 | * | 0.066 | * | 0.057 | * | 0.049 | * | 0.041 | * | 0.035 | * | 0.037 | * |
| BA | 0.000 | 2.391 | 0.000 | 2.384 | 0.000 | 2.344 | 0.000 | 2.341 | 0.000 | 2.259 | 0.000 | 2.066 | 0.000 | 2.016 | 0.000 | 2.067 |
| CL | 0.000 | * | 0.000 | * | 0.000 | * | 0.000 | * | 0.000 | * | 0.000 | * | 0.000 | * | 0.000 | * |
| F | 0.000 | * | 0.000 | * | 0.000 | * | 0.000 | * | 0.000 | * | 0.000 | * | 0.000 | * | 0.000 | * |
| H | 2.000 | 2.000 | 2.000 | 2.000 | 2.000 | 2.000 | 2.000 | 2.000 | 2.000 | 2.000 | 2.000 | 2.000 | 2.000 | 2.000 | 2.000 | 2.000 |
| O | 24.000 | * | 24.000 | * | 24.000 | * | 24.000 | * | 24.000 | * | 24.000 | * | 24.000 | * | 24.000 | * |

9 573 AM425
10 574 AM425
11 575 AM425
12 576 AM425
13 577 AM425
14 578 AM425
15 579 AM425
16 580 AM425

1SUPER RECAL TABLE 3B AMPHIBOLE ANALYSES (OH CALCULATED)

| | 17 | 18 | 19 | 20 | 21 | 22 | 23 | 24 |
|---|---|---|---|---|---|---|---|---|
| SIO2 | 44.48 | 47.40 | 46.35 | 45.06 | 45.10 | 44.65 | 44.64 | 44.77 |
| A2O3 | 10.77 | 9.70 | 10.82 | 12.21 | 12.56 | 13.10 | 13.09 | 12.92 |
| TIO2 | 0.30 | 0.27 | 0.32 | 0.36 | 0.37 | 0.37 | 0.38 | 0.39 |
| FEO | 17.18 | 17.15 | 17.63 | 17.86 | 18.10 | 18.02 | 18.23 | 18.19 |
| MNO | 0.27 | 0.32 | 0.31 | 0.32 | 0.31 | 0.31 | 0.32 | 0.30 |
| MGO | 9.85 | 11.24 | 10.61 | 9.66 | 9.46 | 8.88 | 9.14 | 9.16 |
| CAO | 12.59 | 10.96 | 10.72 | 10.75 | 10.80 | 10.85 | 10.72 | 10.77 |
| NA2O | 1.58 | 1.52 | 1.64 | 1.78 | 1.92 | 1.86 | 1.97 | 1.85 |
| K2O | 0.27 | 0.23 | 0.30 | 0.33 | 0.34 | 0.37 | 0.46 | 0.55 |
| BAO | 0.00 | 0.00 | 0.00 | 0.00 | 0.00 | 0.00 | 0.00 | 0.00 |
| CL | 0.00 | 0.00 | 0.00 | 0.00 | 0.00 | 0.00 | 0.00 | 0.00 |
| F | 0.00 | 0.00 | 0.00 | 0.00 | 0.00 | 0.00 | 0.00 | 0.00 |
| H2O | 1.99 | 2.05 | 2.04 | 2.02 | 2.03 | 2.02 | 2.03 | 2.03 |
| SUM | 99.28 | 100.84 | 100.74 | 100.35 | 100.99 | 100.43 | 100.98 | 100.93 |
| -O= F+CL | 0.00 | 0.00 | 0.00 | 0.00 | 0.00 | 0.00 | 0.00 | 0.00 |
| SUM | 99.28 | 100.84 | 100.74 | 100.35 | 100.99 | 100.43 | 100.98 | 100.93 |

| | | | | | | | | | | | | | | | | |
|---|---|---|---|---|---|---|---|---|---|---|---|---|---|---|---|---|
| SI | 6.690 | * | 6.940 | * | 6.816 | * | 6.673 | * | 6.645 | * | 6.615 | * | 6.589 | * | 6.610 | * |
| AL | 1.310 | 8.000 | 1.060 | 8.000 | 1.184 | 8.000 | 1.327 | 8.000 | 1.355 | 8.000 | 1.385 | 8.000 | 1.411 | 8.000 | 1.390 | 8.000 |
| AL | 0.599 | * | 0.614 | * | 0.691 | * | 0.804 | * | 0.825 | * | 0.902 | * | 0.866 | * | 0.858 | * |
| TI | 0.034 | * | 0.030 | * | 0.035 | * | 0.040 | * | 0.041 | * | 0.041 | * | 0.042 | * | 0.043 | * |
| FE | 2.161 | * | 2.100 | * | 2.168 | * | 2.212 | * | 2.230 | * | 2.233 | * | 2.250 | * | 2.246 | * |
| MN | 0.034 | * | 0.040 | * | 0.039 | * | 0.040 | * | 0.039 | * | 0.039 | * | 0.040 | * | 0.038 | * |
| MG | 2.208 | 5.036 | 2.453 | 5.236 | 2.326 | 5.259 | 2.132 | 5.228 | 2.077 | 5.212 | 1.961 | 5.175 | 2.011 | 5.209 | 2.016 | 5.201 |
| CA | 2.029 | * | 1.719 | * | 1.689 | * | 1.706 | * | 1.705 | * | 1.722 | * | 1.695 | * | 1.704 | * |
| NA | 0.461 | * | 0.431 | * | 0.468 | * | 0.511 | * | 0.548 | * | 0.534 | * | 0.564 | * | 0.530 | * |
| K | 0.052 | * | 0.043 | * | 0.056 | * | 0.062 | * | 0.064 | * | 0.070 | * | 0.087 | * | 0.104 | * |
| BA | 0.000 | 2.541 | 0.000 | 2.194 | 0.000 | 2.213 | 0.000 | 2.279 | 0.000 | 2.317 | 0.000 | 2.326 | 0.000 | 2.346 | 0.000 | 2.337 |
| CL | 0.000 | * | 0.000 | * | 0.000 | * | 0.000 | * | 0.000 | * | 0.000 | * | 0.000 | * | 0.000 | * |
| F | 0.000 | * | 0.000 | * | 0.000 | * | 0.000 | * | 0.000 | * | 0.000 | * | 0.000 | * | 0.000 | * |
| H | 2.000 | 2.000 | 2.000 | 2.000 | 2.000 | 2.000 | 2.000 | 2.000 | 2.000 | 2.000 | 2.000 | 2.000 | 2.000 | 2.000 | 2.000 | 2.000 |
| O | 24.000 | * | 24.000 | * | 24.000 | * | 24.000 | * | 24.000 | * | 24.000 | * | 24.000 | * | 24.000 | * |

17 581 AM425
18 582 AM425
19 583 AM425
20 584 AM425
21 585 AM425
22 586 AM425
23 589 AM425
24 590 AM425

1SUPER RECAL TABLE 3B AMPHIBOLE ANALYSES (OH CALCULATED)

| | 25 | 26 | 27 | 28 | 29 | 30 | 31 | 32 |
|---|---|---|---|---|---|---|---|---|
| SIO2 | 44.25 | 45.59 | 43.01 | 43.18 | 46.49 | 39.98 | 43.60 | 45.61 |
| A2O3 | 13.02 | 10.29 | 14.20 | 13.66 | 10.65 | 10.57 | 13.46 | 15.34 |
| TIO2 | 0.39 | 0.45 | 0.60 | 0.59 | 0.54 | 0.47 | 0.52 | 0.42 |
| FEO | 18.31 | 17.48 | 18.71 | 18.60 | 17.61 | 16.08 | 18.54 | 17.38 |
| MNO | 0.30 | 0.32 | 0.30 | 0.28 | 0.34 | 0.26 | 0 32 | 0.24 |
| MGO | 9.03 | 10.63 | 8.36 | 8.06 | 10.45 | 8.67 | 8.84 | 7.45 |
| CAO | 10.86 | 11.44 | 11.01 | 10.93 | 10.77 | 16.15 | 10.95 | 10.01 |
| NA2O | 1.82 | 1.45 | 1.88 | 1.79 | 1.48 | 1.49 | 1.91 | 3.11 |
| K2O | 0.58 | 0.27 | 0.48 | 0.41 | 0.30 | 0.30 | 0.53 | 0.32 |
| BAO | 0.00 | 0.00 | 0.00 | 0.00 | 0.00 | 0.00 | 0.00 | 0.00 |
| CL | 0.00 | 0.00 | 0.00 | 0.00 | 0.00 | 0.00 | 0.00 | 0.00 |
| F | 0.00 | 0.00 | 0.00 | 0.00 | 0.00 | 0.00 | 0.00 | 0.00 |
| H2O | 2.02 | 2.01 | 2.01 | 1.99 | 2.04 | 1.89 | 2.01 | 2.07 |
| SUM | 100.58 | 99.93 | 100.56 | 99.49 | 100.67 | 95.86 | 100.68 | 101.95 |
| -O= F+CL | 0.00 | 0.00 | 0.00 | 0.00 | 0.00 | 0.00 | 0.00 | 0.00 |
| SUM | 100.58 | 99.93 | 100.56 | 99.49 | 100.67 | 95.86 | 100.68 | 101.95 |

| | | | | | | | | | | | | | | | | |
|---|---|---|---|---|---|---|---|---|---|---|---|---|---|---|---|---|
| SI | 6.570 | * | 6.782 | * | 6.410 | * | 6.495 | * | 6.838 | * | 6.347 | * | 6.484 | * | 6.608 | * |
| AL | 1.430 | 8.000 | 1.218 | 8.000 | 1.590 | 8.000 | 1.505 | 8.000 | 1.162 | 8.000 | 1.653 | 8.000 | 1.516 | 8.000 | 1.392 | 8.000 |
| AL | 0.848 | * | 0.585 | * | 0.904 | * | 0.916 | * | 0.683 | * | 0.324 | * | 0.843 | * | 1.226 | * |
| TI | 0.044 | * | 0.050 | * | 0.067 | * | 0.067 | * | 0.060 | * | 0.056 | * | 0.058 | * | 0.046 | * |
| FE | 2.274 | * | 2.175 | * | 2.332 | * | 2.340 | * | 2.166 | * | 2.135 | * | 2.306 | * | 2.106 | * |
| MN | 0.038 | * | 0.040 | * | 0.038 | * | 0.036 | * | 0.042 | * | 0.035 | * | 0.040 | * | 0.029 | * |
| MG | 1.998 | 5.202 | 2.357 | 5.207 | 1.857 | 5.199 | 1.807 | 5.165 | 2.291 | 5.242 | 2.051 | 4.601 | 1.960 | 5.207 | 1.609 | 5.016 |
| CA | 1.728 | * | 1.823 | * | 1.758 | * | 1.761 | * | 1.697 | * | 2.747 | * | 1.745 | * | 1.554 | * |
| NA | 0.524 | * | 0.418 | * | 0.543 | * | 0.522 | * | 0.422 | * | 0.459 | * | 0.551 | * | 0.874 | * |
| K | 0.110 | * | 0.051 | * | 0.091 | * | 0.079 | * | 0.056 | * | 0.061 | * | 0.101 | * | 0.059 | * |
| BA | 0.000 | 2.361 | 0.000 | 2.293 | 0.000 | 2.393 | 0.000 | 2.362 | 0.000 | 2.175 | 0.000 | 3.266 | 0.000 | 2.396 | 0.000 | 2.486 |
| CL | 0.000 | * | 0.000 | * | 0.000 | * | 0.000 | * | 0.000 | * | 0.000 | * | 0.000 | * | 0.000 | * |
| F | 0.000 | * | 0.000 | * | 0.000 | * | 0.000 | * | 0.000 | * | 0.000 | * | 0.000 | * | 0.000 | * |
| H | 2.000 | 2.000 | 2.000 | 2.000 | 2.000 | 2.000 | 2.000 | 2.000 | 2.000 | 2.000 | 2.000 | 2.000 | 2.000 | 2.000 | 2.000 | 2.000 |
| O | 24.000 | * | 24.000 | * | 24.000 | * | 24.000 | * | 24.000 | * | 24.000 | * | 24.000 | * | 24.000 | * |

25 591 AM425
26 639 AM4425
27 640 AM4425
28 641 AM4425
29 642 AM4425
30 643 AM4425
31 644 AM4425
32 645 AM4425

1SUPER RECAL TABLE 3C AMPHIBOLE ANALYSES (OH CALCULATED)

| | 1 | 2 | 3 | 4 | 5 | 6 | 7 | 8 |
|---|---|---|---|---|---|---|---|---|
| SIO2 | 45.49 | 44.97 | 44.52 | 44.29 | 44.48 | 44.57 | 44.97 | 45.27 |
| A2O3 | 12.22 | 12.58 | 12.39 | 12.56 | 12.42 | 12.69 | 12.34 | 12.13 |
| TIO2 | 0.28 | 0.27 | 0.34 | 0.30 | 0.30 | 0.35 | 0.32 | 0.34 |
| FEO | 15.87 | 16.36 | 16.39 | 16.32 | 16.21 | 16.37 | 16.24 | 16.14 |
| MNO | 0.12 | 0.11 | 0.12 | 0.07 | 0.11 | 0.12 | 0.10 | 0.12 |
| MGO | 10.28 | 10.74 | 10.67 | 10.58 | 10.54 | 10.54 | 10.74 | 10.98 |
| CAO | 11.17 | 11.38 | 11.30 | 11.44 | 11.48 | 11.48 | 11.52 | 11.57 |
| NA2O | 1.74 | 1.72 | 1.81 | 1.81 | 1.80 | 1.92 | 1.80 | 1.83 |
| K2O | 0.32 | 0.34 | 0.35 | 0.38 | 0.38 | 0.40 | 0.40 | 0.38 |
| BAO | -0.14 | -0.15 | -0.14 | -0.13 | -0.15 | -0.14 | -0.11 | -0.12 |
| CL | 0.00 | 0.01 | 0.00 | 0.00 | 0.01 | 0.02 | 0.02 | 0.02 |
| F | 0.01 | 0.02 | 0.01 | 0.02 | 0.01 | 0.02 | 0.03 | 0.02 |
| H2O | 2.02 | 2.02 | 2.02 | 2.01 | 2.01 | 2.02 | 2.02 | 2.03 |
| SUM | 99.38 | 100.37 | 99.78 | 99.65 | 99.60 | 100.36 | 100.39 | 100.71 |
| -O= F+CL | 0.00 | 0.01 | 0.00 | 0.01 | 0.01 | 0.01 | 0.02 | 0.01 |
| SUM | 99.38 | 100.36 | 99.77 | 99.64 | 99.59 | 100.34 | 100.37 | 100.70 |

| | | | | | | | | | | | | | | | | |
|---|---|---|---|---|---|---|---|---|---|---|---|---|---|---|---|---|
| SI | 6.727 | * | 6.612 | * | 6.597 | * | 6.574 | * | 6.601 | * | 6.571 | * | 6.618 | * | 6.637 | * |
| AL | 1.273 | 8.000 | 1.388 | 8.000 | 1.403 | 8.000 | 1.426 | 8.000 | 1.399 | 8.000 | 1.429 | 8.000 | 1.382 | 8.000 | 1.363 | 8.000 |
| AL | 0.857 | * | 0.791 | * | 0.760 | * | 0.771 | * | 0.773 | * | 0.775 | * | 0.758 | * | 0.733 | * |
| TI | 0.031 | * | 0.030 | * | 0.038 | * | 0.033 | * | 0.033 | * | 0.039 | * | 0.035 | * | 0.037 | * |
| FE | 1.963 | * | 2.012 | * | 2.031 | * | 2.026 | * | 2.012 | * | 2.018 | * | 1.999 | * | 1.979 | * |
| MN | 0.015 | * | 0.014 | * | 0.015 | * | 0.009 | * | 0.014 | * | 0.015 | * | 0.012 | * | 0.015 | * |
| MG | 2.266 | 5.132 | 2.354 | 5.200 | 2.357 | 5.201 | 2.341 | 5.180 | 2.331 | 5.163 | 2.316 | 5.163 | 2.356 | 5.161 | 2.399 | 5.163 |
| CA | 1.770 | * | 1.793 | * | 1.794 | * | 1.819 | * | 1.825 | * | 1.813 | * | 1.817 | * | 1.817 | * |
| NA | 0.499 | * | 0.490 | * | 0.520 | * | 0.521 | * | 0.518 | * | 0.549 | * | 0.514 | * | 0.520 | * |
| K | 0.060 | * | 0.064 | * | 0.066 | * | 0.072 | * | 0.072 | * | 0.075 | * | 0.075 | * | 0.071 | * |
| BA | -0.008 | 2.321 | -0.009 | 2.338 | -0.008 | 2.372 | -0.008 | 2.405 | -0.009 | 2.406 | -0.008 | 2.429 | -0.006 | 2.399 | -0.007 | 2.402 |
| CL | 0.000 | * | 0.002 | * | 0.000 | * | 0.000 | * | 0.003 | * | 0.005 | * | 0.005 | * | 0.005 | * |
| F | 0.005 | * | 0.009 | * | 0.005 | * | 0.009 | * | 0.005 | * | 0.009 | * | 0.014 | * | 0.009 | * |
| H | 1.995 | 2.000 | 1.988 | 2.000 | 1.995 | 2.000 | 1.991 | 2.000 | 1.993 | 2.000 | 1.986 | 2.000 | 1.981 | 2.000 | 1.986 | 2.000 |
| O | 24.000 | * | 24.000 | * | 24.000 | * | 24.000 | * | 24.000 | * | 24.000 | * | 24.000 | * | 24.000 | * |

1 41 AM675
2 42 AM675
3 43 AM675
4 44 AM675
5 45 AM675
6 46 AM675
7 47 AM675
8 48 AM675

1SUPER RECAL TABLE 3C AMPHIBOLE ANALYSES (OH CALCULATED)

| | 9 | 10 | 11 | 12 | 13 | 14 | 15 | 16 |
|---|---|---|---|---|---|---|---|---|
| SIO2 | 44.98 | 44.99 | 44.55 | 44.37 | 44.74 | 44.29 | 44.01 | 45.41 |
| A2O3 | 12.16 | 12.15 | 12.00 | 11.95 | 12.16 | 12.88 | 13.07 | 12.07 |
| TIO2 | 0.32 | 0.33 | 1.15 | 1.20 | 0.37 | 0.38 | 0.38 | 0.35 |
| FEO | 16.28 | 16.76 | 16.68 | 16.03 | 16.40 | 16.40 | 16.63 | 15.89 |
| MNO | 0.12 | 0.12 | 0.13 | 0.12 | 0.09 | 0.14 | 0.08 | 0.12 |
| MGO | 10.79 | 10.63 | 10.35 | 10.41 | 10.61 | 10.30 | 10.51 | 11.31 |
| CAO | 11.40 | 11.48 | 11.80 | 11.82 | 11.24 | 11.28 | 11.17 | 11.36 |
| NA2O | 1.79 | 1.78 | 1.81 | 1.79 | 1.87 | 1.99 | 1.85 | 1.88 |
| K2O | 0.38 | 0.37 | 0.36 | 0.36 | 0.37 | 0.39 | 0.34 | 0.31 |
| BAO | -0.10 | -0.08 | -0.12 | -0.16 | -0.18 | -0.14 | -0.17 | -0.19 |
| CL | 0.02 | 0.02 | 0.02 | 0.00 | 0.01 | 0.00 | -0.01 | 0.00 |
| F | 0.03 | 0.05 | 0.04 | 0.05 | -0.01 | 0.06 | 0.02 | -0.01 |
| H2O | 2.01 | 2.01 | 2.01 | 2.00 | 2.02 | 1.99 | 2.02 | 2.05 |
| SUM | 100.18 | 100.60 | 100.78 | 99.94 | 99.69 | 99.96 | 99.90 | 100.55 |
| -O= F+CL | 0.02 | 0.03 | 0.02 | 0.02 | 0.00 | 0.03 | 0.01 | 0.00 |
| SUM | 100.16 | 100.58 | 100.76 | 99.92 | 99.69 | 99.94 | 99.89 | 100.55 |

| | | | | | | | | | | | | | | | | |
|---|---|---|---|---|---|---|---|---|---|---|---|---|---|---|---|---|
| SI | 6.633 | * | 6.623 | * | 6.560 | * | 6.569 | * | 6.632 | * | 6.555 | * | 6.519 | * | 6.651 | * |
| AL | 1.367 | 8.000 | 1.377 | 8.000 | 1.440 | 8.000 | 1.431 | 8.000 | 1.368 | 8.000 | 1.445 | 8.000 | 1.481 | 8.000 | 1.349 | 8.000 |
| AL | 0.747 | * | 0.730 | * | 0.642 | * | 0.654 | * | 0.756 | * | 0.801 | * | 0.800 | * | 0.734 | * |
| TI | 0.035 | * | 0.037 | * | 0.127 | * | 0.134 | * | 0.041 | * | 0.042 | * | 0.042 | * | 0.039 | * |
| FE | 2.008 | * | 2.063 | * | 2.054 | * | 1.985 | * | 2.033 | * | 2.030 | * | 2.060 | * | 1.946 | * |
| MN | 0.015 | * | 0.015 | * | 0.016 | * | 0.015 | * | 0.011 | * | 0.018 | * | 0.010 | * | 0.015 | * |
| MG | 2.372 | 5.177 | 2.332 | 5.177 | 2.272 | 5.112 | 2.297 | 5.085 | 2.344 | 5.186 | 2.272 | 5.162 | 2.320 | 5.233 | 2.469 | 5.203 |
| CA | 1.801 | * | 1.811 | * | 1.862 | * | 1.875 | * | 1.785 | * | 1.789 | * | 1.773 | * | 1.783 | * |
| NA | 0.512 | * | 0.508 | * | 0.517 | * | 0.514 | * | 0.537 | * | 0.571 | * | 0.531 | * | 0.534 | * |
| K | 0.071 | * | 0.069 | * | 0.068 | * | 0.068 | * | 0.070 | * | 0.074 | * | 0.064 | * | 0.058 | * |
| BA | -0.006 | 2.379 | -0.005 | 2.383 | -0.007 | 2.439 | -0.009 | 2.448 | -0.010 | 2.382 | -0.008 | 2.425 | -0.010 | 2.358 | -0.011 | 2.363 |
| CL | 0.005 | * | 0.005 | * | 0.005 | * | 0.000 | * | 0.003 | * | 0.000 | * | -0.003 | * | 0.000 | * |
| F | 0.014 | * | 0.023 | * | 0.019 | * | 0.023 | * | -0.005 | * | 0.028 | * | 0.009 | * | -0.005 | * |
| H | 1.981 | 2.000 | 1.972 | 2.000 | 1.976 | 2.000 | 1.977 | 2.000 | 2.002 | 2.000 | 1.972 | 2.000 | 1.993 | 2.000 | 2.005 | 2.000 |
| O | 24.000 | * | 24.000 | * | 24.000 | * | 24.000 | * | 24.000 | * | 24.000 | * | 24.000 | * | 24.000 | * |

9 49 AM675
10 50 AM675
11 51 AM675
12 53 AM675
13 54 AM675
14 55 AM675
15 56 AM675
16 57 AM675

1SUPER RECAL TABLE 3C AMPHIBOLE ANALYSES (OH CALCULATED)

| | 17 | 18 | 19 | 20 | 21 | 22 | 23 | 24 |
|---|---|---|---|---|---|---|---|---|
| SIO2 | 44.90 | 43.95 | 44.09 | 43.57 | 43.71 | 48.16 | 43.72 | 43.46 |
| A2O3 | 12.94 | 13.16 | 13.40 | 13.64 | 13.54 | 12.40 | 13.50 | 13.78 |
| TIO2 | 0.28 | 0.36 | 0.30 | 0.35 | 0.37 | 0.39 | 0.44 | 0.44 |
| FEO | 16.13 | 15.63 | 15.80 | 15.86 | 15.81 | 14.97 | 16.04 | 16.05 |
| MNO | 0.08 | 0.16 | 0.15 | 0.12 | 0.15 | 0.05 | 0.11 | 0.12 |
| MGO | 9.67 | 10.02 | 9.95 | 10.01 | 9.93 | 9.23 | 10.06 | 10.10 |
| CAO | 11.08 | 11.03 | 11.05 | 11.10 | 11.13 | 10.57 | 11.30 | 11.24 |
| NA2O | 1.85 | 1.81 | 1.88 | 1.78 | 1.80 | 1.65 | 1.88 | 1.97 |
| K2O | 0.39 | 0.36 | 0.37 | 0.38 | 0.37 | 0.31 | 0.36 | 0.36 |
| BAO | -0.15 | -0.14 | -0.22 | -0.13 | -0.14 | -0.17 | -0.15 | -0.20 |
| CL | 0.01 | 0.00 | -0.01 | 0.00 | -0.01 | 0.00 | -0.01 | -0.01 |
| F | 0.04 | 0.04 | 0.03 | 0.05 | 0.05 | 0.04 | 0.02 | 0.03 |
| H2O | 2.00 | 1.98 | 2.00 | 1.98 | 1.98 | 2.04 | 2.01 | 2.00 |
| SUM | 99.22 | 98.36 | 98.79 | 98.71 | 98.69 | 99.64 | 99.28 | 99.34 |
| -O= F+CL | 0.02 | 0.02 | 0.01 | 0.02 | 0.02 | 0.02 | 0.01 | 0.01 |
| SUM | 99.20 | 98.34 | 98.78 | 98.69 | 98.67 | 99.62 | 99.27 | 99.33 |

| | | | | | | | | | | | | | | | | |
|---|---|---|---|---|---|---|---|---|---|---|---|---|---|---|---|---|
| SI | 6.663 | * | 6.578 | * | 6.570 | * | 6.509 | * | 6.529 | * | 6.999 | * | 6.504 | * | 6.463 | * |
| AL | 1.337 | 8.000 | 1.422 | 8.000 | 1.430 | 8.000 | 1.491 | 8.000 | 1.471 | 8.000 | 1.001 | 8.000 | 1.496 | 8.000 | 1.537 | 8.000 |
| AL | 0.925 | * | 0.900 | * | 0.923 | * | 0.910 | * | 0.912 | * | 1.122 | * | 0.871 | * | 0.877 | * |
| TI | 0.031 | * | 0.041 | * | 0.034 | * | 0.039 | * | 0.042 | * | 0.043 | * | 0.049 | * | 0.049 | * |
| FE | 2.002 | * | 1.956 | * | 1.969 | * | 1.981 | * | 1.975 | * | 1.819 | * | 1.996 | * | 1.996 | * |
| MN | 0.010 | * | 0.020 | * | 0.019 | * | 0.015 | * | 0.019 | * | 0.006 | * | 0.014 | * | 0.015 | * |
| MG | 2.139 | 5.107 | 2.235 | 5.152 | 2.210 | 5.155 | 2.229 | 5.175 | 2.211 | 5.158 | 1.999 | 4.989 | 2.231 | 5.161 | 2.239 | 5.176 |
| CA | 1.762 | * | 1.769 | * | 1.764 | * | 1.777 | * | 1.781 | * | 1.646 | * | 1.801 | * | 1.791 | * |
| NA | 0.532 | * | 0.525 | * | 0.543 | * | 0.516 | * | 0.521 | * | 0.465 | * | 0.542 | * | 0.568 | * |
| K | 0.074 | * | 0.069 | * | 0.070 | * | 0.072 | * | 0.070 | * | 0.057 | * | 0.068 | * | 0.068 | * |
| BA | -0.009 | 2.359 | -0.008 | 2.355 | -0.013 | 2.365 | -0.008 | 2.357 | -0.008 | 2.365 | -0.010 | 2.158 | -0.009 | 2.403 | -0.012 | 2.415 |
| CL | 0.003 | * | 0.000 | * | -0.003 | * | 0.000 | * | -0.003 | * | 0.000 | * | -0.003 | * | -0.003 | * |
| F | 0.019 | * | 0.019 | * | 0.014 | * | 0.024 | * | 0.024 | * | 0.018 | * | 0.009 | * | 0.014 | * |
| H | 1.979 | 2.000 | 1.981 | 2.000 | 1.988 | 2.000 | 1.976 | 2.000 | 1.979 | 2.000 | 1.982 | 2.000 | 1.993 | 2.000 | 1.988 | 2.000 |
| O | 24.000 | * | 24.000 | * | 24.000 | * | 24.000 | * | 24.000 | * | 24.000 | * | 24.000 | * | 24.000 | * |

17 82 AM675
18 88 AM675
19 89 AM675
20 90 AM675
21 91 AM675
22 132 AM675
23 133 AM675
24 134 AM675

1SUPER RECAL TABLE 3C AMPHIBOLE ANALYSES (OH CALCULATED)

| | 25 | 26 | 27 | 28 | 29 |
|---|---|---|---|---|---|
| SIO2 | 43.57 | 43.94 | 43.87 | 43.96 | 44.05 |
| A2O3 | 13.54 | 13.57 | 13.51 | 13.55 | 13.70 |
| TIO2 | 0.41 | 0.41 | 0.32 | 0.39 | 0.41 |
| FEO | 16.12 | 16.09 | 15.94 | 16.03 | 15.94 |
| MNO | 0.13 | 0.14 | 0.14 | 0.12 | 0.13 |
| MGO | 10.23 | 10.20 | 10.14 | 10.23 | 10.19 |
| CAO | 11.22 | 11.18 | 11.16 | 11.18 | 11.25 |
| NA2O | 1.98 | 2.04 | 1.98 | 1.96 | 2.00 |
| K2O | 0.37 | 0.38 | 0.39 | 0.38 | 0.38 |
| BAO | -0.17 | -0.18 | -0.14 | -0.17 | -0.14 |
| CL | 0.00 | -0.01 | 0.00 | 0.00 | 0.00 |
| F | 0.02 | 0.02 | 0.06 | 0.06 | 0.02 |
| H2O | 2.00 | 2.02 | 1.99 | 1.99 | 2.02 |
| SUM | 99.42 | 99.80 | 99.36 | 99.68 | 99.95 |
| -O= F+CL | 0.01 | 0.01 | 0.03 | 0.03 | 0.01 |
| SUM | 99.42 | 99.79 | 99.33 | 99.66 | 99.94 |

| | | | | | | | | | | |
|---|---|---|---|---|---|---|---|---|---|---|
| SI | 6.479 | * | 6.503 | * | 6.517 | * | 6.508 | * | 6.504 | * |
| AL | 1.521 | 8.000 | 1.497 | 8.000 | 1.483 | 8.000 | 1.492 | 8.000 | 1.496 | 8.000 |
| AL | 0.851 | * | 0.869 | * | 0.881 | * | 0.871 | * | 0.887 | * |
| TI | 0.046 | * | 0.046 | * | 0.036 | * | 0.043 | * | 0.046 | * |
| FE | 2.005 | * | 1.991 | * | 1.980 | * | 1.985 | * | 1.968 | * |
| MN | 0.016 | * | 0.018 | * | 0.018 | * | 0.015 | * | 0.016 | * |
| MG | 2.267 | 5.185 | 2.250 | 5.173 | 2.245 | 5.160 | 2.257 | 5.171 | 2.242 | 5.160 |
| CA | 1.788 | * | 1.773 | * | 1.776 | * | 1.773 | * | 1.780 | * |
| NA | 0.571 | * | 0.585 | * | 0.570 | * | 0.563 | * | 0.573 | * |
| K | 0.070 | * | 0.072 | * | 0.074 | * | 0.072 | * | 0.072 | * |
| BA | -0.010 | 2.419 | -0.010 | 2.419 | -0.008 | 2.412 | -0.010 | 2.398 | -0.008 | 2.416 |
| CL | 0.000 | * | -0.003 | * | 0.000 | * | 0.000 | * | 0.000 | * |
| F | 0.009 | * | 0.009 | * | 0.028 | * | 0.028 | * | 0.009 | * |
| H | 1.991 | 2.000 | 1.993 | 2.000 | 1.972 | 2.000 | 1.972 | 2.000 | 1.991 | 2.000 |
| O | 24.000 | * | 24.000 | * | 24.000 | * | 24.000 | * | 24.000 | * |

25 135 AM675
26 136 AM675
27 137 AM675
28 138 AM675
29 139 AM675

1SUPER RECAL TABLE 5A FELDSPAR ANALYSES

| | 1 | 2 | 3 | 4 | 5 | 6 | 7 | 8 |
|---|---|---|---|---|---|---|---|---|
| SIO2 | 61.89 | 64.43 | 64.64 | 65.18 | 62.12 | 64.71 | 64.45 | 65.19 |
| A2O3 | 22.23 | 23.17 | 22.78 | 23.07 | 22.64 | 23.16 | 22.76 | 23.02 |
| TIO2 | 0.01 | 0.00 | 0.01 | 0.00 | 0.01 | 0.01 | 0.00 | 0.01 |
| FEO | 1.04 | 0.21 | 0.12 | 0.11 | 0.15 | 0.16 | 0.13 | 0.11 |
| MNO | -0.01 | 0.00 | 0.00 | 0.01 | 0.00 | 0.01 | 0.01 | 0.02 |
| MGO | 0.02 | 0.00 | -0.01 | -0.02 | -0.02 | -0.03 | -0.02 | -0.02 |
| CAO | 3.52 | 3.65 | 3.33 | 3.53 | 3.66 | 3.60 | 3.41 | 3.40 |
| NA2O | 9.66 | 9.99 | 10.24 | 9.88 | 10.06 | 10.21 | 10.06 | 10.27 |
| BAO | 0.00 | 0.00 | 0.00 | 0.00 | 0.00 | 0.00 | 0.00 | 0.00 |
| K2O | 0.06 | 0.07 | 0.07 | 0.07 | 0.06 | 0.07 | 0.07 | 0.06 |
| SUM | 98.42 | 101.52 | 101.18 | 101.83 | 98.68 | 101.90 | 100.87 | 102.06 |

| | | | | | | | | | | | | | | | | |
|---|---|---|---|---|---|---|---|---|---|---|---|---|---|---|---|---|
| SI | 2.795 | * | 2.807 | * | 2.823 | * | 2.824 | * | 2.790 | * | 2.809 | * | 2.822 | * | 2.822 | * |
| AL | 1.183 | * | 1.189 | * | 1.172 | * | 1.178 | * | 1.198 | * | 1.185 | * | 1.174 | * | 1.174 | * |
| TI | 0.000 | 3.978 | 0.000 | 3.996 | 0.000 | 3.995 | 0.000 | 4.002 | 0.000 | 3.989 | 0.000 | 3.994 | 0.000 | 3.997 | 0.000 | 3.996 |
| FE | 0.039 | * | 0.008 | * | 0.004 | * | 0.004 | * | 0.006 | * | 0.008 | * | 0.005 | * | 0.004 | * |
| MN | 0.000 | * | 0.000 | * | 0.000 | * | 0.000 | * | 0.000 | * | 0.000 | * | 0.000 | * | 0.001 | * |
| MG | 0.001 | * | 0.000 | * | -0.001 | * | -0.001 | * | -0.001 | * | -0.002 | * | -0.001 | * | -0.001 | * |
| CA | 0.170 | * | 0.170 | * | 0.156 | * | 0.164 | * | 0.176 | * | 0.167 | * | 0.160 | * | 0.158 | * |
| BA | 0.000 | * | 0.000 | * | 0.000 | * | 0.000 | * | 0.000 | * | 0.000 | * | 0.000 | * | 0.000 | * |
| NA | 0.846 | * | 0.844 | * | 0.867 | * | 0.830 | * | 0.876 | * | 0.859 | * | 0.854 | * | 0.862 | * |
| K | 0.003 | 1.060 | 0.004 | 1.026 | 0.004 | 1.030 | 0.004 | 1.001 | 0.003 | 1.060 | 0.004 | 1.035 | 0.004 | 1.022 | 0.003 | 1.026 |
| O | 8.000 | * | 8.000 | * | 8.000 | * | 8.000 | * | 8.000 | * | 8.000 | * | 8.000 | * | 8.000 | * |

1 26 FE565
2 27 FE565
3 28 FE565
4 29 FE565
5 92 FE565
6 93 FE565
7 94 FE565
8 95 FE565

1SUPER RECAL TABLE 5A FELDSPAR ANALYSES

| | 9 | 10 | 11 | 12 | 13 | 14 | 15 | 16 |
|---|---|---|---|---|---|---|---|---|
| SIO2 | 64.76 | 64.47 | 64.78 | 61.40 | 64.17 | 65.11 | 64.83 | 65.04 |
| A2O3 | 23.06 | 23.32 | 23.59 | 21.78 | 22.95 | 23.51 | 22.99 | 23.01 |
| TIO2 | 0.00 | 0.01 | 0.01 | 0.00 | 0.01 | 0.00 | 0.00 | 0.01 |
| FEO | 0.12 | 0.11 | 0.10 | 0.11 | 0.08 | 0.07 | 0.08 | 0.08 |
| MNO | -0.01 | 0.00 | -0.01 | -0.01 | 0.02 | 0.00 | 0.01 | 0.02 |
| MGO | -0.02 | -0.01 | -0.02 | -0.03 | 0.00 | -0.03 | 0.00 | -0.02 |
| CAO | 3.66 | 3.61 | 3.70 | 3.66 | 3.71 | 3.57 | 3.60 | 3.49 |
| NA2O | 10.12 | 9.99 | 10.02 | 9.06 | 10.01 | 10.26 | 10.08 | 10.26 |
| BAO | 0.00 | 0.00 | 0.00 | 0.00 | 0.00 | 0.00 | 0.00 | 0.00 |
| K2O | 0.07 | 0.06 | 0.07 | 0.06 | 0.08 | 0.08 | 0.07 | 0.07 |
| SUM | 101.76 | 101.56 | 102.24 | 96.03 | 101.03 | 102.57 | 101.66 | 101.96 |

| | | | | | | | | | | | | | | | | |
|---|---|---|---|---|---|---|---|---|---|---|---|---|---|---|---|---|
| SI | 2.814 | * | 2.805 | * | 2.800 | * | 2.822 | * | 2.809 | * | 2.806 | * | 2.818 | * | 2.819 | * |
| AL | 1.181 | * | 1.196 | * | 1.202 | * | 1.179 | * | 1.184 | * | 1.194 | * | 1.177 | * | 1.175 | * |
| TI | 0.000 | 3.994 | 0.000 | 4.001 | 0.000 | 4.003 | 0.000 | 4.001 | 0.000 | 3.993 | 0.000 | 4.000 | 0.000 | 3.995 | 0.000 | 3.995 |
| FE | 0.004 | * | 0.004 | * | 0.004 | * | 0.004 | * | 0.003 | * | 0.003 | * | 0.003 | * | 0.003 | * |
| MN | 0.000 | * | 0.000 | * | 0.000 | * | 0.000 | * | 0.001 | * | 0.000 | * | 0.000 | * | 0.001 | * |
| MG | -0.001 | * | -0.001 | * | -0.001 | * | -0.002 | * | 0.000 | * | -0.002 | * | 0.000 | * | -0.001 | * |
| CA | 0.170 | * | 0.168 | * | 0.171 | * | 0.180 | * | 0.174 | * | 0.165 | * | 0.168 | * | 0.162 | * |
| BA | 0.000 | * | 0.000 | * | 0.000 | * | 0.000 | * | 0.000 | * | 0.000 | * | 0.000 | * | 0.000 | * |
| NA | 0.852 | * | 0.843 | * | 0.840 | * | 0.807 | * | 0.850 | * | 0.857 | * | 0.849 | * | 0.862 | * |
| K | 0.004 | 1.029 | 0.003 | 1.018 | 0.004 | 1.017 | 0.004 | 0.993 | 0.004 | 1.032 | 0.004 | 1.027 | 0.004 | 1.024 | 0.004 | 1.031 |
| O | 8.000 | * | 8.000 | * | 8.000 | * | 8.000 | * | 8.000 | * | 8.000 | * | 8.000 | * | 8.000 | * |

9 96 FE565
10 97 FE565
11 98 FE565
12 99 FE565
13 101 FE565
14 102 FE565
15 103 FE565
16 104 FE565

1SUPER RECAL TABLE 5A FELDSPAR ANALYSES

| | 17 | 18 | 19 | 20 | 21 | 22 | 23 | 24 |
|---|---|---|---|---|---|---|---|---|
| SIO2 | 65.46 | 65.10 | 65.16 | 64.59 | 65.63 | 64.18 | 65.23 | 64.90 |
| A2O3 | 22.97 | 23.14 | 23.41 | 23.42 | 23.63 | 23.18 | 23.56 | 23.27 |
| TIO2 | 0.00 | 0.00 | 0.00 | 0.01 | 0.01 | 0.01 | 0.01 | 0.02 |
| FEO | 0.10 | 0.08 | 0.08 | 0.08 | 0.11 | 0.09 | 0.11 | 0.11 |
| MNO | 0.00 | -0.01 | -0.01 | 0.02 | 0.00 | 0.02 | 0.00 | 0.00 |
| MGO | -0.01 | 0.00 | -0.02 | -0.01 | 0.00 | -0.02 | 0.02 | -0.01 |
| CAO | 3.57 | 3.59 | 3.73 | 3.68 | 3.65 | 3.64 | 3.75 | 3.81 |
| NA2O | 10.22 | 10.11 | 10.00 | 10.23 | 10.06 | 9.92 | 10.08 | 10 00 |
| BAO | 0.00 | 0.00 | 0.00 | 0.00 | 0.00 | 0.00 | 0.00 | 0.00 |
| K2O | 0.07 | 0.07 | 0.07 | 0.07 | 0.08 | 0.08 | 0.08 | 0.07 |
| SUM | 102.38 | 102.08 | 102.42 | 102.09 | 103.17 | 101.10 | 102.84 | 102.17 |

| | | | | | | | | | | | | | | | | |
|---|---|---|---|---|---|---|---|---|---|---|---|---|---|---|---|---|
| SI | 2.825 | * | 2.817 | * | 2.810 | * | 2.799 | * | 2.810 | * | 2.806 | * | 2.804 | * | 2.808 | * |
| AL | 1.168 | * | 1.180 | * | 1.190 | * | 1.196 | * | 1.192 | * | 1.194 | * | 1.193 | * | 1.187 | * |
| TI | 0.000 | 3.993 | 0.000 | 3.997 | 0.000 | 4.000 | 0.000 | 3.996 | 0.000 | 4.002 | 0.000 | 4.000 | 0.000 | 3.998 | 0.001 | 3.996 |
| FE | 0.004 | * | 0.003 | * | 0.003 | * | 0.003 | * | 0.004 | * | 0.003 | * | 0.004 | * | 0.004 | * |

| | | | | | | | | | | | | | | | |
|---|---|---|---|---|---|---|---|---|---|---|---|---|---|---|---|
| MN | 0.000 | * | 0.000 | * | 0.000 | * | 0.001 | * | 0.000 | * | 0.001 | * | 0.000 | * | 0.000 | * |
| MG | -0.001 | * | 0.000 | * | -0.001 | * | -0.001 | * | 0.000 | * | -0.001 | * | 0.001 | * | -0.001 | * |
| CA | 0.165 | * | 0.166 | * | 0.172 | * | 0.171 | * | 0.167 | * | 0.170 | * | 0.173 | * | 0.177 | * |
| BA | 0.000 | * | 0.000 | * | 0.000 | * | 0.000 | * | 0.000 | * | 0.000 | * | 0.000 | * | 0.000 | * |
| NA | 0.855 | * | 0.848 | * | 0.836 | * | 0.860 | * | 0.835 | * | 0.841 | * | 0.840 | * | 0.839 | * |
| K | 0.004 | 1.027 | 0.004 | 1.021 | 0.004 | 1.014 | 0.004 | 1.037 | 0.004 | 1.011 | 0.004 | 1.019 | 0.004 | 1.022 | 0.004 | 1.023 |
| O | 8.000 | * | 8.000 | * | 8.000 | * | 8.000 | * | 8.000 | * | 8.000 | * | 8.000 | * | 8.000 | * |

17 105 FE565
18 106 FE565
19 107 FE565
20 108 FE565
21 109 FE56A
22 110 FE56A
23 111 FE56A
24 112 FE56A

1SUPER RECAL TABLE 5A FELDSPAR ANALYSES

| | 25 | 26 | 27 | 28 | 29 | 30 | 31 | 32 |
|---|---|---|---|---|---|---|---|---|
| SIO2 | 64.99 | 65.18 | 65.09 | 64.71 | 64.10 | 64.71 | 64.06 | 64.15 |
| A2O3 | 23.60 | 23.48 | 23.20 | 23.32 | 23.63 | 23.82 | 24.02 | 23.48 |
| TIO2 | 0.00 | 0.02 | 0.01 | 0.00 | -0.01 | 0.01 | 0.01 | 0.01 |
| FEO | 0.12 | 0.13 | 0.16 | 0.16 | 0.15 | 0.14 | 0.13 | 0.13 |
| MNO | 0.02 | 0.03 | -0.02 | 0.02 | 0.00 | 0.02 | 0.00 | 0.00 |
| MGO | -0.01 | 0.00 | -0.02 | -0.01 | -0.02 | -0.02 | 0.00 | -0.03 |
| CAO | 3.66 | 3.72 | 3.72 | 3.71 | 4.14 | 4.17 | 4.32 | 4.19 |
| NA2O | 10.10 | 9.99 | 9.78 | 10.02 | 9.65 | 9.76 | 9.69 | 9.53 |
| BAO | 0.00 | 0.00 | 0.00 | 0.00 | 0.00 | 0.00 | 0.00 | 0.00 |
| K2O | 0.07 | 0.07 | 0.08 | 0.07 | 0.07 | 0.07 | 0.07 | 0.07 |
| SUM | 102.55 | 102.62 | 102.00 | 102.00 | 101.71 | 102.68 | 102.30 | 101.53 |

| | | | | | | | | | | | | | | | |
|---|---|---|---|---|---|---|---|---|---|---|---|---|---|---|---|
| SI | 2.802 | * | 2.807 | * | 2.817 | * | 2.806 | * | 2.789 | * | 2.789 | * | 2.773 | * | 2.794 | * |
| AL | 1.199 | * | 1.192 | * | 1.183 | * | 1.191 | * | 1.211 | * | 1.210 | * | 1.225 | * | 1.205 | * |
| TI | 0.000 | 4.001 | 0.001 | 3.999 | 0.000 | 4.001 | 0.000 | 3.997 | 0.000 | 4.000 | 0.000 | 3.999 | 0.000 | 3.999 | 0.000 | 4.000 |
| FE | 0.004 | * | 0.005 | * | 0.006 | * | 0.006 | * | 0.005 | * | 0.005 | * | 0.005 | * | 0.005 | * |
| MN | 0.001 | * | 0.001 | * | -0.001 | * | 0.001 | * | 0.000 | * | 0.001 | * | 0.000 | * | 0.000 | * |
| MG | -0.001 | * | 0.000 | * | -0.001 | * | -0.001 | * | -0.001 | * | -0.001 | * | 0.000 | * | -0.002 | * |
| CA | 0.169 | * | 0.172 | * | 0.173 | * | 0.172 | * | 0.193 | * | 0.193 | * | 0.200 | * | 0.196 | * |
| BA | 0.000 | * | 0.000 | * | 0.000 | * | 0.000 | * | 0.000 | * | 0.000 | * | 0.000 | * | 0.000 | * |
| NA | 0.844 | * | 0.834 | * | 0.821 | * | 0.842 | * | 0.814 | * | 0.816 | * | 0.813 | * | 0.805 | * |
| K | 0.004 | 1.022 | 0.004 | 1.015 | 0.004 | 1.001 | 0.004 | 1.024 | 0.004 | 1.015 | 0.004 | 1.016 | 0.004 | 1.022 | 0.004 | 1.007 |
| O | 8.000 | * | 8.000 | * | 8.000 | * | 8.000 | * | 8.000 | * | 8.000 | * | 8.000 | * | 8.000 | * |

25 113 FE565
26 114 FE565
27 115 FE565
28 116 FE565
29 126 FE565
30 127 FE565
31 128 FE565
32 129 FE565

1SUPER RECAL TABLE 5A FELDSPAR ANALYSES

| | 33 | 34 | 35 | 36 | 37 | 38 | 39 | 40 |
|---|---|---|---|---|---|---|---|---|
| SIO2 | 63.86 | 64.27 | 63.55 | 64.35 | 64.61 | 63.68 | 64.11 | 64.49 |
| A2O3 | 23.75 | 23.84 | 23.74 | 24.02 | 24.12 | 23.54 | 23.84 | 23.84 |
| TIO2 | 0.01 | 0.01 | 0.01 | 0.01 | 0.00 | 0.01 | 0.01 | 0.01 |
| FEO | 0.14 | 0.12 | 0.14 | 0.13 | 0.15 | 0.13 | 0.15 | 0.14 |
| MNO | 0.01 | -0.02 | 0.00 | 0.01 | 0.00 | 0.01 | 0.01 | 0.00 |
| MGO | 0.00 | -0.02 | -0.02 | -0.01 | 0.00 | -0.01 | 0.01 | -0.03 |
| CAO | 4.24 | 4.26 | 4.21 | 4.25 | 4.24 | 4.21 | 4.27 | 4.34 |
| NA2O | 9.62 | 9.85 | 9.78 | 9.76 | 9.40 | 9.60 | 9.64 | 9.59 |
| BAO | 0.00 | 0.00 | 0.00 | 0.00 | 0.00 | 0.00 | 0.00 | 0.00 |
| K2O | 0.07 | 0.07 | 0.07 | 0.07 | 0.08 | 0.08 | 0.07 | 0.07 |
| SUM | 101.70 | 102.38 | 101.48 | 102.59 | 102.60 | 101.25 | 102.11 | 102.45 |

| | | | | | | | | | | | | | | | |
|---|---|---|---|---|---|---|---|---|---|---|---|---|---|---|---|
| SI | 2.780 | * | 2.780 | * | 2.775 | * | 2.777 | * | 2.783 | * | 2.784 | * | 2.780 | * | 2.786 | * |
| AL | 1.218 | * | 1.215 | * | 1.221 | * | 1.222 | * | 1.224 | * | 1.213 | * | 1.218 | * | 1.213 | * |
| TI | 0.000 | 3.999 | 0.000 | 3.996 | 0.000 | 3.997 | 0.000 | 3.999 | 0.000 | 4.008 | 0.000 | 3.997 | 0.000 | 3.998 | 0.000 | 3.999 |
| FE | 0.005 | * | 0.004 | * | 0.005 | * | 0.005 | * | 0.005 | * | 0.005 | * | 0.005 | * | 0.005 | * |
| MN | 0.000 | * | -0.001 | * | 0.000 | * | 0.000 | * | 0.000 | * | 0.000 | * | 0.000 | * | 0.000 | * |
| MG | 0.000 | * | -0.001 | * | -0.001 | * | -0.001 | * | 0.000 | * | -0.001 | * | 0.001 | * | -0.002 | * |
| CA | 0.198 | * | 0.197 | * | 0.197 | * | 0.197 | * | 0.196 | * | 0.197 | * | 0.198 | * | 0.201 | * |
| BA | 0.000 | * | 0.000 | * | 0.000 | * | 0.000 | * | 0.000 | * | 0.000 | * | 0.000 | * | 0.000 | * |
| NA | 0.812 | * | 0.826 | * | 0.828 | * | 0.817 | * | 0.785 | * | 0.814 | * | 0.810 | * | 0.803 | * |
| K | 0.004 | 1.019 | 0.004 | 1.030 | 0.004 | 1.033 | 0.004 | 1.022 | 0.004 | 0.991 | 0.004 | 1.020 | 0.004 | 1.019 | 0.004 | 1.011 |
| O | 8.000 | * | 8.000 | * | 8.000 | * | 8.000 | * | 8.000 | * | 8.000 | * | 8.000 | * | 8.000 | * |

33 130 FE565
34 131 FE565
35 132 FE565
36 133 FE565
37 134 FE565
38 135 FE565
39 136 FE565
40 137 FE565

1SUPER RECAL TABLE 5A FELDSPAR ANALYSES

| | 41 | 42 | 43 | 44 |
|---|---|---|---|---|
| SIO2 | 64.34 | 64.24 | 63.99 | 64.42 |
| A2O3 | 23.99 | 24.01 | 23.90 | 23.61 |
| TIO2 | 0.01 | 0.01 | 0.00 | 0.01 |

| | | | | | | | | |
|---|---|---|---|---|---|---|---|---|
| FEO | | 0.17 | | 0.17 | | 0.23 | | 0.25 |
| MNO | | 0.00 | | 0.01 | | 0.01 | | 0.01 |
| MGO | | 0.00 | | -0.04 | | 0.01 | | 0.01 |
| CAO | | 4.38 | | 4.43 | | 4.34 | | 4.35 |
| NA2O | | 9.62 | | 9.54 | | 9.50 | | 9.58 |
| BAO | | 0.00 | | 0.00 | | 0.00 | | 0.00 |
| K2O | | 0.07 | | 0.06 | | 0.07 | | 0.07 |
| SUM | | 102.58 | | 102.43 | | 102.05 | | 102.31 |
| SI | 2.777 | * | 2.777 | * | 2.777 | * | 2.788 | * |
| AL | 1.220 | * | 1.223 | * | 1.222 | * | 1.204 | * |
| TI | 0.000 | 3.998 | 0.000 | 4.000 | 0.000 | 3.999 | 0.000 | 3.993 |
| FE | 0.006 | * | 0.006 | * | 0.008 | * | 0.009 | * |
| MN | 0.000 | * | 0.000 | * | 0.000 | * | 0.000 | * |
| MG | 0.000 | * | -0.003 | * | 0.001 | * | 0.001 | * |
| CA | 0.203 | * | 0.205 | * | 0.202 | * | 0.202 | * |
| BA | 0.000 | * | 0.000 | * | 0.000 | * | 0.000 | * |
| NA | 0.805 | * | 0.800 | * | 0.799 | * | 0.804 | * |
| K | 0.004 | 1.018 | 0.003 | 1.012 | 0.004 | 1.014 | 0.004 | 1.020 |
| O | 8.000 | * | 8.000 | * | 8.000 | * | 8.000 | * |

41 138 FE565
42 139 FE565
43 140 FE565
44 141 FE565

1SUPER RECAL TABLE 5B FELDSPAR ANALYSES

| | 1 | 2 | 3 | 4 | 5 | 6 | 7 | 8 |
|---|---|---|---|---|---|---|---|---|
| SIO2 | 68.68 | 68.70 | 68.90 | 69.00 | 68.73 | 67.37 | 63.99 | 65.75 |
| A2O3 | 20.41 | 20.33 | 20.33 | 20.69 | 19.93 | 21.31 | 23.11 | 19.66 |
| TIO2 | 0.01 | 0.02 | 0.05 | 0.01 | 0.01 | 0.02 | 0.05 | 0.02 |
| FEO | 0.22 | 0.16 | 0.26 | 0.24 | 0.16 | 0.34 | 0.39 | 0.25 |
| MNO | 0.01 | 0.00 | 0.00 | 0.00 | -0.01 | 0.01 | 0.02 | 0.00 |
| MGO | -0.03 | -0.02 | -0.03 | -0.02 | -0.02 | -0.02 | -0.02 | -0.01 |
| CAO | 0.72 | 0.62 | 0.63 | 0.65 | 0.37 | 1.76 | 3.73 | 3.01 |
| NA2O | 11.23 | 11.28 | 11.04 | 11.30 | 11.23 | 10.64 | 9.41 | 10.74 |
| BAO | 0.00 | 0.00 | 0.00 | 0.00 | 0.00 | 0.00 | 0.00 | 0.00 |
| K2O | 0.04 | 0.04 | 0.04 | 0.04 | 0.05 | 0.04 | 0.05 | 0.04 |
| SUM | 101.29 | 101.13 | 101.22 | 101.91 | 100.45 | 101.47 | 100.73 | 99.46 |

| | | | | | | | | | | | | | | | | |
|---|---|---|---|---|---|---|---|---|---|---|---|---|---|---|---|---|
| SI | 2.965 | * | 2.969 | * | 2.973 | * | 2.961 | * | 2.986 | * | 2.914 | * | 2.807 | * | 2.920 | * |
| AL | 1.038 | * | 1.035 | * | 1.034 | * | 1.046 | * | 1.020 | * | 1.086 | * | 1.195 | * | 1.029 | * |
| TI | 0.000 | 4.004 | 0.001 | 4.005 | 0.002 | 4.008 | 0.000 | 4.007 | 0.000 | 4.007 | 0.001 | 4.001 | 0.002 | 4.003 | 0.001 | 3.949 |
| FE | 0.008 | * | 0.006 | * | 0.009 | * | 0.009 | * | 0.006 | * | 0.012 | * | 0.014 | * | 0.009 | * |
| MN | 0.000 | * | 0.000 | * | 0.000 | * | 0.000 | * | 0.000 | * | 0.000 | * | 0.001 | * | 0.000 | * |
| MG | -0.002 | * | -0.001 | * | -0.002 | * | -0.001 | * | -0.001 | * | -0.001 | * | -0.001 | * | -0.001 | * |
| CA | 0.033 | * | 0.029 | * | 0.029 | * | 0.030 | * | 0.017 | * | 0.082 | * | 0.175 | * | 0.143 | * |
| BA | 0.000 | * | 0.000 | * | 0.000 | * | 0.000 | * | 0.000 | * | 0.000 | * | 0.000 | * | 0.000 | * |
| NA | 0.940 | * | 0.945 | * | 0.924 | * | 0.940 | * | 0.946 | * | 0.892 | * | 0.800 | * | 0.925 | * |
| K | 0.002 | 0.982 | 0.002 | 0.981 | 0.002 | 0.962 | 0.002 | 0.979 | 0.003 | 0.970 | 0.002 | 0.988 | 0.003 | 0.992 | 0.002 | 1.079 |
| O | 8.000 | * | 8.000 | * | 8.000 | * | 8.000 | * | 8.000 | * | 8.000 | * | 8.000 | * | 8.000 | * |

1 647 FE425
2 648 FE425
3 649 FE425
4 650 FE425
5 651 FE425
6 657 FE425
7 658 FE425
8 659 FE425

1SUPER RECAL TABLE 5B FELDSPAR ANALYSES

| | 9 | 10 | 11 |
|---|---|---|---|
| SIO2 | 67.79 | 66.37 | 68.38 |
| A2O3 | 20.52 | 19.82 | 20.47 |
| TIO2 | 0.01 | 0.00 | 0.01 |
| FEO | 0.28 | 0.23 | 0.27 |
| MNO | 0.01 | 0.00 | 0.02 |
| MGO | -0.03 | -0.03 | -0.05 |
| CAO | 1.03 | 2.16 | 0.59 |
| NA2O | 11.11 | 10.98 | 11.22 |
| BAO | 0.00 | 0.00 | 0.00 |
| K2O | 0.04 | 0.04 | 0.04 |
| SUM | 100.76 | 99.57 | 100.95 |

| | | | | | | |
|---|---|---|---|---|---|---|
| SI | 2.948 | * | 2.935 | * | 2.962 | * |
| AL | 1.051 | * | 1.033 | * | 1.045 | * |
| TI | 0.000 | 4.000 | 0.000 | 3.968 | 0.000 | 4.007 |
| FE | 0.010 | * | 0.009 | * | 0.010 | * |
| MN | 0.000 | * | 0.000 | * | 0.001 | * |
| MG | -0.002 | * | -0.002 | * | -0.003 | * |
| CA | 0.048 | * | 0.102 | * | 0.027 | * |
| BA | 0.000 | * | 0.000 | * | 0.000 | * |
| NA | 0.937 | * | 0.941 | * | 0.942 | * |
| K | 0.002 | 0.995 | 0.002 | 1.052 | 0.002 | 0.979 |
| O | 8.000 | * | 8.000 | * | 8.000 | * |

9 660 FE425
10 661 FE425
11 662 FE425

1SUPER RECAL TABLE 5B CHLORITE ANALYSES

| | 1 | 2 | 3 | 4 | 5 | 6 | 7 | 8 |
|---|---|---|---|---|---|---|---|---|
| SIO2 | 28.30 | 25.35 | 30.57 | 25.75 | 27.16 | 25.81 | 25.11 | 29.39 |
| A2O3 | 21.95 | 19.76 | 18.93 | 21.17 | 20.37 | 20.94 | 20.38 | 20.49 |
| TIO2 | 0.15 | 0.12 | 0.30 | 0.16 | 0.20 | 0.10 | 0.11 | 0.10 |
| FEO | 21.55 | 22.01 | 22.15 | 23.09 | 23.71 | 22.67 | 22.26 | 20.71 |
| MNO | 0.15 | 0.20 | 0.19 | 0.17 | 0.15 | 0.19 | 0.17 | 0.15 |
| MGO | 15.79 | 16.63 | 15.61 | 17.48 | 17.52 | 16.87 | 16.39 | 15.14 |
| CAO | 1.02 | 2.82 | 1.99 | 0.10 | 0.10 | 0.06 | 0.08 | 0.22 |
| NA2O | 0.30 | 0.03 | 0.35 | 0.09 | 0.07 | 0.00 | 0.00 | 1.02 |
| K2O | 0.08 | 0.03 | 0.62 | 0.04 | 0.03 | 0.02 | 0.02 | 0.02 |
| BAO | 0.00 | 0.00 | 0.00 | 0.00 | 0.00 | 0.00 | 0.00 | 0.00 |
| CL | 0.00 | 0.00 | 0.00 | 0.00 | 0.00 | 0.00 | 0.00 | 0.00 |
| F | 0.00 | 0.00 | 0.00 | 0.00 | 0.00 | 0.00 | 0.00 | 0.00 |
| H2O | 11.88 | 11.32 | 11.97 | 11.55 | 11.72 | 11.40 | 11.10 | 11.68 |
| SUM | 101.17 | 98.27 | 102.68 | 99.60 | 101.03 | 98.06 | 95.62 | 98.92 |
| -O= F+CL | 0.00 | 0.00 | 0.00 | 0.00 | 0.00 | 0.00 | 0.00 | 0.00 |
| SUM | 101.17 | 98.27 | 102.68 | 99.60 | 101.03 | 98.06 | 95.62 | 98.92 |

| | | | | | | | | | | | | | | | | |
|---|---|---|---|---|---|---|---|---|---|---|---|---|---|---|---|---|
| SI | 2.855 | * | 2.684 | * | 3.060 | * | 2.672 | * | 2.777 | * | 2.714 | * | 2.710 | * | 3.016 | * |
| AL | 1.145 | 4.000 | 1.316 | 4.000 | 0.940 | 4.000 | 1.328 | 4.000 | 1.223 | 4.000 | 1.286 | 4.000 | 1.290 | 4.000 | 0.984 | 4.000 |
| AL | 1.465 | * | 1.148 | * | 1.292 | * | 1.261 | * | 1.232 | * | 1.309 | * | 1.302 | * | 1.494 | * |
| TI | 0.011 | * | 0.010 | * | 0.023 | * | 0.012 | * | 0.015 | * | 0.008 | * | 0.009 | * | 0.008 | * |
| FE | 1.818 | * | 1.948 | * | 1.854 | * | 2.004 | * | 2.028 | * | 1.994 | * | 2.009 | * | 1.778 | * |
| MN | 0.013 | * | 0.018 | * | 0.016 | * | 0.015 | * | 0.013 | * | 0.017 | * | 0.016 | * | 0.013 | * |
| MG | 2.375 | * | 2.624 | * | 2.329 | * | 2.704 | * | 2.670 | * | 2.644 | * | 2.637 | * | 2.316 | * |
| CA | 0.110 | * | 0.320 | * | 0.213 | * | 0.011 | * | 0.011 | * | 0.007 | * | 0.009 | * | 0.024 | * |
| NA | 0.059 | * | 0.006 | * | 0.068 | * | 0.018 | * | 0.014 | * | 0.000 | * | 0.000 | * | 0.203 | * |
| K | 0.010 | * | 0.004 | * | 0.079 | * | 0.005 | * | 0.004 | * | 0.003 | * | 0.003 | * | 0.003 | * |
| BA | 0.000 | 5.862 | 0.000 | 6.078 | 0.000 | 5.874 | 0.000 | 6.031 | 0.000 | 5.987 | 0.000 | 5.981 | 0.000 | 5.985 | 0.000 | 5.838 |
| CL | 0.000 | * | 0.000 | * | 0.000 | * | 0.000 | * | 0.000 | * | 0.000 | * | 0.000 | * | 0.000 | * |
| F | 0.000 | * | 0.000 | * | 0.000 | * | 0.000 | * | 0.000 | * | 0.000 | * | 0.000 | * | 0.000 | * |
| H | 8.000 | 8.000 | 8.000 | 8.000 | 8.000 | 8.000 | 8.000 | 8.000 | 8.000 | 8.000 | 8.000 | 8.000 | 8.000 | 8.000 | 8.000 | 8.000 |
| O | 18.000 | * | 18.000 | * | 18.000 | * | 18.000 | * | 18.000 | * | 18.000 | * | 18.000 | * | 18.000 | * |

1 652 CH425
2 653 CH425
3 654 CH425
4 655 CH425
5 656 CH425
6 663 CH425
7 664 CH425
8 665 CH425

1SUPER RECAL TABLE 5C FELDSPAR ANALYSES

| | 1 | 2 | 3 | 4 | 5 | 6 | 7 | 8 |
|---|---|---|---|---|---|---|---|---|
| SIO2 | 62.74 | 62.89 | 64.19 | 63.41 | 63.32 | 61.39 | 62.23 | 63.08 |
| A2O3 | 22.87 | 22.88 | 22.50 | 23.22 | 23.33 | 21.19 | 23.38 | 23.36 |
| TIO2 | 0.03 | 1.01 | 0.06 | -0.02 | -0.01 | -0.03 | -0.08 | -0.06 |
| FEO | 0.28 | 0.44 | 0.33 | 0.20 | 0.21 | 2.25 | 0.63 | 0.17 |
| MNO | -0.12 | -0.13 | -0.15 | -0.14 | -0.15 | -0.11 | -0.13 | -0.12 |
| MGO | -0.06 | -0.05 | -0.01 | -0.06 | -0.05 | 1.09 | 0.27 | -0.05 |
| CAO | 4.36 | 4.86 | 4.12 | 4.45 | 4.68 | 4.60 | 4.99 | 4.50 |
| BAO | -0.19 | -0.10 | -0.16 | -0.24 | -0.20 | -0.23 | -0.20 | -0.17 |
| NA2O | 9.34 | 9.61 | 8.76 | 9.58 | 9.04 | 9.29 | 8.86 | 9.34 |
| K2O | 0.05 | 0.03 | 0.04 | 0.05 | 0.05 | 0.07 | 0.05 | 0.05 |
| SUM | 99.30 | 101.44 | 99.68 | 100.45 | 100.22 | 99.51 | 100.00 | 100.10 |

| | | | | | | | | | | | | | | | | |
|---|---|---|---|---|---|---|---|---|---|---|---|---|---|---|---|---|
| SI | 2.793 | * | 2.758 | * | 2.833 | * | 2.790 | * | 2.790 | * | 2.767 | * | 2.760 | * | 2.785 | * |
| AL | 1.200 | * | 1.182 | * | 1.170 | * | 1.204 | * | 1.211 | * | 1.125 | * | 1.222 | * | 1.215 | * |
| TI | 0.001 | 3.994 | 0.033 | 3.973 | 0.002 | 4.005 | -0.001 | 3.994 | 0.000 | 4.001 | -0.001 | 3.891 | -0.003 | 3.979 | -0.002 | 3.999 |
| FE | 0.010 | * | 0.016 | * | 0.012 | * | 0.007 | * | 0.008 | * | 0.085 | * | 0.023 | * | 0.006 | * |
| MN | -0.005 | * | -0.005 | * | -0.006 | * | -0.005 | * | -0.006 | * | -0.004 | * | -0.005 | * | -0.004 | * |
| MG | -0.004 | * | -0.003 | * | -0.001 | * | -0.004 | * | -0.003 | * | 0.073 | * | 0.018 | * | -0.003 | * |
| CA | 0.208 | * | 0.228 | * | 0.195 | * | 0.210 | * | 0.221 | * | 0.222 | * | 0.237 | * | 0.213 | * |
| BA | -0.003 | * | -0.002 | * | -0.003 | * | -0.004 | * | -0.003 | * | -0.004 | * | -0.003 | * | -0.003 | * |
| NA | 0.806 | * | 0.817 | * | 0.750 | * | 0.817 | * | 0.772 | * | 0.812 | * | 0.762 | * | 0.800 | * |
| K | 0.003 | 1.016 | 0.002 | 1.053 | 0.002 | 0.950 | 0.003 | 1.024 | 0.003 | 0.991 | 0.004 | 1.188 | 0.003 | 1.035 | 0.003 | 1.011 |
| O | 8.000 | * | 8.000 | * | 8.000 | * | 8.000 | * | 8.000 | * | 8.000 | * | 8.000 | * | 8.000 | * |

1 60 FE675
2 63 FE675
3 64 FE675
4 65 FE675
5 66 FE675
6 76 FE675
7 80 FE675
8 81 FE675

1SUPER RECAL TABLE 5C FELDSPAR ANALYSES

| | 9 | 10 | 11 | 12 | 13 | 14 | 15 | 16 |
|---|---|---|---|---|---|---|---|---|
| SIO2 | 62.36 | 62.56 | 63.60 | 63.79 | 63.69 | 63.65 | 63.50 | 63.13 |
| A2O3 | 22.75 | 22.75 | 23.46 | 23.26 | 23.25 | 23.15 | 23.41 | 23.27 |
| TIO2 | -0.04 | -0.05 | -0.09 | -0.09 | -0.09 | -0.07 | -0.10 | -0.08 |
| FEO | 1.06 | 1.00 | 0.15 | 0.14 | 0.13 | 0.13 | 0.14 | 0.14 |
| MNO | -0.13 | -0.12 | -0.13 | -0.12 | -0.14 | -0.13 | -0.14 | -0.16 |
| MGO | 0.50 | 0.44 | -0.05 | -0.05 | -0.05 | -0.06 | -0.05 | -0.06 |
| CAO | 4.64 | 4.61 | 4.30 | 4.27 | 4.26 | 4.25 | 4.29 | 4.31 |
| BAO | -0.23 | -0.13 | -0.14 | -0.19 | -0.16 | -0.20 | -0.18 | -0.15 |
| NA2O | 9.41 | 9.38 | 9.69 | 9.66 | 9.77 | 9.70 | 9.88 | 9.82 |
| K2O | 0.09 | 0.15 | 0.09 | 0.05 | 0.05 | 0.05 | 0.04 | 0.04 |
| SUM | 100.41 | 100.59 | 100.88 | 100.72 | 100.71 | 100.47 | 100.79 | 100.26 |

| | | | | | | | | | | | | | | | | |
|---|---|---|---|---|---|---|---|---|---|---|---|---|---|---|---|---|
| SI | 2.764 | * | 2.769 | * | 2.788 | * | 2.798 | * | 2.795 | * | 2.799 | * | 2.787 | * | 2.786 | * |
| AL | 1.188 | * | 1.187 | * | 1.212 | * | 1.202 | * | 1.202 | * | 1.199 | * | 1.211 | * | 1.210 | * |
| TI | -0.001 | 3.951 | -0.002 | 3.954 | -0.003 | 3.997 | -0.003 | 3.997 | -0.003 | 3.995 | -0.002 | 3.996 | -0.003 | 3.994 | -0.003 | 3.993 |
| FE | 0.039 | * | 0.037 | * | 0.005 | * | 0.005 | * | 0.005 | * | 0.005 | * | 0.005 | * | 0.005 | * |
| MN | -0.005 | * | -0.004 | * | -0.005 | * | -0.004 | * | -0.005 | * | -0.005 | * | -0.005 | * | -0.006 | * |
| MG | 0.033 | * | 0.029 | * | -0.003 | * | -0.003 | * | -0.003 | * | -0.004 | * | -0.003 | * | -0.004 | * |
| CA | 0.220 | * | 0.219 | * | 0.202 | * | 0.201 | * | 0.200 | * | 0.200 | * | 0.202 | * | 0.204 | * |
| BA | -0.004 | * | -0.002 | * | -0.002 | * | -0.003 | * | -0.003 | * | -0.003 | * | -0.003 | * | -0.003 | * |
| NA | 0.809 | * | 0.805 | * | 0.824 | * | 0.821 | * | 0.831 | * | 0.827 | * | 0.841 | * | 0.840 | * |
| K | 0.005 | 1.098 | 0.008 | 1.091 | 0.005 | 1.026 | 0.003 | 1.019 | 0.003 | 1.028 | 0.003 | 1.022 | 0.002 | 1.038 | 0.002 | 1.039 |
| O | 8.000 | * | 8.000 | * | 8.000 | * | 8.000 | * | 8.000 | * | 8.000 | * | 8.000 | * | 8.000 | * |

9 148 FE675
10 149 FE675
11 150 FE675
12 151 FE675
13 152 FE675
14 153 FE675
15 154 FE675
16 155 FE675

1SUPER RECAL TABLE 5C FELDSPAR ANALYSES

| | 17 | 18 | 19 | 20 | 21 | 22 | 23 | 24 |
|---|---|---|---|---|---|---|---|---|
| SIO2 | 62.52 | 63.57 | 63.29 | 67.70 | 62.90 | 63.05 | 76.30 | 87.71 |
| A2O3 | 23.24 | 23.55 | 23.38 | 20.42 | 23.43 | 21.98 | 12.09 | 7.81 |
| TIO2 | -0.07 | -0.08 | -0.08 | -0.07 | -0.09 | -0.05 | 0.08 | -0.04 |
| FEO | 0.16 | 0.17 | 0.19 | 0.17 | 0.17 | 0.34 | 1.60 | 0.45 |
| MNO | -0.14 | -0.12 | -0.13 | -0.14 | -0.12 | -0.13 | -0.12 | -0.12 |
| MGO | -0.06 | -0.05 | -0.03 | -0.04 | -0.05 | 0.13 | 1.16 | 0.27 |
| CAO | 4.34 | 4.43 | 4.57 | 4.26 | 4.90 | 4.50 | 2.04 | 1.40 |
| BAO | -0.14 | -0.16 | -0.16 | -0.16 | -0.19 | -0.15 | -0.16 | -0.17 |
| NA2O | 9.54 | 9.65 | 9.48 | 7.39 | 8.85 | 8.64 | 4.54 | 2.96 |
| K2O | 0.06 | 0.05 | 0.05 | 0.03 | 0.05 | 0.17 | 0.91 | 0.21 |
| SUM | 99.45 | 101.01 | 100.54 | 99.56 | 99.85 | 98.48 | 98.44 | 100.48 |

| | | | | | | | | | | | | | | | | |
|---|---|---|---|---|---|---|---|---|---|---|---|---|---|---|---|---|
| SI | 2.781 | * | 2.784 | * | 2.785 | * | 2.959 | * | 2.782 | * | 2.826 | * | 3.314 | * | 3.612 | * |
| AL | 1.218 | * | 1.215 | * | 1.211 | * | 1.052 | * | 1.221 | * | 1.161 | * | 0.619 | * | 0.379 | * |
| TI | -0.002 | 3.997 | -0.003 | 3.996 | -0.003 | 3.993 | -0.002 | 4.008 | -0.003 | 4.001 | -0.002 | 3.985 | 0.003 | 3.936 | -0.001 | 3.989 |
| FE | 0.006 | * | 0.006 | * | 0.007 | * | 0.006 | * | 0.006 | * | 0.013 | * | 0.058 | * | 0.015 | * |

| | | | | | | | | | | | | | | | |
|---|---|---|---|---|---|---|---|---|---|---|---|---|---|---|---|
| MN | -0.005 | * | -0.004 | * | -0.005 | * | -0.005 | * | -0.004 | * | -0.005 | * | -0.004 | * | -0.004 | * |
| MG | -0.004 | * | -0.003 | * | -0.002 | * | -0.003 | * | -0.003 | * | 0.009 | * | 0.075 | * | 0.017 | * |
| CA | 0.207 | * | 0.208 | * | 0.215 | * | 0.199 | * | 0.232 | * | 0.216 | * | 0.095 | * | 0.062 | * |
| BA | -0.002 | * | -0.003 | * | -0.003 | * | -0.003 | * | -0.003 | * | -0.003 | * | -0.003 | * | -0.003 | * |
| NA | 0.823 | * | 0.819 | * | 0.809 | * | 0.626 | * | 0.759 | * | 0.751 | * | 0.382 | * | 0.236 | * |
| K | 0.003 | 1.027 | 0.003 | 1.026 | 0.003 | 1.024 | 0.002 | 0.823 | 0.003 | 0.989 | 0.010 | 0.990 | 0.050 | 0.654 | 0.011 | 0.334 |
| O | 8.000 | * | 8.000 | * | 8.000 | * | 8.000 | * | 8.000 | * | 8.000 | * | 8.000 | * | 8.000 | * |

17 156 FE675
18 157 FE675
19 158 FE675
20 219 FE467
21 220 FE467
22 221 FE467
23 222 FE467
24 223 FE675

1SUPER RECAL TABLE 5C FELDSPAR ANALYSES

| | 25 | 26 | 27 | 28 | 29 | 30 | 31 | 32 |
|---|---|---|---|---|---|---|---|---|
| SIO2 | 84.69 | 75.02 | 64.24 | 62.41 | 62.54 | 61.22 | 55.11 | 43.87 |
| A2O3 | 9.59 | 15.18 | 21.55 | 23.39 | 23.55 | 23.33 | 22.71 | 18.29 |
| TIO2 | -0.07 | -0.07 | -0.09 | -0.06 | -0.07 | -0.07 | 0.00 | 0.85 |
| FEO | 0.16 | 0.15 | 0.20 | 0.19 | 0.21 | 0.59 | 3.59 | 11.61 |
| MNO | -0.12 | -0.12 | -0.12 | -0.13 | -0.12 | -0.12 | -0.06 | 0.05 |
| MGO | -0.04 | -0.05 | -0.06 | -0.05 | -0.06 | -0.06 | 0.40 | 4.43 |
| CAO | 1.75 | 2.72 | 4.03 | 4.50 | 4.59 | 5.38 | 9.91 | 15.04 |
| BAO | -0.16 | -0.20 | -0.19 | -0.14 | -0.16 | -0.19 | -0.15 | -0.12 |
| NA2O | 3.88 | 6.46 | 8.24 | 9.14 | 8.81 | 8.70 | 6.74 | 2.20 |
| K2O | 0.00 | 0.02 | 0.03 | 0.04 | 0.04 | 0.03 | 0.10 | 0.29 |
| SUM | 99.68 | 99.11 | 97.83 | 99.29 | 99.33 | 98.81 | 98.35 | 96.51 |

| | | | | | | | | | | | | | | | |
|---|---|---|---|---|---|---|---|---|---|---|---|---|---|---|---|
| SI | 3.533 | * | 3.230 | * | 2.876 | * | 2.778 | * | 2.779 | * | 2.751 | * | 2.577 | * | 2.248 | * |
| AL | 0.471 | * | 0.770 | * | 1.137 | * | 1.227 | * | 1.233 | * | 1.235 | * | 1.251 | * | 1.105 | * |
| TI | -0.002 | 4.002 | -0.002 | 3.997 | -0.003 | 4.010 | -0.002 | 4.003 | -0.002 | 4.010 | -0.002 | 3.984 | 0.000 | 3.828 | 0.033 | 3.386 |
| FE | 0.006 | * | 0.005 | * | 0.007 | * | 0.007 | * | 0.008 | * | 0.022 | * | 0.140 | * | 0.498 | * |
| MN | -0.004 | * | -0.004 | * | -0.005 | * | -0.005 | * | -0.005 | * | -0.005 | * | -0.002 | * | 0.002 | * |
| MG | -0.002 | * | -0.003 | * | -0.004 | * | -0.003 | * | -0.004 | * | -0.004 | * | 0.028 | * | 0.338 | * |
| CA | 0.078 | * | 0.125 | * | 0.193 | * | 0.215 | * | 0.219 | * | 0.259 | * | 0.497 | * | 0.826 | * |
| BA | -0.003 | * | -0.003 | * | -0.003 | * | -0.002 | * | -0.003 | * | -0.003 | * | -0.003 | * | -0.002 | * |
| NA | 0.314 | * | 0.539 | * | 0.715 | * | 0.789 | * | 0.759 | * | 0.758 | * | 0.611 | * | 0.219 | * |
| K | 0.000 | 0.388 | 0.001 | 0.660 | 0.002 | 0.906 | 0.002 | 1.002 | 0.002 | 0.976 | 0.002 | 1.029 | 0.006 | 1.277 | 0.019 | 1.899 |
| O | 8.000 | * | 8.000 | * | 8.000 | * | 8.000 | * | 8.000 | * | 8.000 | * | 8.000 | * | 8.000 | * |

25 224 FE675
26 225 FE675
27 226 FE675
28 227 FE675
29 228 FE675
30 229 FE675
31 230 FE675
32 231 FE675

1SUPER RECAL TABLE 5C FELDSPAR ANALYSES

| | 33 | 34 | 35 | 36 | 37 | 38 | 39 |
|---|---|---|---|---|---|---|---|
| SIO2 | 86.70 | 64.93 | 62.46 | 62.41 | 62.78 | 62.46 | 62.63 |
| A2O3 | 1.17 | 21.74 | 23.38 | 23.16 | 23.31 | 23.26 | 23.68 |
| TIO2 | 5.64 | 0.08 | 0.01 | 0.00 | -0.05 | -0.02 | -0.04 |
| FEO | 4.86 | 0.29 | 0.22 | 0.20 | 0.19 | 0.21 | 0.25 |
| MNO | 0.02 | -0.13 | -0.12 | -0.13 | -0.12 | -0.12 | -0.13 |
| MGO | -0.05 | -0.06 | -0.06 | -0.05 | -0.05 | -0.05 | -0.05 |
| CAO | 0.21 | 3.92 | 4.54 | 4.39 | 4.32 | 4.28 | 4.55 |
| BAO | -0.16 | -0.13 | -0.18 | -0.16 | -0.18 | -0.17 | -0.19 |
| NA2O | 0.37 | 8.83 | 9.18 | 9.43 | 9.40 | 9.51 | 9.30 |
| K2O | 0.00 | 0.04 | 0.04 | 0.05 | 0.05 | 0.05 | 0.05 |
| SUM | 98.76 | 99.51 | 99.47 | 99.30 | 99.65 | 99.41 | 100.05 |

| | | | | | | | | | | | | | | | |
|---|---|---|---|---|---|---|---|---|---|---|---|---|---|---|---|
| SI | 3.680 | * | 2.867 | * | 2.776 | * | 2.780 | * | 2.784 | * | 2.779 | * | 2.769 | * | | |
| AL | 0.059 | * | 1.131 | * | 1.225 | * | 1.216 | * | 1.218 | * | 1.220 | * | 1.234 | * | | |
| TI | 0.180 | 3.919 | 0.003 | 4.000 | 0.000 | 4.001 | 0.000 | 3.996 | -0.002 | 4.001 | -0.001 | 3.998 | -0.001 | 4.001 | | |
| FE | 0.173 | * | 0.011 | * | 0.008 | * | 0.007 | * | 0.007 | * | 0.008 | * | 0.009 | * | | |
| MN | 0.001 | * | -0.005 | * | -0.005 | * | -0.005 | * | -0.005 | * | -0.005 | * | -0.005 | * | | |
| MG | -0.003 | * | -0.004 | * | -0.004 | * | -0.003 | * | -0.003 | * | -0.003 | * | -0.003 | * | | |
| CA | 0.010 | * | 0.185 | * | 0.216 | * | 0.210 | * | 0.205 | * | 0.204 | * | 0.216 | * | | |
| BA | -0.003 | * | -0.002 | * | -0.003 | * | -0.003 | * | -0.003 | * | -0.003 | * | -0.003 | * | | |
| NA | 0.030 | * | 0.756 | * | 0.791 | * | 0.815 | * | 0.808 | * | 0.820 | * | 0.797 | * | | |
| K | 0.000 | 0.207 | 0.002 | 0.943 | 0.002 | 1.006 | 0.003 | 1.023 | 0.003 | 1.012 | 0.003 | 1.024 | 0.003 | 1.013 | | |
| O | 8.000 | * | 8.000 | * | 8.000 | * | 8.000 | * | 8.000 | * | 8.000 | * | 8.000 | * | | |

33 232 FE567
34 233 FE567
35 235 FE567
36 236 FE675
37 237 FE675
38 238 FE675
39 239 FE675

1SUPER RECAL TABLE 5C CHLORITE ANALYSES

| | 1 | 2 | 3 | 4 | 5 | 6 | 7 | 8 |
|---|---|---|---|---|---|---|---|---|
| SIO2 | 26.68 | 26.63 | 26.34 | 26.36 | 26.60 | 26.74 | 26.67 | 26.43 |
| A2O3 | 20.57 | 20.82 | 20.51 | 20.52 | 20.69 | 19.79 | 20.60 | 20.68 |
| TIO2 | 0.09 | 0.19 | 0.12 | 0.12 | 0.17 | 0.09 | 0.06 | 0.11 |
| FEO | 20.06 | 20.42 | 20.25 | 20.33 | 19.79 | 19.50 | 19.78 | 19.75 |
| MNO | 0.16 | 0.15 | 0.20 | 0.20 | 0.18 | 0.16 | 0.16 | 0.15 |
| MGO | 19.22 | 18.77 | 18.99 | 19.02 | 19.32 | 19.29 | 19.37 | 19.31 |
| CAO | 0.09 | 0.13 | 0.13 | 0.10 | 0.09 | 0.11 | 0.09 | 0.06 |
| NA2O | 0.02 | 0.02 | 0.03 | 0.01 | 0.07 | 0.11 | 0.06 | 0.11 |
| K2O | 0.01 | 0.02 | 0.02 | 0.02 | 0.02 | 0.04 | 0.03 | 0.03 |
| BAO | 0.00 | 0.00 | 0.00 | 0.00 | 0.00 | 0.00 | 0.00 | 0.00 |
| CL | 0.00 | 0.00 | 0.00 | 0.00 | 0.00 | 0.00 | 0.00 | 0.00 |
| F | 0.00 | 0.00 | 0.00 | 0.00 | 0.00 | 0.00 | 0.00 | 0.00 |
| H2O | 11.60 | 11.62 | 11.53 | 11.54 | 11.62 | 11.47 | 11.60 | 11.57 |
| SUM | 98.50 | 98.77 | 98.12 | 98.22 | 98.55 | 97.30 | 98.42 | 98.20 |
| -O= F+CL | 0.00 | 0.00 | 0.00 | 0.00 | 0.00 | 0.00 | 0.00 | 0.00 |
| SUM | 98.50 | 98.77 | 98.12 | 98.22 | 98.55 | 97.30 | 98.42 | 98.20 |

| | | | | | | | | | | | | | | | | |
|---|---|---|---|---|---|---|---|---|---|---|---|---|---|---|---|---|
| SI | 2.756 | * | 2.747 | * | 2.737 | * | 2.737 | * | 2.744 | * | 2.793 | * | 2.754 | * | 2.737 | * |
| AL | 1.244 | 4.000 | 1.253 | 4.000 | 1.263 | 4.000 | 1.263 | 4.000 | 1.256 | 4.000 | 1.207 | 4.000 | 1.246 | 4.000 | 1.263 | 4.000 |
| AL | 1.259 | * | 1.278 | * | 1.249 | * | 1.248 | * | 1.259 | * | 1.228 | * | 1.261 | * | 1.260 | * |
| TI | 0.007 | * | 0.015 | * | 0.009 | * | 0.009 | * | 0.013 | * | 0.007 | * | 0.005 | * | 0.009 | * |
| FE | 1.733 | * | 1.762 | * | 1.760 | * | 1.765 | * | 1.707 | * | 1.703 | * | 1.708 | * | 1.710 | * |
| MN | 0.014 | * | 0.013 | * | 0.018 | * | 0.018 | * | 0.016 | * | 0.014 | * | 0.014 | * | 0.013 | * |
| MG | 2.959 | * | 2.886 | * | 2.941 | * | 2.944 | * | 2.971 | * | 3.003 | * | 2.981 | * | 2.980 | * |
| CA | 0.010 | * | 0.014 | * | 0.014 | * | 0.011 | * | 0.010 | * | 0.012 | * | 0.010 | * | 0.007 | * |
| NA | 0.004 | * | 0.004 | * | 0.006 | * | 0.002 | * | 0.014 | * | 0.022 | * | 0.012 | * | 0.022 | * |
| K | 0.001 | * | 0.003 | * | 0.003 | * | 0.003 | * | 0.003 | * | 0.005 | * | 0.004 | * | 0.004 | * |
| BA | 0.000 | 5.987 | 0.000 | 5.975 | 0.000 | 6.001 | 0.000 | 5.999 | 0.000 | 5.992 | 0.000 | 5.995 | 0.000 | 5.995 | 0.000 | 6.005 |
| CL | 0.000 | * | 0.000 | * | 0.000 | * | 0.000 | * | 0.000 | * | 0.000 | * | 0.000 | * | 0.000 | * |
| F | 0.000 | * | 0.000 | * | 0.000 | * | 0.000 | * | 0.000 | * | 0.000 | * | 0.000 | * | 0.000 | * |
| H | 8.000 | 8.000 | 8.000 | 8.000 | 8.000 | 8.000 | 8.000 | 8.000 | 8.000 | 8.000 | 8.000 | 8.000 | 8.000 | 8.000 | 8.000 | 8.000 |
| O | 18.000 | * | 18.000 | * | 18.000 | * | 18.000 | * | 18.000 | * | 18.000 | * | 18.000 | * | 18.000 | * |

1 10 CH675
2 11 CH675
3 12 CH675
4 13 CH675
5 14 CH675
6 15 CH675
7 16 CH675
8 18 CH675

1

1SUPER RECAL TABLE 5C CHLORITE ANALYSES

| | 9 |
|---|---|
| SIO2 | 26.52 |
| A2O3 | 20.67 |
| TIO2 | 0.12 |
| FEO | 19.97 |
| MNO | 0.15 |
| MGO | 19.11 |
| CAO | 0.09 |
| NA2O | 0.11 |
| K2O | 0.03 |
| BAO | 0.00 |
| CL | 0.00 |
| F | 0.00 |
| H2O | 11.58 |
| SUM | 98.35 |
| -O= F+CL | 0.00 |
| SUM | 98.35 |

| | | |
|---|---|---|
| SI | 2.744 | * |
| AL | 1.256 | 4.000 |
| AL | 1.264 | * |
| TI | 0.009 | * |
| FE | 1.728 | * |
| MN | 0.013 | * |
| MG | 2.947 | * |
| CA | 0.010 | * |
| NA | 0.022 | * |
| K | 0.004 | * |
| BA | 0.000 | 5.998 |
| CL | 0.000 | * |
| F | 0.000 | * |
| H | 8.000 | 8.000 |
| O | 18.000 | * |

9 20 CH675

SUPER RECAL

TABLE 7a GARNET ANALYSES

| | 1 | 2 | 3 | 4 | 5 | 6 | 7 |
|---|---|---|---|---|---|---|---|
| SIO2 | 39.20 | 38.98 | 38.97 | 38.91 | 39.48 | 38.91 | 37.22 |
| TIO2 | 0.08 | 0.07 | 0.09 | 0.07 | 0.10 | 0.00 | 0.12 |
| A2O3 | 21.15 | 21.21 | 20.70 | 20.64 | 21.59 | 21.72 | 20.25 |
| FEO | 31.59 | 30.83 | 31.10 | 30.73 | 30.74 | 30.32 | 29.19 |
| MGO | 3.66 | 3.89 | 3.84 | 3.93 | 3.75 | 3.56 | 3.50 |
| MNO | 2.13 | 1.96 | 2.24 | 2.18 | 2.28 | 2.23 | 3.07 |
| CAO | 4.20 | 4.26 | 4.10 | 4.35 | 4.40 | 4.66 | 4.74 |
| NA2O | 0.04 | -0.01 | 0.08 | 0.07 | 0.03 | 0.03 | 0.05 |
| K2O | 0.02 | 0.01 | 0.01 | 0.01 | 0.00 | 0.00 | -0.02 |
| SUM | 102.07 | 101.20 | 101.13 | 100.89 | 102.41 | 101.51 | 98.12 |

| | | | | | | | | | | | | | | |
|---|---|---|---|---|---|---|---|---|---|---|---|---|---|---|
| SI | 3.052 | | 3.050 | | 3.061 | | 3.061 | | 3.051 | | 3.034 | | 3.023 | |
| TI | 0.005 | | 0.004 | | 0.005 | | 0.004 | | 0.006 | | 0.005 | | 0.007 | |
| AL | 0.000 | 3.056 | 0.000 | 3.054 | 0.000 | 3.066 | 0.000 | 3.065 | 0.000 | 3.057 | 0.000 | 3.038 | 0.000 | 3.030 |
| AL | 1.940 | | 1.956 | | 1.916 | | 1.913 | | 1.966 | | 1.995 | | 1.938 | |
| FE | 0.060 | 2.000 | 0.044 | 2.000 | 0.084 | 2.000 | 0.087 | 2.000 | 0.034 | 2.000 | 0.005 | 2.000 | 0.062 | 2.000 |
| FE | 1.997 | | 1.973 | | 1.959 | | 1.935 | | 1.952 | | 1.972 | | 1.920 | |
| MG | 0.425 | | 0.454 | | 0.450 | | 0.461 | | 0.432 | | 0.414 | | 0.424 | |
| MN | 0.140 | | 0.130 | | 0.149 | | 0.145 | | 0.149 | | 0.147 | | 0.211 | |
| CA | 0.350 | | 0.357 | | 0.345 | | 0.367 | | 0.364 | | 0.389 | | 0.412 | |
| NA | 0.006 | | -0.002 | | 0.012 | | 0.011 | | 0.010 | | 0.005 | | 0.008 | |
| K | 0.002 | 2.920 | 0.001 | 2.913 | 0.001 | 2.915 | 0.001 | 2.919 | 0.000 | 2.908 | 0.000 | 2.927 | -0.002 | 2.973 |
| O | 12.000 | | 12.000 | | 12.000 | | 12.000 | | 12.000 | | 12.000 | | 12.000 | |
| AL | | 69.20 | | 68.20 | | 68.40 | | 67.52 | | 67.75 | | 67.54 | | 65.43 |
| PY | | 14.29 | | 15.34 | | 15.05 | | 15.39 | | 14.73 | | 14.13 | | 13.98 |
| SP | | 4.73 | | 4.39 | | 4.99 | | 4.85 | | 5.09 | | 5.03 | | 6.97 |
| GR | | 11.79 | | 12.07 | | 11.55 | | 12.24 | | 12.42 | | 13.30 | | 13.61 |
| F/M | | 5.033 | | 4.635 | | 4.688 | | 4.514 | | 4.866 | | 5.123 | | 5.031 |
| F/FM | | 0.834 | | 0.823 | | 0.824 | | 0.819 | | 0.830 | | 0.837 | | 0.834 |
| A* = | | 0.281 | | 0.283 | | 0.278 | | 0.278 | | 0.289 | | 0.294 | | 0.287 |
| A = | | 0.280 | | 0.283 | | 0.277 | | 0.278 | | 0.289 | | 0.294 | | 0.288 |
| M = | | 0.171 | | 0.184 | | 0.180 | | 0.186 | | 0.179 | | 0.173 | | 0.176 |

1 24 GA495
2 44 GA495
3 64 GA495
4 84 GA495
5 104 GA495
6 124 GA495
7 223 GA495

SUPER RECAL

TABLE 7b GARNET ANALYSES

| | 1 | 2 | 3 | 4 | 5 | 6 |
|---|---|---|---|---|---|---|
| SIO2 | 37.34 | 37.78 | 38.02 | 37.89 | 37.77 | 38.44 |
| TIO2 | 0.11 | 0.11 | 0.17 | 0.14 | 0.12 | 0.09 |
| A2O3 | 19.95 | 20.26 | 19.46 | 19.72 | 20.17 | 19.76 |
| FEO | 30.50 | 30.59 | 31.10 | 31.09 | 30.48 | 30.55 |
| MGO | 4.24 | 4.13 | 4.22 | 4.20 | 4.23 | 4.09 |
| MNO | 1.35 | 1.46 | 1.12 | 1.16 | 1.42 | 1.16 |
| CAO | 4.66 | 4.74 | 4.52 | 4.41 | 4.58 | 4.25 |
| NA2O | 0.01 | 0.02 | 0.01 | 0.01 | 0.04 | 0.02 |
| K2O | 0.05 | 0.04 | 0.04 | 0.04 | 0.04 | 0.27 |
| SUM | 98.21 | 99.13 | 98.66 | 98.66 | 98.85 | 98.63 |

| | | | | | | | | | | | | |
|---|---|---|---|---|---|---|---|---|---|---|---|---|
| SI | 3.025 | * | 3.030 | * | 3.066 | * | 3.054 | * | 3.035 | * | 3.089 | * |
| TI | 0.007 | * | 0.007 | * | 0.010 | * | 0.008 | * | 0.007 | * | 0.005 | * |
| AL | 0.000 | 3.032 | 0.000 | 3.036 | 0.000 | 3.076 | 0.000 | 3.063 | 0.000 | 3.042 | 0.000 | 3.094 |
| AL | 1.904 | * | 1.914 | * | 1.849 | * | 1.873 | * | 1.910 | * | 1.871 | * |
| FE | 0.096 | 2.000 | 0.086 | 2.000 | 0.151 | 2.000 | 0.127 | 2.000 | 0.090 | 2.000 | 0.129 | 2.000 |
| FE | 1.971 | * | 1.966 | * | 1.946 | * | 1.969 | * | 1.958 | * | 1.924 | * |
| MG | 0.512 | * | 0.494 | * | 0.507 | * | 0.505 | * | 0.507 | * | 0.490 | * |
| MN | 0.093 | * | 0.099 | * | 0.076 | * | 0.079 | * | 0.097 | * | 0.079 | * |
| CA | 0.404 | * | 0.407 | * | 0.390 | * | 0.381 | * | 0.394 | * | 0.366 | * |
| NA | 0.002 | * | 0.003 | * | 0.002 | * | 0.002 | * | 0.006 | * | 0.003 | * |
| K | 0.005 | 2.987 | 0.004 | 2.973 | 0.004 | 2.926 | 0.004 | 2.940 | 0.004 | 2.965 | 0.028 | 2.890 |
| O | 12.000 | * | 12.000 | * | 12.000 | * | 12.000 | * | 12.000 | * | 12.000 | * |
| AL | | 67.19 | | 67.23 | | 68.28 | | 68.48 | | 67.25 | | 68.71 |
| PY | | 16.65 | | 16.18 | | 16.51 | | 16.49 | | 16.63 | | 16.40 |
| SP | | 3.01 | | 3.25 | | 2.49 | | 2.59 | | 3.17 | | 2.64 |
| GR | | 13.15 | | 13.35 | | 12.71 | | 12.44 | | 12.95 | | 12.25 |
| F/M | | 4.030 | | 4.183 | | 3.988 | | 4.059 | | 4.055 | | 4.089 |
| F/FM | | 0.801 | | 0.807 | | 0.800 | | 0.802 | | 0.802 | | 0.804 |
| A* = | | 0.269 | | 0.273 | | 0.262 | | 0.264 | | 0.272 | | 0.266 |
| A = | | 0.268 | | 0.272 | | 0.261 | | 0.264 | | 0.271 | | 0.260 |
| M = | | 0.199 | | 0.194 | | 0.195 | | 0.194 | | 0.198 | | 0.193 |

1 385 GA11D
2 389 GA11D
3 399 GA11D
4 400 GA11D
5 434 GA11D
6 436 GA11D

SUPER RECAL

TABLE 7c GARNET ANALYSES

| | 1 | | 2 | | 3 | | 4 | | 5 | |
|---|---|---|---|---|---|---|---|---|---|---|
| SIO2 | 38.27 | | 38.84 T | | 38.08 | | 35.18 | | 38.24 | |
| TIO2 | 0.11 | | 0.13 | | 0.16 | | 0.20 | | 0.15 | |
| A2O3 | 20.81 | | 20.75 | | 20.67 | | 26.19 | | 20.87 | |
| FEO | 27.79 | | 27.71 | | 28.16 | | 25.65 | | 27.82 | |
| MGO | 2.03 | | 2.05 | | 2.12 | | 2.15 | | 2.10 | |
| MNO | 5.08 | | 5.03 | | 5.29 | | 4.81 | | 5.03 | |
| CAO | 6.66 | | 6.94 | | 6.34 | | 6.09 | | 6.49 | |
| NA2O | 0.03 | | 0.03 | | 0.02 | | 0.01 | | 0.03 | |
| K2O | 0.01 | | -0.01 | | 0.00 | | 0.05 | | -0.01 | |
| SUM | 100.79 | | 100.87 | | 100.84 | | 100.33 | | 100.72 | |
| SI | 3.036 | * | 3.033 | * | 3.027 | * | 2.773 | * | 3.034 | * |
| TI | 0.007 | * | 0.008 | * | 0.010 | * | 0.012 | * | 0.009 | * |
| AL | 0.000 | 3.043 | 0.000 | 3.040 | 0.000 | 3.037 | 0.216 | 3.000 | 0.000 | 3.043 |
| AL | 1.946 | * | 1.939 | * | 1.936 | * | 2.217 | * | 1.951 | * |
| FE | 0.054 | 2.000 | 0.061 | 2.000 | 0.064 | 2.000 | 0.000 | 2.217 | 0.049 | 2.000 |
| FE | 1.790 | * | 1.777 | * | 1.808 | * | 1.691 | * | 1.797 | * |
| MG | 0.240 | * | 0.242 | * | 0.251 | * | 0.253 | * | 0.248 | * |
| MN | 0.341 | * | 0.338 | * | 0.336 | * | 0.321 | * | 0.338 | * |
| CA | 0.566 | * | 0.590 | * | 0.540 | * | 0.514 | * | 0.552 | * |
| NA | 0.005 | * | 0.005 | * | 0.003 | * | 0.002 | * | 0.005 | * |
| K | 0.001 | 2.943 | -0.001 | 2.950 | 0.000 | 2.959 | 0.005 | 2.785 | -0.001 | 2.939 |
| O | 12.000 | * | 12.000 | * | 12.000 | * | 12.000 | * | 12.000 | * |
| AL | | 61.64 | | 61.10 | | 62.00 | | 60.85 | | 61.86 |
| PY | | 8.02 | | 8.06 | | 8.32 | | 9.09 | | 8.32 |
| SP | | 11.41 | | 11.23 | | 11.80 | | 11.56 | | 11.33 |
| GR | | 18.93 | | 19.61 | | 17.88 | | 18.51 | | 18.49 |
| F/M | | 8.877 | | 8.727 | | 8.617 | | 7.965 | | 8.598 |
| F/FM | | 0.899 | | 0.897 | | 0.896 | | 0.888 | | 0.896 |
| AM = | | 0.310 | | 0.310 | | 0.313 | | 0.304 | | 0.310 |
| A = | | 0.318 | | 0.318 | | 0.313 | | 0.384 | | 0.318 |
| M = | | 0.115 | | 0.116 | | 0.118 | | 0.130 | | 0.119 |

1 544 GA793
2 546 GA793
3 559 GA793
4 560 GA793
5 638 GA793

SUPER RECAL

TABLE 7d GARNET ANALYSES

| | 1 | 2 | 3 | 4 | 5 | 6 |
|---|---|---|---|---|---|---|
| SIO2 | 38.46 | 38.34 | 38.86 | 37.78 | 37.72 | 37.75 |
| TIO2 | 0.10 | 0.12 | 0.17 | 0.12 | 0.12 | 0.14 |
| A2O3 | 20.17 | 20.39 | 20.33 | 20.01 | 19.87 | 19.76 |
| FEO | 29.74 | 28.70 | 27.08 | 29.80 | 29.51 | 29.27 |
| MGO | 2.06 | 2.19 | 1.96 | 2.23 | 2.17 | 2.17 |
| MNO | 4.04 | 4.31 | 5.36 | 4.11 | 4.00 | 4.12 |
| CAO | 5.90 | 6.57 | 7.55 | 5.74 | 6.06 | 6.30 |
| NA2O | 0.01 | 0.05 | 0.03 | 0.08 | 0.05 | 0.02 |
| K2O | 0.09 | 0.04 | 0.06 | 0.05 | 0.05 | 0.04 |
| SUM | 100.57 | 100.71 | 101.40 | 99.92 | 99.55 | 99.57 |

| | | | | | | | | | | | | |
|---|---|---|---|---|---|---|---|---|---|---|---|---|
| SI | 3.067 | * | | 3.048 | * | | 3.064 | * | | 3.040 | * | |
| TI | 0.006 | * | | 0.007 | * | | 0.010 | * | | 0.007 | * | |
| AL | 0.000 | * | 3.073 | 0.000 | * | 3.055 | 0.000 | * | 3.074 | 0.000 | * | 3.048 |
| AL | 1.895 | * | | 1.910 | * | | 1.889 | * | | 1.898 | * | |
| FE | 0.105 | * | 2.000 | 0.090 | * | 2.000 | 0.111 | * | 2.000 | 0.102 | * | 2.000 |
| FE | 1.879 | * | | 1.818 | * | | 1.675 | * | | 1.903 | * | |
| MG | 0.245 | * | | 0.260 | * | | 0.230 | * | | 0.267 | * | |
| MN | 0.273 | * | | 0.290 | * | | 0.358 | * | | 0.280 | * | |
| CA | 0.504 | * | | 0.560 | * | | 0.638 | * | | 0.495 | * | |
| NA | 0.002 | * | | 0.008 | * | | 0.005 | * | | 0.012 | * | |
| K | 0.009 | * | 2.911 | 0.004 | * | 2.939 | 0.006 | * | 2.911 | 0.005 | * | 2.963 |
| O | 12.000 | * | | 12.000 | * | | 12.000 | * | | 12.000 | * | |

| | | | | | | | | | | | | |
|---|---|---|---|---|---|---|---|---|---|---|---|---|
| | 5 | | | 6 | | | | | | | | |
| SI | 3.045 | * | | 3.047 | * | | | | | | | |
| TI | 0.007 | * | | 0.008 | * | | | | | | | |
| AL | 0.000 | * | 3.053 | 0.000 | * | 3.056 | | | | | | |
| AL | 1.890 | * | | 1.880 | * | | | | | | | |
| FE | 0.110 | * | 2.000 | 0.120 | * | 2.000 | | | | | | |
| FE | 1.883 | * | | 1.856 | * | | | | | | | |
| MG | 0.261 | * | | 0.261 | * | | | | | | | |
| MN | 0.274 | * | | 0.282 | * | | | | | | | |
| CA | 0.524 | * | | 0.545 | * | | | | | | | |
| NA | 0.008 | * | | 0.003 | * | | | | | | | |
| K | 0.005 | * | 2.955 | 0.004 | * | 2.951 | | | | | | |
| O | 12.000 | * | | 12.000 | * | | | | | | | |

| | | | | | | | | | | | | |
|---|---|---|---|---|---|---|---|---|---|---|---|---|
| AL | 66.00 | | | 63.24 | | | 59.29 | | | 65.80 | | |
| PY | 8.15 | | | 8.60 | | | 7.65 | | | 8.78 | | |
| SP | 9.08 | | | 9.62 | | | 11.89 | | | 9.19 | | |
| GR | 16.77 | | | 18.55 | | | 21.18 | | | 16.24 | | |
| F/M | 8.787 | | | 8.125 | | | 8.824 | | | 8.162 | | |
| F/FM | 0.898 | | | 0.890 | | | 0.898 | | | 0.891 | | |
| A* = | 0.297 | | | 0.305 | | | 0.318 | | | 0.294 | | |
| A = | 0.295 | | | 0.305 | | | 0.317 | | | 0.293 | | |
| M = | 0.110 | | | 0.120 | | | 0.114 | | | 0.118 | | |

| | | | | | | | | | | | | |
|---|---|---|---|---|---|---|---|---|---|---|---|---|
| | | | | | | | | | | 4 | 253 | GA608 |
| | | | | | | | | | | 5 | 254 | GA608 |
| 1 | 159 | GA608 | | | | | | | | 6 | 255 | GA608 |
| 2 | 160 | GA608 | | | | | | | | | | |
| 3 | 184 | GA608 | | | | | | | | | | |

1SUPER RECAL TABLE 8A BIOTITE ANALYSES (H2O CALCULATED)

| | 1 | 2 | 3 | 4 | 5 | 6 | 7 | 8 |
|---|---|---|---|---|---|---|---|---|
| SIO2 | 37.07 | 36.74 | 37.65 | 36.80 | 36.77 | 36.66 | 37.13 | 37.00 |
| A2O3 | 19.53 | 19.45 | 19.75 | 19.46 | 19.93 | 19.91 | 19.76 | 20.44 |
| TIO2 | 1.60 | 1.58 | 1.62 | 1.58 | 1.60 | 1.61 | 1.54 | 1.58 |
| FEO | 15.35 | 15.11 | 14.86 | 14.74 | 14.85 | 15.02 | 14.66 | 14.74 |
| MNO | -0.01 | 0.01 | 0.00 | 0.00 | -0.03 | -0.03 | -0.03 | -0.08 |
| MGO | 13.23 | 12.93 | 12.95 | 13.16 | 13.07 | 13.07 | 13.28 | 13.10 |
| CAO | 0.01 | 0.01 | 0.00 | -0.02 | 0.00 | -0.01 | 0.00 | 0.00 |
| NA2O | 0.42 | 0.38 | 0.44 | 0.35 | 0.39 | 0.43 | 0.35 | 0.45 |
| K2O | 7.87 | 8.02 | 8.13 | 8.14 | 8.30 | 8.18 | 8.07 | 8.02 |
| BAO | 0.00 | 0.00 | 0.00 | 0.00 | 0.00 | 0.00 | 0.00 | 0.00 |
| CL | 0.00 | 0.00 | 0.00 | 0.00 | 0.00 | 0.00 | 0.00 | 0.00 |
| F | 0.00 | 0.00 | 0.00 | 0.00 | 0.00 | 0.00 | 0.00 | 0.00 |
| H2O | 4.06 | 4.02 | 4.08 | 4.03 | 4.05 | 4.05 | 4.06 | 4.08 |
| SUM | 99.13 | 98.25 | 99.48 | 98.24 | 98.93 | 98.89 | 98.82 | 99.33 |
| -O= F+CL | 0.00 | 0.00 | 0.00 | 0.00 | 0.00 | 0.00 | 0.00 | 0.00 |
| SUM | 99.13 | 98.25 | 99.48 | 98.24 | 98.93 | 98.89 | 98.82 | 99.33 |

| | | | | | | | | | | | | | | | | |
|---|---|---|---|---|---|---|---|---|---|---|---|---|---|---|---|---|
| SI | 5.471 | * | 5.474 | * | 5.522 | * | 5.476 | * | 5.439 | * | 5.428 | * | 5.481 | * | 5.432 | * |
| AL | 2.529 | 8.000 | 2.526 | 8.000 | 2.478 | 8.000 | 2.524 | 8.000 | 2.561 | 8.000 | 2.572 | 8.000 | 2.519 | 8.000 | 2.568 | 8.000 |
| AL | 0.867 | * | 0.889 | * | 0.935 | * | 0.889 | * | 0.913 | * | 0.902 | * | 0.918 | * | 0.968 | * |
| TI | 0.178 | * | 0.177 | * | 0.179 | * | 0.177 | * | 0.178 | * | 0.179 | * | 0.171 | * | 0.174 | * |
| FE | 1.895 | * | 1.883 | * | 1.823 | * | 1.834 | * | 1.837 | * | 1.860 | * | 1.810 | * | 1.810 | * |
| MN | -0.001 | * | 0.001 | * | 0.000 | * | 0.000 | * | -0.004 | * | -0.004 | * | -0.004 | * | -0.010 | * |
| MG | 2.910 | 5.849 | 2.871 | 5.821 | 2.831 | 5.767 | 2.919 | 5.819 | 2.881 | 5.805 | 2.884 | 5.821 | 2.922 | 5.817 | 2.866 | 5.808 |
| CA | 0.002 | * | 0.002 | * | 0.000 | * | -0.003 | * | 0.000 | * | -0.002 | * | 0.000 | * | 0.000 | * |
| NA | 0.120 | * | 0.110 | * | 0.125 | * | 0.101 | * | 0.112 | * | 0.123 | * | 0.100 | * | 0.128 | * |
| K | 1.481 | * | 1.524 | * | 1.521 | * | 1.545 | * | 1.566 | * | 1.545 | * | 1.519 | * | 1.502 | * |
| BA | 0.000 | 1.603 | 0.000 | 1.635 | 0.000 | 1.646 | 0.000 | 1.643 | 0.000 | 1.678 | 0.000 | 1.667 | 0.000 | 1.620 | 0.000 | 1.630 |
| CL | 0.000 | * | 0.000 | * | 0.000 | * | 0.000 | * | 0.000 | * | 0.000 | * | 0.000 | * | 0.000 | * |
| F | 0.000 | * | 0.000 | * | 0.000 | * | 0.000 | * | 0.000 | * | 0.000 | * | 0.000 | * | 0.000 | * |
| H | 4.000 | 4.000 | 4.000 | 4.000 | 4.000 | 4.000 | 4.000 | 4.000 | 4.000 | 4.000 | 4.000 | 4.000 | 4.000 | 4.000 | 4.000 | 4.000 |
| O | 24.000 | * | 24.000 | * | 24.000 | * | 24.000 | * | 24.000 | * | 24.000 | * | 24.000 | * | 24.000 | * |

1 241 BI495
2 243 BI495
3 244 BI495
4 245 BI495
5 246 BI495
6 247 BI495
7 248 BI495
8 249 BI495

1SUPER RECAL TABLE 8A BIOTITE ANALYSES (H2O CALCULATED)

| | 9 | 10 | 11 | 12 | 13 | 14 | 15 | 16 |
|---|---|---|---|---|---|---|---|---|
| SIO2 | 36.95 | 37.30 | 37.71 | 37.61 | 37.84 | 37.78 | 37.62 | 37.88 |
| A2O3 | 18.98 | 19.23 | 19.31 | 18.95 | 19.41 | 19.17 | 19.20 | 19.35 |
| TIO2 | 1.72 | 1.69 | 1.70 | 1.68 | 1.64 | 1.62 | 1.62 | 1.61 |
| FEO | 14.84 | 14.80 | 14.73 | 14.80 | 14.78 | 14.70 | 14.76 | 14.73 |
| MNO | -0.04 | -0.01 | -0.03 | 0.00 | -0.01 | -0.02 | -0.02 | -0.02 |
| MGO | 12.64 | 12.71 | 12.78 | 13.03 | 12.85 | 12.80 | 12.76 | 12.86 |
| CAO | 0.03 | 0.08 | 0.00 | -0.01 | 0.01 | 0.00 | 0.00 | 0.02 |
| NA2O | 0.36 | 0.39 | 0.40 | 0.40 | 0.41 | 0.39 | 0.41 | 0.40 |
| K2O | 7.90 | 7.68 | 8.05 | 8.04 | 8.10 | 8.10 | 8.09 | 8.02 |
| BAO | 0.00 | 0.00 | 0.00 | 0.00 | 0.00 | 0.00 | 0.00 | 0.00 |
| CL | 0.00 | 0.00 | 0.00 | 0.00 | 0.00 | 0.00 | 0.00 | 0.00 |
| F | 0.00 | 0.00 | 0.00 | 0.00 | 0.00 | 0.00 | 0.00 | 0.00 |
| H2O | 3.99 | 4.03 | 4.06 | 4.05 | 4.07 | 4.05 | 4.04 | 4.07 |
| SUM | 97.37 | 97.90 | 98.71 | 98.55 | 99.10 | 98.59 | 98.48 | 98.92 |
| -O= F+CL | 0.00 | 0.00 | 0.00 | 0.00 | 0.00 | 0.00 | 0.00 | 0.00 |
| SUM | 97.37 | 97.90 | 98.71 | 98.55 | 99.10 | 98.59 | 98.48 | 98.92 |

| | | | | | | | | | | | | | | | | |
|---|---|---|---|---|---|---|---|---|---|---|---|---|---|---|---|---|
| SI | 5.542 | * | 5.551 | * | 5.568 | * | 5.570 | * | 5.567 | * | 5.586 | * | 5.572 | * | 5.578 | * |
| AL | 2.458 | 8.000 | 2.449 | 8.000 | 2.432 | 8.000 | 2.430 | 8.000 | 2.433 | 8.000 | 2.414 | 8.000 | 2.428 | 8.000 | 2.422 | 8.000 |
| AL | 0.896 | * | 0.924 | * | 0.928 | * | 0.876 | * | 0.931 | * | 0.926 | * | 0.923 | * | 0.936 | * |
| TI | 0.194 | * | 0.189 | * | 0.189 | * | 0.187 | * | 0.181 | * | 0.180 | * | 0.180 | * | 0.178 | * |
| FE | 1.861 | * | 1.842 | * | 1.819 | * | 1.833 | * | 1.818 | * | 1.818 | * | 1.828 | * | 1.814 | * |
| MN | -0.005 | * | -0.001 | * | -0.004 | * | 0.000 | * | -0.001 | * | -0.003 | * | -0.003 | * | -0.002 | * |
| MG | 2.826 | 5.772 | 2.819 | 5.773 | 2.813 | 5.745 | 2.876 | 5.772 | 2.818 | 5.747 | 2.821 | 5.742 | 2.817 | 5.747 | 2.823 | 5.749 |
| CA | 0.005 | * | 0.013 | * | 0.000 | * | -0.002 | * | 0.002 | * | 0.000 | * | 0.000 | * | 0.003 | * |
| NA | 0.105 | * | 0.113 | * | 0.115 | * | 0.115 | * | 0.117 | * | 0.112 | * | 0.118 | * | 0.114 | * |
| K | 1.511 | * | 1.458 | * | 1.516 | * | 1.519 | * | 1.520 | * | 1.528 | * | 1.528 | * | 1.506 | * |
| BA | 0.000 | 1.621 | 0.000 | 1.583 | 0.000 | 1.631 | 0.000 | 1.632 | 0.000 | 1.638 | 0.000 | 1.639 | 0.000 | 1.646 | 0.000 | 1.624 |
| CL | 0.000 | * | 0.000 | * | 0.000 | * | 0.000 | * | 0.000 | * | 0.000 | * | 0.000 | * | 0.000 | * |
| F | 0.000 | * | 0.000 | * | 0.000 | * | 0.000 | * | 0.000 | * | 0.000 | * | 0.000 | * | 0.000 | * |
| H | 4.000 | 4.000 | 4.000 | 4.000 | 4.000 | 4.000 | 4.000 | 4.000 | 4.000 | 4.000 | 4.000 | 4.000 | 4.000 | 4.000 | 4.000 | 4.000 |
| O | 24.000 | * | 24.000 | * | 24.000 | * | 24.000 | * | 24.000 | * | 24.000 | * | 24.000 | * | 24.000 | * |

9 329 BI495
10 330 BI495
11 331 BI495
12 332 BI3495
13 337 BI495
14 338 BI495
15 339 BI495
16 340 BI495

1SUPER RECAL TABLE 8A BIOTITE ANALYSES (H2O CALCULATED)

| | 17 | 18 | 19 | 20 | 21 | 22 | 23 | 24 |
|---|---|---|---|---|---|---|---|---|
| SIO2 | 37.84 | 37.69 | 37.18 | 37.50 | 37.10 | 37.66 | 38.15 | 37.93 |
| A2O3 | 19.69 | 19.33 | 19.04 | 18.89 | 19.58 | 19.38 | 19.44 | 19.28 |
| TIO2 | 1.61 | 1.64 | 1.46 | 1.47 | 1.73 | 1.73 | 1.69 | 1.60 |
| FEO | 14.65 | 14.81 | 14.55 | 14.46 | 15.11 | 15.14 | 15.18 | 14.96 |
| MNO | -0.02 | -0.01 | -0.02 | 0.00 | -0.02 | -0.01 | -0.02 | 0.00 |
| MGO | 12.60 | 12.78 | 11.95 | 11.98 | 13.38 | 13.10 | 12.94 | 12.81 |
| CAO | 0.01 | 0.00 | -0.02 | -0.02 | 0.02 | 0.01 | 0.00 | 0.05 |
| NA2O | 0.37 | 0.37 | 0.39 | 0.39 | 0.38 | 0.37 | 0.41 | 0.40 |
| K2O | 8.06 | 8.11 | 8.06 | 8.04 | 7.94 | 8.12 | 8.19 | 7.97 |
| BAO | 0.00 | 0.00 | 0.00 | 0.00 | 0.00 | 0.00 | 0.00 | 0.00 |
| CL | 0.00 | 0.00 | 0.00 | 0.00 | 0.00 | 0.00 | 0.00 | 0.00 |
| F | 0.00 | 0.00 | 0.00 | 0.00 | 0.00 | 0.00 | 0.00 | 0.00 |
| H2O | 4.07 | 4.06 | 3.97 | 3.98 | 4.07 | 4.08 | 4.11 | 4.07 |
| SUM | 98.88 | 98.78 | 96.56 | 96.69 | 99.29 | 99.58 | 100.09 | 99.07 |
| -O= F+CL | 0.00 | 0.00 | 0.00 | 0.00 | 0.00 | 0.00 | 0.00 | 0.00 |
| SUM | 98.88 | 98.78 | 96.56 | 96.69 | 99.29 | 99.58 | 100.09 | 99.07 |

| | | | | | | | | | | | | | | | | |
|---|---|---|---|---|---|---|---|---|---|---|---|---|---|---|---|---|
| SI | 5.570 | * | 5.566 | * | 5.615 | * | 5.649 | * | 5.462 | * | 5.526 | * | 5.565 | * | 5.582 | * |
| AL | 2.430 | 8.000 | 2.434 | 8.000 | 2.385 | 8.000 | 2.351 | 8.000 | 2.538 | 8.000 | 2.474 | 8.000 | 2.435 | 8.000 | 2.418 | 8.000 |
| AL | 0.986 | * | 0.929 | * | 1.003 | * | 1.002 | * | 0.858 | * | 0.878 | * | 0.907 | * | 0.926 | * |
| TI | 0.178 | * | 0.182 | * | 0.166 | * | 0.167 | * | 0.192 | * | 0.191 | * | 0.185 | * | 0.177 | * |
| FE | 1.804 | * | 1.829 | * | 1.837 | * | 1.822 | * | 1.860 | * | 1.858 | * | 1.852 | * | 1.841 | * |
| MN | -0.002 | * | -0.001 | * | -0.003 | * | 0.000 | * | -0.002 | * | -0.001 | * | -0.002 | * | 0.000 | * |
| MG | 2.765 | 5.730 | 2.813 | 5.752 | 2.690 | 5.693 | 2.690 | 5.680 | 2.936 | 5.843 | 2.865 | 5.791 | 2.814 | 5.756 | 2.810 | 5.754 |
| CA | 0.002 | * | 0.000 | * | -0.003 | * | -0.003 | * | 0.003 | * | 0.002 | * | 0.000 | * | 0.008 | * |
| NA | 0.106 | * | 0.106 | * | 0.114 | * | 0.114 | * | 0.108 | * | 0.105 | * | 0.116 | * | 0.114 | * |
| K | 1.513 | * | 1.527 | * | 1.552 | * | 1.545 | * | 1.491 | * | 1.520 | * | 1.524 | * | 1.496 | * |
| BA | 0.000 | 1.621 | 0.000 | 1.633 | 0.000 | 1.663 | 0.000 | 1.655 | 0.000 | 1.602 | 0.000 | 1.627 | 0.000 | 1.640 | 0.000 | 1.618 |
| CL | 0.000 | * | 0.000 | * | 0.000 | * | 0.000 | * | 0.000 | * | 0.000 | * | 0.000 | * | 0.000 | * |
| F | 0.000 | * | 0.000 | * | 0.000 | * | 0.000 | * | 0.000 | * | 0.000 | * | 0.000 | * | 0.000 | * |
| H | 4.000 | 4.000 | 4.000 | 4.000 | 4.000 | 4.000 | 4.000 | 4.000 | 4.000 | 4.000 | 4.000 | 4.000 | 4.000 | 4.000 | 4.000 | 4.000 |
| O | 24.000 | * | 24.000 | * | 24.000 | * | 24.000 | * | 24.000 | * | 24.000 | * | 24.000 | * | 24.000 | * |

17 341 BI495
18 342 BI495
19 343 BI495
20 345 BI495
21 418 BI495
22 419 BI495
23 421 BI495
24 422 BI495

1SUPER RECAL TABLE 8A BIOTITE ANALYSES (H2O CALCULATED)

| | 25 | 26 | 27 | 28 | 29 | 30 | 31 | 32 |
|---|---|---|---|---|---|---|---|---|
| SIO2 | 37.68 | 37.55 | 37.86 | 37.33 | 37.83 | 37.71 | 37.33 | 37.34 |
| A2O3 | 19.32 | 19.23 | 19.45 | 19.33 | 19.14 | 19.33 | 18.92 | 19.30 |
| TIO2 | 1.61 | 1.58 | 1.55 | 1.54 | 1.51 | 1.52 | 1.53 | 1.51 |
| FEO | 15.19 | 15.05 | 15.03 | 14.80 | 14.75 | 14.92 | 14.65 | 14.67 |
| MNO | -0.02 | -0.02 | 0.00 | -0.04 | -0.01 | -0.01 | 0.00 | -0.01 |
| MGO | 12.81 | 12.60 | 12.73 | 12.60 | 12.70 | 12.44 | 12.27 | 12.42 |
| CAO | 0.03 | 0.02 | 0.02 | -0.02 | -0.02 | -0.02 | -0.01 | 0.00 |
| NA2O | 0.45 | 0.42 | 0.43 | 0.42 | 0.39 | 0.40 | 0.37 | 0.39 |
| K2O | 8.07 | 8.05 | 7.99 | 8.17 | 8.17 | 8.17 | 8.06 | 8.06 |
| BAO | 0.00 | 0.00 | 0.00 | 0.00 | 0.00 | 0.00 | 0.00 | 0.00 |
| CL | 0.00 | 0.00 | 0.00 | 0.00 | 0.00 | 0.00 | 0.00 | 0.00 |
| F | 0.00 | 0.00 | 0.00 | 0.00 | 0.00 | 0.00 | 0.00 | 0.00 |
| H2O | 4.07 | 4.04 | 4.07 | 4.03 | 4.05 | 4.04 | 3.99 | 4.01 |
| SUM | 99.21 | 98.52 | 99.13 | 98.16 | 98.51 | 98.50 | 97.11 | 97.69 |
| -O= F+CL | 0.00 | 0.00 | 0.00 | 0.00 | 0.00 | 0.00 | 0.00 | 0.00 |
| SUM | 99.21 | 98.52 | 99.13 | 98.16 | 98.51 | 98.50 | 97.11 | 97.69 |

| | | | | | | | | | | | | | | | | |
|---|---|---|---|---|---|---|---|---|---|---|---|---|---|---|---|---|
| SI | 5.551 | * | 5.567 | * | 5.571 | * | 5.554 | * | 5.601 | * | 5.588 | * | 5.608 | * | 5.574 | * |
| AL | 2.449 | 8.000 | 2.433 | 8.000 | 2.429 | 8.000 | 2.446 | 8.000 | 2.399 | 8.000 | 2.412 | 8.000 | 2.392 | 8.000 | 2.426 | 8.000 |
| AL | 0.905 | * | 0.926 | * | 0.943 | * | 0.942 | * | 0.940 | * | 0.963 | * | 0.957 | * | 0.969 | * |
| TI | 0.178 | * | 0.176 | * | 0.172 | * | 0.172 | * | 0.168 | * | 0.169 | * | 0.173 | * | 0.170 | * |
| FE | 1.871 | * | 1.866 | * | 1.849 | * | 1.841 | * | 1.826 | * | 1.849 | * | 1.841 | * | 1.831 | * |
| MN | -0.002 | * | -0.003 | * | 0.000 | * | -0.005 | * | -0.001 | * | -0.001 | * | 0.000 | * | -0.001 | * |
| MG | 2.813 | 5.765 | 2.784 | 5.750 | 2.792 | 5.755 | 2.794 | 5.745 | 2.802 | 5.735 | 2.747 | 5.727 | 2.747 | 5.718 | 2.764 | 5.733 |
| CA | 0.005 | * | 0.003 | * | 0.003 | * | -0.003 | * | -0.003 | * | -0.003 | * | -0.002 | * | 0.000 | * |
| NA | 0.129 | * | 0.121 | * | 0.123 | * | 0.121 | * | 0.112 | * | 0.115 | * | 0.108 | * | 0.113 | * |
| K | 1.516 | * | 1.522 | * | 1.499 | * | 1.550 | * | 1.543 | * | 1.544 | * | 1.544 | * | 1.535 | * |
| BA | 0.000 | 1.650 | 0.000 | 1.646 | 0.000 | 1.625 | 0.000 | 1.668 | 0.000 | 1.652 | 0.000 | 1.656 | 0.000 | 1.651 | 0.000 | 1.648 |
| CL | 0.000 | * | 0.000 | * | 0.000 | * | 0.000 | * | 0.000 | * | 0.000 | * | 0.000 | * | 0.000 | * |
| F | 0.000 | * | 0.000 | * | 0.000 | * | 0.000 | * | 0.000 | * | 0.000 | * | 0.000 | * | 0.000 | * |
| H | 4.000 | 4.000 | 4.000 | 4.000 | 4.000 | 4.000 | 4.000 | 4.000 | 4.000 | 4.000 | 4.000 | 4.000 | 4.000 | 4.000 | 4.000 | 4.000 |
| O | 24.000 | * | 24.000 | * | 24.000 | * | 24.000 | * | 24.000 | * | 24.000 | * | 24.000 | * | 24.000 | * |

25 423 BI495
26 424 BI495
27 425 BI495
28 427 BI495
29 428 BI495
30 429 BI495
31 430 BI495
32 431 BI495

1SUPER RECAL TABLE 8A BIOTITE ANALYSES (H2O CALCULATED)

| | 33 | 34 | 35 | 36 | 37 | 38 | 39 | 40 |
|---|---|---|---|---|---|---|---|---|
| SIO2 | 37.33 | 37.20 | 37.30 | 36.60 | 37.40 | 37.60 | 37.52 | 36.94 |
| A2O3 | 19.35 | 18.81 | 19.21 | 20.78 | 20.69 | 19.30 | 19.38 | 19.21 |
| TIO2 | 1.51 | 1.55 | 1.57 | 1.56 | 1.70 | 1.49 | 1.52 | 1.65 |
| FEO | 14.61 | 14.70 | 14.72 | 14.63 | 12.94 | 14.65 | 14.60 | 14.80 |
| MNO | -0.01 | -0.01 | -0.02 | -0.02 | -0.05 | -0.01 | -0.02 | -0.02 |
| MGO | 12.10 | 12.31 | 12.18 | 11.74 | 11.49 | 12.49 | 12.50 | 12.45 |
| CAO | 0.00 | -0.02 | -0.02 | 0.01 | 0.02 | 0.00 | 0.00 | -0.01 |
| NA2O | 0.39 | 0.37 | 0.40 | 0.61 | 0.78 | 0.41 | 0.37 | 0.36 |
| K2O | 8.05 | 7.95 | 8.08 | 7.66 | 7.45 | 8.13 | 8.10 | 8.11 |
| BAO | 0.00 | 0.00 | 0.00 | 0.00 | 0.00 | 0.00 | 0.00 | 0.00 |
| CL | 0.00 | 0.00 | 0.00 | 0.00 | 0.00 | 0.00 | 0.00 | 0.00 |
| F | 0.00 | 0.00 | 0.00 | 0.00 | 0.00 | 0.00 | 0.00 | 0.00 |
| H2O | 4.00 | 3.98 | 4.00 | 4.02 | 4.01 | 4.03 | 4.03 | 4.00 |
| SUM | 97.33 | 96.84 | 97.42 | 97.59 | 96.43 | 98.09 | 98.00 | 97.49 |
| -O= F+CL | 0.00 | 0.00 | 0.00 | 0.00 | 0.00 | 0.00 | 0.00 | 0.00 |
| SUM | 97.33 | 96.84 | 97.42 | 97.59 | 96.43 | 98.09 | 98.00 | 97.49 |

| | | | | | | | | | | | | | | | | |
|---|---|---|---|---|---|---|---|---|---|---|---|---|---|---|---|---|
| SI | 5.590 | * | 5.604 | * | 5.586 | * | 5.459 | * | 5.583 | * | 5.589 | * | 5.579 | * | 5.538 | * |
| AL | 2.410 | 8.000 | 2.396 | 8.000 | 2.414 | 8.000 | 2.541 | 8.000 | 2.417 | 8.000 | 2.411 | 8.000 | 2.421 | 8.000 | 2.462 | 8.000 |
| AL | 1.005 | * | 0.943 | * | 0.976 | * | 1.111 | * | 1.222 | * | 0.969 | * | 0.975 | * | 0.931 | * |
| TI | 0.170 | * | 0.176 | * | 0.177 | * | 0.175 | * | 0.191 | * | 0.167 | * | 0.170 | * | 0.186 | * |
| FE | 1.830 | * | 1.852 | * | 1.844 | * | 1.825 | * | 1.615 | * | 1.821 | * | 1.816 | * | 1.855 | * |
| MN | -0.001 | * | -0.001 | * | -0.003 | * | -0.003 | * | -0.006 | * | -0.001 | * | -0.003 | * | -0.003 | * |
| MG | 2.701 | 5.704 | 2.764 | 5.734 | 2.719 | 5.713 | 2.610 | 5.719 | 2.557 | 5.579 | 2.767 | 5.723 | 2.771 | 5.729 | 2.782 | 5.751 |
| CA | 0.000 | * | -0.003 | * | -0.003 | * | 0.002 | * | 0.003 | * | 0.000 | * | 0.000 | * | -0.002 | * |
| NA | 0.113 | * | 0.108 | * | 0.116 | * | 0.176 | * | 0.226 | * | 0.118 | * | 0.107 | * | 0.105 | * |
| K | 1.538 | * | 1.528 | * | 1.543 | * | 1.457 | * | 1.418 | * | 1.541 | * | 1.536 | * | 1.551 | * |
| BA | 0.000 | 1.651 | 0.000 | 1.632 | 0.000 | 1.656 | 0.000 | 1.635 | 0.000 | 1.647 | 0.000 | 1.659 | 0.000 | 1.643 | 0.000 | 1.654 |
| CL | 0.000 | * | 0.000 | * | 0.000 | * | 0.000 | * | 0.000 | * | 0.000 | * | 0.000 | * | 0.000 | * |
| F | 0.000 | * | 0.000 | * | 0.000 | * | 0.000 | * | 0.000 | * | 0.000 | * | 0.000 | * | 0.000 | * |
| H | 4.000 | 4.000 | 4.000 | 4.000 | 4.000 | 4.000 | 4.000 | 4.000 | 4.000 | 4.000 | 4.000 | 4.000 | 4.000 | 4.000 | 4.000 | 4.000 |
| O | 24.000 | * | 24.000 | * | 24.000 | * | 24.000 | * | 24.000 | * | 24.000 | * | 24.000 | * | 24.000 | * |

33 432 BI495
34 433 BI495
35 434 BI495
36 435 BI495
37 436 BI495
38 437 BI495
39 438 BI495
40 447 BI495

1SUPER RECAL TABLE 8A BIOTITE ANALYSES (H2O CALCULATED)

| | 41 |
|---|---|
| SIO2 | 37.17 |
| A2O3 | 19.21 |
| TIO2 | 1.62 |
| FEO | 14.98 |
| MNO | -0.02 |
| MGO | 12.65 |
| CAO | -0.02 |
| NA2O | 0.41 |
| K2O | 8.28 |
| BAO | 0.00 |
| CL | 0.00 |
| F | 0.00 |
| H2O | 4.02 |
| SUM | 98.30 |
| -O= F+CL | 0.00 |
| SUM | 98.30 |

| | | | |
|---|---|---|---|
| SI | 5.534 | * | |
| AL | 2.466 | 8.000 | |
| AL | 0.904 | * | |
| TI | 0.181 | * | |
| FE | 1.865 | * | |
| MN | -0.003 | * | |
| MG | 2.807 | 5.755 | |
| CA | -0.003 | * | |
| NA | 0.118 | * | |
| K | 1.572 | * | |
| BA | 0.000 | 1.687 | |
| CL | 0.000 | * | |
| F | 0.000 | * | |
| H | 4.000 | 4.000 | |
| O | 24.000 | * | |

41 448 BI495

1SUPER RECAL TABLE 8B BIOTITE ANALYSES (H2O CALCULATED)

| | 1 | 2 | 3 | 4 | 5 | 6 | 7 | 8 |
|---|---|---|---|---|---|---|---|---|
| SIO2 | 37.18 | 36.76 | 37.03 | 37.22 | 36.79 | 37.01 | 36.42 | 35.73 |
| A2O3 | 19.11 | 18.99 | 19.24 | 19.53 | 19.49 | 19.72 | 19.52 | 19.13 |
| TIO2 | 1.51 | 1.49 | 1.43 | 1.44 | 1.43 | 1.45 | 1.38 | 1.31 |
| FEO | 13.97 | 14.39 | 14.04 | 14.09 | 13.88 | 13.80 | 14.35 | 14.93 |
| MNO | 0.04 | 0.04 | 0.04 | 0.06 | 0.04 | 0.07 | 0.04 | 0.04 |
| MGO | 12.96 | 13.07 | 12.95 | 12.88 | 12.86 | 12.88 | 12.88 | 13.25 |
| CAO | 0.04 | 0.04 | 0.04 | 0.06 | 0.06 | 0.05 | 0.06 | 0.07 |
| NA2O | 0.42 | 0.44 | 0.47 | 0.43 | 0.42 | 0.44 | 0.44 | 0.39 |
| K2O | 8.35 | 8.28 | 8.28 | 8.23 | 8.23 | 8.35 | 8.05 | 7.42 |
| BAO | 0.00 | 0.00 | 0.00 | 0.00 | 0.00 | 0.00 | 0.00 | 0.00 |
| CL | 0.00 | 0.00 | 0.00 | 0.00 | 0.00 | 0.00 | 0.00 | 0.00 |
| F | 0.00 | 0.00 | 0.00 | 0.00 | 0.00 | 0.00 | 0.00 | 0.00 |
| H2O | 4.01 | 3.99 | 4.01 | 4.03 | 4.00 | 4.02 | 3.98 | 3.94 |
| SUM | 97.59 | 97.49 | 97.53 | 97.97 | 97.20 | 97.79 | 97.12 | 96.21 |
| -O= F+CL | 0.00 | 0.00 | 0.00 | 0.00 | 0.00 | 0.00 | 0.00 | 0.00 |
| SUM | 97.59 | 97.49 | 97.53 | 97.97 | 97.20 | 97.79 | 97.12 | 96.21 |

| | | | | | | | | | | | | | | | | |
|---|---|---|---|---|---|---|---|---|---|---|---|---|---|---|---|---|
| SI | 5.556 | * | 5.515 | * | 5.538 | * | 5.536 | * | 5.516 | * | 5.514 | * | 5.477 | * | 5.432 | * |
| AL | 2.444 | 8.000 | 2.485 | 8.000 | 2.462 | 8.000 | 2.464 | 8.000 | 2.484 | 8.000 | 2.486 | 8.000 | 2.523 | 8.000 | 2.568 | 8.000 |
| AL | 0.920 | * | 0.872 | * | 0.929 | * | 0.959 | * | 0.960 | * | 0.975 | * | 0.936 | * | 0.859 | * |
| TI | 0.170 | * | 0.168 | * | 0.161 | * | 0.161 | * | 0.161 | * | 0.162 | * | 0.156 | * | 0.150 | * |
| FE | 1.746 | * | 1.805 | * | 1.756 | * | 1.753 | * | 1.740 | * | 1.719 | * | 1.805 | * | 1.898 | * |
| MN | 0.005 | * | 0.005 | * | 0.005 | * | 0.008 | * | 0.005 | * | 0.009 | * | 0.005 | * | 0.005 | * |
| MG | 2.886 | 5.727 | 2.923 | 5.773 | 2.887 | 5.739 | 2.856 | 5.736 | 2.874 | 5.741 | 2.860 | 5.726 | 2.887 | 5.789 | 3.002 | 5.914 |
| CA | 0.006 | * | 0.006 | * | 0.006 | * | 0.010 | * | 0.010 | * | 0.008 | * | 0.010 | * | 0.011 | * |
| NA | 0.122 | * | 0.128 | * | 0.136 | * | 0.124 | * | 0.122 | * | 0.127 | * | 0.128 | * | 0.115 | * |
| K | 1.591 | * | 1.584 | * | 1.580 | * | 1.561 | * | 1.574 | * | 1.587 | * | 1.544 | * | 1.439 | * |
| BA | 0.000 | 1.719 | 0.000 | 1.719 | 0.000 | 1.722 | 0.000 | 1.695 | 0.000 | 1.706 | 0.000 | 1.722 | 0.000 | 1.682 | 0.000 | 1.565 |
| CL | 0.000 | * | 0.000 | * | 0.000 | * | 0.000 | * | 0.000 | * | 0.000 | * | 0.000 | * | 0.000 | * |
| F | 0.000 | * | 0.000 | * | 0.000 | * | 0.000 | * | 0.000 | * | 0.000 | * | 0.000 | * | 0.000 | * |
| H | 4.000 | 4.000 | 4.000 | 4.000 | 4.000 | 4.000 | 4.000 | 4.000 | 4.000 | 4.000 | 4.000 | 4.000 | 4.000 | 4.000 | 4.000 | 4.000 |
| O | 24.000 | * | 24.000 | * | 24.000 | * | 24.000 | * | 24.000 | * | 24.000 | * | 24.000 | * | 24.000 | * |

1 438 BI11D
2 439 BI11D
3 440 BI11D
4 441 BI11D
5 442 BI11D
6 443 BI11D
7 446 BI11D
8 447 BI11D

1SUPER RECAL TABLE 8B BIOTITE ANALYSES (H2O CALCULATED)

| | 9 | 10 | 11 | 12 | 13 | 14 | 15 | 16 |
|---|---|---|---|---|---|---|---|---|
| SIO2 | 56.21 | 37.21 | 36.43 | 37.36 | 37.22 | 37.06 | 36.48 | 39.44 |
| A2O3 | 23.34 | 19.45 | 19.36 | 19.55 | 19.47 | 19.18 | 18.98 | 18.82 |
| TIO2 | 0.44 | 1.85 | 1.67 | 1.59 | 1.48 | 1.52 | 1.44 | 2.23 |
| FEO | 3.41 | 14.17 | 14.63 | 14.61 | 14.43 | 14.43 | 14.69 | 12.49 |
| MNO | 0.01 | 0.05 | 0.06 | 0.04 | 0.04 | 0.05 | 0.05 | 0.05 |
| MGO | 2.79 | 12.85 | 13.22 | 13.16 | 13.20 | 13.07 | 13.34 | 10.93 |
| CAO | 3.91 | 0.08 | 0.07 | 0.06 | 0.06 | 0.07 | 0.07 | 0.78 |
| NA2O | 6.98 | 0.39 | 0.37 | 0.45 | 0.39 | 0.48 | 0.37 | 0.64 |
| K2O | 1.84 | 8.16 | 8.01 | 8.24 | 8.02 | 8.08 | 7.95 | 8.13 |
| BAO | 0.00 | 0.00 | 0.00 | 0.00 | 0.00 | 0.00 | 0.00 | 0.00 |
| CL | 0.00 | 0.00 | 0.00 | 0.00 | 0.00 | 0.00 | 0.00 | 0.00 |
| F | 0.00 | 0.00 | 0.00 | 0.00 | 0.00 | 0.00 | 0.00 | 0.00 |
| H2O | 4.72 | 4.04 | 4.01 | 4.07 | 4.04 | 4.02 | 3.99 | 4.06 |
| SUM | 103.65 | 98.25 | 97.83 | 99.13 | 98.35 | 97.96 | 97.36 | 97.57 |
| -O= F+CL | 0.00 | 0.00 | 0.00 | 0.00 | 0.00 | 0.00 | 0.00 | 0.00 |
| SUM | 103.65 | 98.25 | 97.83 | 99.13 | 98.35 | 97.96 | 97.36 | 97.57 |

| | | | | | | | | | | | | | | | | |
|---|---|---|---|---|---|---|---|---|---|---|---|---|---|---|---|---|
| SI | 7.128 | * | 5.520 | * | 5.447 | * | 5.505 | * | 5.517 | * | 5.524 | * | 5.482 | * | 5.826 | * |
| AL | 0.872 | 8.000 | 2.480 | 8.000 | 2.553 | 8.000 | 2.495 | 8.000 | 2.483 | 8.000 | 2.476 | 8.000 | 2.518 | 8.000 | 2.174 | 8.000 |
| AL | 2.615 | * | 0.919 | * | 0.858 | * | 0.899 | * | 0.917 | * | 0.892 | * | 0.843 | * | 1.102 | * |
| TI | 0.042 | * | 0.206 | * | 0.188 | * | 0.176 | * | 0.165 | * | 0.170 | * | 0.163 | * | 0.248 | * |
| FE | 0.362 | * | 1.758 | * | 1.829 | * | 1.800 | * | 1.789 | * | 1.799 | * | 1.846 | * | 1.543 | * |
| MN | 0.001 | * | 0.006 | * | 0.008 | * | 0.005 | * | 0.005 | * | 0.006 | * | 0.006 | * | 0.006 | * |
| MG | 0.527 | 3.547 | 2.841 | 5.731 | 2.946 | 5.829 | 2.890 | 5.771 | 2.916 | 5.792 | 2.904 | 5.771 | 2.988 | 5.846 | 2.406 | 5.305 |
| CA | 0.531 | * | 0.013 | * | 0.011 | * | 0.009 | * | 0.010 | * | 0.011 | * | 0.011 | * | 0.123 | * |
| NA | 1.716 | * | 0.112 | * | 0.107 | * | 0.129 | * | 0.112 | * | 0.139 | * | 0.108 | * | 0.183 | * |
| K | 0.298 | * | 1.544 | * | 1.528 | * | 1.549 | * | 1.516 | * | 1.536 | * | 1.524 | * | 1.532 | * |
| BA | 0.000 | 2.545 | 0.000 | 1.669 | 0.000 | 1.646 | 0.000 | 1.687 | 0.000 | 1.638 | 0.000 | 1.686 | 0.000 | 1.643 | 0.000 | 1.839 |
| CL | 0.000 | * | 0.000 | * | 0.000 | * | 0.000 | * | 0.000 | * | 0.000 | * | 0.000 | * | 0.000 | * |
| F | 0.000 | * | 0.000 | * | 0.000 | * | 0.000 | * | 0.000 | * | 0.000 | * | 0.000 | * | 0.000 | * |
| H | 4.000 | 4.000 | 4.000 | 4.000 | 4.000 | 4.000 | 4.000 | 4.000 | 4.000 | 4.000 | 4.000 | 4.000 | 4.000 | 4.000 | 4.000 | 4.000 |
| O | 24.000 | * | 24.000 | * | 24.000 | * | 24.000 | * | 24.000 | * | 24.000 | * | 24.000 | * | 24.000 | * |

9 449 BI11D
10 450 BI11D
11 451 BI11D
12 452 BI11D
13 454 BI11D
14 455 BI11D
15 457 BI11D
16 469 BI11D

1SUPER RECAL TABLE 8B BIOTITE ANALYSES (H2O CALCULATED)

| | 17 | 18 | 19 |
|---|---|---|---|
| SIO2 | 36.94 | 36.87 | 36.93 |
| A2O3 | 18.98 | 18.66 | 19.03 |
| TIO2 | 1.70 | 1.64 | 1.65 |
| FEO | 14.31 | 14.50 | 14.53 |
| MNO | 0.07 | 0.04 | 0.05 |
| MGO | 12.77 | 12.81 | 12.68 |
| CAO | 0.05 | 0.04 | 0.02 |
| NA2O | 0.39 | 0.36 | 0.37 |
| K2O | 8.16 | 8.16 | 8.18 |
| BAO | 0.00 | 0.00 | 0.00 |
| CL | 0.00 | 0.00 | 0.00 |
| F | 0.00 | 0.00 | 0.00 |
| H2O | 3.99 | 3.98 | 3.99 |
| SUM | 97.36 | 97.06 | 97.43 |
| -O= F+CL | 0.00 | 0.00 | 0.00 |
| SUM | 97.36 | 97.06 | 97.43 |

| | | | | | | |
|---|---|---|---|---|---|---|
| SI | 5.540 | * | 5.554 | * | 5.539 | * |
| AL | 2.460 | 8.000 | 2.446 | 8.000 | 2.461 | 8.000 |
| AL | 0.894 | * | 0.866 | * | 0.902 | * |
| TI | 0.192 | * | 0.186 | * | 0.186 | * |
| FE | 1.795 | * | 1.827 | * | 1.822 | * |
| MN | 0.009 | * | 0.005 | * | 0.006 | * |
| MG | 2.854 | 5.744 | 2.876 | 5.759 | 2.835 | 5.752 |
| CA | 0.008 | * | 0.006 | * | 0.003 | * |
| NA | 0.113 | * | 0.105 | * | 0.108 | * |
| K | 1.561 | * | 1.568 | * | 1.565 | * |
| BA | 0.000 | 1.682 | 0.000 | 1.679 | 0.000 | 1.676 |
| CL | 0.000 | * | 0.000 | * | 0.000 | * |
| F | 0.000 | * | 0.000 | * | 0.000 | * |
| H | 4.000 | 4.000 | 4.000 | 4.000 | 4.000 | 4.000 |
| O | 24.000 | * | 24.000 | * | 24.000 | * |

17 471 BI11D
18 472 BI11D
19 473 BI11D

1SUPER RECAL TABLE 8C BIOTITE ANALYSES (H2O CALCULATED)

| | 1 | 2 | 3 | 4 | 5 | 6 | 7 | 8 |
|---|---|---|---|---|---|---|---|---|
| SIO2 | 35.92 | 36.08 | 36.03 | 37.12 | 36.42 | 40.16 | 36.57 | 35.90 |
| A2O3 | 19.07 | 18.79 | 18.95 | 19.67 | 18.84 | 22.16 | 19.08 | 20.18 |
| TIO2 | 1.73 | 1.77 | 1.71 | 1.70 | 1.68 | 1.20 | 1.68 | 1.60 |
| FEO | 17.42 | 17.33 | 17.34 | 16.82 | 17.06 | 13.18 | 17.10 | 16.80 |
| MNO | 0.05 | 0.06 | 0.08 | 0.05 | 0.06 | 0.01 | 0.04 | 0.06 |
| MGO | 11.08 | 11.12 | 10.97 | 10.48 | 11.13 | 8.35 | 11.28 | 11.19 |
| CAO | 0.09 | 0.08 | 0.10 | 0.18 | 0.11 | 1.07 | 0.07 | 0.08 |
| NA2O | 0.14 | 0.14 | 0.15 | 0.61 | 0.15 | 1.65 | 0.18 | 0.17 |
| K2O | 8.41 | 8.42 | 8.36 | 7.93 | 8.38 | 6.17 | 8.49 | 8.16 |
| BAO | 0.00 | 0.00 | 0.00 | 0.00 | 0.00 | 0.00 | 0.00 | 0.00 |
| CL | 0.00 | 0.00 | 0.00 | 0.00 | 0.00 | 0.00 | 0.00 | 0.00 |
| F | 0.00 | 0.00 | 0.00 | 0.00 | 0.00 | 0.00 | 0.00 | 0.00 |
| H2O | 3.95 | 3.94 | 3.94 | 4.01 | 3.95 | 4.12 | 3.98 | 3.98 |
| SUM | 97.86 | 97.73 | 97.63 | 98.57 | 97.78 | 98.07 | 98.47 | 98.12 |
| -O= F+CL | 0.00 | 0.00 | 0.00 | 0.00 | 0.00 | 0.00 | 0.00 | 0.00 |
| SUM | 97.86 | 97.73 | 97.63 | 98.57 | 97.78 | 98.07 | 98.47 | 98.12 |

| | | | | | | | | | | | | | | | | |
|---|---|---|---|---|---|---|---|---|---|---|---|---|---|---|---|---|
| SI | 5.454 | * | 5.483 | * | 5.480 | * | 5.550 | * | 5.518 | * | 5.833 | * | 5.502 | * | 5.405 | * |
| AL | 2.546 | 8.000 | 2.517 | 8.000 | 2.520 | 8.000 | 2.450 | 8.000 | 2.482 | 8.000 | 2.167 | 8.000 | 2.498 | 8.000 | 2.595 | 8.000 |
| AL | 0.866 | * | 0.848 | * | 0.876 | * | 1.015 | * | 0.882 | * | 1.626 | * | 0.885 | * | 0.985 | * |
| TI | 0.198 | * | 0.202 | * | 0.196 | * | 0.191 | * | 0.191 | * | 0.131 | * | 0.190 | * | 0.181 | * |
| FE | 2.212 | * | 2.203 | * | 2.206 | * | 2.103 | * | 2.162 | * | 1.601 | * | 2.152 | * | 2.115 | * |
| MN | 0.006 | * | 0.008 | * | 0.010 | * | 0.006 | * | 0.008 | * | 0.001 | * | 0.005 | * | 0.008 | * |
| MG | 2.508 | 5.790 | 2.519 | 5.780 | 2.487 | 5.775 | 2.335 | 5.651 | 2.514 | 5.756 | 1.808 | 5.167 | 2.530 | 5.762 | 2.511 | 5.800 |
| CA | 0.015 | * | 0.013 | * | 0.016 | * | 0.029 | * | 0.018 | * | 0.167 | * | 0.011 | * | 0.013 | * |
| NA | 0.041 | * | 0.041 | * | 0.044 | * | 0.177 | * | 0.044 | * | 0.465 | * | 0.053 | * | 0.050 | * |
| K | 1.629 | * | 1.632 | * | 1.622 | * | 1.512 | * | 1.619 | * | 1.143 | * | 1.629 | * | 1.567 | * |
| BA | 0.000 | 1.685 | 0.000 | 1.686 | 0.000 | 1.682 | 0.000 | 1.718 | 0.000 | 1.681 | 0.000 | 1.774 | 0.000 | 1.693 | 0.000 | 1.629 |
| CL | 0.000 | * | 0.000 | * | 0.000 | * | 0.000 | * | 0.000 | * | 0.000 | * | 0.000 | * | 0.000 | * |
| F | 0.000 | * | 0.000 | * | 0.000 | * | 0.000 | * | 0.000 | * | 0.000 | * | 0.000 | * | 0.000 | * |
| H | 4.000 | 4.000 | 4.000 | 4.000 | 4.000 | 4.000 | 4.000 | 4.000 | 4.000 | 4.000 | 4.000 | 4.000 | 4.000 | 4.000 | 4.000 | 4.000 |
| O | 24.000 | * | 24.000 | * | 24.000 | * | 24.000 | * | 24.000 | * | 24.000 | * | 24.000 | * | 24.000 | * |

1 608 BI793
2 609 BI793
3 610 BI793
4 611 BI793
5 613 BI793
6 614 BI793
7 618 BI793
8 619 BI793

1SUPER RECAL TABLE 8D BIOTITE ANALYSES (H2O CALCULATED)

| | 1 | 2 | 3 | 4 | 5 | 6 | 7 | 8 |
|---|---|---|---|---|---|---|---|---|
| SIO2 | 36.72 | 37.23 | 37.04 | 37.56 | 37.52 | 37.57 | 43.10 | 46.55 |
| A2O3 | 18.73 | 18.61 | 18.47 | 18.16 | 18.37 | 17.99 | 16.60 | 15.30 |
| TIO2 | 1.58 | 1.61 | 1.58 | 1.59 | 1.64 | 1.67 | 1.61 | 1.40 |
| FEO | 18.57 | 18.44 | 18.45 | 18.66 | 18.55 | 18.26 | 16.97 | 15.89 |
| MNO | 0.12 | 0.10 | 0.13 | 0.12 | 0.10 | 0.12 | 0.09 | 0.09 |
| MGO | 10.78 | 10.86 | 10.92 | 10.97 | 10.98 | 10.76 | 9.82 | 9.53 |
| CAO | 0.09 | 0.07 | 0.05 | 0.05 | 0.08 | 0.09 | 0.11 | 0.12 |
| NA2O | 0.19 | 0.19 | 0.20 | 0.18 | 0.18 | 0.18 | 0.16 | 0.11 |
| K2O | 8.90 | 8.91 | 9.06 | 9.00 | 8.89 | 8.63 | 7.97 | 5.25 |
| BAO | 0.00 | 0.00 | 0.00 | 0.00 | 0.00 | 0.00 | 0.00 | 0.00 |
| CL | 0.00 | 0.00 | 0.00 | 0.00 | 0.00 | 0.00 | 0.00 | 0.00 |
| F | 0.00 | 0.00 | 0.00 | 0.00 | 0.00 | 0.00 | 0.00 | 0.00 |
| H2O | 3.99 | 4.01 | 4.00 | 4.02 | 4.03 | 3.99 | 4.15 | 4.18 |
| SUM | 99.67 | 100.03 | 99.90 | 100.31 | 100.34 | 99.26 | 100.58 | 98.42 |
| -O= F+CL | 0.00 | 0.00 | 0.00 | 0.00 | 0.00 | 0.00 | 0.00 | 0.00 |
| SUM | 99.67 | 100.03 | 99.90 | 100.31 | 100.34 | 99.26 | 100.58 | 98.42 |

| | | | | | | | | | | | | | | | | |
|---|---|---|---|---|---|---|---|---|---|---|---|---|---|---|---|---|
| SI | 5.511 | * | 5.556 | * | 5.545 | * | 5.596 | * | 5.582 | * | 5.636 | * | 6.228 | * | 6.675 | * |
| AL | 2.489 | 8.000 | 2.444 | 8.000 | 2.455 | 8.000 | 2.404 | 8.000 | 2.418 | 8.000 | 2.364 | 8.000 | 1.772 | 8.000 | 1.325 | 8.000 |
| AL | 0.823 | * | 0.828 | * | 0.803 | * | 0.785 | * | 0.802 | * | 0.816 | * | 1.055 | * | 1.261 | * |
| TI | 0.178 | * | 0.181 | * | 0.178 | * | 0.178 | * | 0.183 | * | 0.188 | * | 0.175 | * | 0.151 | * |
| FE | 2.331 | * | 2.301 | * | 2.310 | * | 2.325 | * | 2.308 | * | 2.291 | * | 2.051 | * | 1.906 | * |
| MN | 0.015 | * | 0.013 | * | 0.016 | * | 0.015 | * | 0.013 | * | 0.015 | * | 0.011 | * | 0.011 | * |
| MG | 2.411 | 5.759 | 2.416 | 5.738 | 2.437 | 5.744 | 2.436 | 5.740 | 2.435 | 5.740 | 2.406 | 5.717 | 2.115 | 5.407 | 2.037 | 5.365 |
| CA | 0.014 | * | 0.011 | * | 0.008 | * | 0.008 | * | 0.013 | * | 0.014 | * | 0.017 | * | 0.018 | * |
| NA | 0.055 | * | 0.055 | * | 0.058 | * | 0.052 | * | 0.052 | * | 0.052 | * | 0.045 | * | 0.031 | * |
| K | 1.704 | * | 1.696 | * | 1.730 | * | 1.710 | * | 1.687 | * | 1.651 | * | 1.469 | * | 0.960 | * |
| BA | 0.000 | 1.773 | 0.000 | 1.762 | 0.000 | 1.796 | 0.000 | 1.770 | 0.000 | 1.752 | 0.000 | 1.718 | 0.000 | 1.531 | 0.000 | 1.009 |
| CL | 0.000 | * | 0.000 | * | 0.000 | * | 0.000 | * | 0.000 | * | 0.000 | * | 0.000 | * | 0.000 | * |
| F | 0.000 | * | 0.000 | * | 0.000 | * | 0.000 | * | 0.000 | * | 0.000 | * | 0.000 | * | 0.000 | * |
| H | 4.000 | 4.000 | 4.000 | 4.000 | 4.000 | 4.000 | 4.000 | 4.000 | 4.000 | 4.000 | 4.000 | 4.000 | 4.000 | 4.000 | 4.000 | 4.000 |
| O | 24.000 | * | 24.000 | * | 24.000 | * | 24.000 | * | 24.000 | * | 24.000 | * | 24.000 | * | 24.000 | * |

1 120 BI608
2 121 BI608
3 122 BI608
4 123 BI608
5 124 BI608
6 125 BI608
7 126 BI608
8 127 BI608

1SUPER RECAL TABLE 8D BIOTITE ANALYSES (H2O CALCULATED)

| | 9 | 10 | 11 | 12 | 13 | 14 | 15 | 16 |
|---|---|---|---|---|---|---|---|---|
| SIO2 | 35.55 | 36.62 | 36.86 | 36.50 | 36.12 | 36.62 | 36.40 | 35.97 |
| A2O3 | 18.74 | 18.37 | 18.26 | 18.04 | 18.29 | 18.09 | 18.10 | 18.47 |
| TIO2 | 1.56 | 1.68 | 1.64 | 1.70 | 1.66 | 1.63 | 1.70 | 1.69 |
| FEO | 18.71 | 18.54 | 18.67 | 18.69 | 18.89 | 17.88 | 18.10 | 18.10 |
| MNO | 0.12 | 0.12 | 0.12 | 0.10 | 0.12 | 0.10 | 0.11 | 0.10 |
| MGO | 10.69 | 10.48 | 10.58 | 10.44 | 10.53 | 10.80 | 10.96 | 10.92 |
| CAO | 0.06 | 0.05 | 0.06 | 0.05 | 0.08 | 0.11 | 0.07 | 0.05 |
| NA2O | 0.16 | 0.18 | 0.18 | 0.20 | 0.19 | 0.32 | 0.19 | 0.20 |
| K2O | 8.16 | 9.00 | 9.01 | 8.85 | 8.56 | 8.90 | 8.98 | 9.06 |
| BAO | 0.00 | 0.00 | 0.00 | 0.00 | 0.00 | 0.00 | 0.00 | 0.00 |
| CL | 0.00 | 0.00 | 0.00 | 0.00 | 0.00 | 0.00 | 0.00 | 0.00 |
| F | 0.00 | 0.00 | 0.00 | 0.00 | 0.00 | 0.00 | 0.00 | 0.00 |
| H2O | 3.91 | 3.96 | 3.97 | 3.94 | 3.93 | 3.95 | 3.95 | 3.94 |
| SUM | 97.66 | 99.00 | 99.35 | 98.51 | 98.37 | 98.40 | 98.56 | 98.50 |
| -O= F+CL | 0.00 | 0.00 | 0.00 | 0.00 | 0.00 | 0.00 | 0.00 | 0.00 |
| SUM | 97.66 | 99.00 | 99.35 | 98.51 | 98.37 | 98.40 | 98.56 | 98.50 |

| | | | | | | | | | | | | | | | | |
|---|---|---|---|---|---|---|---|---|---|---|---|---|---|---|---|---|
| SI | 5.443 | * | 5.539 | * | 5.556 | * | 5.552 | * | 5.503 | * | 5.559 | * | 5.526 | * | 5.470 | * |
| AL | 2.557 | 8.000 | 2.461 | 8.000 | 2.444 | 8.000 | 2.448 | 8.000 | 2.497 | 8.000 | 2.441 | 8.000 | 2.474 | 8.000 | 2.530 | 8.000 |
| AL | 0.824 | * | 0.813 | * | 0.800 | * | 0.786 | * | 0.786 | * | 0.795 | * | 0.764 | * | 0.780 | * |
| TI | 0.180 | * | 0.191 | * | 0.186 | * | 0.194 | * | 0.190 | * | 0.186 | * | 0.194 | * | 0.193 | * |
| FE | 2.396 | * | 2.345 | * | 2.354 | * | 2.378 | * | 2.407 | * | 2.270 | * | 2.298 | * | 2.302 | * |
| MN | 0.016 | * | 0.015 | * | 0.015 | * | 0.013 | * | 0.015 | * | 0.013 | * | 0.014 | * | 0.013 | * |
| MG | 2.440 | 5.854 | 2.363 | 5.728 | 2.377 | 5.732 | 2.367 | 5.738 | 2.391 | 5.790 | 2.444 | 5.708 | 2.480 | 5.750 | 2.475 | 5.763 |
| CA | 0.010 | * | 0.008 | * | 0.010 | * | 0.008 | * | 0.013 | * | 0.018 | * | 0.011 | * | 0.008 | * |
| NA | 0.047 | * | 0.053 | * | 0.053 | * | 0.059 | * | 0.056 | * | 0.094 | * | 0.056 | * | 0.059 | * |
| K | 1.594 | * | 1.736 | * | 1.732 | * | 1.717 | * | 1.663 | * | 1.723 | * | 1.739 | * | 1.757 | * |
| BA | 0.000 | 1.651 | 0.000 | 1.797 | 0.000 | 1.795 | 0.000 | 1.784 | 0.000 | 1.733 | 0.000 | 1.835 | 0.000 | 1.808 | 0.000 | 1.824 |
| CL | 0.000 | * | 0.000 | * | 0.000 | * | 0.000 | * | 0.000 | * | 0.000 | * | 0.000 | * | 0.000 | * |
| F | 0.000 | * | 0.000 | * | 0.000 | * | 0.000 | * | 0.000 | * | 0.000 | * | 0.000 | * | 0.000 | * |
| H | 4.000 | 4.000 | 4.000 | 4.000 | 4.000 | 4.000 | 4.000 | 4.000 | 4.000 | 4.000 | 4.000 | 4.000 | 4.000 | 4.000 | 4.000 | 4.000 |
| O | 24.000 | * | 24.000 | * | 24.000 | * | 24.000 | * | 24.000 | * | 24.000 | * | 24.000 | * | 24.000 | * |

9 188 BI608
10 189 BI608
11 190 BI608
12 191 BI608
13 192 BI608
14 213 BI608
15 214 BI608
16 215 BI608

1SUPER RECAL TABLE 8D BIOTITE ANALYSES (H2O CALCULATED)

| | 17 | 18 | 19 | 20 | 21 | 22 | 23 | 24 |
|---|---|---|---|---|---|---|---|---|
| SIO2 | 36.29 | 36.25 | 45.08 | 38.87 | 35.89 | 36.05 | 36.10 | 36.10 |
| A2O3 | 18.57 | 18.23 | 15.95 | 16.93 | 18.31 | 18.24 | 18.33 | 18.15 |
| TIO2 | 1.66 | 1.71 | 1.49 | 1.74 | 1.80 | 1.85 | 1.84 | 1.83 |
| FEO | 17.98 | 17.90 | 16.08 | 18.03 | 18.08 | 18.23 | 18.26 | 18.16 |
| MNO | 0.11 | 0.12 | 0.09 | 0.10 | 0.12 | 0.12 | 0.13 | 0.12 |
| MGO | 10.97 | 11.01 | 8.18 | 10.22 | 10.78 | 11.06 | 10.88 | 10.94 |
| CAO | 0.07 | 0.07 | 0.47 | 0.08 | 0.12 | 0.08 | 0.07 | 0.07 |
| NA2O | 0.22 | 0.17 | 0.85 | 0.15 | 0.19 | 0.19 | 0.18 | 0.19 |
| K2O | 8.86 | 8.96 | 6.84 | 8.31 | 8.70 | 9.01 | 9.15 | 9.14 |
| BAO | 0.00 | 0.00 | 0.00 | 0.00 | 0.00 | 0.00 | 0.00 | 0.00 |
| CL | 0.00 | 0.00 | 0.00 | 0.00 | 0.00 | 0.00 | 0.00 | 0.00 |
| F | 0.00 | 0.00 | 0.00 | 0.00 | 0.00 | 0.00 | 0.00 | 0.00 |
| H2O | 3.96 | 3.94 | 4.14 | 3.98 | 3.92 | 3.95 | 3.95 | 3.94 |
| SUM | 98.69 | 98.36 | 99.17 | 98.41 | 97.91 | 98.78 | 98.89 | 98.64 |
| -O= F+CL | 0.00 | 0.00 | 0.00 | 0.00 | 0.00 | 0.00 | 0.00 | 0.00 |
| SUM | 98.69 | 98.36 | 99.17 | 98.41 | 97.91 | 98.78 | 98.89 | 98.64 |

| | | | | | | | | | | | | | | | | |
|---|---|---|---|---|---|---|---|---|---|---|---|---|---|---|---|---|
| SI | 5.493 | * | 5.510 | * | 6.524 | * | 5.848 | * | 5.483 | * | 5.470 | * | 5.475 | * | 5.487 | * |
| AL | 2.507 | 8.000 | 2.490 | 8.000 | 1.476 | 8.000 | 2.152 | 8.000 | 2.517 | 8.000 | 2.530 | 8.000 | 2.525 | 8.000 | 2.513 | 8.000 |
| AL | 0.806 | * | 0.775 | * | 1.244 | * | 0.850 | * | 0.778 | * | 0.732 | * | 0.751 | * | 0.738 | * |
| TI | 0.189 | * | 0.195 | * | 0.162 | * | 0.197 | * | 0.207 | * | 0.211 | * | 0.210 | * | 0.209 | * |
| FE | 2.276 | * | 2.275 | * | 1.946 | * | 2.269 | * | 2.310 | * | 2.313 | * | 2.316 | * | 2.309 | * |
| MN | 0.014 | * | 0.015 | * | 0.011 | * | 0.013 | * | 0.016 | * | 0.015 | * | 0.017 | * | 0.015 | * |
| MG | 2.475 | 5.760 | 2.494 | 5.755 | 1.765 | 5.128 | 2.292 | 5.620 | 2.455 | 5.765 | 2.501 | 5.773 | 2.459 | 5.752 | 2.479 | 5.750 |
| CA | 0.011 | * | 0.011 | * | 0.073 | * | 0.013 | * | 0.020 | * | 0.013 | * | 0.011 | * | 0.011 | * |
| NA | 0.065 | * | 0.050 | * | 0.239 | * | 0.044 | * | 0.056 | * | 0.056 | * | 0.053 | * | 0.056 | * |
| K | 1.711 | * | 1.737 | * | 1.263 | * | 1.595 | * | 1.695 | * | 1.744 | * | 1.770 | * | 1.772 | * |
| BA | 0.000 | 1.787 | 0.000 | 1.798 | 0.000 | 1.574 | 0.000 | 1.651 | 0.000 | 1.771 | 0.000 | 1.813 | 0.000 | 1.834 | 0.000 | 1.839 |
| CL | 0.000 | * | 0.000 | * | 0.000 | * | 0.000 | * | 0.000 | * | 0.000 | * | 0.000 | * | 0.000 | * |
| F | 0.000 | * | 0.000 | * | 0.000 | * | 0.000 | * | 0.000 | * | 0.000 | * | 0.000 | * | 0.000 | * |
| H | 4.000 | 4.000 | 4.000 | 4.000 | 4.000 | 4.000 | 4.000 | 4.000 | 4.000 | 4.000 | 4.000 | 4.000 | 4.000 | 4.000 | 4.000 | 4.000 |
| O | 24.000 | * | 24.000 | * | 24.000 | * | 24.000 | * | 24.000 | * | 24.000 | * | 24.000 | * | 24.000 | * |

17 216 BI608
18 217 BI608
19 232 BI608
20 233 BI608
21 234 BI608
22 235 BI608
23 236 BI608
24 237 BI608

1SUPER RECAL TABLE 8D BIOTITE ANALYSES (H2O CALCULATED)

| | 25 | 26 | 27 |
|---|---|---|---|
| SIO2 | 35.04 | 36.15 | 35.41 |
| A2O3 | 18.84 | 18.13 | 18.09 |
| TIO2 | 1.45 | 1.71 | 1.67 |
| FEO | 18.79 | 18.54 | 18.23 |
| MNO | 0.14 | 0.11 | 0.11 |
| MGO | 11.86 | 11.16 | 10.66 |
| CAO | 0.06 | 0.06 | 0.11 |
| NA2O | 0.14 | 0.17 | 0.16 |
| K2O | 7.76 | 9.01 | 8.32 |
| BAO | 0.00 | 0.00 | 0.00 |
| CL | 0.00 | 0.00 | 0.00 |
| F | 0.00 | 0.00 | 0.00 |
| H2O | 3.93 | 3.95 | 3.87 |
| SUM | 98.01 | 98.99 | 96.63 |
| -O= F+CL | 0.00 | 0.00 | 0.00 |
| SUM | 98.01 | 98.99 | 96.63 |

| | | | | | | |
|---|---|---|---|---|---|---|
| SI | 5.345 | * | 5.480 | * | 5.481 | * |
| AL | 2.655 | 8.000 | 2.520 | 8.000 | 2.519 | 8.000 |
| AL | 0.731 | * | 0.718 | * | 0.781 | * |
| TI | 0.166 | * | 0.195 | * | 0.194 | * |
| FE | 2.397 | * | 2.350 | * | 2.360 | * |
| MN | 0.018 | * | 0.014 | * | 0.014 | * |
| MG | 2.696 | 6.008 | 2.521 | 5.798 | 2.459 | 5.809 |
| CA | 0.010 | * | 0.010 | * | 0.018 | * |
| NA | 0.041 | * | 0.050 | * | 0.048 | * |
| K | 1.510 | * | 1.742 | * | 1.643 | * |
| BA | 0.000 | 1.561 | 0.000 | 1.802 | 0.000 | 1.709 |
| CL | 0.000 | * | 0.000 | * | 0.000 | * |
| F | 0.000 | * | 0.000 | * | 0.000 | * |
| H | 4.000 | 4.000 | 4.000 | 4.000 | 4.000 | 4.000 |
| O | 24.000 | * | 24.000 | * | 24.000 | * |

25 247 BI608
26 248 BI608
27 249 BI608

1SUPER RECAL TABLE 10A FELDSPAR ANALYSES

| | 1 | 2 | 3 | 4 | 5 | 6 | 7 | 8 |
|---|---|---|---|---|---|---|---|---|
| SIO2 | 61.55 | 60.99 | 60.72 | 61.46 | 60.96 | 62.06 | 60.54 | 61.52 |
| A2O3 | 24.59 | 24.29 | 24.29 | 24.60 | 24.30 | 25.48 | 24.99 | 24.94 |
| TIO2 | 0.02 | 0.01 | -0.01 | -0.01 | 0.00 | 0.00 | -0.01 | -0.03 |
| FEO | -0.02 | -0.09 | -0.12 | -0.11 | -0.13 | -0.14 | -0.14 | -0.10 |
| MNO | -0.09 | -0.07 | -0.06 | -0.08 | -0.07 | -0.07 | -0.10 | -0.05 |
| MGO | -0.01 | 0.01 | 0.02 | 0.04 | -0.02 | -0.03 | -0.01 | 0.01 |
| CAO | 5.47 | 5.27 | 4.99 | 5.12 | 5.00 | 5.20 | 5.18 | 5.18 |
| NA2O | 8.69 | 8.78 | 8.77 | 8.72 | 8.71 | 8.74 | 8.56 | 8.81 |
| BAO | 0.00 | 0.00 | 0.00 | 0.00 | 0.00 | 0.00 | 0.00 | 0.00 |
| K2O | 0.01 | 0.02 | 0.03 | 0.06 | 0.02 | 0.02 | 0.23 | 0.01 |
| SUM | 100.21 | 99.21 | 98.63 | 99.80 | 98.77 | 101.26 | 99.24 | 100.29 |

| | | | | | | | | | | | | | | | | |
|---|---|---|---|---|---|---|---|---|---|---|---|---|---|---|---|---|
| SI | 2.724 | * | 2.726 | * | 2.727 | * | 2.727 | * | 2.732 | * | 2.713 | * | 2.705 | * | 2.718 | * |
| AL | 1.282 | * | 1.279 | * | 1.286 | * | 1.286 | * | 1.283 | * | 1.313 | * | 1.316 | * | 1.298 | * |
| TI | 0.001 | 4.006 | 0.000 | 4.005 | 0.000 | 4.012 | 0.000 | 4.013 | 0.000 | 4.015 | 0.000 | 4.025 | 0.000 | 4.021 | -0.001 | 4.015 |
| FE | -0.001 | * | -0.003 | * | -0.005 | * | -0.004 | * | -0.005 | * | -0.005 | * | -0.005 | * | -0.004 | * |
| MN | -0.003 | * | -0.003 | * | -0.002 | * | -0.003 | * | -0.003 | * | -0.003 | * | -0.004 | * | -0.002 | * |
| MG | -0.001 | * | 0.001 | * | 0.001 | * | 0.003 | * | -0.001 | * | -0.002 | * | -0.001 | * | 0.001 | * |
| CA | 0.259 | * | 0.252 | * | 0.240 | * | 0.243 | * | 0.240 | * | 0.244 | * | 0.248 | * | 0.245 | * |
| BA | 0.000 | * | 0.000 | * | 0.000 | * | 0.000 | * | 0.000 | * | 0.000 | * | 0.000 | * | 0.000 | * |
| NA | 0.746 | * | 0.761 | * | 0.764 | * | 0.750 | * | 0.757 | * | 0.741 | * | 0.742 | * | 0.755 | * |
| K | 0.001 | 1.001 | 0.001 | 1.009 | 0.002 | 1.000 | 0.003 | 0.993 | 0.001 | 0.989 | 0.001 | 0.976 | 0.013 | 0.993 | 0.001 | 0.995 |
| O | 8.000 | * | 8.000 | * | 8.000 | * | 8.000 | * | 8.000 | * | 8.000 | * | 8.000 | * | 8.000 | * |

1 227 FE495
2 228 FE495
3 229 FE495
4 230 FE495
5 231 FE495
6 232 FE495
7 233 FE495
8 234 FE495

1SUPER RECAL TABLE 10A FELDSPAR ANALYSES

| | 9 | 10 | 11 | 12 | 13 | 14 | 15 | 16 |
|---|---|---|---|---|---|---|---|---|
| SIO2 | 61.76 | 62.00 | 61.33 | 59.66 | 60.63 | 61.59 | 61.60 | 61.74 |
| A2O3 | 24.81 | 24.54 | 24.62 | 25.84 | 25.15 | 24.18 | 24.33 | 24.25 |
| TIO2 | 0.01 | 0.02 | 0.02 | -0.01 | 0.01 | 0.00 | -0.01 | 0.01 |
| FEO | -0.12 | -0.11 | -0.10 | -0.08 | 0.04 | 0.03 | 0.05 | 0.03 |
| MNO | -0.06 | -0.04 | -0.06 | -0.09 | -0.08 | -0.08 | -0.05 | -0.07 |
| MGO | 0.03 | 0.06 | 0.03 | 0.01 | 0.03 | 0.02 | 0.00 | 0.01 |
| CAO | 4.94 | 5.04 | 4.92 | 5.23 | 5.65 | 4.59 | 4.82 | 4.77 |
| NA2O | 8.91 | 8.98 | 9.10 | 8.65 | 8.60 | 9.15 | 9.16 | 9.08 |
| BAO | 0.00 | 0.00 | 0.00 | 0.00 | 0.00 | 0.00 | 0.00 | 0.00 |
| K2O | 0.04 | 0.00 | 0.02 | 0.02 | 0.01 | 0.03 | 0.03 | 0.02 |
| SUM | 100.32 | 100.49 | 99.88 | 99.23 | 100.04 | 99.51 | 99.93 | 99.84 |

| | | | | | | | | | | | | | | | | |
|---|---|---|---|---|---|---|---|---|---|---|---|---|---|---|---|---|
| SI | 2.726 | * | 2.733 | * | 2.722 | * | 2.668 | * | 2.692 | * | 2.741 | * | 2.734 | * | 2.740 | * |
| AL | 1.290 | * | 1.275 | * | 1.288 | * | 1.362 | * | 1.316 | * | 1.268 | * | 1.272 | * | 1.268 | * |
| TI | 0.000 | 4.017 | 0.001 | 4.008 | 0.001 | 4.011 | 0.000 | 4.030 | 0.000 | 4.009 | 0.000 | 4.010 | 0.000 | 4.006 | 0.000 | 4.008 |
| FE | -0.004 | * | -0.004 | * | -0.004 | * | -0.003 | * | 0.001 | * | 0.001 | * | 0.002 | * | 0.001 | * |
| MN | -0.002 | * | -0.001 | * | -0.002 | * | -0.003 | * | -0.003 | * | -0.003 | * | -0.002 | * | -0.003 | * |
| MG | 0.002 | * | 0.004 | * | 0.002 | * | 0.001 | * | 0.002 | * | 0.001 | * | 0.000 | * | 0.001 | * |
| CA | 0.234 | * | 0.238 | * | 0.234 | * | 0.251 | * | 0.269 | * | 0.219 | * | 0.229 | * | 0.227 | * |
| BA | 0.000 | * | 0.000 | * | 0.000 | * | 0.000 | * | 0.000 | * | 0.000 | * | 0.000 | * | 0.000 | * |
| NA | 0.762 | * | 0.767 | * | 0.783 | * | 0.750 | * | 0.740 | * | 0.790 | * | 0.788 | * | 0.781 | * |
| K | 0.002 | 0.994 | 0.000 | 1.004 | 0.001 | 1.014 | 0.001 | 0.996 | 0.001 | 1.010 | 0.002 | 1.010 | 0.002 | 1.019 | 0.001 | 1.008 |
| O | 8.000 | * | 8.000 | * | 8.000 | * | 8.000 | * | 8.000 | * | 8.000 | * | 8.000 | * | 8.000 | * |

9 235 FE495
10 236 FE495
11 237 FE495
12 238 FE495
13 239 FE495
14 265 FE495
15 266 FE495
16 267 FE495

1SUPER RECAL TABLE 10A FELDSPAR ANALYSES

| | 17 | 18 | 19 | 20 | 21 | 22 | 23 | 24 |
|---|---|---|---|---|---|---|---|---|
| SIO2 | 62.04 | 62.49 | 61.61 | 61.06 | 61.91 | 61.49 | 61.66 | 61.84 |
| A2O3 | 24.54 | 24.81 | 24.53 | 24.93 | 24.75 | 24.51 | 24.54 | 24.55 |
| TIO2 | 0.00 | -0.01 | 0.00 | 0.00 | -0.02 | -0.01 | -0.01 | 0.00 |
| FEO | 0.04 | 0.02 | -0.12 | -0.15 | -0.15 | -0.15 | -0.17 | -0.16 |
| MNO | -0.08 | -0.07 | -0.07 | -0.09 | -0.06 | -0.05 | -0.07 | -0.07 |
| MGO | 0.01 | 0.01 | 0.00 | 0.00 | 0.01 | -0.01 | 0.00 | 0.01 |
| CAO | 4.78 | 4.84 | 4.98 | 5.53 | 5.10 | 5.10 | 4.99 | 5.06 |
| NA2O | 8.69 | 7.45 | 8.93 | 8.39 | 8.81 | 8.96 | 8.88 | 8.71 |
| BAO | 0.00 | 0.00 | 0.00 | 0.00 | 0.00 | 0.00 | 0.00 | 0.00 |
| K2O | 0.03 | 0.02 | 0.01 | -0.01 | 0.02 | 0.03 | 0.03 | 0.03 |
| SUM | 100.05 | 99.56 | 99.87 | 99.66 | 100.37 | 99.87 | 99.85 | 99.97 |

| | | | | | | | | | | | | | | | | |
|---|---|---|---|---|---|---|---|---|---|---|---|---|---|---|---|---|
| SI | 2.742 | * | 2.759 | * | 2.732 | * | 2.713 | * | 2.730 | * | 2.729 | * | 2.733 | * | 2.736 | * |
| AL | 1.278 | * | 1.291 | * | 1.282 | * | 1.305 | * | 1.286 | * | 1.282 | * | 1.282 | * | 1.280 | * |
| TI | 0.000 | 4.020 | 0.000 | 4.049 | 0.000 | 4.013 | 0.000 | 4.018 | -0.001 | 4.016 | 0.000 | 4.010 | 0.000 | 4.015 | 0.000 | 4.016 |
| FE | 0.001 | * | 0.001 | * | -0.004 | * | -0.006 | * | -0.006 | * | -0.006 | * | -0.006 | * | -0.006 | * |

| | | | | | | | | | | | | | | | |
|---|---|---|---|---|---|---|---|---|---|---|---|---|---|---|---|
| MN | -0.003 | * | -0.003 | * | -0.003 | * | -0.003 | * | -0.002 | * | -0.002 | * | -0.003 | * | -0.003 | * |
| MG | 0.001 | * | 0.001 | * | 0.000 | * | 0.000 | * | 0.001 | * | -0.001 | * | 0.000 | * | 0.001 | * |
| CA | 0.226 | * | 0.229 | * | 0.237 | * | 0.263 | * | 0.241 | * | 0.242 | * | 0.237 | * | 0.240 | * |
| BA | 0.000 | * | 0.000 | * | 0.000 | * | 0.000 | * | 0.000 | * | 0.000 | * | 0.000 | * | 0.000 | * |
| NA | 0.745 | * | 0.638 | * | 0.768 | * | 0.723 | * | 0.753 | * | 0.771 | * | 0.763 | * | 0.747 | * |
| K | 0.002 | 0.972 | 0.001 | 0.866 | 0.001 | 0.998 | -0.001 | 0.976 | 0.001 | 0.988 | 0.002 | 1.007 | 0.002 | 0.993 | 0.002 | 0.981 |
| O | 8.000 | * | 8.000 | * | 8.000 | * | 8.000 | * | 8.000 | * | 8.000 | * | 8.000 | * | 8.000 | * |

17 268 FE495
18 269 FE495
19 270 FE495
20 271 FE495
21 272 FE495
22 273 FE495
23 274 FE495
24 275 FE495

1SUPER RECAL TABLE 10A FELDSPAR ANALYSES

| | 25 | 26 | 27 | 28 | 29 | 30 | 31 | 32 |
|---|---|---|---|---|---|---|---|---|
| SIO2 | 57.52 | 61.62 | 61.74 | 62.31 | 62.31 | 62.13 | 62.10 | 61.88 |
| A2O3 | 25.78 | 24.68 | 24.55 | 24.60 | 24.54 | 24.49 | 24.59 | 24.57 |
| TIO2 | 0.00 | -0.01 | -0.01 | -0.01 | -0.02 | -0.01 | 0.00 | -0.01 |
| FEO | -0.08 | -0.17 | -0.19 | -0.17 | -0.18 | -0.19 | -0.17 | -0.17 |
| MNO | -0.08 | -0.08 | -0.06 | -0.09 | -0.09 | -0.09 | -0.07 | -0.08 |
| MGO | 0.09 | 0.00 | 0.00 | 0.00 | 0.01 | 0.01 | -0.01 | -0.01 |
| CAO | 4.90 | 5.27 | 5.26 | 5.15 | 5.17 | 5.14 | 5.18 | 5.09 |
| NA2O | 7.79 | 8.72 | 8.64 | 8.79 | 8.73 | 8.70 | 8.78 | 8.70 |
| BAO | 0.00 | 0.00 | 0.00 | 0.00 | 0.00 | 0.00 | 0.00 | 0.00 |
| K2O | 0.09 | 0.01 | 0.00 | 0.01 | 0.02 | 0.03 | 0.03 | 0.04 |
| SUM | 96.01 | 100.04 | 99.93 | 100.59 | 100.49 | 100.21 | 100.43 | 100.01 |

| | | | | | | | | | | | | | | | |
|---|---|---|---|---|---|---|---|---|---|---|---|---|---|---|---|
| SI | 2.652 | * | 2.727 | * | 2.734 | * | 2.740 | * | 2.742 | * | 2.742 | * | 2.737 | * | 2.737 | * |
| AL | 1.401 | * | 1.287 | * | 1.281 | * | 1.275 | * | 1.273 | * | 1.273 | * | 1.277 | * | 1.281 | * |
| TI | 0.000 | 4.053 | 0.000 | 4.014 | 0.000 | 4.014 | 0.000 | 4.014 | -0.001 | 4.014 | 0.000 | 4.015 | 0.000 | 4.013 | 0.000 | 4.017 |
| FE | -0.003 | * | -0.006 | * | -0.007 | * | -0.006 | * | -0.007 | * | -0.007 | * | -0.006 | * | -0.006 | * |
| MN | -0.003 | * | -0.003 | * | -0.002 | * | -0.003 | * | -0.003 | * | -0.003 | * | -0.003 | * | -0.003 | * |
| MG | 0.006 | * | 0.000 | * | 0.000 | * | 0.000 | * | 0.001 | * | 0.001 | * | -0.001 | * | -0.001 | * |
| CA | 0.242 | * | 0.250 | * | 0.250 | * | 0.243 | * | 0.244 | * | 0.243 | * | 0.245 | * | 0.241 | * |
| BA | 0.000 | * | 0.000 | * | 0.000 | * | 0.000 | * | 0.000 | * | 0.000 | * | 0.000 | * | 0.000 | * |
| NA | 0.696 | * | 0.748 | * | 0.742 | * | 0.749 | * | 0.745 | * | 0.744 | * | 0.750 | * | 0.746 | * |
| K | 0.005 | 0.944 | 0.001 | 0.989 | 0.000 | 0.982 | 0.001 | 0.983 | 0.001 | 0.980 | 0.002 | 0.979 | 0.002 | 0.987 | 0.002 | 0.980 |
| O | 8.000 | * | 8.000 | * | 8.000 | * | 8.000 | * | 8.000 | * | 8.000 | * | 8.000 | * | 8.000 | * |

25 276 FE495
26 277 FE495
27 278 FE495
28 279 FE495
29 281 FE495
30 282 FE495
31 283 FE495
32 284 FE495

1SUPER RECAL TABLE 10A FELDSPAR ANALYSES

| | 33 | 34 | 35 | 36 | 37 | 38 |
|---|---|---|---|---|---|---|
| SIO2 | 62.12 | 62.61 | 62.53 | 61.58 | 61.93 | 62.08 |
| A2O3 | 24.70 | 24.33 | 24.76 | 24.60 | 24.55 | 25.05 |
| TIO2 | -0.02 | 0.00 | -0.01 | -0.01 | 0.00 | -0.01 |
| FEO | -0.17 | -0.15 | -0.16 | -0.13 | -0.16 | -0.16 |
| MNO | -0.08 | -0.08 | -0.07 | -0.08 | -0.08 | -0.07 |
| MGO | 0.02 | 0.00 | 0.01 | 0.01 | 0.01 | 0.01 |
| CAO | 5.19 | 5.09 | 5.27 | 5.51 | 5.24 | 5.35 |
| NA2O | 8.69 | 8.78 | 8.59 | 8.58 | 8.63 | 8.61 |
| BAO | 0.00 | 0.00 | 0.00 | 0.00 | 0.00 | 0.00 |
| K2O | 0.03 | 0.03 | 0.03 | 0.00 | 0.02 | 0.03 |
| SUM | 100.48 | 100.61 | 100.95 | 100.06 | 100.14 | 100.89 |

| | | | | | | | | | | | | | | | |
|---|---|---|---|---|---|---|---|---|---|---|---|---|---|---|---|
| SI | 2.735 | * | 2.752 | * | 2.739 | * | 2.726 | * | 2.736 | * | 2.723 | * | | | |
| AL | 1.281 | * | 1.260 | * | 1.278 | * | 1.283 | * | 1.278 | * | 1.295 | * | | | |
| TI | -0.001 | 4.016 | 0.000 | 4.012 | 0.000 | 4.017 | 0.000 | 4.009 | 0.000 | 4.014 | 0.000 | 4.018 | | | |
| FE | -0.006 | * | -0.006 | * | -0.006 | * | -0.005 | * | -0.006 | * | -0.006 | * | | | |
| MN | -0.003 | * | -0.003 | * | -0.003 | * | -0.003 | * | -0.003 | * | -0.003 | * | | | |
| MG | 0.001 | * | 0.000 | * | 0.001 | * | 0.001 | * | 0.001 | * | 0.001 | * | | | |
| CA | 0.245 | * | 0.240 | * | 0.247 | * | 0.261 | * | 0.248 | * | 0.251 | * | | | |
| BA | 0.000 | * | 0.000 | * | 0.000 | * | 0.000 | * | 0.000 | * | 0.000 | * | | | |
| NA | 0.742 | * | 0.748 | * | 0.730 | * | 0.736 | * | 0.739 | * | 0.732 | * | | | |
| K | 0.002 | 0.980 | 0.002 | 0.981 | 0.002 | 0.971 | 0.000 | 0.991 | 0.001 | 0.980 | 0.002 | 0.978 | | | |
| O | 8.000 | * | 8.000 | * | 8.000 | * | 8.000 | * | 8.000 | * | 8.000 | * | | | |

33 285 FE495
34 286 FE495
35 287 FE495
36 293 FE495
37 294 FE495
38 295 FE495

**The vita has been removed from the scanned document**

# Geology of the Ålen Area, Central Norway

Charles W. Mandeville

Orogenic Studies Laboratory, Department of Geological Sciences
Virginia Tech, Blacksburg, Virginia

1988

LOWER ORDOVICIAN TO SILURIAN(?)

TREMADOCIAN - LOWER ORDOVICIAN

## STRATIGRAPHY

### INTRUSIVES

**T** — *Trondjhemite, T* : light colored fine - coarse grained, massive equigranular to strongly foliated and/or lineated varities. Mineralogy consists of plagioclase quartz and biotite occasionally with accessory garnet. Probably more than one generation of Trondjhemite.

**Mqd** — *Meta-Quartz diorite, Mqd* : fine - coarse grained equigranular textured to strongly foliated and/or lineated varieties. Mineralogy consists of plagioclase, quartz, biotite, hornblende, chlorite with accessory zolsite, sphene, epidote and calcite. Possibly coeval with the Fundsjø Group.

**Mg** — *Meta-Gabbro, Mg* : medium - coarse grained, equigranular textured to strongly foliated and/or lineated varieties. Mineralogy composed almost entirely of plagioclase partially altered to zolsite and sericite, and dark blue-green hornblende. May have accessory garnet and sulphides. Most are probably coeval with the Fundsjø Group.

### FUNDSJØ GROUP

**Fs** — *Slågrov Fm, Fs* : dominantly interbedded dark grey muscovite + biotite + quartz ± graphite phyllite, biotite + muscovite + quartz ± graphite schist, and muscovite + quartz + biotite schist. Common intercalations of plagioclase + quartz + biotite semischist, and quartz + plagioclase + biotite ± chlorite psammite.

**Frv / Frm** — *Reitan Fm, Frv* : dominantly interbedded fine grained dark green amphibolite mafic tuff and light grey quartz keratophyre tuff, lapilli tuff, tuff breccia, and rarely, coarse pyroclastic breccia. Commonly intercalated with biotite + quartz + plagioclase ± garnet ± chlorite schist and plagioclase + hornblende + quartz ± chlorite ± calcite garbenschist. Intruded by fine grained and occasionally porphyritic mafic sills; *Frm* : light to dark grey impure marble and calc-silicate schist.

**Fk** — *Kjurudal Fm, Fk* : dominantly interbedded dark grey biotite + muscovite + quartz ± graphite schist, muscovite + biotite + quartz + graphite phyllite, biotite + quartz + hornblende ± chlorite ± garnet garbenschist. Commonly a chlorite + biotite + quartz + garnet + albite ± calcite schist, quartz + biotite ± garnet ± muscovite psammite, muscovite + chlorite + biotite ± garnet schist, and rarely a dark grey calc-silicate schist.

**Fh / Fhm** — *Hersjø Fm, Fh* : dominantly interbedded fine grained dark green amphibolite mafic tuff and light grey quartz keratophyre tuff, plagioclase quartz crystal tuff, lapilli tuff, tuff breccia and coarse pyroclastic breccia, commonly with minor intercalations of plagioclase + quartz + hornblende ± chlorite ± garnet garbenschist, quartz + plagioclase + biotite ± garnet ± hornblende semischist, and biotite + quartz ± garnet ± hornblende schist. Intruded by characteristic 1 - 2m thick porphyritic dolerite sills and fine grained amphibolite sills; *Fhm* : light grey impure marble with minor amounts of quartz, albite, tremolite, chlorite, and biotite.

**Fg** — *Gudå Fm, Fg* : dominantly interbedded dark grey-brown biotite + quartz + muscovite ± garnet schist, biotite + muscovite + quartz ± graphite phyllite and schist, biotite + quartz + muscovite + garnet ± staurolite ± kyanite schist, common intercalations of plagioclase + quartz + hornblende ± chlorite garbenschist, plagioclase + hornblende ± quartz calc-silicate layers, and quartz + plagioclase + biotite ± muscovite psammite, minor fine grained amphibolite mafic tuff layers and light to dark grey marble layers.

## STRUCTURE

- $S_0$ strike and dip of overturned bedding (determined from graded beds)
- $S_1$ strike and dip of schistosity; inclined, vertical: parallel to $S_0$ generally
- $S_2$ strike and dip of spaced cleavage, locally a crenulation cleavage, rarely a continuous cleavage
- $S_1$ strike and dip of foliation of uncertain generation developed in intrusive lithologies
- $F_2$ trend and plunge of $F_2$ mesoscopic (open to tight) fold axes: form (S or Z) as viewed down plunge indicated by S or Z at base of arrow shaft
- $F_2$ trend and plunge of $F_2$ mesoscopic (open to tight) fold axes: form (S or Z) undetermined due to incomplete exposure of long and short limbs
- $S_1/S_2$ trend and plunge of intersection lineation of $S_1$ continuous and $S_2$ spaced cleavages: also trend and plunge of $L_2$ crenulation on $S_1$
- $L_1$ trend and plunge of mineral lineation defined by hornblende and/or elongated plagioclase or quartz grains
- $F_2$ trend and plunge of $F_2$ kink folds
- $S_1 \wedge S_2/S_2$ trend and plunge of crenulation lineation on $S_1$ and $S_2$ surfaces
- $S_1$, $S_2$ and $S_1/S_2$ measured at a single point within an outcrop
- strike and dip of $S_1$, and trend and plunge of mineral lineation on $S_1$
- strike and dip of $S_1$, strike and dip of $S_2$ measured at separate points within a single outcrop
- strike and dip of $S_1$, strike and dip of $S_2$ measured at a single point within an outcrop
- $D_1$ overturned bedding plane fault; solid where approximate, short dashes where assumed, base of sawteeth on upper plate, sawteeth point in direction of overturned dip
- $D_2$? thrust fault; as on NGU 1 : 250,000 Røros and Sveg quadrangle
- geologic contacts; solid where known to within 100m, short dashes where approximate, and long dashes where NGU 1 : 250,000 Røros and Sveg quadrangle contacts are used
- axial trace of $F_2$ antiformal syncline (approximately located)
- axial trace of $F_2$ synformal anticline (approximately located)



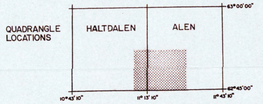



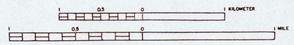


Numbered lines on topographic base indicate UTM grid, zone 32, international Spheroid